



Callum Scullion, MSci

PhD Thesis

**Synthesis and Reactivity of
Superelectrophilic Amidine Disalts**

A thesis submitted to the University of Strathclyde in part fulfilment of regulations for the degree of PhD in Chemistry.

WestCHEM, Department of Pure & Applied Chemistry, University of Strathclyde,

Thomas Graham Building, 295 Cathedral Street, Glasgow G1 1 XL

2014

Declaration of Copyright

This thesis is the result of the author's original research. It has been composed by the author and has not been previously submitted for examination which has led to the award of a degree.

The copyright of this thesis belongs to the author under the terms of the United Kingdom Copyright Acts as qualified by University of Strathclyde Regulation 3.50. Due acknowledgement must always be made of the use of any material contained in, or derived from, this thesis.

Signed:

Date:

Acknowledgements

Firstly, I would like to thank Prof. John A. Murphy for the opportunity to work in his research group for the last few years. I am grateful for all of the guidance and support that he has afforded me as well as the opportunity to work independently – a four month placement at the Université of Montréal in the second year of my research was an experience that I will always be appreciative of.

I would then like to thank the Murphy group, past and present, for providing a fantastic arena to develop as a chemist. “Guru” Zhou, Steve-O, Luka, Phil, Doni, Ryan, Jonathan, Greg, Mike, Neil and those that I may have missed out unintentionally, have been fantastic colleagues and good friends.

I would also like to acknowledge the university staff that kept the instruments working, including Craig Irving, Patricia Keating and Gavin Bain. Alan Kennedy also obtained the X-ray structure of an amidine disalt.

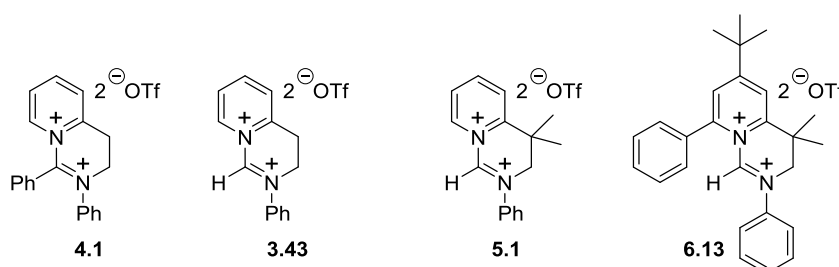
An acknowledgement must also go to my parents and four older brothers. They have all helped instill a great enjoyment in learning and used to answer my many questions about the world when growing up.

Lastly, and most importantly, I would like to thank my wife Lynsey for all of the support that she has provided me with. Having met as undergraduates on the same course, to then go on and work towards PhDs in the same department, I now look forward to the many adventures that lie ahead of us outside of academia. I must also quickly mention our cat Jimmy, who is currently trying to help me write this acknowledgement by jumping on to the laptop.

Abstract

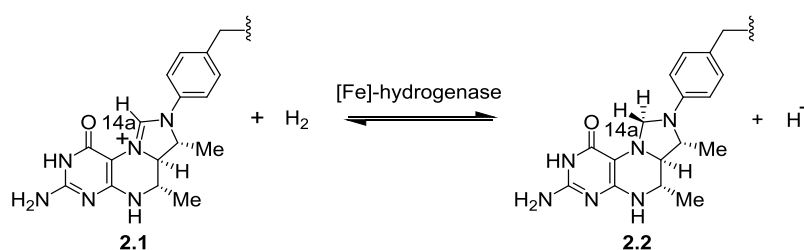
This work describes the successful synthesis and full characterization of amidine disalt **4.1** (Scheme A), which was made from the reaction of a tertiary amide with triflic anhydride and an amine; this disalt contains a dication which can be considered as a superelectrophile. Various related disalts (not limited to, but including disalts **3.43**, **5.1** and **6.13**, Scheme A) have also been synthesised and their reactivities further investigated.

Scheme A Various synthesised disalts.



Chapter 1 gives an introduction to the concept of superelectrophiles, including the original discoveries in this area of chemistry. Chapter 2 focuses on reviewing the chemistry of [Fe]-hydrogenase, which converts amidine molecule **2.1** into diamino methylene **2.2** (Scheme B); the possibility of a mechanism involving superelectrophiles is briefly highlighted.

Scheme B The reaction carried out by [Fe]-hydrogenase.



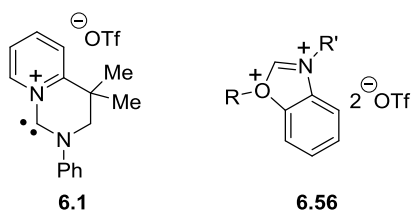
Chapter 3 reviews the previous work carried out within the Murphy group regarding superelectrophiles, leading on to the synthesis of disalt **3.43**. (Scheme A). Chapter 4 discusses the route to synthesising and isolating disalt **4.1** (Scheme A). Additionally,

Chapter 4 describes attempts at carrying out [Fe]-hydrogenase-related reactivity with disalt **3.43** and also describes the limitations of this disalt due to side-reactivity.

The reasoning behind the synthesis of disalt **5.1** (Scheme A) is discussed in Chapter 5; this chapter also discusses the successful reduction of this disalt with an iron hydride in a reversible process – the first successful model reaction of amidine disalts and iron hydrides, intended to mimic the possible reactivity within [Fe]-hydrogenase.

Chapter 6 discusses non-hydrogenase reactivity of amidine disalts; evidence for the formation of monocationic carbene **6.1** (Scheme C), the synthesis and reactivity of further substituted disalt **6.13** (Scheme A) and the possibility of oxygen-containing disalts of type **6.56** (Scheme C) are all discussed.

Scheme C Cationic carbene **6.1** and oxygen-containing disalt structure **6.56**.



Abbreviations

°C	degree(s) Celsius
Å	Ångström(s)
AcOH	acetic acid
Ala	alanine
Ar	aryl
atm	atmosphere(s)
b	broad
b.p.	boiling point
d	doublet
CD	circular dichroism
CH≡H ₄ MPT ⁺	<i>N</i> ⁵ , <i>N</i> ¹⁰ -methenyltetrahydromethanopterin
CH ₂ =H ₄ MPT	<i>N</i> ⁵ , <i>N</i> ¹⁰ -methylenetetrahydromethanopterin
COSY	correlation spectroscopy
CPK	a space-filling molecular modeling system designed by Robert Corey and Linus Pauling, later improved by Walter Koltun
Cys	cysteine
Cy	cyclohexyl
DCE	1,2-dichloroethane
dec.	decomposed
DEPT	distortionless enhancement by polarization transfer
DFT	density functional theory
Diip	2,6-di- <i>iso</i> -propylphenyl
DIPEA	di- <i>iso</i> -propylethylamine
2-DMAP	2-dimethylaminopyridine
4-DMAP	4-dimethylaminopyridine

DMF	dimethylformamide
DMSO	dimethyl sulfoxide
2,4-DNPH	2,4-dinitrophenylhydrazine
DTT	dithiothreitol
E_0	standard potential
$E_{1/2}$	half-wave potential
EI	electron impact
EPSRC	Engineering and Physical Sciences Research Council
ESI	electrospray ionisation
FeGP	iron (II) guanylyl pyridone
Fp	cyclopentadienyliron dicarbonyl
g	gram(s)
h	hour(s)
His	histidine
HMBC	heteronuclear multiple-bond correlation
HRMS	high resolution mass spectrometry
HSQC	heteronuclear single quantum coherence
IR	infrared
KOtBu	potassium <i>tertiary</i> -butoxide
L	litre
LA	Lewis acid
LDA	lithium diisopropylamide
LiHMDS	lithium hexamethyldisilazide
liq.	liquid
M	molar or generic metal
m	milli or multiplet
Me	methyl

Mes	mesityl (2,4,6-trimethylphenyl)
Met	methionine
MHz	megahertz
min	minute(s)
m.p.	melting point
MS	mass spectrometry
<i>m/z</i>	mass-to-charge ratio
N	normality or nitrogen
NaO <i>t</i> Bu	sodium <i>tertiary</i> -butoxide
NHC	<i>N</i> -heterocyclic carbene
NMR	nuclear magnetic resonance
nOe	nuclear Overhauser effect
NOESY	nuclear Overhauser effect spectroscopy
NRVS	nuclear resonance vibrational spectroscopy
OTf	trifluoromethanesulfonate
PEG	poly(ethylene glycol)
Ph	phenyl
ppm	parts per million
psi	pounds per square inch
Q135	pulse of 135 °
R	generic alkyl/aryl group
RCSB	Research Collaboratory for Structural Bioinformatics
r.t.	room temperature
s	singlet
sat.	saturated
SED	super electron-donor
t	triplet

Thr	threonine
TFA	trifluoroacetic acid
TfOH	trifluoromethanesulfonic acid or triflic acid
THF	tetrahydrofuran
TLC	thin layer chromatography
TMS	trimethylsilyl
Tyr	tyrosine
U	unknown ligand
VMD	Virtual Molecular Dynamics
vs.	<i>versus</i>

Contents

Abbreviations:	i
Chapter 1 : Superelectrophiles	1
1.1 : Introduction to Superelectrophiles	1
1.2 : Initial Discoveries of Superelectrophilic Activation	1
1.3 : Superelectrophiles in Organic Synthesis – Using Superacidic Media	4
1.4 : Superelectrophiles in Organic Synthesis – Without Superacidic Media	5
1.5 : Nitrogen-based Heterocyclic Disalts	11
Chapter 2 : [Fe]-Hydrogenase	17
2.1 : Introduction	17
2.2 : Initial Studies of Hmd	18
2.3 : Discovery that Hmd Contains a Bound Cofactor	22
2.4 : Discovery that Hmd is a Metalloenzyme	22
2.5 : Crystal Structure Studies of [Fe]-Hydrogenase	25
2.6 : Mechanistic Models of [Fe]-Hydrogenase	33
2.6.1 : Studies Before the Most Recent Assignment of the FeGP Cofactor	33
2.6.2 : Studies After the Most Recent Assignment of the FeGP Cofactor	36
2.7 : Synthesised Model Complexes of the FeGP Cofactor	43
Chapter 3 : Previous Work	55
3.1 : Initial Search and Development of Superelectrophiles	55
3.2 : A New Series of Disalts	60
Chapter 4 : Results and Discussion: Providing Evidence for the Formation of Amidine Disalts	64
4.1 : Project Aims	64
4.2 : Isolation and Full Characterisation of a New Amidine Disalt	65
4.3 : Synthesis of Disalts Related to Disalt 4.1	68
4.4 : Initial [Fe]-Hydrogenase Model Reactions	73

4.4.1 :	Hydrogenation Under 1 Atmosphere of Hydrogen	74
4.4.2 :	High Pressure Hydrogenation	77
4.5 :	Chapter 4 Summary	79
Chapter 5 :	Results and Discussion: Development of Amidine Disalts That Do Not Undergo Oxidation	81
5.1 :	The Synthesis of a Disalt That Does Not Undergo Oxidation	81
5.2 :	Reaction of Disalt 5.1 with Triethylsilane	83
5.3 :	Reaction of Disalt 5.1 with an Iron Hydride	87
5.4 :	Chapter 5 Summary	96
Chapter 6 :	Results and Discussion: Extending the Reactivity of Superelectrophilic Disalts	98
6.1 :	Further Investigations into the Reactivity of Disalt 5.1	98
6.2 :	The Synthesis and Reactivity of Disalts Related to Disalt 5.1 : Breaking <i>N</i> -Phenyl Bonds	105
6.3 :	Amidine Disalts As Formylating Agents	112
6.4 :	Oxygen-Containing, Amide-Derived Disalts	115
6.5 :	Chapter 6 Summary	121
Chapter 7 :	Conclusions and Future Work	124
Chapter 8 :	Experimental Section	129
References :		202
Appendices :		211
	Appendix A: Treatment of Disalt 5.1 with 1 eq Et ₃ SiH	211
	Appendix B: ¹ H NMR of FpH Formed in C ₆ D ₆	215
	Appendix C: Treatment of a Solution of Disalt 5.1 in CD ₃ CN with a Solution of FpH in C ₆ D ₆	216
	Appendix D: NMR Spectra of Disalt 5.1 Reaction with Pyridine	217
	Appendix E: ¹ H NMR of Possible <i>N</i> -Ph Cleavage Reaction	224
	Appendix F: ¹ H NMR Experiment: Treatment of Amide 6.91 with Tf ₂ O at r.t.	225
	Appendix G: ¹ H NMR Experiment: Treatment of Amide 6.91 with Tf ₂ O at r.t. Followed by Heating at 80 °C Then	226

Cooling to r.t.

Appendix H: ^{19}F NMR experiment: Treatment of Amide
6.91 with Tf_2O at r.t. Followed by Heating at $80\text{ }^\circ\text{C}$ Then
Cooling to r.t. 230

Chapter 1: Superelectrophiles

As the main focus of work to be discussed in this Thesis is the synthesis and reactivity of amidine disalts as superelectrophilic compounds, a brief history of superelectrophiles will be detailed in this chapter. The amidine disalts that were prepared in this work were also used as model compounds for the reactivity observed in [Fe]-hydrogenase; Chapter 2 will introduce and review the history of [Fe]-hydrogenase and will also include a short section describing the possible role of superelectrophilic activation within this enzyme.

1.1 Introduction to Superelectrophiles

Investigations into superelectrophilic activation were first carried out by Olah in 1975,¹ and developed from his research into reactions carried out in superacidic media. Superelectrophiles are generally defined as “doubly electron-deficient, activated species”,² which primarily involve dicationic species. Superelectrophilic activation of an electrophile causes the resulting compound to have greatly increased reactivity over its parent compound.³

Traditionally, research into superelectrophiles has been carried out in superacidic media, which have low nucleophilicity and high ionising ability.² Electrophiles can often be further activated by protosolvation or coordination in superacidic media – thus giving superelectrophiles. However, superelectrophilic activation is an area of research that has also grown to include reactions in organic synthesis and has also been proposed to have a presence in some enzymatic reactions.

This chapter will now go on to discuss three areas of superelectrophilic activation: the initial discoveries of superelectrophilic activation, superelectrophiles in organic synthesis and possible enzymatic superelectrophiles.

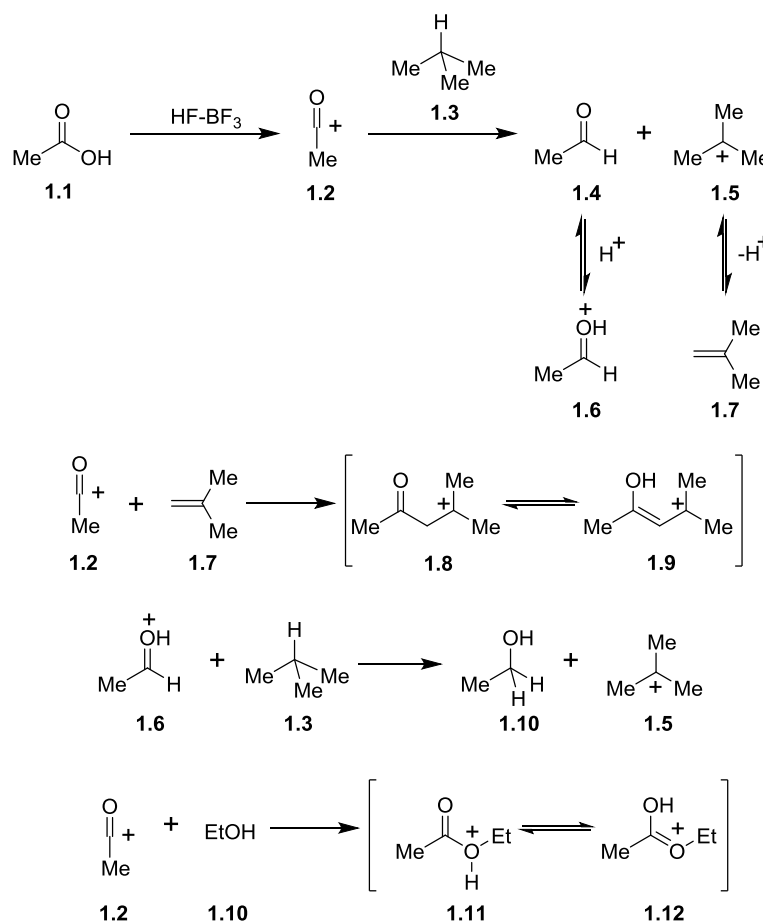
1.2 Initial Discoveries of Superelectrophilic Activation

In 1975,¹ Olah *et al.* revisited work originally carried out by Brouwer and Kiffen,⁴ which looked into the hydride transfer reaction from 2-methylpropane **1.3** to the

acetyl cation **1.2**, which occurs in the reaction between 2-methylpropane **1.3** and acetic acid **1.1** in HF-BF₃ (Scheme 1.1). Products observed from the reaction were protonated mesityl oxide **1.9** and protonated ethyl acetate **1.12**, produced in a ratio of 2:1 and the rate constant of hydride transfer was calculated as $3.0 \times 10^{-5} \text{ M}^{-1}\text{s}^{-1}$.

To explain these results, Brouwer and Kiffen suggested that protonated acetaldehyde **1.6** and *iso*-butene **1.7** were produced as reaction intermediates which would, in turn, have derived from acetaldehyde **1.4** and the *t*-butyl cation **1.5**, respectively. Reaction of acetyl cation **1.2** with *iso*-butene **1.7** could account for formation of protonated mesityl oxide **1.9**, while protonated acetaldehyde **1.6** and 2-methylpropane **1.3** could react to give ethanol **1.10** which then reacts with acetyl cation **1.2** to give protonated ethyl acetate **1.12**.

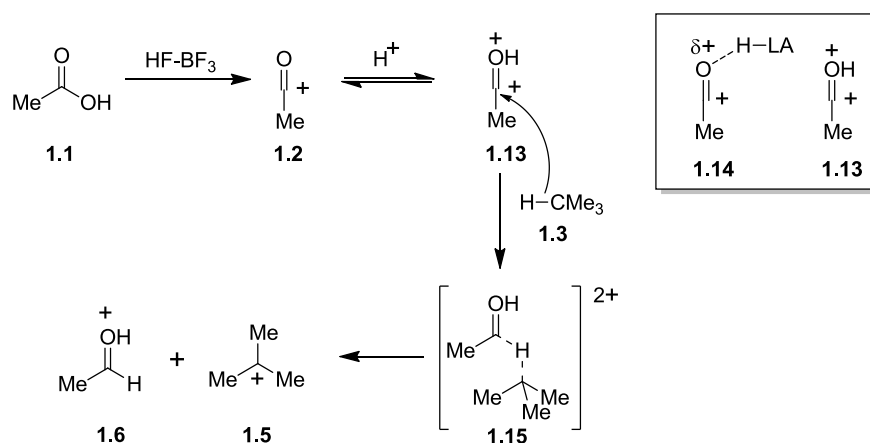
Scheme 1.1 Proposed mechanism of the reaction of acetyl cation **1.2** and 2-methylpropane **1.3**.



The reaction was also studied in HF-SbF₅ (which has a greater acidity) and the same hydride transfer was observed, this time with a calculated rate constant of $2.0 \times 10^{-5} \text{ M}^{-1}\text{s}^{-1}$. In their explanation of the hydride transfer in the two different superacidic systems, the authors concluded that both occurred in the same way (with acetyl cation **1.2** as the electrophile) and that added activation by protonation of the carbonyl group of acetyl cation **1.2** was not occurring.

Olah *et al.*¹ later revisited the work of Brouwer and Kiffen. This time, the reaction was tried under several different conditions, including in aprotic solvents (examples include CH₂Cl₂, SO₂, SO₂ClF and AsF₃). Other conditions employed by Olah and co-workers also involved using an excess of methylpropane **1.3** and also trying the reaction with alternative hydrocarbons.¹ These experiments did not afford any hydride transfer reactions; this was contradictory to Brouwer and Kiffen's proposal that protonation of the carbonyl group of acetyl cation **1.2** was not occurring. If protonation of acetyl cation **1.2** was not essential, these reactions in aprotic solvents would have resulted in hydride transfer.

Scheme 1.2 Superelectrophilic activation of acetyl cation **1.2**.

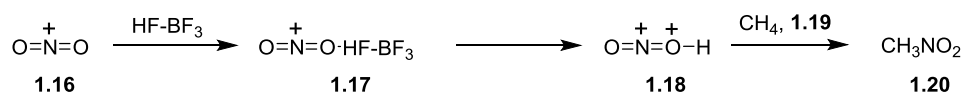


According to Olah *et al.*,¹ the non-bonding electron pair on the oxygen of acetyl cation **1.2** must interact further with the superacidic solvent. This could be done by either coordination of the superacidic solvent to the acetyl cation **1.2** to give a superelectrophilic hydrogen-bonded species such as **1.14** or with full protonation (protosolvation) of **1.2** to give dication **1.13** (Scheme 1.2). Both modes of interaction provided Olah *et al.* with a mechanism for the hydride abstraction in which **1.13** or

1.14 can abstract a hydride from 2-methylpropane **1.3** and give species **1.5** and **1.6** via a 3-centre-2-electron (3c-2e) bonded transition state **1.15**.

In the same paper,¹ Olah *et al.* refer to previous work that they had carried out,⁵ showing similar reactivity between nitronium salts and alkanes such as methane **1.19** (Scheme 1.3). Some evidence for the coordination of FSO₃H with the nitronium ion **1.16** was obtained from IR spectra in AsF₃.¹ On addition of approximately 10% NO₂⁺PF₆⁻ to the system, the H-O stretching frequency of the acid was shifted from about 3300 to 3265 cm⁻¹ and was also broadened. Simultaneously, the N-O stretching frequency at 2380 cm⁻¹ remained unchanged, indicating no change in the N-O bond strength.

Scheme 1.3 Superelectrophilic activation of nitronium salts.



Since these initial studies of superelectrophilic activation in superacidic media, many more examples have been observed and extensive reviews of this area now exist, providing many examples of oxygen, nitrogen and carbon superelectrophiles.^{3,6,7} This chapter, rather than extensively covering the area of superelectrophiles in superacidic media, will now go on to review superelectrophiles in organic synthesis – with some examples in superacidic media described first.

1.3 Superelectrophiles in Organic Synthesis – Using Superacidic Media

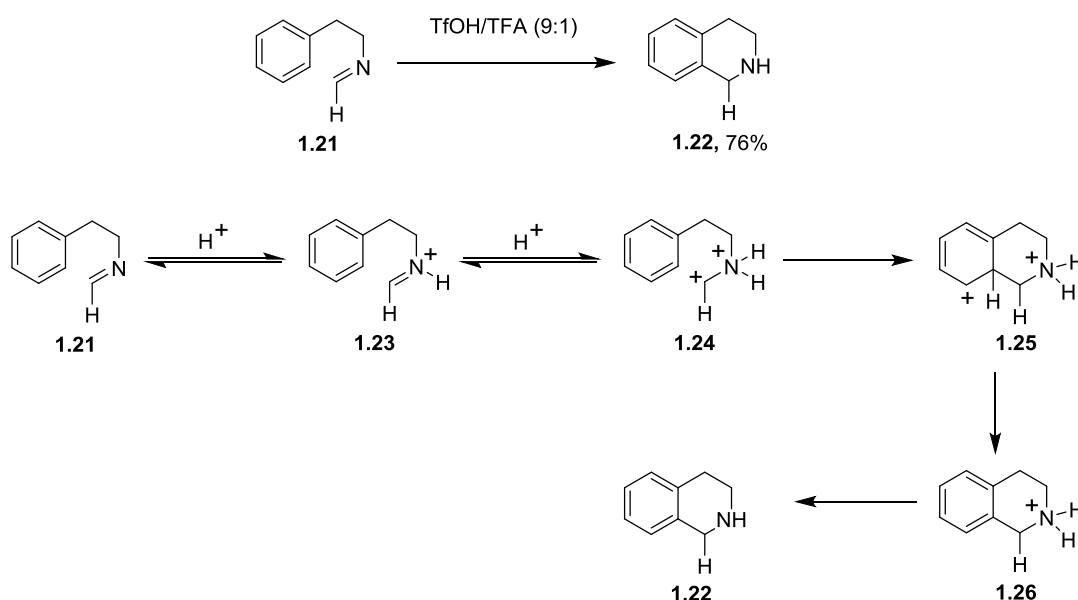
The Pictet-Spengler^{8,9} and Bischler-Napieralski¹⁰ reactions are used in organic synthesis to provide the useful isoquinoline ring structure. In reactions carried out with monocationic iminium ions, cyclisation normally requires activated aryl nucleophiles to provide adequate reactivity. Shudo and Ohwada,¹¹ however, have carried out Pictet-Spengler reactions on non-activated species in superacidic media and have found kinetic evidence for the involvement of superelectrophilic activation.

Imine **1.21** (which has an unactivated arene) was cyclised to 1,2,3,4-tetrahydroisoquinoline **1.22** in a yield of 76 % (Scheme 1.4). The rate of cyclisation

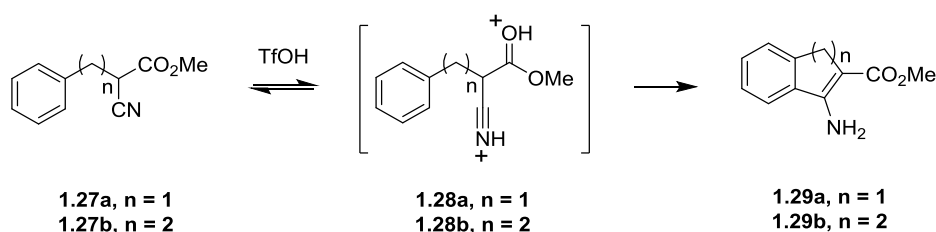
was shown to have a linear relationship to acidity (varied by changing the TFA/TfOH ratio; $H_0 < -10$), which Shudo and Ohwada propose would only occur if imine **1.21** was protonated twice to give dication **1.24**.¹¹

Ohwada *et al.* have also carried out the cyclisation of arylcyano species **1.27** to give cyclised 5- and 6- membered β -enamino esters **1.29**¹² (Scheme 1.5). These reactions are proposed to go *via distonic* (distant, i.e. greater than 1 atom between both positive charges) superelectrophilic species **1.28**.

Scheme 1.4 Pictet-Spengler reaction of unactivated imine **1.21**.



Scheme 1.5 Distonic superelectrophilic activation of arylcyanopropionates **1.27**.



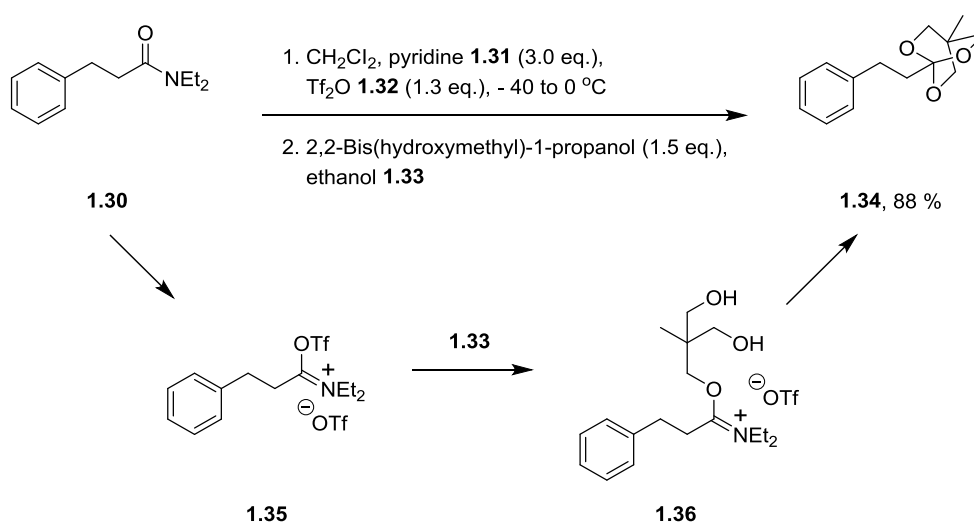
1.4 Superelectrophiles in Organic Synthesis – Without Superacidic Media

Superelectrophiles are normally associated with work carried out in superacidic media, which act both to produce the superelectrophile from the starting materials

and then also provide a solvent that will not nucleophilically attack the superelectrophile. However, work has been published in recent years regarding the existence of superelectrophilic intermediates in conventional reaction conditions and this will now be discussed.

In 1997, Charette and Chua¹³ prepared bridged orthoesters from the treatment of secondary and tertiary amides with triflic anhydride **1.32** and pyridine **1.31**, followed by treatment with a branched triol. Activation of tertiary amide **1.30** followed by treatment with triol **1.33** afforded orthoester **1.34** in an 88 % yield (Scheme 1.6).

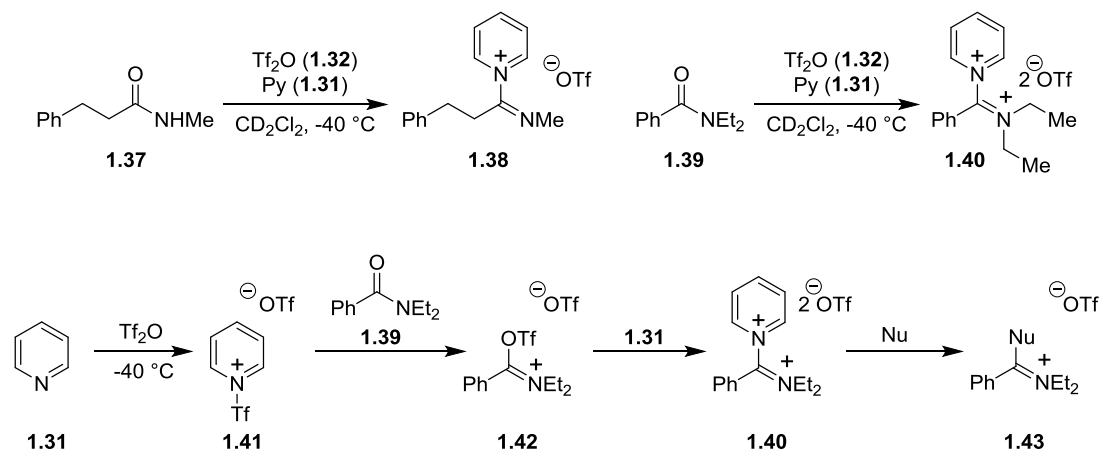
Scheme 1.6 Preparation of bridged orthoester **1.34**.



Charette *et al.* originally proposed the intermediacy of iminium triflate **1.35** when the pyridine/anhydride mixture was added to the amide, before attack of the triol **1.33** to form **1.36**, which would go on to form the bridged orthoester **1.34** after intramolecular attack on the iminium group by the alcohol groups. Molecule **1.35**, however, was not isolated nor detected by spectroscopy.

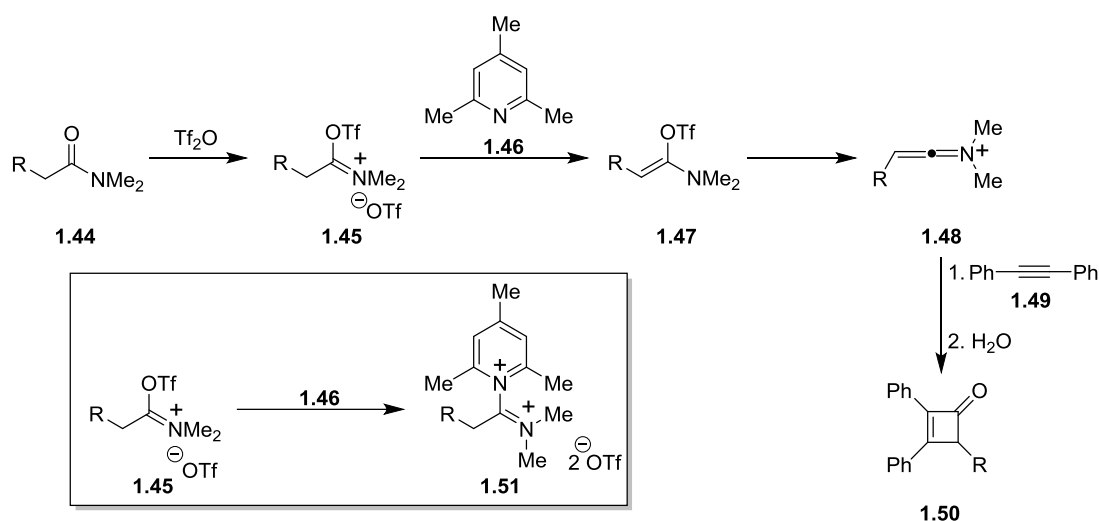
Charette and Grenon¹⁴ later published an NMR study that investigated the reaction of amides with pyridine **1.31** and triflic anhydride **1.32** (Scheme 1.7). ^1H NMR and ^{19}F NMR were used to identify the pyridine salt **1.38** in a mixture of products formed by the reaction of secondary amide **1.37** with pyridine **1.31** and triflic anhydride **1.32**. When carrying out the reaction of tertiary amide **1.39** under the same conditions, instead of forming an iminium triflate compound (analogous to **1.35**), dicationic product **1.40** was proposed based on ^1H NMR and ^{19}F NMR spectroscopy.

Scheme 1.7 NMR study of reaction of secondary and tertiary amides with Tf₂O/pyridine (1.32/1.31).

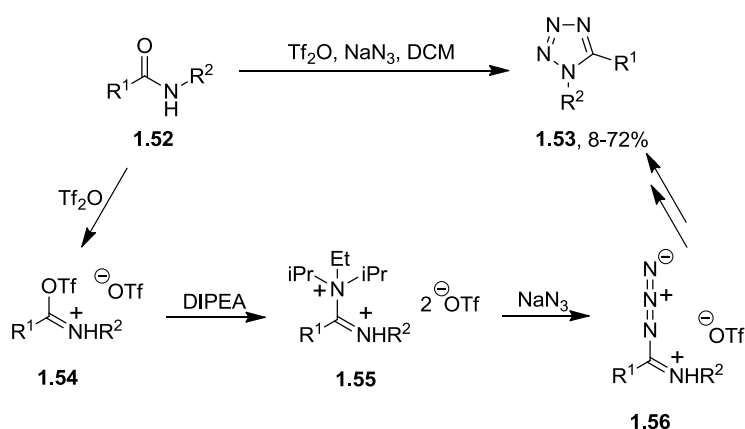


Dication **1.40** was believed to be part of a mixture that also contained *N*-(trifluoromethanesulfonyl)pyridinium salt **1.41** – the triflating agent in the reaction with the amides (Scheme 1.7)¹⁴ As the mixture was proposed to contain **1.41** and the ¹⁹F NMR of the mixture only showed two fluorine peaks (-75.9 ppm for the *N*-(trifluoromethylsulfonyl)pyridinium and -79.8 ppm for the triflate anion), dication **1.40** was proposed to be present in the mixture and account for some of the signal at -79.8 ppm. ¹H NMR also showed a considerable downfield shift in peaks compared to **1.31** and **1.39**, which would be expected with the increase in positive charge. Although these results could not provide conclusive evidence of dicationic intermediates, their proposed existence was used to explain the reactivity observed in such systems.

The spectroscopic studies of Charette *et al.*¹⁴ suggest that dicationic intermediates (and the iminium triflates that these intermediates are most likely produced from) may be present in the previous preparations of bridged orthoesters (Scheme 1.6) as well as in other reactions which Charette *et al.* have carried out on tertiary amides with triflic anhydride and pyridines.¹⁵⁻²⁴ It also shows that the pyridines utilised in these reactions are not only important because of their abilities in acid scavenging, as previously believed,¹⁷ but often as catalysts to produce highly electrophilic intermediates. The use of 4-DMAP and related pyridines in nucleophilic catalysis is well established²⁵ and some parallels in the role of pyridines to produce superelectrophiles may be seen.

Scheme 1.8 Reaction of amide **1.44** with Tf₂O **1.32** and base **1.46**.

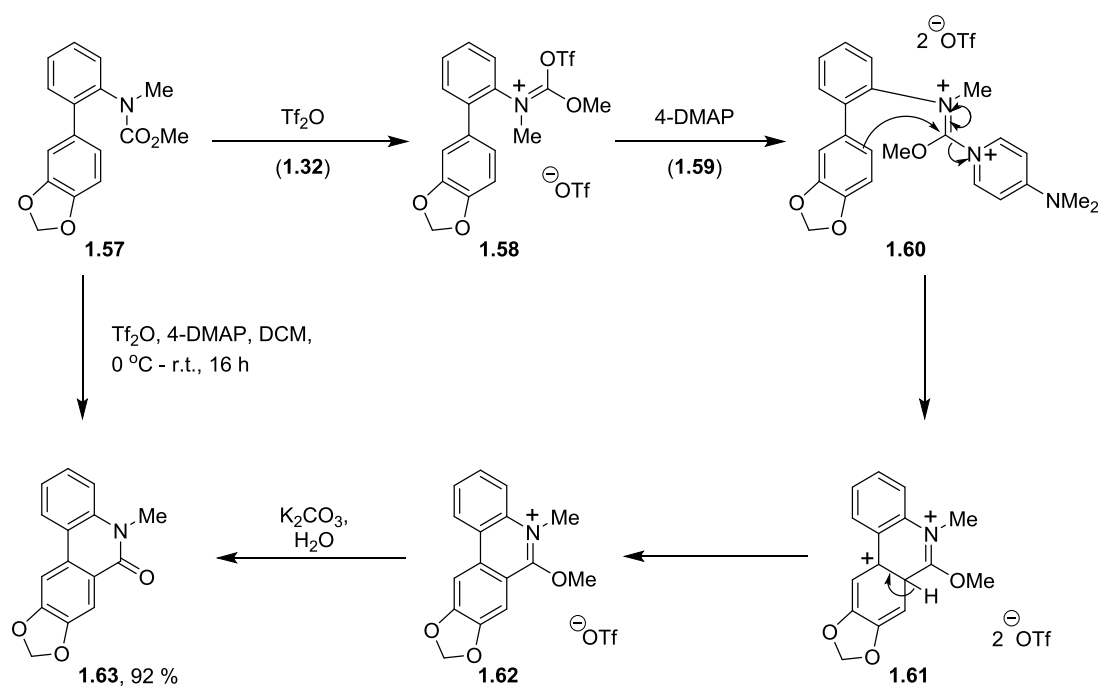
The reaction of amides with triflic anhydride **1.32** and a pyridine base was actually reported earlier by Ghosez *et al.* in 1981.²⁶ This work was carried out using 2,4,6-trimethylpyridine **1.46** and was used to prepare cyclobutene species **1.50** from amides **1.44** (Scheme 1.8). The reaction was proposed to proceed *via* keteniminium salt **1.48**. However, this was never isolated from the reaction mixture nor seen spectroscopically during the reaction. Corr²⁷ suggested that it would be equally reasonable to expect dicationic species **1.51** to exist in this reaction, although steric hindrance from the base **1.46** could make this less favourable. Ghosez *et al.* also used this kind of reaction in further syntheses.²⁸

Scheme 1.9 Synthesis of tetrazoles **1.53** from amides **1.52**.

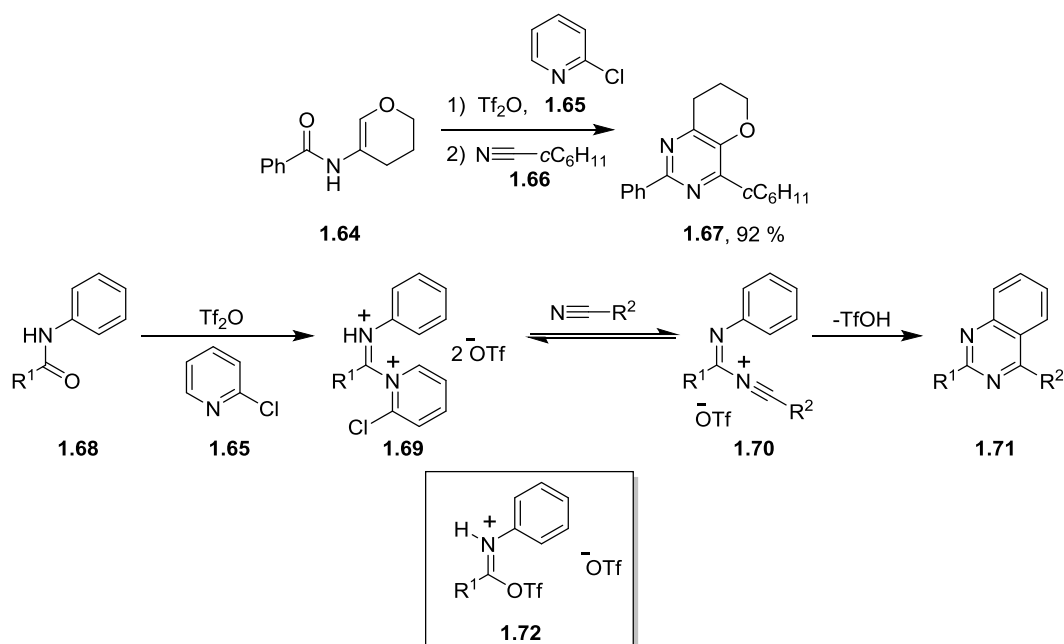
In 1993, Thomas also reported the use of triflic anhydride and an amine base to activate amides.²⁹ His work involved the conversion of secondary amides **1.52** to

tetrazoles **1.53** using NaN_3 (Scheme 1.9). It was found that the addition of DIPEA to the reaction mixture increased the rate of tetrazole formation and, in fact, some tetrazoles could not be formed without the addition of DIPEA. No mechanism was given by the author at the time, but it could be possible that the reaction proceeds *via* iminium salt **1.54**, which can be attacked by NaN_3 to form **1.53** or, in the presence of DIPEA, form dication **1.55** before NaN_3 attack – this mechanism has been suggested by Corr.²⁷

Scheme 1.10 Possible mechanism for formation of **1.63**.



Before the work of Charette *et al.*,^{13,14} Banwell *et al.*³⁰ carried out the activation of tertiary amides with triflic anhydride **1.32** and 4-DMAP **1.59** in Bischler-Napieralski reactions, with substrates that required exceptionally forceful conditions using the traditional POCl_3 method (and which actually failed to work at all in some cases). Again, no mechanism was provided, but Corr²⁷ has since suggested that substrate **1.57** could form dicationic intermediate **1.60** on the way to forming iminium ether **1.62** which, when treated under basic conditions, forms *N*-methylcrinasiadine **1.63** (Scheme 1.10).

Scheme 1.11 Synthesis of pyrimidine derivatives **1.67** and **1.71**.

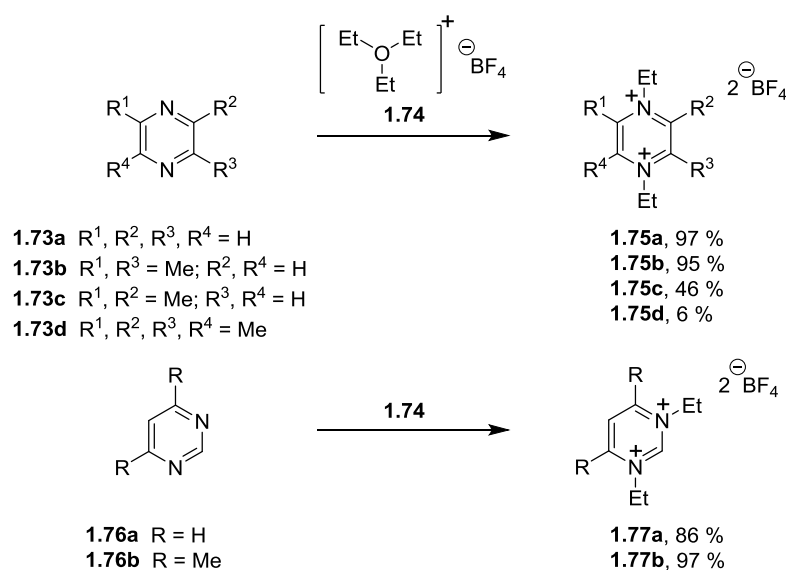
More recently, Movassaghi's group have published reactions involving the activation of amides with triflic anhydride and bases including 2-chloropyridine **1.65**³¹⁻³⁵ and 2-fluoropyridine.^{34,36} In their preparation of substituted pyrimidines such as **1.67** (Scheme 1.11)³² the authors treated secondary amides such as **1.64** with a mixture of 2-chloropyridine **1.65** and triflic anhydride **1.32**, before treating with nitrile species such as **1.66**. In the same paper and with other substrates, an equilibrium between dicationic salt **1.69** and iminium triflate **1.72** was suggested, although neither type of intermediate was isolated. The deprotonation of dication **1.69** by 2-chloropyridine **1.65** would also seem a possible route to the final product.

As can be seen in this section, the superelectrophiles proposed to be present in organic synthesis consist of nitrogen-based heterocyclic dications. Evidence for these dications, however, is very limited with NMR studies carried out using mixtures rather than pure disalts.¹⁴ The next section will discuss examples of organic disalts and polycations that have appeared in the literature and have been isolated; these disalts can be considered organic superelectrophiles.

1.5 Nitrogen-Based Heterocyclic Disalts

Although Section 1.4 has discussed the *possible* presence of nitrogen-based disalts in organic synthesis, nitrogen-based heterocyclic disalts and polycations have been isolated as synthetic products for over 40 years, without the need of superacids.

Scheme 1.12 Various dicationic pyrazines **1.75** and pyrimidines **1.77**.

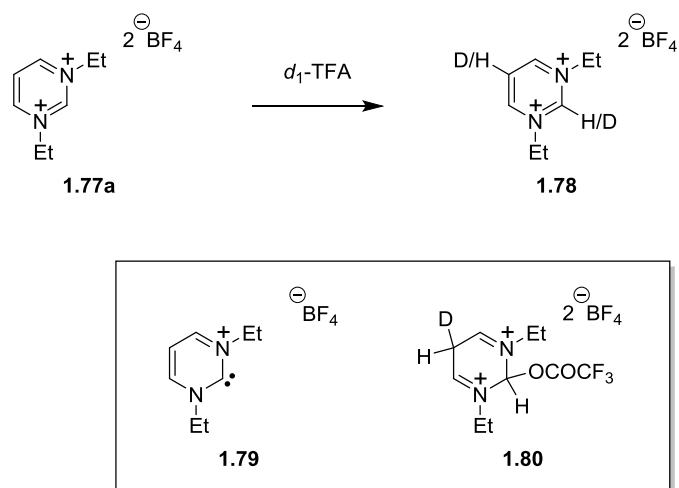


In 1965, Curphey³⁷ published the first syntheses of diquaternary salts of pyrazines **1.73** and pyrimidines **1.76**; disalts **1.75** and **1.77** (Scheme 1.12). These disalts were synthesised by reacting the starting pyrazine **1.73** and pyrimidine **1.76** with Meerwein's salt **1.74** (Scheme 1.12) and gave compounds with very unusual reactivity. In alcoholic solvents or in the presence of TFA with zinc granules, the pyrazines disalts were observed to generate radical cations, following electron transfer from the zinc.

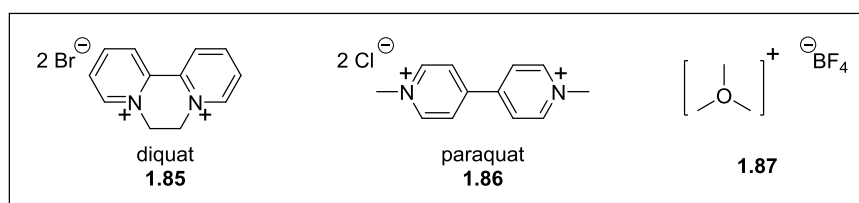
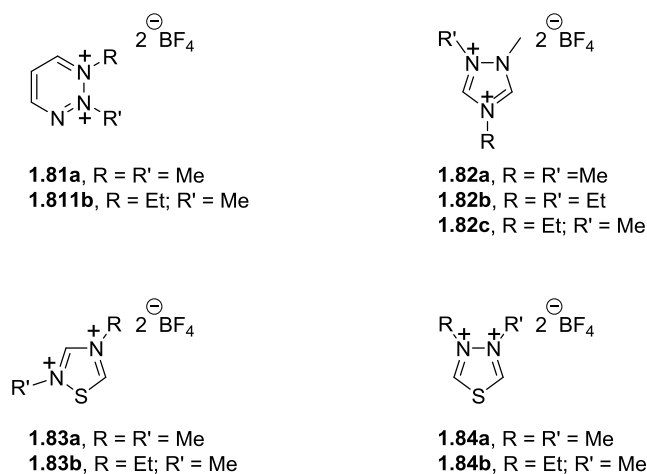
While no deuterium exchange was observed with the pyrazine-derived disalts **1.75** in the presence of deuterated TFA, disalt **1.77a** underwent deuterium exchange in both the 2- and the 5-positions (Scheme 1.13), with half-lives of 12 and 29 h, respectively. Deuteration in the 2-position was thought to occur through carbene (cation ylide) **1.79**, driven by the decrease in charge repulsion. Rearomatisation can then drive the uptake of deuterium in this position. As for the 5-position, formation of a carbene is very unlikely to be the route to deuteration. Curphey suggested trifluoroacetate

adduct **1.80** as being the route to this substitution; loss of trifluoroacetic acid from this structure would generate the 5-labelled product.

Scheme 1.13 Deuterium exchange of disalt **1.77a**.



Scheme 1.14 Various disalts synthesized by Curphey and Prasad.

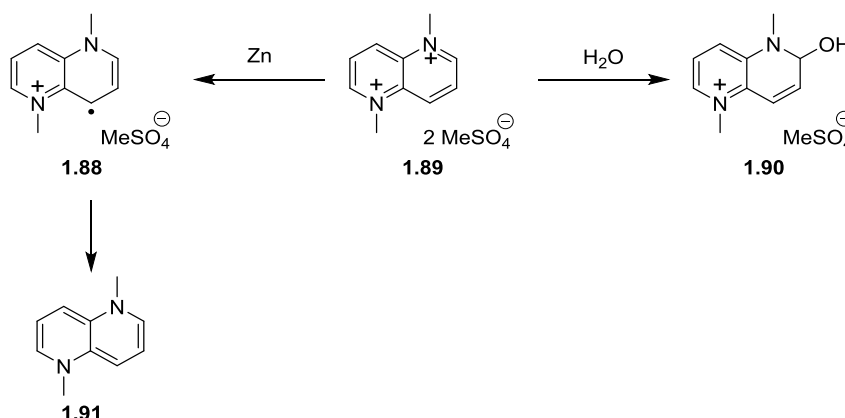


Curphey and Prasad³⁸ later published further dicationic structures (Scheme 1.14) which had been obtained using either Meerwein's salt **1.74** or the stronger quaternizing reagent trimethyloxonium tetrafluoroborate **1.87**. The rationale behind synthesising these molecules was driven by both their expected high reactivity and

the known herbicidal reactivity of other diquaternised salts such as the diquat **1.85**³⁹ and paraquat **1.86**.^{40,41}

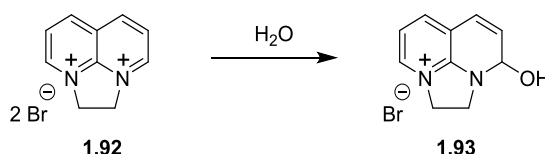
Summers *et al.*^{42,43} reported on the intriguing chemistry of disalts related to **1.85** and **1.86**. The 1,5-naphthyridine-derived disalt **1.89** was found to reduce in the presence of zinc to form radical cation **1.88** and to react with water to form 2-hydroxynaphthyridine species **1.90** (Scheme 1.15).⁴³ In electrochemical experiments, two symmetrical half-wave potentials [$E_{1/2}$ (note that the paper incorrectly uses the symbol for standard potential, E_0)] of +0.02 and -0.33 V were found, independent of pH and concentration and were attributed to the formation of radical cation **1.88** and further reduced species **1.91**.

Scheme 1.15 The chemistry of disalt **1.89**.



The attempted reduction of disalt **1.92** (Scheme 1.16) with zinc dust to form a radical cation was found to be unsuccessful; however, formation of 2-hydroxynaphthyridine species **1.93** was observed.⁴² Both disalts **1.89** and **1.92** were found to be inactive as herbicides, due to their instability at physiological pH.

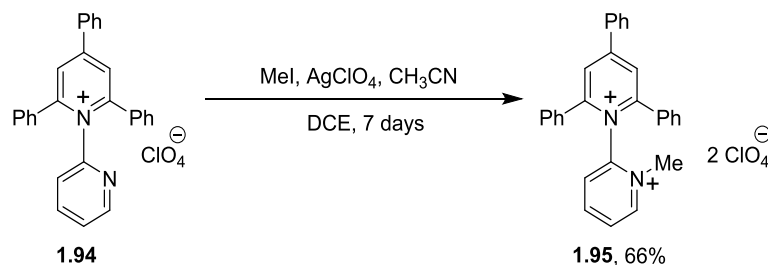
Scheme 1.16 Reaction of disalt **1.92** with water.



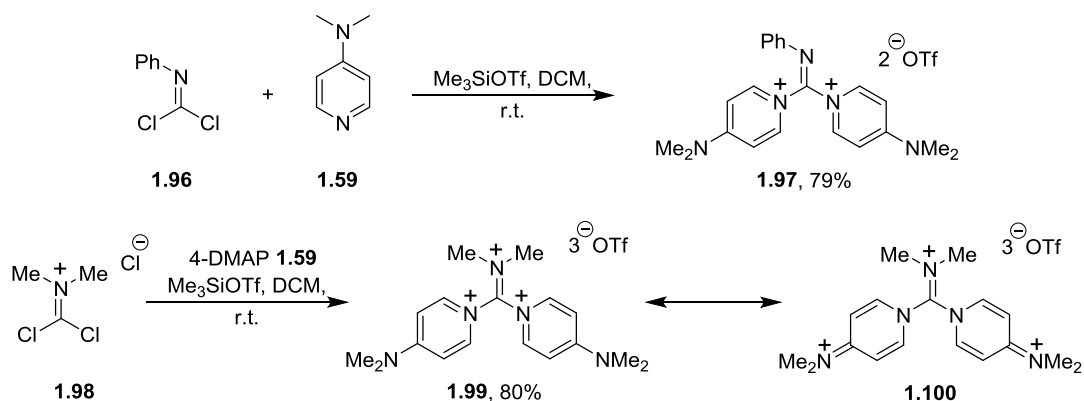
In 1979, Katritzky *et al.* reported the synthesis of disalt **1.95** from pyridinium salt **1.94** (Scheme 1.17).⁴⁴ To test the reactivity of disalt **1.95**, the authors attempted a

reaction with sodium borohydride, but this gave a complicated mixture of products from which nothing was isolated.

Scheme 1.17 Synthesis of disalt **1.95**.

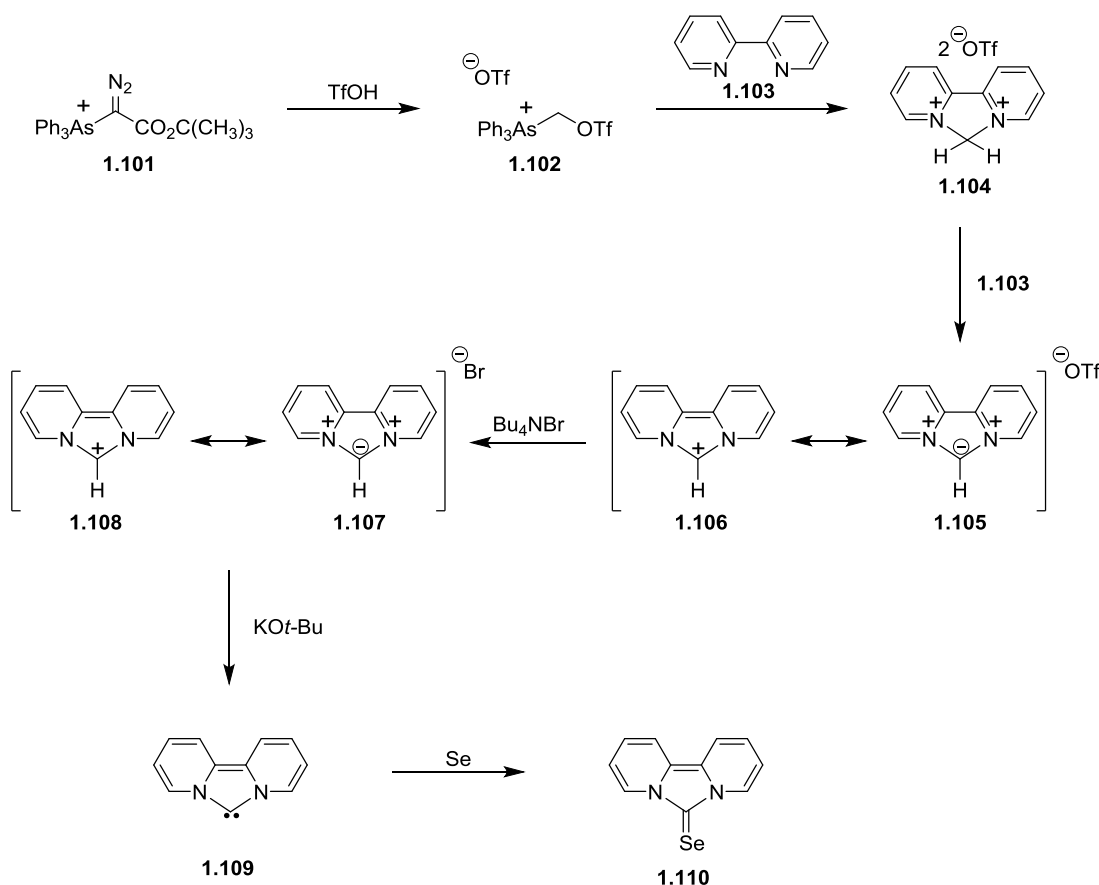


Scheme 1.18 Synthesis of disalt **1.97** and trication **1.99**.

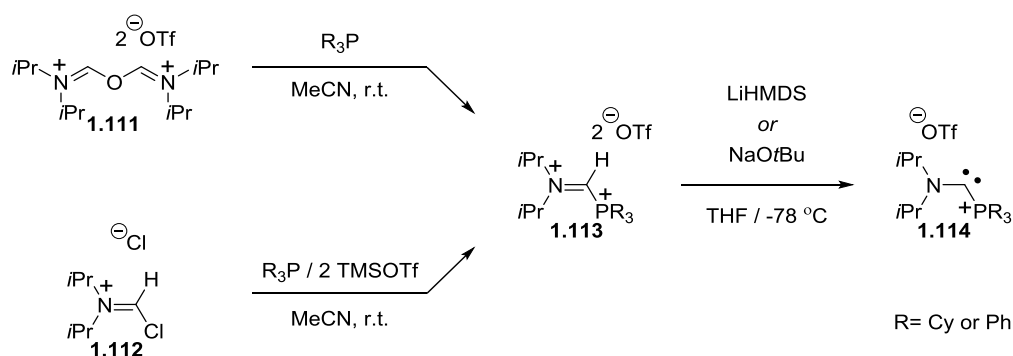


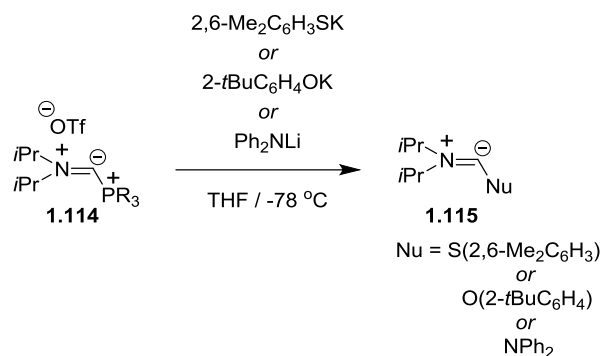
Weiss and Roth developed a successful method of isolating di- and tricationic species derived from 4-DMAP **1.59** (Scheme 1.18).⁴⁵ Disalt **1.97** was formed from the reaction of phenylisocyanidedichloride **1.96** and 4-DMAP **1.59**, with trimethylsilyl triflate (TMSOTf) added to the reaction mixture to produce the ditriflate salt (the triflate counter-ion is not as nucleophilic as the chloride anion). Similarly, trication **1.99** was formed from iminium chloride **1.98**, 4-DMAP **1.59** and TMSOTf to afford a very unique species in polycationic chemistry. The reactivity of this compound was never published; however, its reactivity may be moderated by resonance stabilization.

Weiss *et al.*⁴⁶ later reported the synthesis of dicationic species **1.104**; although they did not isolate this dication, they isolated (confirmed by X-ray crystal structure) the deprotonated species **1.108**, after counter-ion exchange from **1.105/1.106** (Scheme 1.19). Cation **1.108** was then further deprotonated to give carbene species **1.109**, which was reacted with selenium to give compound **1.110**.

Scheme 1.19 The chemistry of disalt **1.104**.

Bertrand *et al.*⁴⁷ also carried out the synthesis of dicationic species **1.113** (this time containing a phosphorus as well as a nitrogen) which they then deprotonated to form carbenes **1.114** (Scheme 1.20). The disalts and resulting carbenes were all characterised by X-ray crystallography as well as by NMR, giving firm evidence of their formation. The carbenes were then reacted with various bases to displace the phosphorus, giving new carbene species **1.115** (Scheme 1.21) without net positive charges.

Scheme 1.20 Disalts **1.113** used for forming carbenes **1.114**.

Scheme 1.21 Reaction of carbenes **1.114** with several bases.

As this chapter illustrates, there are several dicationic and polycationic species that have been isolated and characterised over the years from various academic groups. In recent years, the Murphy Group have been interested in the synthesis and reactivity of amidine dications; this work will be reviewed in Chapter 3, Previous Work.

Before discussing previous work carried out by the Murphy Group, the next Chapter will go on to discuss the chemistry of [Fe]-hydrogenase. The chapter will mention the possible existence of superelectrophiles within the enzymatic reaction. The use of previously synthesized disalts as models for the reactivity observed in [Fe]-hydrogenase will be detailed in Chapter 3, Previous Work, while the use of the novel disalts reported in this thesis will be described in Chapters 4, 5 and 6.

Chapter 2: [Fe]-Hydrogenase

As mentioned in the previous chapter, the chemistry of [Fe]-hydrogenase may involve superelectrophilic species. A major part of the work reported in this thesis involves model reactions designed to mimic the reactivity of the amidine substrate present in the reaction of [Fe]-hydrogenase. To fully place this work in context, this chapter will review the literature surrounding [Fe]-hydrogenase.

2.1 Introduction

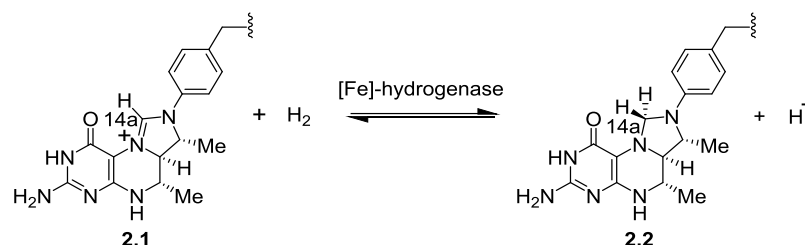
Hydrogenases are a group of enzymes that catalyze the reversible cleavage of molecular hydrogen and are present within aerobic and anaerobic bacteria, archaea and eucarya.⁴⁸ The consumption of dihydrogen by hydrogenase-containing microorganisms exists in syntrophy with the production of hydrogen from H₂-forming microorganisms such as *Escherichia coli*.⁴⁸ There are three distinct classes of hydrogenase with two of these classes containing iron-sulfur clusters; [NiFe]-hydrogenase contains nickel-iron-sulfur clusters while [FeFe]-hydrogenase contains iron-sulfur clusters only.

The third class of hydrogenase (which can be obtained from methanogenic archaea grown in nickel-limiting and red light conditions)⁴⁹ was originally believed to be metal-free, resulting in it being known as the iron-sulfur-cluster free hydrogenase or H₂-forming methylenetetrahydromethanopterin dehydrogenase (Hmd). However, in more recent years, the third hydrogenase has been found to contain an essential iron cofactor resulting in the new name of [Fe]-hydrogenase. Although the iron cofactor within [Fe]-hydrogenase contains a cysteine ligand, the chemistry at this iron centre is quite distinct from that of the hydrogenases that contain iron-sulfur clusters.

[Fe]-hydrogenase catalyses the reversible reduction of *N*⁵,*N*¹⁰-methenyltetrahydromethanopterin (CH≡H₄MPT⁺) **2.1** with H₂ to *N*⁵,*N*¹⁰-methylenetetrahydromethanopterin (CH₂=H₄MPT) **2.2** and a proton (Figure 2.1).⁴⁹ This represents the

reduction from the formic acid oxidation level to the formaldehyde oxidation level at the carbon centre C_{14a}, which is originally derived from carbon dioxide within methanogenic archaea.⁴⁸

Figure 2.1 Reaction catalyzed by [Fe]-hydrogenase.



As this chapter will discuss studies carried out on [Fe]-hydrogenase before and after the discovery of the Fe-cofactor, the abbreviation Hmd will be used for the enzyme for results before this major discovery.

2.2 Initial Studies of Hmd

Thauer and his colleagues first described the hydrogenase activity of Hmd in 1990⁴⁹ after isolating the pure enzyme from *methanobacterium thermoautotrophicum*. In this study, Hmd was found to dehydrogenate CH₂=H₄MPT **2.2** to form CH≡H₄MPT⁺ **2.1** and H₂ as well as carry out the reduction of **2.1** to **2.2** with the liberation of a proton (Figure 2.1). Additionally, it was found that the purified enzyme did not catalyze the reduction of coenzyme F₄₂₀, NAD⁺, NADP⁺ or methylviologen (it has been found that Hmd has a role in providing CH₂=H₄MPT **2.2** for F₄₂₀-dependent methylenetetrahydromethanopterin dehydrogenase, which is needed for the reduction of coenzyme F₄₂₀ in *M. thermoautotrophicum* grown under nickel-limiting conditions).⁵¹ While nickel was found in insufficient quantities to be active (less than 0.1 equivalents to 1 equivalent of enzyme), 1 equivalent of iron to 1 equivalent of enzyme was identified; however, this finding was initially thought to be influenced by background contamination of iron rather than indicative of the presence of an active iron species within the enzyme.⁴⁹ This conclusion was perhaps influenced by the differences seen with [NiFe]-hydrogenase and [FeFe]-hydrogenase, which are redox active with viologens and which have absorbances above 340 nm in UV-visible spectroscopy, which were not present with Hmd.⁵⁰ It was also established

that the enzyme activity of [Fe]-hydrogenase was rapidly lost under aerobic conditions and in the presence of dithiothreitol or mercaptoethanol.⁴⁹

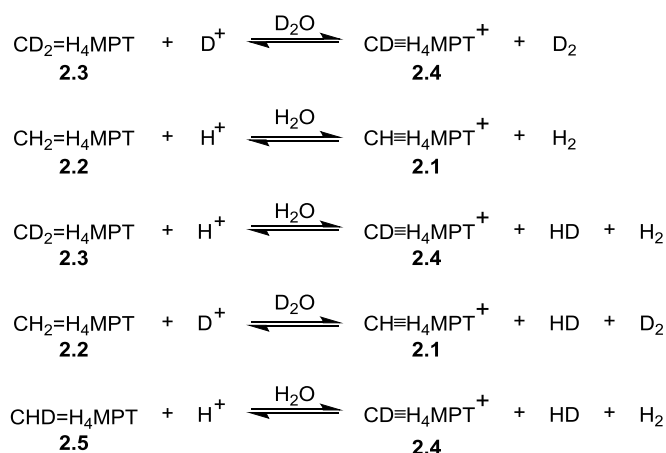
The effect of using standard inhibitors of transition metal-containing enzymes in the presence of Hmd was examined in both redox directions. CO (5 % and 50 % in the gas phase), acetylene (5 % and 50 % in the gas phase), NO (1mM and 10 mM) and azide (1mM and 10mM) were found to have no effect on enzyme activity.⁵⁰ Cyanide was found have no effect at 0.1 mM but caused a 50 % decrease in activity at 10 mM concentration.⁵⁰

To assess the conditions required for hydrogen cleavage in Hmd, tritium exchange experiments were carried out.⁵⁰ When pure Hmd was used alone, no exchange between $^3\text{H}_2$ and $^1\text{H}_2\text{O}$ was observed at a range of temperatures and pH values. However, when $\text{CH}\equiv\text{H}_4\text{MPT}^+$ **2.1** or $\text{CH}_2=\text{H}_4\text{MPT}$ **2.2** were added to the enzyme, exchange between $^3\text{H}_2$ and $^1\text{H}_2\text{O}$ was observed, with incorporation of tritium into the aqueous solution as well as into substrates $\text{CH}\equiv\text{H}_4\text{MPT}^+$ **2.1** and $\text{CH}_2=\text{H}_4\text{MPT}$ **2.2**. After the reaction of $\text{CH}\equiv\text{H}_4\text{MPT}^+$ **2.1** with $^3\text{H}_2$ was carried out, HPLC separation of the products and radioactivity experiments showed that for every equivalent of $\text{CH}_2=\text{H}_4\text{MPT}$ **2.2** formed, 0.5 equivalents of $^3\text{H}_2$ was incorporated. The substrate dependence for tritium exchange in Hmd is in contrast to [FeFe]-hydrogenase and [NiFe]-hydrogenase, which both actively carry out $^3\text{H}_2/{}^1\text{H}_2\text{O}$ exchange with no substrate present.⁵⁰

Several NMR studies have been carried out in order to gain information on the reversible process between $\text{CH}\equiv\text{H}_4\text{MPT}^+$ **2.1** and H_2 . In 1993, Schwörer *et al.*⁵² examined the mechanism of dihydrogen formation in Hmd using deuterium labeling. Firstly, the kinetic isotope effect was determined by comparing D_2 formation from $\text{CD}_2=\text{H}_4\text{MPT}$ **2.3** in D_2O and H_2 formation from $\text{CH}_2=\text{H}_4\text{MPT}$ **2.2** in H_2O (Figure 2.2) giving a value of ~ 4.7 for $k_{\text{H}}/k_{\text{D}}$.⁵² The oxidation of $\text{CD}_2=\text{H}_4\text{MPT}$ **2.3** in H_2O was then examined, showing HD and H_2 formation, while HD and D_2 were produced from $\text{CH}_2=\text{H}_4\text{MPT}$ **2.2** in D_2O (Figure 2.2). The production of H_2 from $\text{CD}_2=\text{H}_4\text{MPT}$ **2.3** in H_2O was accounted for by the reduction of $\text{CD}\equiv\text{H}_4\text{MPT}^+$ **2.4** by the HD produced, giving some amounts of $\text{CHD}=\text{H}_4\text{MPT}^+$ **2.5** which could dehydrogenate to

give H₂ (Figure 2.2). Indeed, CHD=H₄MPT⁺ **2.5** was synthesized and subjected to the reaction conditions to form H₂ at a rate four times faster than HD. No exchange was observed between substrates **2.2** or **2.3** with gas or solvent without the presence of Hmd when blank experiments were run. When subjected to the same oxidative conditions with Hmd, but in the absence of CH₂=H₄MPT **2.2** or CD₂=H₄MPT **2.3**, no exchange between H₂ and D₂O or D₂ and H₂O was observed, complementing the previous tritium labeling studies.⁵⁰ These results indicated that only one of the hydrogens from CH₂=H₄MPT **2.2** was used in the formation of dihydrogen, with the other hydrogen being obtained from solution. In forming dihydrogen, one atom is obtained from a proton in solution and the other from what is formally a hydride from CH₂=H₄MPT **2.2**;⁵⁰ the pH dependence on the equilibrium of products confirms this, with alkaline pH (pH>7) favoring the reduction of CH≡H₄MPT⁺ **2.1** with H₂ and acidic pH (pH<7) favoring the dehydrogenation of CH₂=H₄MPT **2.2**.

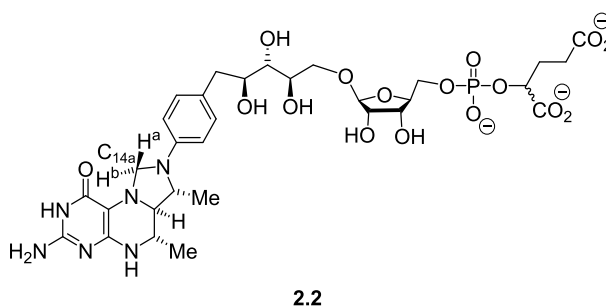
Figure 2.2 Various reactions investigated by Schwörer *et al.*⁵²



Schleucher *et al.*⁵³ used two-dimensional NMR spectroscopy to determine the stereoselectivity of hydride transfer to CH≡H₄MPT⁺ **2.1** catalyzed by Hmd. Due to the complexity observed in the ¹H NMR of CH₂=H₄MPT **2.2**, they simplified their analysis by using various deuterium-incorporating reactions and looking at the HSQC spectra of the products – this technique was further aided by ¹³C labeling of the C_{14a} of the CH≡H₄MPT⁺ **2.1** or CD≡H₄MPT⁺ **2.4** starting materials. Due to the chirality of CH₂=H₄MPT **2.2**, the methylene protons (H^a and H^b shown in Figure 2.3)

are chemically and magnetically distinct, with H^a observed at 4.9 ppm and H^b at 3.3 ppm in ¹H NMR. Table 2.1 gives a summary of the six reactions studied.

Figure 2.3 Structure of CH₂=H₄MPT **2.2** showing magnetically distinct methylene protons H^a and H^b.



The results of these reactions showed that hydride is delivered stereoselectively to the *Re*-face of the amidine centre in CH≡H₄MPT⁺ **2.1** to take up the *pro-R* position (H^b) of C_{14a} in CH₂=H₄MPT **2.2**.⁵³

Table 2.1 Deuterium Labeled Experiments to Determine Stereoselectivity of Hmd Process.

Entry Number	Reaction	Major Product
1	¹³ CH≡H ₄ MPT ⁺ + D ₂ , D ₂ O	¹³ CH ^a D ^b =H ₄ MPT
2	¹³ CD≡H ₄ MPT ⁺ + H ₂ , H ₂ O	¹³ CD ^a H ^b =H ₄ MPT
3	¹³ CD≡H ₄ MPT ⁺ + H ₂ , D ₂ O	¹³ CD ^a H ^b =H ₄ MPT
4	¹³ CH≡H ₄ MPT ⁺ + D ₂ , H ₂ O	¹³ CH ^a D ^b =H ₄ MPT
5	¹³ CD≡H ₄ MPT ⁺ + D ₂ , H ₂ O	¹³ CD ₂ =H ₄ MPT
6	¹³ CH≡H ₄ MPT ⁺ + H ₂ , D ₂ O	¹³ CH ₂ =H ₄ MPT

The CH≡H₄MPT⁺ **2.1** dependent exchange of H and D is also nicely complemented by the observed conversion of *para*-H₂ to *ortho*-H₂ catalyzed by Hmd, which is also dependent on the presence of CH≡H₄MPT⁺ **2.1**.^{54,55}

2.3 Discovery That Hmd Contains a Bound Cofactor

In 2000, Buurman *et al.*⁵⁶ obtained Hmd enzyme from the heterologous expression of Hmd genes from *methanopyrus kandleri* and *methanococcus jannaschi* in *escherichia coli*. The purified enzymes were found to be completely inactive. In the same study, Hmd purified from *methanothermobacter marburgensis* was denatured in urea and the resulting mixture separated through a 10 kDa molecular mass cut-off membrane. The resulting ultrafiltrate was considered to contain components of too low molecular weight to contain active enzyme. When the ultrafiltrate was added to the heterologously expressed Hmd, enzymatic activity (both hydrogenation and dehydrogenation) was observed, suggesting the presence of a bound cofactor in the wild enzyme.⁵⁶ HPLC of the ultrafiltrate followed by mass spectral analysis showed the active fractions to have apparent masses well below 10 kDa. UV-visible spectroscopy showed absorbance at 280 nm which accounted for the decrease in extinction coefficient at this value in the denatured enzyme.⁵⁶ In the same work, analysis by total reflection X-ray fluorescence spectrometry showed that the ultrafiltrate contained no nickel and only traces of iron and zinc (a result that was later explained by the conditions required for handling the enzyme).⁵⁷ This further added to the opinion that Hmd did not contain a redox-active transition metal.⁵⁶

2.4 Discovery that Hmd is a Metalloenzyme

In 2004, Thauer and co-workers⁵⁷ made one of the most significant discoveries in the investigations into Hmd; they discovered that the 1 equivalent of iron found in the sample of Hmd in 1990⁴⁹ was due to an essential iron present within the enzyme.

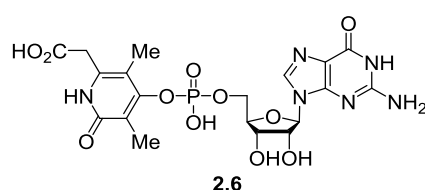
Previously, Thauer *et al.*^{49,50} had shown that the Hmd that they had prepared had no absorption above 340 nm in UV/visible spectroscopy. However, the discovery that UV-A (320-400 nm) and blue-light (400-500 nm) inactivate and bleach Hmd and its cofactor, suggested that the enzyme absorbed UV/visible light above 340 nm.⁵⁷ By preparing and isolating Hmd enzyme in the dark at 4 °C (and storing anaerobically at -80 °C), it was possible to obtain a UV/visible spectrum of Hmd with absorbance maximum at approximately 360 nm.⁵⁷ This absorbance was seen to decrease the

longer that the sample of enzyme was exposed to UV-A/blue light. Along with showing a decrease in activity when exposed to UV-A/blue light, iron was seen to be released by the enzyme, giving a strong indication that the iron was necessary for enzymatic activity.⁵⁷

Thauer and co-workers⁵⁷ also established that the enzyme is in fact inhibited by carbon monoxide, contrary to the previous investigations.⁵⁰ At a concentration of 100 % v/v carbon monoxide atmosphere, they observed 50 % inhibition of enzyme, a process that was found to be reversible when the same sample was used in the absence of carbon monoxide. Carbon monoxide inhibition provided a way of protecting the Hmd from light inactivation – a protection that was presumed to be due to the formation of an Fe-CO complex.⁵⁷ Again, cyanide inhibition was investigated and showed that the inhibition was most likely due to Hmd-cyanide complex formation rather than reaction with $\text{CH}\equiv\text{H}_4\text{MPT}^+$ **2.1** or $\text{CD}\equiv\text{H}_4\text{MPT}^+$ **2.2**, as originally proposed.⁵⁰ It should be noted here, that although all three of the hydrogenase families are inhibited by CO, only Hmd is known to be inhibited by cyanide.^{57,58}

Shima *et al.*⁵⁹ proposed a structure **2.6** (Figure 2.4) for the light-inactivation product from Hmd, most likely derived from the active cofactor. This species, which was separated by HPLC, had a mass of 542 Da, (consistent with structure **2.6**), was proposed to contain a phosphodiester due to its reactivity with phosphodiesterase and the presence of a signal at -6.18 ppm in ³¹P NMR. By isolating the light-inactivated product from Hmd produced in cells grown in ¹⁵NH₄Cl rather than ¹⁴NH₄Cl, a mass of 548 Da rather than 542 Da was observed, which suggested that the product contained 6 nitrogens. Using various other mass spectroscopy, UV/vis and NMR techniques, it was concluded that structure **2.6** was the most likely structure for the light-inactivated compound.

Figure 2.4 Light-inactivation product isolated from Hmd.



Lyon *et al.*⁵⁸ reported further analysis of the products of light-inactivation in Hmd. They found that for every mole of Hmd enzyme containing cofactor, approximately 2.4 ± 0.2 mol of CO was released; for Hmd apoenzyme, no CO was released. Analysis of the amount of Fe released also showed a value of 2.4 ± 0.2 mol of CO to Fe, suggesting the number of CO molecules in Hmd to be 2 or 3. The authors reported that the infrared analysis of the cofactor before light inactivation showed the presence of two bands of equal intensity at 2011 and 1944 cm^{-1} . It was suggested that this would account for the presence of an $\text{Fe}(\text{CO})_2$ unit with an approximate 90° angle between the CO groups.⁵⁸ Considering the inhibition of Hmd by CO, the authors suggested that an $\text{Fe}(\text{CO})_3$ compound was formed, indicating that an iron in the Fe^0 , Fe^{I} or Fe^{II} was present in Hmd.⁵⁸ The observed inhibition of Hmd by cyanide and the rarity of $\text{Fe}^0\text{-CN}$ compounds were used to propose that the iron present in the enzyme was not present in the Fe^0 oxidation state. Finally, EPR measurements were used to rule out an Fe^{I} centre, and so it was proposed that the Hmd cofactor was an $\text{Fe}^{\text{II}}(\text{CO})_2$ complex which would be likely to be low-spin and 6-coordinate.⁵⁸

It was also shown that when the Fe-containing cofactor was isolated, the CO bands in the infrared spectrum shifted from 2011 and 1944 cm^{-1} to 2031 and 1972 cm^{-1} . This was indicative of decreased electron density at the iron centre, suggesting either an exchange of ligands or a change in the total number of ligands attached, i.e. going from 6-coordinate to 5-coordinate.⁵⁸

Addition of $\text{CH}\equiv\text{H}_4\text{MPT}^+$ **2.1** or $\text{CD}\equiv\text{H}_4\text{MPT}^+$ **2.2** in argon to the Hmd enzyme showed slight changes in the infrared spectra recorded, indicative of binding close to or at the iron site in the enzyme.⁵⁸ The addition of H_2 increased the effects of $\text{CH}\equiv\text{H}_4\text{MPT}^+$ **2.1** on the IR spectrum of Hmd, possibly suggesting interaction between hydrogen and the iron centre in the presence of **2.1**; however, no evidence of Fe-H or Fe-D stretches in the IR spectrum were found. This change in IR spectrum in argon or hydrogen was not observed without the presence of substrate **2.1** or **2.2**.⁵⁸

To gain further information about the electronic structure of iron in Hmd (and due to this centre being EPR silent),⁵⁸ Shima *et al.*⁶⁰ studied the Mössbauer spectrum of ⁵⁷Fe-labelled Hmd prepared in dark conditions. The results showed a low isomer shift for Hmd and indicated the presence of a low-spin iron in a low oxidation state. Introduction of CO or cyanide inhibitors to the enzyme showed changes in isomer shift of the iron centre; changes that the authors proposed indicated direct binding of the inhibitors to the iron. On the other hand, introduction of H₂ and/or CH≡H₄MPT⁺ 2.1 to the enzyme had no significant effect in the spectrum, which shows that when Hmd interacts with its substrates or products, the electronic state of the iron site is not affected sufficiently to be detected by the Mössbauer-active nucleus.⁶⁰

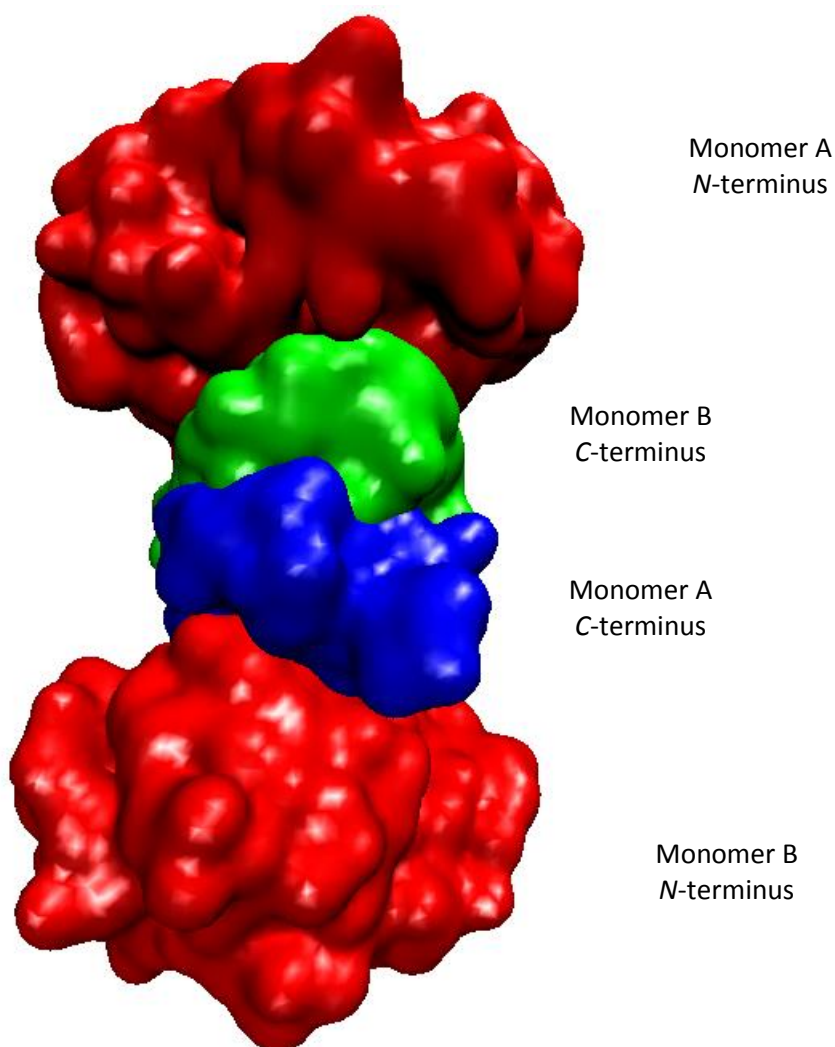
Measurement of the magnetic properties suggested that the iron centre in Hmd was diamagnetic with spin $S = 0$, consistent with Fe^{II} or Fe⁰.⁶⁰ Based on the infrared⁵⁸ and Mössbauer⁶⁰ studies together, it was proposed that an Fe^{II} was the more likely electronic state of the iron centre. Additional information gained from the Mössbauer spectra of Hmd was a value of 1.14 ± 0.25 atoms of iron per protein monomer.

From these studies,⁵⁷⁻⁶⁰ it was concluded that the iron centre in Hmd was an iron (II) guanylyl pyridone cofactor (FeGP cofactor) and that due to the effects of CO or cyanide on this centre (causing changes in the properties of the iron and inhibiting enzymatic activity) it must be key to enzymatic activity. To gain further information on this cofactor, it was necessary to obtain information on the 3D structure of Hmd, which will henceforth be referred to as [Fe]-hydrogenase.

2.5 Crystal Structure Studies of [Fe]-Hydrogenase

In 2006,⁶¹ the first X-ray crystal structures of [Fe]-hydrogenase were reported, with the apoenzyme (without FeGP cofactor) isolated and crystallized from both *M. jannaschii* (Figure 2.5) and *M. kandleri*, giving structures of 1.75 Å and 2.4 Å resolution, respectively.

Figure 2.5 Crystal structure of homodimer of [Fe]-hydrogenase apoenzyme isolated from *M. jannaschii*; 2B0J in RCSB Protein Data Bank; quaternary structure file available from EMBL-EBI's Protein Data Bank in Europe (PDBe). Red sections show *N*-termini (residues 1-250 of both monomers) and blue and green sections show *C*-termini (residues 251-358 of both monomers). Image generated using VMD.⁶²



[Fe]-hydrogenase was found to be a homodimer with dimensions of approximately 90 Å x 50 Å x 40 Å, and with the architecture of one central and two identical peripheral globular units. The peripheral units corresponded to the *N*-terminal domains (red in Figure 2.5) of each subunit and were composed of Rossman fold-like α/β structure. The central globular unit corresponded to the *C*-terminal segments (green and blue in Figure 2.5) of both subunits, each containing four α -helices that form an intertwined intersubunit helix bundle.⁶¹ Analysis of the relative

arrangements of the globular units showed that [Fe]-hydrogenase from *M. jannaschii* was present in a closed conformational state, while [Fe]-hydrogenase from *M. kandleri* was in an open conformational state.

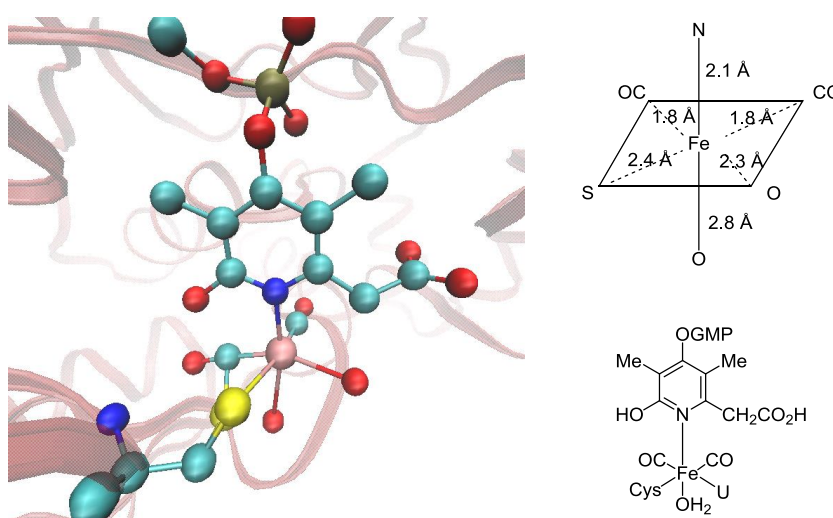
In the same study, activity measurements of mutant [Fe]-hydrogenase were used to suggest that the iron binding site was located in the pocket containing Cys176.⁶¹ Of the three conserved cysteine residues in [Fe]-hydrogenase, only Cys176 was essential for activity. The authors mention the presence of an iron-ligating sulfur ligand in an unpublished X-ray absorption spectrum of the [Fe]-hydrogenase holoenzyme. Due to the importance of Cys176, they suggest that this is the source of the ligation to iron.⁶¹ Additionally, in the case of *M. jannaschii* [Fe]-hydrogenase, a 13 Å long U-shaped electron density was observed in a relatively close region to the Cys176 residue (~ 6 Å away). This U-shape was assigned to polyethylene glycol present in the crystallization solution and this site was proposed (aided by some modeling) to be where $\text{CH}\equiv\text{H}_4\text{MPT}^+$ **2.1** binds.⁶¹

In 2008, Shima *et al.*⁶² obtained a 1.75 Å resolution X-ray crystal structure for the Hmd holoenzyme (the enzyme including the iron cofactor), isolated from *M. jannaschii*. By reconstituting [Fe]-hydrogenase apoenzyme with labile FeGP cofactor under completely anaerobic and red-light conditions, the authors were able to form crystals of the enzyme. It was reported that the guanosine monophosphate moiety functions to anchor the FeGP cofactor to the enzyme.⁶² In the active site, they found the iron centre to be surrounded by a distorted square pyramidal or octahedral ligation shell dependent on enzymatic state (Figure 2.6). They found that the nitrogen of the guanylylpyridinol was ligated to the iron, while the pyridinol and carboxylate substituents were not, although they noted that the latter substituent was partly disordered and so had to be interpreted with caution. The other species in the coordination sphere of iron were assigned as two CO molecules at 90° angles to each other, the sulfur from Cys176, a solvent water molecule and an unknown ligand (shown as an oxygen in the X-ray structure) that could not be determined due to the high levels of disorder.

When the crystals were soaked in 3mM cyanide, this led to an enhancement (1.6 times) in the electron density at the site of the unknown ligand, suggesting that it could be the site of reversible cyanide inhibition; the Fe-CN distance was determined

as 1.8 Å. Additionally, despite the water molecule being assigned *trans* to the nitrogen of the guanylylpyridinol, the oxygen atom was considered to be too far to be a ligand (2.8 Å for the holoenzyme and 2.7 Å for the cyanide-inhibited holoenzyme).⁶² This site was suggested to be the site of H₂ binding in the reaction with CH≡H₄MPT⁺ **2.1** and also the possible site for the binding of extrinsic CO.

Figure 2.6 Crystal structure of FeGP cofactor binding site in [Fe]-hydrogenase holoenzyme isolated from *M. jannaschii*; 3DAG in RCSB Protein Data Bank. Fe centre, 2 CO ligands, guanylyl pyridone ligand and Cys176 shown as CPK structures. Image generated using VMD.⁶³

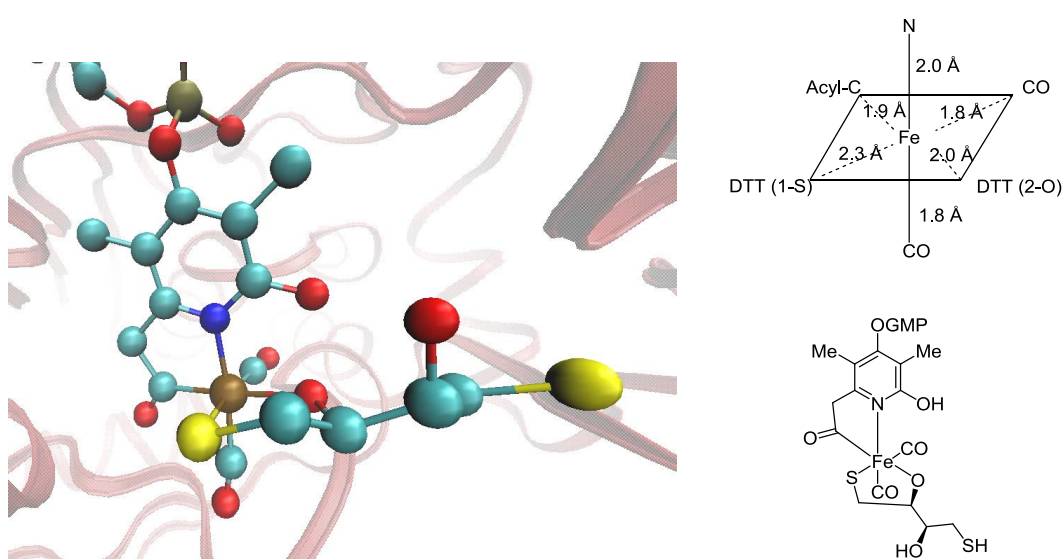


The authors proposed a mechanism for hydride delivery to CH≡H₄MPT⁺ **2.1** based on these results.⁶² They suggested that by binding H₂ in a side-on fashion to the iron centre, the *pK_a* of H₂ could be lowered (the *pK_a* of molecular H₂ being 35)⁶⁴ and that hydride could be delivered to “the strong hydride acceptor” CH≡H₄MPT⁺ **2.1** while the resulting proton could be accepted by a nearby proton acceptor. The candidate proton acceptors were suggested as the Cys176 ligand, the pyridinol ligand (nitrogen, oxygen or carboxylate) or one of two histidines (His14 and His201) all within 6.5 Å of the iron. It was noted that His14 → Ala mutation had a significant effect on the activity of the enzyme (while His201 → Ala mutation had little effect) and so it could be possible for this to be the proton acceptor.⁶²

In 2009,⁶⁵ the crystal structure of the FeGP cofactor within [Fe]-hydrogenase was revised, based on the crystal structure of a mutated [Fe]-hydrogenase enzyme. The holoenzyme of Cys176 → Ala mutated [Fe]-hydrogenase from *M. jannaschii* was

crystallized in the presence of dithiothreitol (DTT) to give a structure at 1.95 Å resolution (Figure 2.7). The structure showed an iron centre octahedrally coordinated by one DTT-sulfur, one DTT-oxygen, two CO groups at 90 ° to each other (also shown by IR analysis), the 2-pyridinol's nitrogen and the 2-pyridinol's 6-acylmethyl group in an acyl-iron ligation.⁶⁵ The DTT-sulfur had displaced the binding site of the Cys176 from the wild-type enzyme, while the DTT-oxygen had displaced the unknown ligand (Figures 2.6 and 2.7). The acyl-iron ligation showed that the previous “carboxylate” group assignment for the FeGP cofactor was also incorrect. This resulted in the pyridinyl ligand chelating the iron centre, rotating it 180 ° from the previously determined structure. Additionally, one of the CO ligands was determined to actually occupy the site previously suggested to be occupied by water (the water that was too distant to actually be a ligand). The acyl group oxygen was shown to link to the polypeptide chain by the formation of a hydrogen bond with the amide group of Ala176 (which would be Cys176 in the wild-type enzyme), while the 2-oxygen of the pyridinol ligand was shown to be in close proximity to the imidazole group of His14 and the 2- and 3-oxygens of DTT.

Figure 2.7 Crystal structure of FeGP cofactor binding site of DTT-treated, C176A-mutated [Fe]-hydrogenase holoenzyme isolated from *M. jannaschii*; 3F46 in RCSB Protein Data Bank. Fe centre, 2 CO ligands, guanylyl pyridone ligand and DTT shown as CPK structures. Image generated using VMD.⁶³

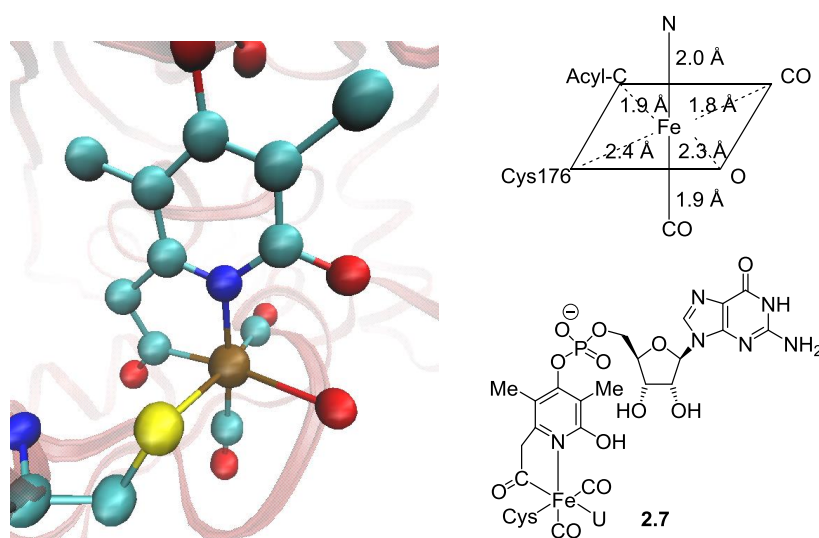


Based on the unprecedented finding of a biological acyl-iron complex, the structure of the wild-type [Fe]-hydrogenase holoenzyme was reinterpreted. This newly

interpreted mode of ligation was found to agree better with the electron density observed not only in the holoenzyme, but also the CO- and cyanide-inhibited structures. Hydrogen bonding was observed between the acyl group and the amide group of Cys176; however, no hydrogen bonding was observed between the pyridinol's hydroxyl group and His14, although an interaction with a solvent molecule anchored to Thr13 was observed.

To explain the reason for the original misinterpretation of the wild-type enzyme, the authors describe a “lack of imagination” concerning the possibility of an acyl ligand on the iron which had resulted in a carboxylate facing towards the non-polar interior of protein. Based on these results, structure **2.7** (Figure 2.8) was proposed for the FeGP cofactor of [Fe]-hydrogenase, where U is an unknown ligand. Further mass spectrometry and infrared spectroscopy evidence for structure **2.7** has recently been reported by Shima *et al.*⁶⁶ who extracted the FeGP cofactor from [Fe]-hydrogenase using acetic acid. The mass of an adduct with an acetate ligand binding in the Cys176 and “unknown” binding site was observed – previous attempts using 2-mercaptoethanol had proved unsuccessful for mass spectral analysis.⁶⁶

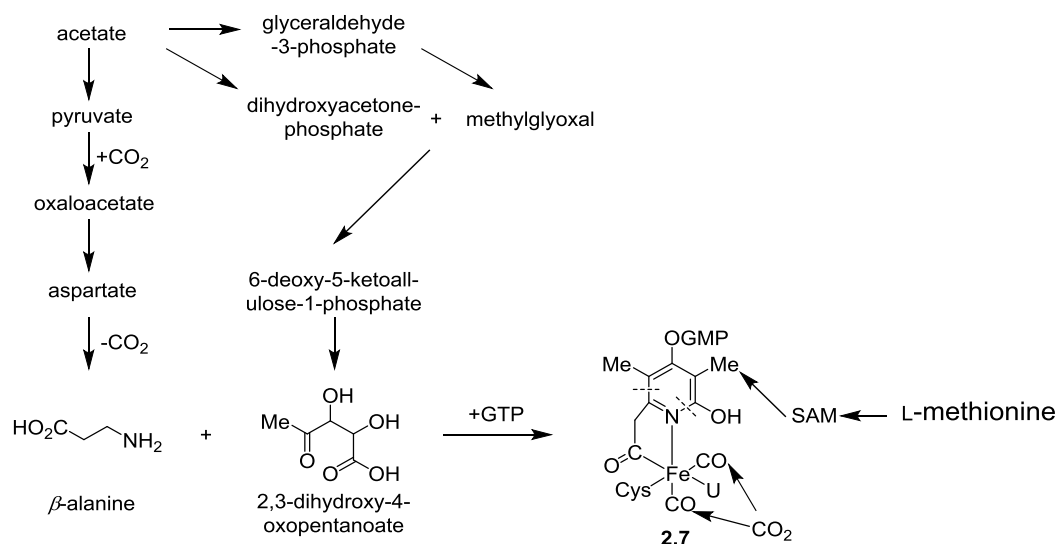
Figure 2.8 Reinterpreted crystal structure of the FeGP cofactor binding site of [Fe]-hydrogenase holoenzyme isolated from *M. jannaschii*; 3F47 in RCSB Protein Data Bank. Fe centre, 2 CO ligands, guanylyl pyridone ligand and DTT shown as CPK structures. Image generated using VMD.⁶³



Recently, Shima and co-workers⁶⁷ carried out ¹³C and ²H labeling studies into the biosynthesis of FeGP cofactor **2.7** by feeding labeled acetate, pyruvate and

methionine to growing methanogenic archaea. The proposed pathway is shown (Scheme 2.1) and it was concluded that the ligands of the cofactor were derived from an acetate, two pyruvates, three carbon dioxides and a methyl group from methionine.⁶⁷

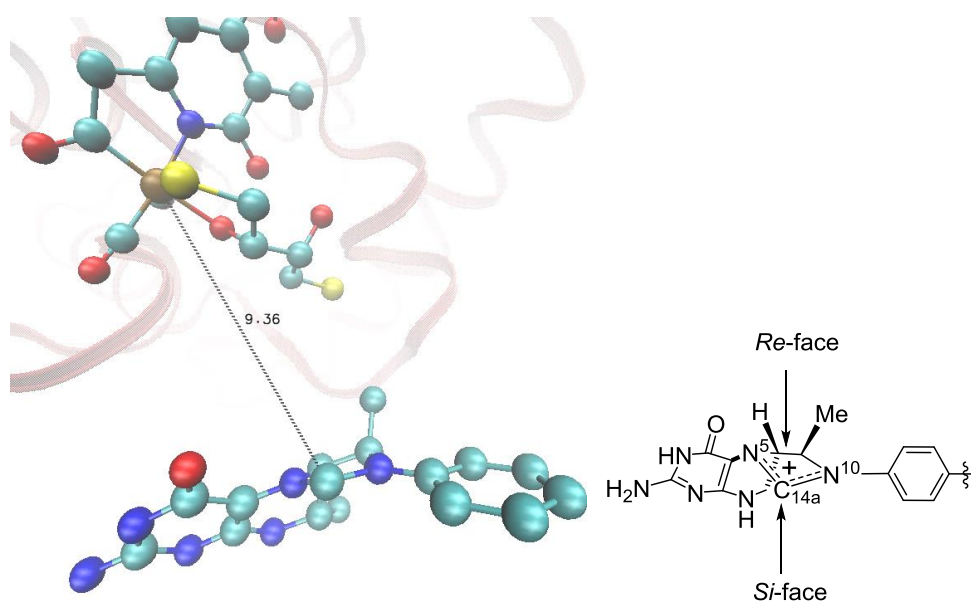
Scheme 2.1 Proposed biosynthesis of the FeGP cofactor.



In 2009, Hiromoto *et al.*⁶⁸ published the structure of a DTT-treated, C176A-mutated [Fe]-hydrogenase with CH₂=H₄MPT **2.2** bound to it (Figure 2.9). The activity of this enzyme was inhibited by the formation of a DTT-chelate complex and removal of Cys176, preventing the reaction of CH₂=H₄MPT **2.2** which had previously hampered cocrystallization.⁶⁸ In the structure, the pterin, imidazolidine and phenyl rings (the “head”) of CH₂=H₄MPT **2.2** were present in the active cleft, with the remaining end (the “tail”) of the molecule exposed to bulk solvent and appearing disordered. The authors interpreted the conformations at N5 and N10 to be planar in the observed X-ray crystal structure of CH₂=H₄MPT **2.2** (Figure 2.9), whereas (citing the NMR and computational investigations of Griesinger and co-workers)^{69,70} they noted that in solution these two nitrogen atoms appeared to be sp³. The authors reasoned that this difference in substrate conformation was because the crystal structure of the substrate was not present in an activated conformation.⁶⁸ The enzyme crystal structure was deemed to be in an “open” form, leading to the conclusion that important interactions were missing on the *Re*-side of the methylene of substrate **2.2**, allowing it to lay planar. Upon “closure” of the enzyme, the authors suggested rotation of the phenyl

ring on substrate **2.2** (again citing the work of Griesinger)⁷⁰ would facilitate the formation of a non-planar conformation.

Figure 2.9 Crystal structure of $\text{CH}_2=\text{H}_4\text{MPT}^+$ **2.2** binding in DTT-treated, C176A-mutated [Fe]-hydrogenase holoenzyme isolated from *M. jannaschii*; 3H65 in RCSB Protein Data Bank. Fe centre, 2 CO ligands, guanylyl pyridone ligand, DTT and $\text{CH}_2=\text{H}_4\text{MPT}^+$ **2.2** shown as CPK structures. Image generated using VMD.⁶³



A distance of 9.3 Å lay between the iron centre and C_{14a} of $\text{CH}_2=\text{H}_4\text{MPT}^+$ **2.2** (Figure 2.9), which would be too long for transferring a hydride ion originating from an iron dihydrogen complex to $\text{CH}\equiv\text{H}_4\text{MPT}^+$ **2.1** in the hydrogenation reaction.⁶⁸ As such, the authors modeled closed forms of the apoenzyme with the FeGP cofactor **2.7** and substrate **2.1**, to explain the possible mechanism involved in the reaction of [Fe]-hydrogenase. The models suggested that, in the closed form, the enzyme would be expected to position the iron centre and C_{14a} of $\text{CH}\equiv\text{H}_4\text{MPT}^+$ **2.1** within 3 Å of each other. $\text{CH}\equiv\text{H}_4\text{MPT}^+$ **2.1** would be facing the “unknown” (U) site of the FeGP cofactor **2.7** and, so, it was reasoned that this site is where H_2 binds. These mechanistic investigations will be described further in the next section, along with other related investigations.

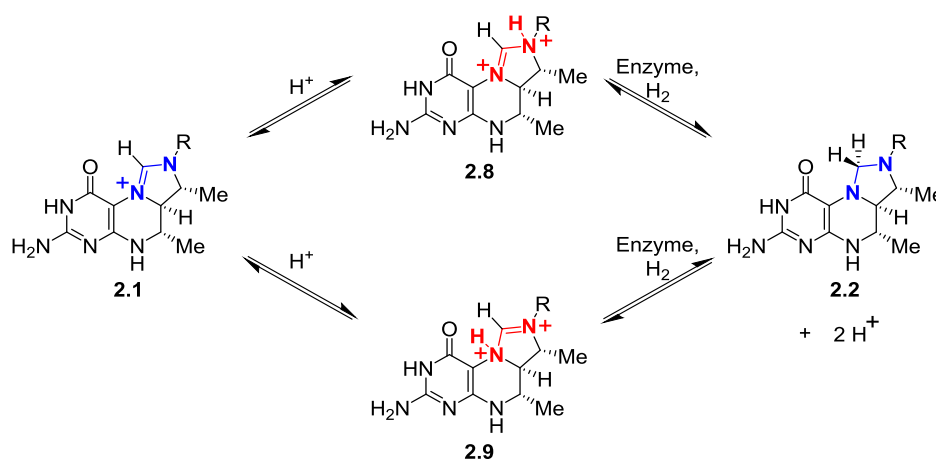
2.6 Mechanistic Models of [Fe]-Hydrogenase

2.6.1 Studies Before the Most Recent Assignment of the FeGP

Cofactor

In 1995, before it had been established that [Fe]-hydrogenase had a cofactor (and an essential iron) Berkessel and Thauer⁷¹ presented an intriguing mechanistic proposal for the reaction of this enzyme based on superelectrophilic activation.¹ Their proposal was that protonation of $\text{CH}\equiv\text{H}_4\text{MPT}^+$ **2.1** in the enzyme active site would lead to formation of a suitably activated substrate, which would result in possible dications **2.8** or **2.9** (Scheme 2.2). As Olah had shown that organic dications could abstract hydride from alkanes, the authors proposed that protonated $\text{CH}\equiv\text{H}_4\text{MPT}^+$ **2.1** (dication **2.8** or **2.9**) might be active enough to abstract hydride from H_2 . A functional group that would be powerful enough to protonate $\text{CH}\equiv\text{H}_4\text{MPT}^+$ **2.1** was not identified in [Fe]-hydrogenase, and a carboxyl group (Berkessel and Thauer suggested aspartate or glutamate as the proton source in the enzyme)⁷¹ is not present in the vicinity the imidazoline ring of substrate **2.1**.⁶⁸

Scheme 2.2 Proposed superelectrophilic activation in [Fe]-hydrogenase.

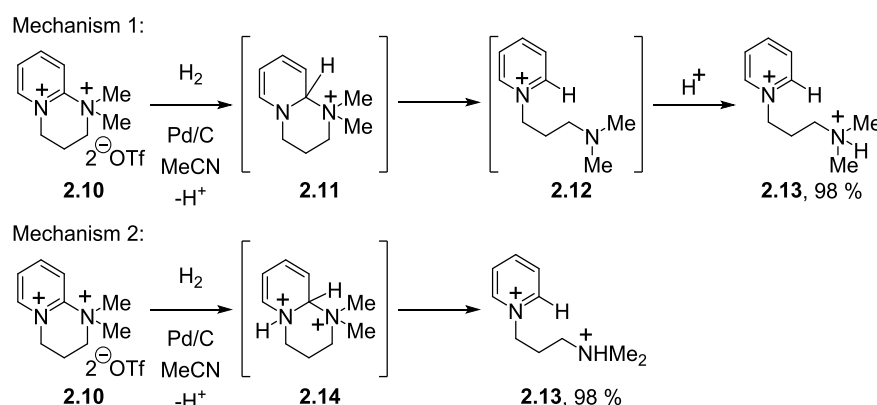


Although the FeGP cofactor **2.7** is known to be essential to enzymatic activity, its role has not yet been established. As will be discussed later, the pyridinol-ligand of the FeGP cofactor **2.7** presents an acidic functional group that is in the vicinity of the imidazoline ring of substrate **2.1**.⁶⁸ Additionally, as described in the first chapter, superelectrophilic activation can also occur through hydrogen-bonding, rather than full protonation;¹ therefore, a group that does not fully protonate $\text{CH}\equiv\text{H}_4\text{MPT}^+$ **2.1**, but rather hydrogen-bonds to N5 or N10 of the substrate may provide suitable

activation. The pyridinol-ligand, if not a sufficiently powerful acid to protonate $\text{CH}\equiv\text{H}_4\text{MPT}^+$ **2.1**, could possibly hydrogen-bond to N5 or N10.

Inspired by the possibility of superelectrophilic activation in [Fe]-hydrogenase, the Murphy Group synthesised amidine disalt **2.10** to carry out hydrogenation reactions with it (Scheme 2.3).^{72,73} Chapter 3, Previous Work, will discuss this area of research in more detail.

Scheme 2.3 Pd-catalyzed reaction of amidine dication **2.10** with H_2 .

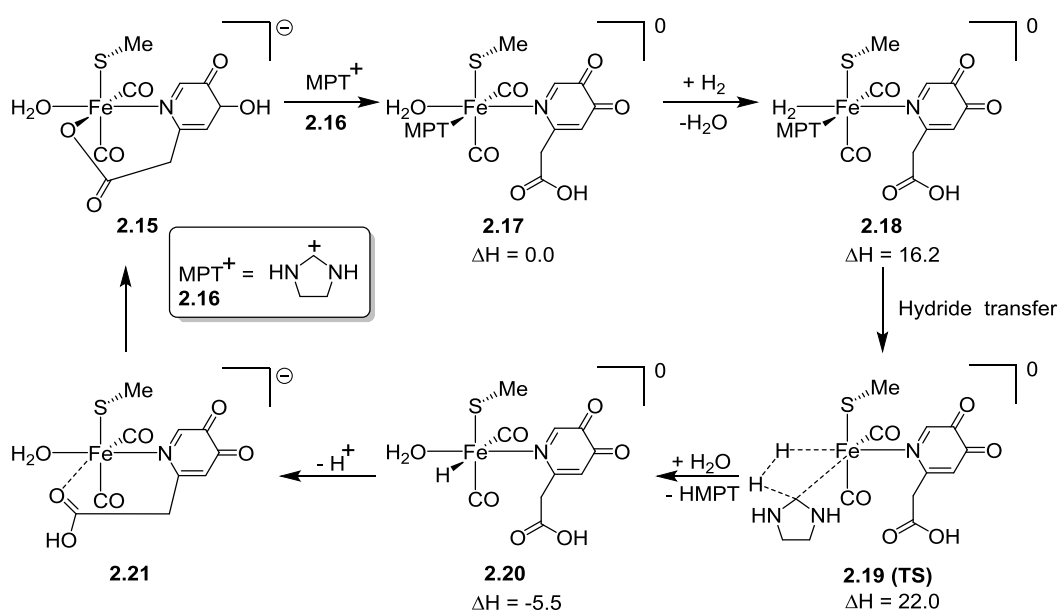


After the original (incorrect) crystal structure of the FeGP cofactor was suggested, Yang and Hall⁷⁴ carried out computational studies (DFT calculations) on the possible role of the iron in activating hydrogen. They reported a trigger mechanism in which they used complex **2.15** (Scheme 2.4) as a model of the FeGP cofactor, where the 2-hydroxyl group has been moved to the 3-position in the pyridinol ligand (this could dramatically change the role of the hydroxyl group) which has also been used in the pyridone form rather than the pyridinol form. In fact, the negative charge on complex **2.15** would be better represented with the α -anionic carbonyl drawn as an enolate and so would present a 3-pyridinolate. Additionally, they modelled the ligation of carboxylate to the iron centre in the unknown ligand position – a bond that has never been identified in [Fe]-hydrogenase. The calculated IR values of the CO ligands in model **2.15** were 1957 and 2014 cm^{-1} , which were comparable to those in [Fe]-hydrogenase (1944 and 2011).⁵⁸

In the absence of MPT^+ **2.16** (the simplified model of $\text{CH}\equiv\text{H}_4\text{MPT}^+$ **2.1**), the splitting of H_2 was calculated to have a barrier of 39.7 kcal mol^{-1} . In the presence of MPT^+ **2.16**, the activation barrier was decreased to 22.0 kcal mol^{-1} (transition state **2.19**

forming complex **2.20**). Before reaching this transition state, the first step involved the coordination of MPT^+ **2.16** to complex **2.15** to form complex **2.17**. The mechanism of this step is not fully presented and does not appear to be entirely sensible – the description is of deprotonation to form the “quinone-like structure”. The deprotonation appears to occur from the carboxylate ligand if it is to form the “quinone-like structure” within complex **2.17**. This process is proposed to leave the negative charge on the iron centre and then MPT^+ **2.16** “binds” to the iron centre; this suggests nucleophilic attack of an iron anion on an amidine cation is taking place. As such, the first step in this process (complex **2.15** to complex **2.17**) appears to be a rather unlikely process.

Scheme 2.4 “Trigger” mechanism of complex **2.15** with MPT^+ **2.16** and H_2 ; units for energy are in kcal mol^{-1} .



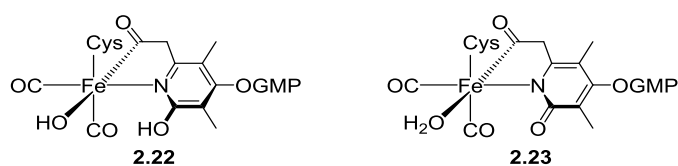
The next stage in the mechanism proposed by Yang and Hall then involves $\text{H}_2/\text{H}_2\text{O}$ exchange in complex **2.17** to form structure **2.18** and was calculated to occur with an enthalpy change of $16.2 \text{ kcal mol}^{-1}$. This mechanism was used to explain the dependence of H_2/H^+ exchange on the presence of MPT^+ **2.16**. The importance of the pyridone ligand was proposed to be due to its ability to “trigger” a change in its donor ability on the binding of MPT^+ **2.16**; this aided the polarization and cleavage of hydrogen and delivery of hydride to MPT^+ **2.16**.

The process of forming complex **2.21** from complex **2.20** is also unclear. The Fe-H bond of complex **2.20** appears to be deprotonated to form an iron anion which then coordinates to the oxygen of a carboxylic acid which is not a likely process. The final proton transfer from unlikely complex **2.21** is again a more complicated process than that presented by the authors and would merit further explanation.

2.6.2 Studies After the Most Recent Assignment of the FeGP Cofactor

As the original interpretation of the crystal structure⁶² differed from the most recently proposed structure of the [Fe]-hydrogenase holoenzyme,⁶⁵ Nakatani *et al.*⁷⁵ carried out DFT calculations on various model complexes of the active site to propose the mode of binding from the pyridinol ligand. Based on comparison of calculated vibrational frequencies to those recorded experimentally for the [Fe]-hydrogenase enzyme, the authors suggested that the FeGP cofactor **2.7** was present as either complex **2.22** or complex **2.23** (Figure 2.10). Complex **2.22** consists of an acylpyridinol ligand, while complex **2.23** consists of an acylpyridone ligand. Additionally, complex **2.22** has a hydroxide in the “unknown” coordination site, while complex **2.23** has a water molecule.

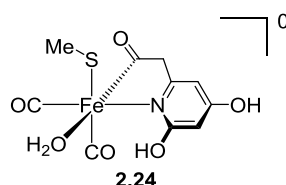
Figure 2.10 The proposed structure of the FeGP cofactor present in [Fe]-hydrogenase suggested by Nakatani *et al.*⁷⁵



After the reinterpretation of the FeGP cofactor **2.7** by Hiromoto *et al.*,⁶⁵ Yang and Hall⁷⁶ provided a new computational model for the possible mechanism in [Fe]-hydrogenase. The authors based their DFT calculations on structure **2.24** (Figure 2.11) representing the FeGP cofactor **2.7**, where Cys176 is replaced by a methylthiolate ligand and the pyridinol ligand is simplified with the removal of 3,5-methyls and the guanosine monophosphate group. The site of the unknown ligand is occupied by a water molecule, which it was proposed can be exchanged with a

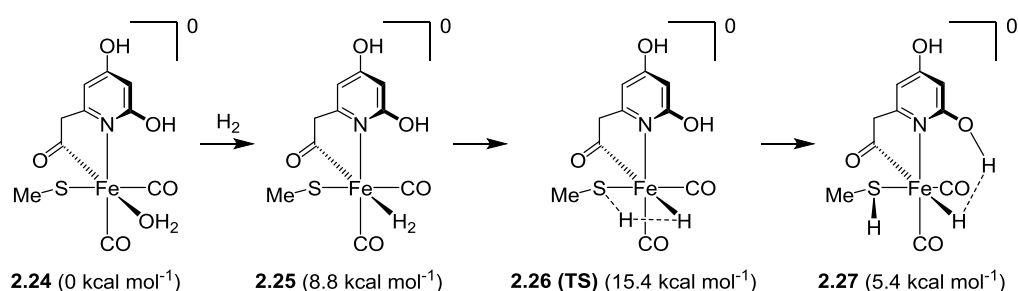
molecule of hydrogen in an energetically neutral process aided by the favourable hydrogen bonding of the water molecule in bulk solution.⁷⁶

Figure 2.11 Yang and Hall's FeGP cofactor model **2.24**.



Scheme 2.5 shows the energy for exchange of hydrogen and water (taking complex **2.24** to start at 0 kcal mol⁻¹ and without considering the favourable effect of solvation) to form complex **2.25** (8.8 kcal mol⁻¹). Through transition state **2.26** (with a free energy barrier of 6.6 kcal mol⁻¹ above **2.25**), structure **2.27** can be formed which is 3.4 kcal mol⁻¹ more stable than **2.25**. In this structure, the dihydrogen has been cleaved, with one hydrogen atom bonded to the iron-bound-thiolate sulfur and the other hydrogen atom bonded to the iron centre, stabilized by a dihydrogen bond to the 2-hydroxyl of the pyridinol ligand. This shows the potential importance of both the thiolate (Cys176) and the pyridinol hydroxyl group in the activation of hydrogen by [Fe]-hydrogenase.

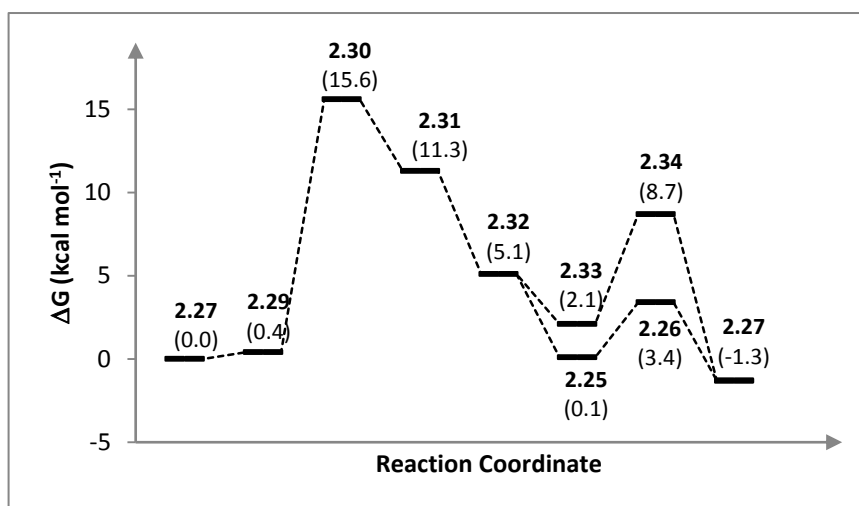
Scheme 2.5 Calculated energies for the substitution of hydrogen with water in complex **2.24** and the subsequent formation of complex **2.27**.



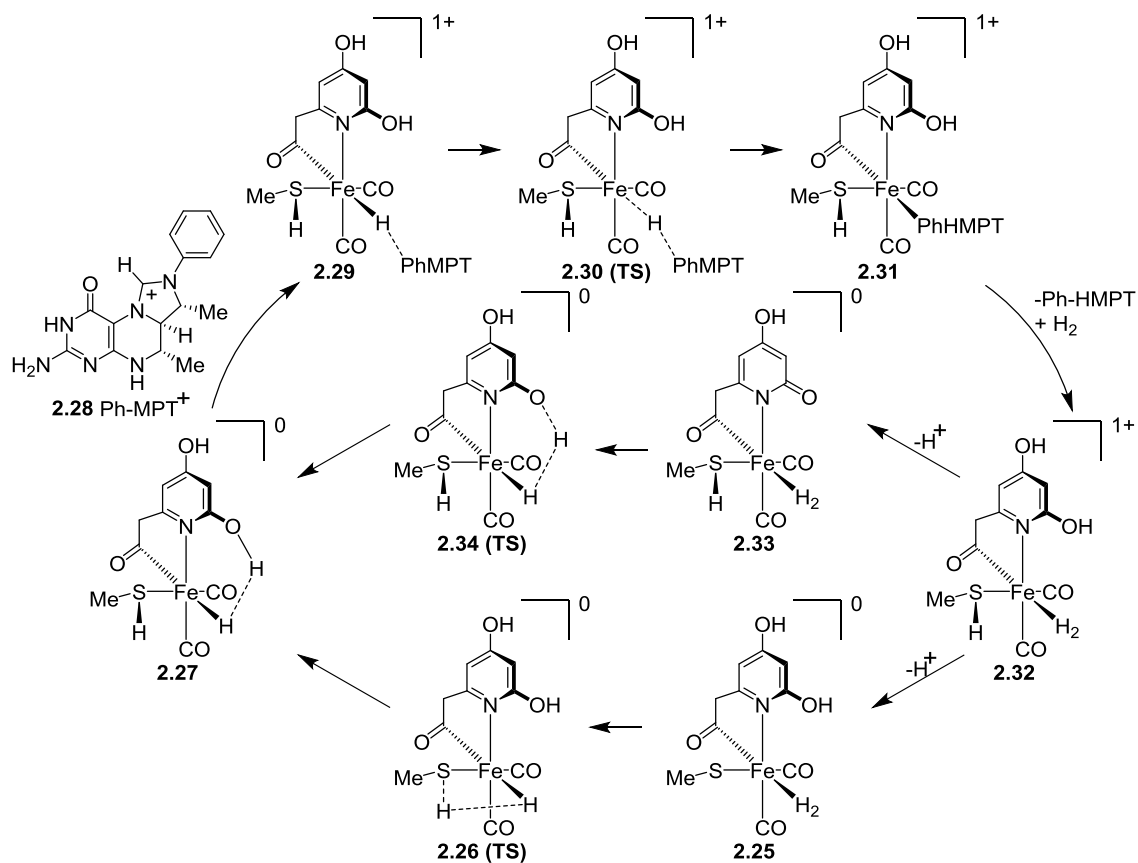
The authors reported calculated values of 2007 and 1947 cm⁻¹ for the vibrational frequencies of the two CO units in structure **2.24**, with structure **2.27** showing values of 2007 and 1949 cm⁻¹.⁷⁶ As these values showed very little difference and were very close to the infrared spectrum values found for the wild type [Fe]-hydrogenase enzyme (2011 and 1944 cm⁻¹),⁵⁸ it was suggested that the resting state of the enzyme could be represented by either structure. As the formation of **2.27** appeared to give a

possible resting state, Yang and Hall proceeded from this structure in their mechanistic calculations to provide a possible substrate-triggered hydride transfer mechanism.⁷⁶

Figure 2.12 Calculated energy values (kcal mol⁻¹) for the mechanism shown in Scheme 2.6.

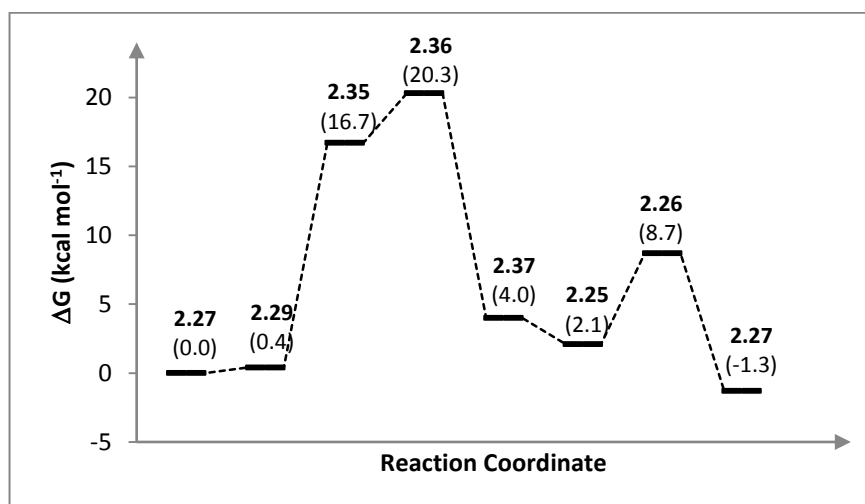


Scheme 2.6 Proposed mechanism for the reduction of Ph-MPT⁺ 2.28 by complex 2.27.



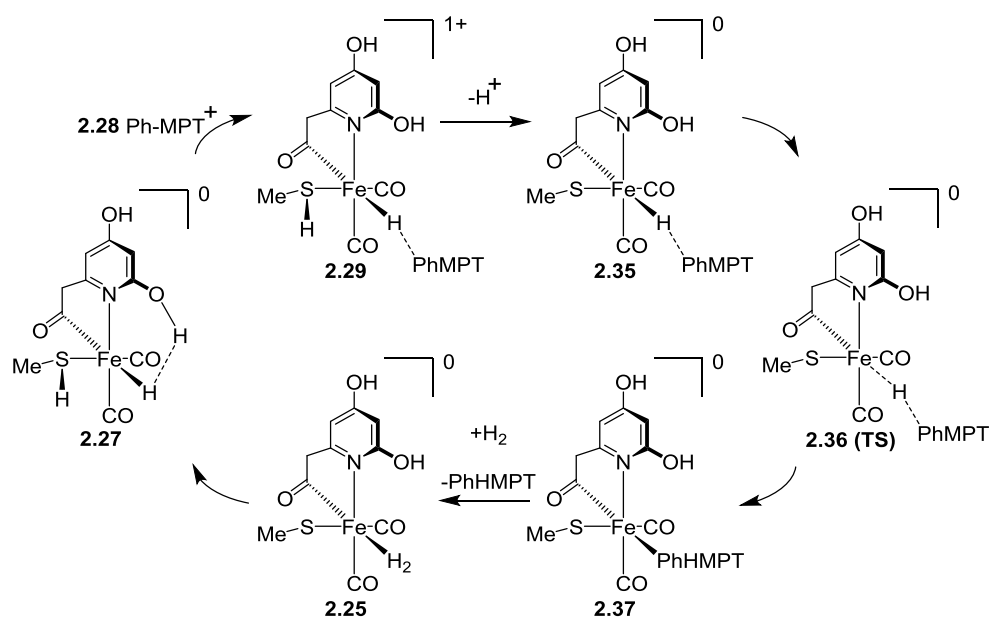
The mechanism outlined in Scheme 2.6 and Figure 2.12 represents the first of two possible reaction pathways proposed by the authors. When Ph-MPT⁺ **2.28** interacts with complex **2.27** to form complex **2.29**, a slight increase in energy is observed (0.4 kcal mol⁻¹) and a hydride can be transferred to Ph-MPT⁺ **2.28** *via* transition state **2.30** which lies at an energy value of 15.6 kcal mol⁻¹ (the value for the total free energy value of the catalytic cycle). Simultaneous dissociation of Ph-HMPT and coordination of H₂ allows for the formation of complex **2.32** which can proceed to reform complex **2.27** upon loss of a proton from two possible routes. The first route involves deprotonation of complex **2.32** on the pyridinol to give complex **2.33**, which was found to proceed at a higher energy than the route involving the deprotonation of the sulfur (i.e. *via* complex **2.25**).

Figure 2.13 Calculated energy values (kcal mol⁻¹) for the mechanism shown in Scheme 2.7.



A second possible route to hydrogen transfer between the iron centre and Ph-MPT⁺ **2.28** was explored (see Scheme 2.7 and Figure 2.13).⁷⁶ In this case, before the transfer of the hydride, complex **2.29** deprotonates to give complex **2.35** with an associated 16.3 kcal mol⁻¹ increase in energy above complex **2.29**. A further 3.6 kcal mol⁻¹ (to give transition state **2.36** at a total free energy of 20.3 kcal mol⁻¹) is then present for the transfer of hydride to the Ph-MPT and formation of complex **2.37**. Loss of Ph-HMPT and coordination of hydrogen then allows for the formation of complex **2.25**, which can go on to form complex **2.27** to allow the catalytic cycle to begin again.

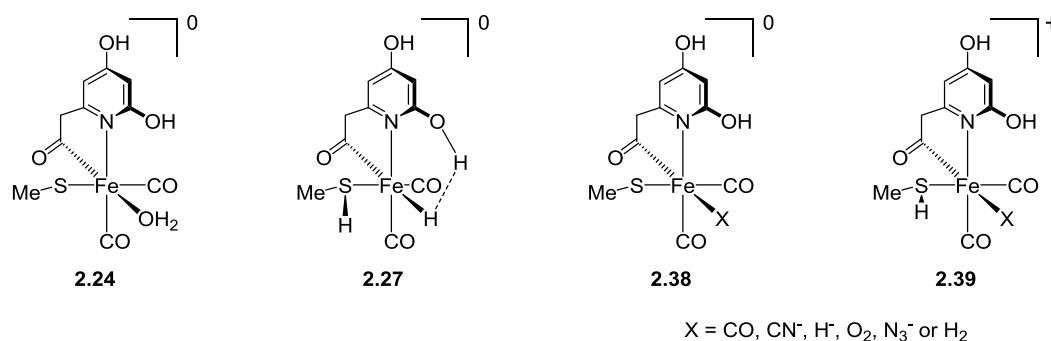
Scheme 2.7 A second proposed mechanism for the reduction of Ph-MPT⁺ **2.28** by complex **2.27**.⁷⁶



In 2010, Dey⁷⁷ also published a DFT study of model FeGP cofactor complexes, in which complex **2.24** (Figure 2.14) was used as the resting complex. The substitution of the water ligand of complex **2.24** was investigated using CO, cyanide, hydride, oxygen, azide and dihydrogen model complexes **2.38** (the corresponding thiol-bound complexes **2.39** were also investigated, as it was unclear if Cys176 was bound as a thiol or thiolate). In the case of $X = H_2$ for complex **2.38**, Dey reported the same structure as that reported by Yang and Hall (complex **2.27**),⁷⁶ in which heterolytic cleavage of dihydrogen had been stabilized by a dihydrogen bond. Removal of this dihydrogen bond by a 180 ° rotation of the 2-hydroxy group was associated with an 8 kcal mol⁻¹ energy penalty. In this study, Dey's results agreed with Yang and Hall's findings⁷⁶ that substitution of water from complex **2.24** with H_2 was energetically unfavourable (without considering the energy gained from solvation). However, Dey claimed⁷⁷ that the space available between the iron centre of the FeGP cofactor **2.7** and $CH\equiv H_4MPT^+$ **2.1** in the active (closed) form of [Fe]-hydrogenase was too small to accommodate a water ligand. The author suggested that in the presence of substrate **2.1** and H_2 , water would be dissociated from the FeGP cofactor and H_2 would be sufficiently small to bind in the free coordination site of the iron. This concept was also used to explain why CO and CN were not stronger inhibitors of [Fe]-hydrogenase (both of these ligands were found to bind to the iron centre more

favorably than water in complexes **2.38** where $X = \text{CO}$ and CN^-), as both of these species are more sterically demanding than H_2 .

Figure 2.14 Complexes studied in the computational work of Dey.⁷⁷



Although the complexes and pathways presented by Yang and Hall,⁷⁶ and Dey⁷⁷ appear to provide attractive mechanisms for the cleavage of dihydrogen, a fundamental issue may be present with the initial starting complex **2.24**. This complex presents a pyridinol ligand, which is likely to be deprotonated at physiological pH (this is further explained in Chapter 6). To appropriately compute the mechanism of dihydrogen cleavage, starting with a deprotonated version of complex **2.24** would provide a better evaluation of the function of the pyridinol ligand's 2-hydroxyl group.

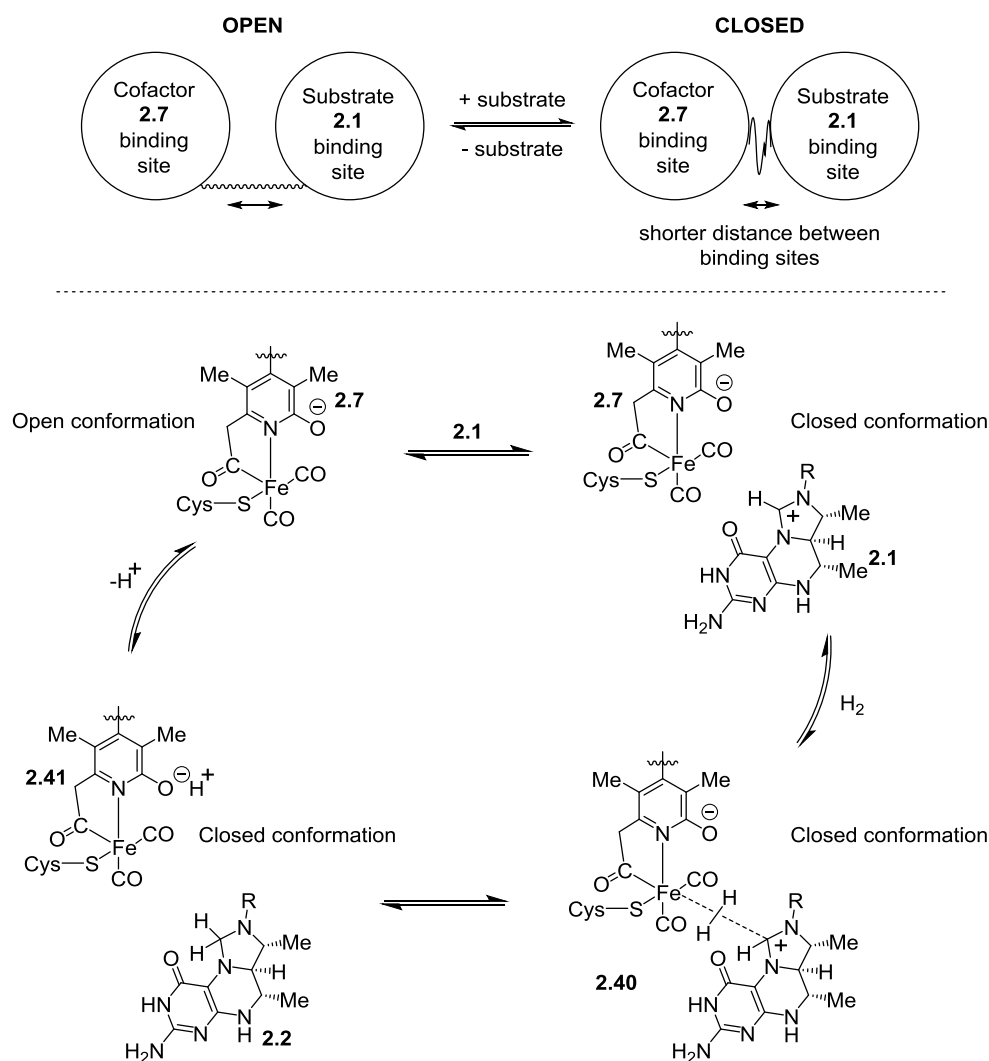
As mentioned in Section 2.5, Hiromoto *et al.*⁶⁸ reported the crystal structure of a DTT-treated, (Cys176 to Ala176) mutated [Fe]-hydrogenase in which $\text{CH}_2=\text{H}_4\text{MPT}^+$ **2.2** was bound. In this study they superimposed the structures of the apoenzyme, the holoenzyme and the C176A-holoenzyme-substrate complex. This showed that the apoenzyme was in a “closed” form, while the holoenzyme was in a “open” form. The C176A-holoenzyme-substrate complex was shown to be closer to the “open” form, but had “closed” to some degree, with the slight rotation of the peripheral unit to the central cleft of the enzyme. The apoenzyme (which contains a PEG molecule in the $\text{CH}_2=\text{H}_4\text{MPT}^+$ **2.2** binding position) and the C176A-holoenzyme-substrate complex contain a hydrogen bond between Tyr267 and Ala282, while the holoenzyme contains a hydrogen bond between Tyr267 and Met252. In the apoenzyme and the C176A-holoenzyme-substrate complex, the amide of Met252 is hydrogen bonded to the PEG and the carbonyl of pterin-containing **2.2**, respectively. This is what prevents the Tyr267 hydrogen bonding to Met252 and causes a

reorganization of the enzyme. Met252 and Ala255 as well as Tyr267 and Ala282 create new hydrogen bonds to each other and could be the cause of the peripheral unit rotating towards the central cleft. The more pronounced “closing” seen in the apoenzyme over the C176-holoenzyme-substrate complex is attributed to the presence of the DTT ligated onto the FeGP cofactor in the latter. It is suggested that this difference is enough to make the “closing” of the enzyme less energetically favourable.

The authors proposed a mechanism for hydrogenation of $\text{CH}\equiv\text{H}_4\text{MPT}^+$ **2.1** (Scheme 2.8) based on this “opening” and “closing” of the enzyme.⁶⁸ The first step involves binding of $\text{CH}\equiv\text{H}_4\text{MPT}^+$ **2.1** to the enzyme in the “open” form which causes the enzyme to “close” and brings the $\text{CH}\equiv\text{H}_4\text{MPT}^+$ **2.1** binding site closer to the FeGP cofactor **2.7**. In the presence of hydrogen, H_2 binds to the “unknown” coordination site of (proposed) Fe^{II} centre of the cofactor. The authors suggest a side-on binding for dihydrogen then provides sufficient polarization of the molecule to allow hydride to be delivered to $\text{CH}\equiv\text{H}_4\text{MPT}^+$ **2.1** via complex **2.40**. At the same time, they suggest the proton could be accepted by the deprotonated pyridinol from complex **2.41** (equally the sulfur of Cys176 was suggested as a possible proton acceptor). As the 2-hydroxy of the pyridinol is shown to be close to His14 (His14 to Ala14 mutation causes a big loss in activity), this might be a strong candidate for accepting a proton and then releasing it.

Further evidence for the conformational change of the [Fe]-hydrogenase enzyme upon the binding of $\text{CH}\equiv\text{H}_4\text{MPT}^+$ **2.1** and H_2 was obtained in the circular dichroism (CD) studies of Shima *et al.*⁷⁸ In these studies, the CD signals of the enzyme were not significantly altered when $\text{CH}\equiv\text{H}_4\text{MPT}^+$ **2.1** was added to [Fe]-hydrogenase under an atmosphere of N_2 . However, when $\text{CH}\equiv\text{H}_4\text{MPT}^+$ **2.1** was added to the enzyme under an atmosphere of H_2 , the CD signals were significantly altered. The authors described the change of signals in the 350-500 nm region as being indicative of changes in the environment of the FeGP cofactor **2.7** (in the presence of both substrate $\text{CH}\equiv\text{H}_4\text{MPT}^+$ **2.1** and H_2). As such, Shima and co-workers⁷⁸ concluded that these results support the idea that [Fe]-hydrogenase rearranges to the “closed” form when substrate is bound.

Scheme 2.8 Proposed “opening” and “closing” mechanism of [Fe]-hydrogenase by Hiromoto *et al.*⁶⁸



The “opening” and “closing” of [Fe]-hydrogenase presented by Hiromoto⁶⁸ and Shima⁷⁸ does provide evidence that conformational change in the enzyme may allow the FeGP cofactor **2.7** to approach close enough to the substrate **2.1** to enable a reaction. The authors did not provide evidence for how dihydrogen binds within the enzyme and how it then cleaves to deliver a hydride to substrate **2.1**.

2.7 Synthesised Model Complexes of the FeGP Cofactor

To date, several model complexes of the FeGP cofactor **2.7** have been synthesized; however, all of the compounds that have been described have had key differences to

the natural complex. As model reactions of [Fe]-hydrogenase reactivity are presented in this thesis (Chapter 5), this section is designed to show the limitations of the complexes available for these studies and should inform the reader why certain compounds were chosen to function the role of the FeGP cofactor **2.7**.

In 2008, Royer *et al.*⁷⁹ reported the synthesis of rhodium and iridium complexes **2.42** and **2.43** as models for the active-site of [Fe]-hydrogenase (Scheme 2.9). Indeed, complex **2.43** showed some hydrogenase-related reactivity by dehydrogenating alcohol **2.44** to acetophenone **2.45**, with a turnover number of 339 over 24 h and as a 50 % solution in toluene. Although interesting for this dehydrogenation reactivity, the authors did not report any hydrogenation activity. Additionally, the model did not contain the same metal as in the enzyme and once the crystal structure of the FeGP cofactor **2.7** was obtained,⁶⁵ it was clear that the pyridinol ligated to the metal through the nitrogen and an acyl carbon rather than the nitrogen and a carboxylate oxygen.

Scheme 2.9 Rhodium and iridium complexes **2.42** and **2.43** and the dehydrogenation of **2.44** to **2.45**.

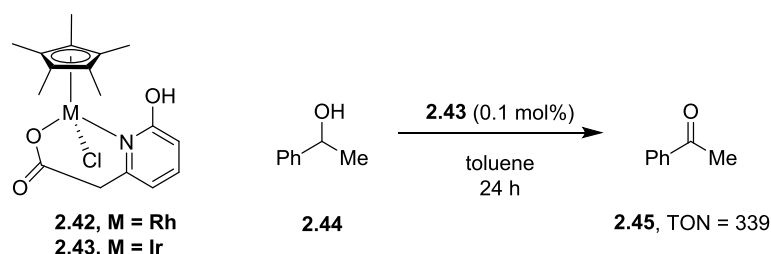
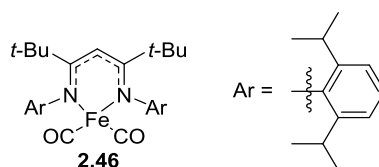


Figure 2.15 4-coordinate Fe^I complex **2.46**.

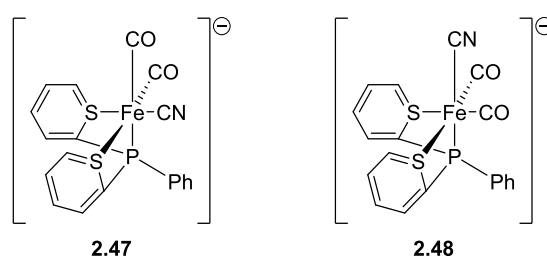


Sadique *et al.*⁸⁰ reported the synthesis of low-valent iron complex **2.46** (Figure 2.15) in which the centre was found to be Fe^I, with vibrational carbonyl stretches at 1917 and 1996 cm⁻¹. This was the first example of a 4-coordinate iron dicarbonyl complex and was synthesized before the reinterpreted crystal structure of the [Fe]-

hydrogenase enzyme had been published,⁶⁵ when the possibility of a 4-coordinate cofactor was still being considered.

Complexes **2.47** and **2.48** (Figure 2.16) were prepared by Koch and co-workers.⁸¹ These two complexes were reported to have infrared spectra that closely resembled the spectrum of the cyanide-inhibited [Fe]-hydrogenase enzyme and it was suggested that the electron density at the iron centre in the enzyme was similar to these complexes.

Figure 2.16 Complexes **2.47** and **2.48** prepared by Koch and co-workers.⁸¹



As part of an investigation into the ⁵⁷Fe nuclear resonance vibrational spectroscopy (NRVS) of the active site of [Fe]-hydrogenase, Rauchfuss and co-workers^{82,83} prepared complex **2.49** (Figure 2.17). The comparison of the NRVS spectrum of this compound and the active site were used to propose a minimal ligand set for the enzyme cofactor consisting of two *cis* carbonyls, a sulfur and a light atom, suggested to be the nitrogen of the pyridinol cofactor.

Figure 2.17 Complex **2.49** prepared by Rauchfuss and co-workers.^{82,83}

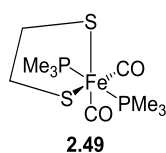
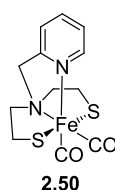
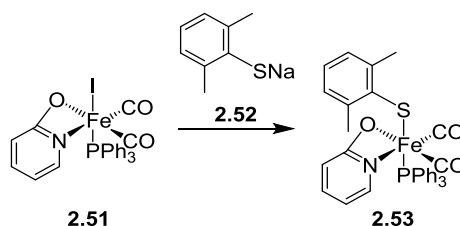


Figure 2.18 Complex **2.50** containing a tetradentate ligand.



Wang *et al.*⁸⁴ reported the synthesis of complex **2.50** (Figure 2.18), which had a tetradentate ligand composed of a pyridine, two thiolates and a tertiary amine. This model was used to compare the Mössbauer and infrared spectra to those of [Fe]-hydrogenase. The results were used to suggest that the iron centre [Fe]-hydrogenase is Fe^{II} and not Fe⁰.⁸⁴

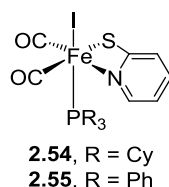
Scheme 2.10 Reaction of complex **2.51** to form complex **2.53**.



In 2009, Hu and co-workers⁸⁵ synthesized complex **2.51** which was also shown to be a precursor to compound **2.53** (Scheme 2.10). The carbonyl vibrational stretching values of these two complexes were 1987 and 2032 cm⁻¹ and 1967 and 2021 cm⁻¹. The authors suggested that the complexes gave further evidence for the Fe^{II} state in the FeGP cofactor **2.7** of [Fe]-hydrogenase. In both structures, the oxygen in the 2-position of the pyridine ligand was bound to the iron centre, which differed from the crystal structure of [Fe]-hydrogenase.⁶⁵

Darensbourg and co-workers⁸⁶ developed complexes **2.54** and **2.55** (Figure 2.19) as analogues of the FeGP cofactor **2.7**. In these complexes, the oxygen in the 2-position of the pyridine ligand had been replaced by a sulfur and was shown to be bound as a thiolate to the metal centre.

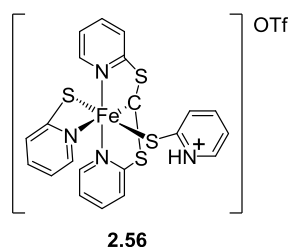
Figure 2.19 2-Thiopyridyl-containing complexes **2.54** and **2.55**.



Later, Halder *et al.*^{87,88} synthesized complex **2.56** (Figure 2.20) which was the first FeGP mimic to contain a bond between Fe^{II} and a carbon ligand that was not a carbonyl. The lack of carbonyls and the fact that the carbon ligand was actually a

carbene (of which there are none on the FeGP cofactor **2.7**) limited this system as a FeGP cofactor model.

Figure 2.20 Complex **2.56** prepared by Halder *et al.*^{87,88}



In 2010, Darensbourg and co-workers⁸⁹ synthesized pentacoordinate complexes **2.57**, **2.58** and **2.59** (Figure 2.21) as analogues of the [Fe]-hydrogenase active site, citing the mechanistic proposal of Thauer and co-workers that the “unknown” coordination site of the FeGP cofactor **2.7** could remain free before coordination of hydrogen and delivery of hydride to $\text{CH}\equiv\text{H}_4\text{MPT}^+$ **2.1**.⁶⁸ No reactivity with hydrogen was discussed, but it was found that when complex **2.57** was protonated, it could accommodate an additional CO in the vacant site of iron. Under these conditions, extrinsic ^{13}CO was found to exchange with intrinsic CO,⁸⁹ which differs from the behavior of [Fe]-hydrogenase in which the intrinsic CO ligands are not exchanged.⁵⁰

Figure 2.21 Pentacoordinate complexes **2.57-2.59** synthesized by Darensbourg and co-workers.⁸⁹

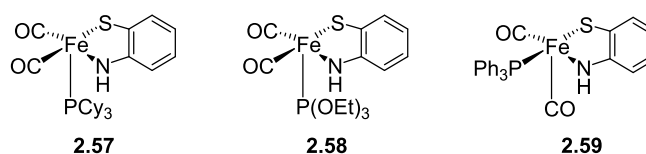
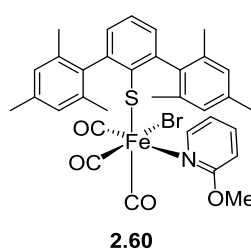


Figure 2.22 Model complex **2.60** with *fac*{(CO)₃Fe} group.

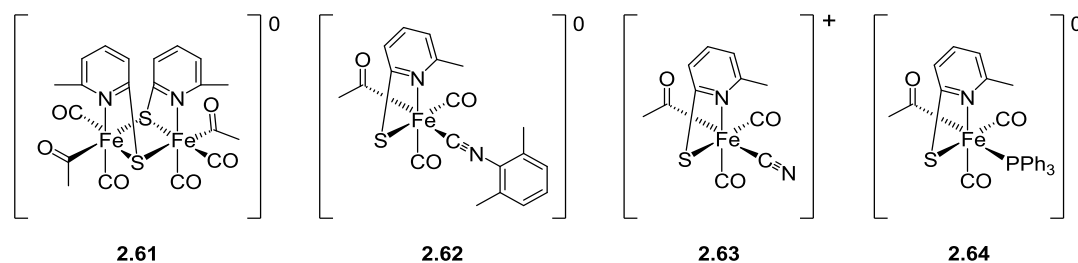


Tanino *et al.*⁹⁰ synthesized complex **2.60** (Figure 2.22) as a model for the active site of [Fe]-hydrogenase. The authors highlighted this complex for its *fac*{(CO)₃Fe} group.

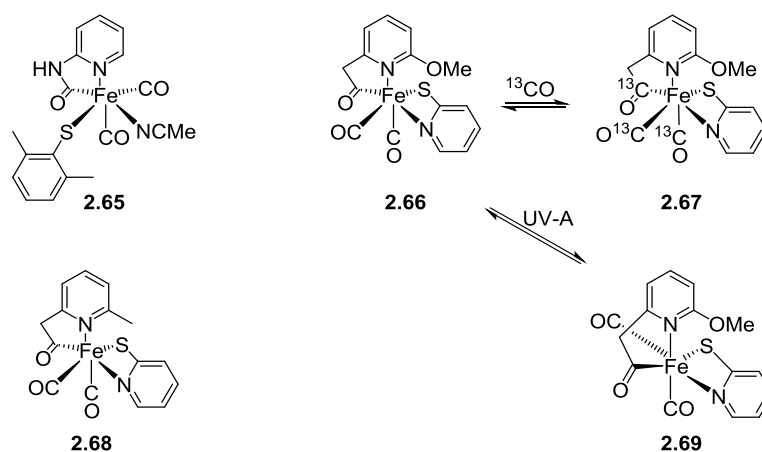
group and suggested this compound could be used as a model for the CO-inhibited [Fe]-hydrogenase. Differences to the FeGP were highlighted, such as the bromide ligand instead of an acyl ligand and the presence of π -stacking between the pyridine ring and one of the mesityl groups of the thiolate ligand.⁹⁰

Hu and co-workers⁹¹ synthesized [Fe]-hydrogenase model complexes **2.61-2.64** (Figure 2.23) with acyl ligands and tight bite angle 2-thiopyridyl ligands. The authors reported that all of the carbonyls of complex **2.61** were exchangeable with ^{13}CO (including the acyl carbonyl), but no reactivity was observed with hydrogen.

Figure 2.23 2-Thiopyridyl-containing complexes **2.61-2.64**.



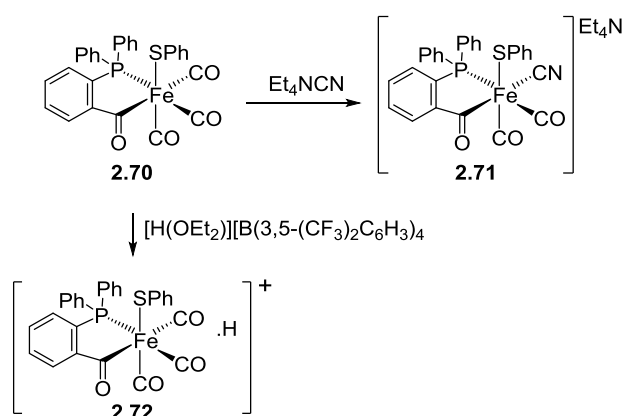
Scheme 2.11 Carbamoyl complex **2.65** and acylmethylpyridinyl complexes **2.66** and **2.68**.



Later, Pickett and co-workers⁹² synthesized carbamoyl complex **2.65** (Scheme 2.11), of which they obtained a crystal structure that showed the same stereochemical arrangement as obtained for the FeGP cofactor **2.7** in [Fe]-hydrogenase.⁶⁵ In the same journal issue, Hu and co-workers⁹³ synthesized compounds **2.66** and **2.68** (with the crystal structure of the latter disclosed), which were the first examples of [Fe]-hydrogenase model complexes containing an acylmethylpyridinyl ligand, like the natural cofactor. In the case of compound **2.66**, when monitored by ^{13}C NMR, all of

the carbonyls are observed to exchange with $^{13}\text{C}\text{O}$ to form compound **2.67**; a phenomenon not observed in [Fe]-hydrogenase, in which the intrinsic carbonyls are not exchanged.⁵⁰ In the presence of UV-A light and absence of extrinsic CO, complex **2.66** isomerizes to complex **2.69**.⁹³

Scheme 2.12 Reactions of acyl-containing complex **2.70**.

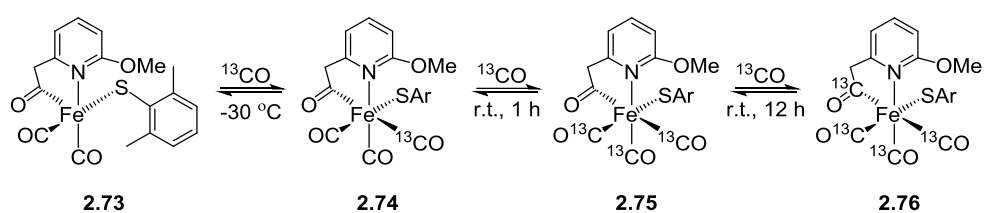


Royer *et al.*^{94,95} synthesised model complex **2.70** (Scheme 2.12) which they found to be indefinitely stable as a solid at room temperature, but that slowly decomposed as a solution kept at $-10\text{ }^\circ\text{C}$. This complex was reacted with Et_4NCN to afford complex **2.71**, in which the cyanide ligand had been placed in the position *trans* to the acyl group, mimicking the stereochemical outcome of the reaction of cyanide with the FeGP cofactor **2.7**,^{62,65} where cyanide is placed in the “unknown” position *trans* to the acyl group of the pyridinol ligand. Complex **2.72** was additionally prepared by the protonation of complex **2.70**, in which the authors suggested that protonation of the thiolate sulfur or the acyl oxygen had occurred.

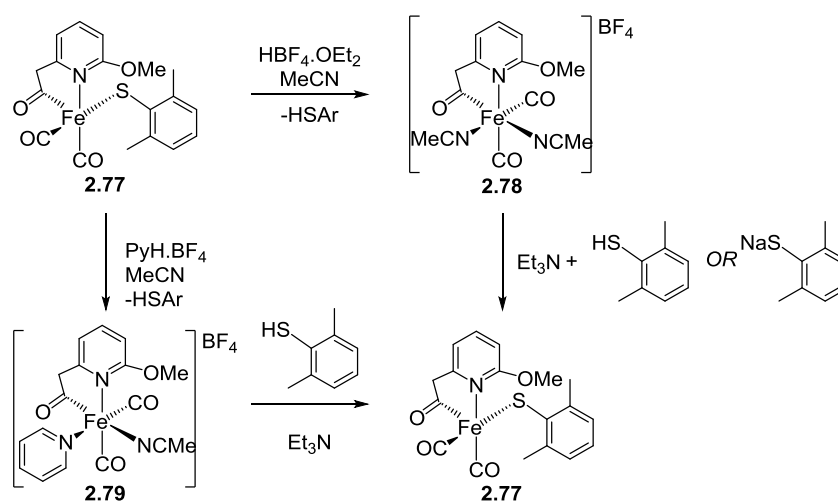
In 2011, Hu and co-workers⁹⁶ isolated complex **2.73** (Scheme 2.13) and obtained a crystal structure. They found that this 5-coordinate complex could accommodate a 3rd carbonyl ligand in the presence of CO. With ^{13}C NMR and the use of $^{13}\text{C}\text{O}$ gas, the authors followed the incorporation of the 6th ligand *trans* to the acyl group to form complex **2.74** and then followed the subsequent exchange of the intrinsic carbonyl ligands to form complexes **2.75** and **2.76** (Scheme 2.13). The authors also reported that no H/D exchange occurred between H_2O , H_2 and D_2 in the presence of complex **2.73**, proposing that a mimic of $\text{CH}\equiv\text{H}_4\text{MPT}^+$ **1** may need to be present. Complex **2.73** was observed to be unreactive towards donor ligands such as water, acetonitrile, pyridine and triethylamine, as well as with O_2 . Due to the fact that PPh_3

and 2-mercapto-6-methylpyridine were found to react with **2.73**, it was judged that the steric effect of the 2-methoxy of the pyridinyl ligand was not enough to account for the lack of reactivity with donor ligands. The authors suggested that the strong *trans* influence of the acyl ligand diminishes the ligand-binding affinity at the vacant site and that the iron centre was also too electron-rich to bind σ -only donors and poor π -acceptors.

Scheme 2.13 5-coordinate complex **2.73** and its reactivity with ^{13}CO .



Scheme 2.14 Complex **2.77** and the reversible loss of the thiolate ligand upon protonation.



More recently, Hu and co-workers⁹⁷ have studied the protonation chemistry of complex **2.77** (Scheme 2.14). In this work, complex **2.77** was protonated in the presence of a donor ligand (MeCN or pyridine) to afford complexes **2.78** and **2.79**, where the thiolate is lost as a thiol. Complex **2.77** can then be regenerated from complexes **2.78** and **2.79** by treating them with sodium thiolate or the thiol in the presence of triethylamine (Scheme 2.14). The authors proposed that this reversible protonation process indicates that Cys176 in [Fe]-hydrogenase is the immediate proton acceptor in the presence of H_2 when hydride is delivered to $\text{CH}\equiv\text{H}_4\text{MPT}^+$ **2.1**.

Hu and co-workers⁹⁸ have also disclosed the infrared and Mössbauer analysis of complexes **2.52**, **2.55**, **2.61-2.64** and **2.80-2.88** (Figure 2.24). The Mössbauer spectrum⁶⁰ of [Fe]-hydrogenase had previously been reported and values of the complexes presented in Figure 2.24 were compared towards this. Although some of the complexes provided comparable Mössbauer spectra to the iron centre in [Fe]-hydrogenase,⁹⁸ none of these complexes contains the potentially vital acylmethylpyridinol ligand present in FeGP cofactor **2.7**.

Figure 2.24 Various complexes synthesized by Hu and co-workers and analyzed by Mössbauer spectroscopy.

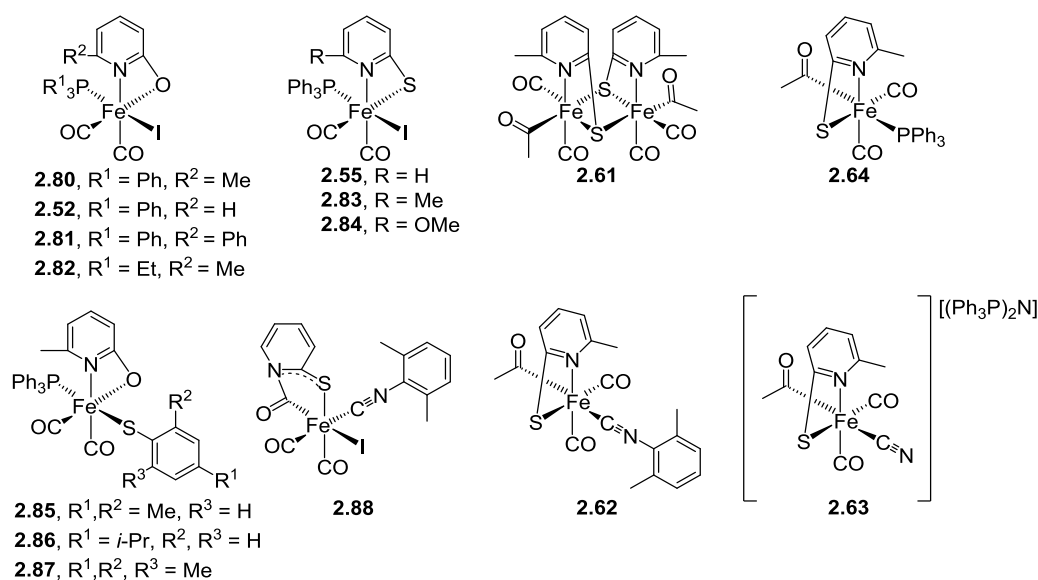
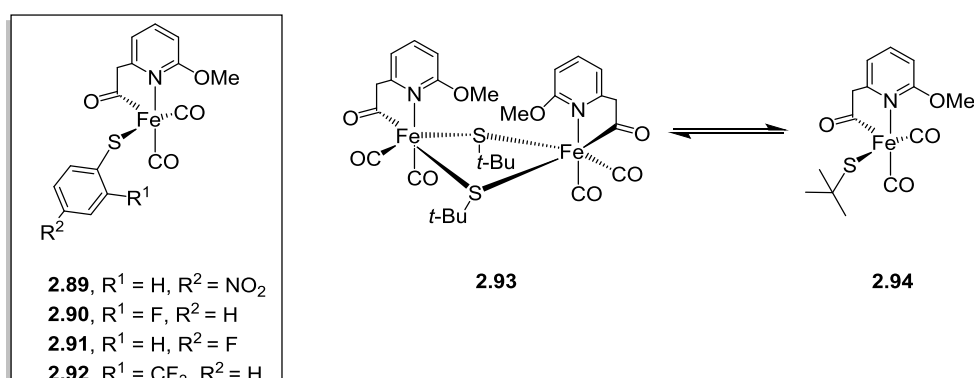


Figure 2.25 5-coordinate complexes of Hu and co-workers.⁹⁹

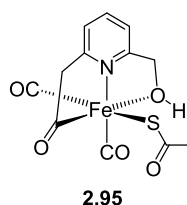


Hu and co-workers⁹⁹ have recently prepared 5-coordinate complexes **2.89** to **2.92** (Figure 2.25). Complexes **2.89** to **2.91** were shown to exist as dimers in solid state and as the 5-coordinate complexes depicted, in solution. Complex **2.92** was shown

to exist as drawn in both the solid and solution state. In the same report, the authors also presented the first 5-coordinate FeGP cofactor model complex **2.94** with an alkyl thiol ligand; this compound was not isolated but shown to form in solution from complex **2.93** by IR spectroscopy.⁹⁹ These complexes contained a methylated version of the acylmethylpyridinol ligand present on FeGP cofactor **2.7**; as the 2-hydroxyl on the pyridinol of cofactor **2.7** may provide vital interactions in the reactivity of [Fe]-hydrogenase, this is a clear limitation present in this series of complexes. To date, no hydrogenation reactions have been reported using complexes such as those in Figure 2.25.

Recently, Song and co-workers¹⁰⁰ reported structure **2.95** (Figure 2.26) as a biomimetic model of the active site of [Fe]-hydrogenase. Other than the rhodium and iridium complexes of Royer *et al.*,⁷⁹ this structure represented the first model complex of [Fe]-hydrogenase with a hydroxyl-containing ligand. X-ray crystallography showed the distance between the iron and the hydroxyl oxygen was 2.128 Å (with an N-Fe-O angle of 78.13 °), which is considerably shorter than the distance of 3.19 Å (with an N-Fe-O angle of 46.76 °) between the hydroxyl oxygen and the iron in the [Fe]-hydrogenase enzyme.⁶⁵ As there is the methylene between the hydroxyl and the pyridine ligand (unlike the pyridinol ligand of the FeGP cofactor **2.7**) this allows the oxygen to fill a ligand position on the iron and affects the properties of the hydroxyl (e.g. pK_a). The authors suggest the binding of the hydroxyl to the iron centre may mimic the potential binding of water to the “unknown” ligand site in [Fe]-hydrogenase.⁶⁵

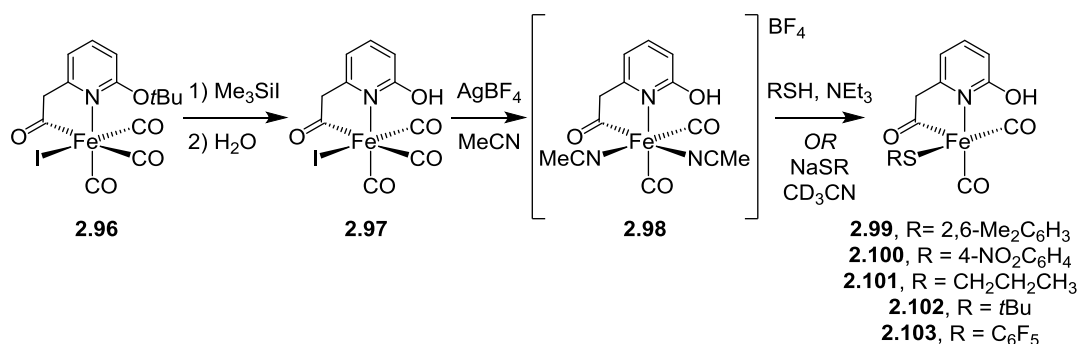
Figure 2.26 Acylmethylpyridyl-complex **2.95**, which contains a hydroxyl group.



In 2014, the syntheses of the first FeGP cofactor **2.7** models containing mononuclear iron centres with an acylmethylpyridinol ligand were reported by Hu *et al.*¹⁰¹ The authors reported the synthesis of *t*-butyl-protected complex **2.96** (Scheme 2.15) which was characterised by X-ray crystallography. The deprotection of the *t*-butoxy group of complex **2.96**, following treatment with trimethylsilyl iodide and an

aqueous work-up, afforded complex **2.97**. This complex was characterised by ^1H NMR, IR and elemental analysis, as was salt **2.98** which was formed after reacting complex **2.97** with silver tetrafluoroborate in acetonitrile. Salt **2.98** was then used to form complexes **2.99** to **2.103**, which each contain a thiolate ligand. Complexes **2.99** to **2.102** were only characterised by IR spectroscopy, while complex **2.103** was characterised by IR spectroscopy when prepared from the thiol and triethylamine in acetonitrile, and characterised by ^1H NMR when prepared from the sodium thiolate salt in deuterated acetonitrile. The (poorly resolved)¹⁰¹ ^1H NMR spectrum of **2.103** was only observed immediately after the reaction mixture was prepared at $-30\text{ }^\circ\text{C}$. It would be fair to assume with the lack of data for complexes **2.99** to **2.103**, that it is unclear if the iron centre is 5-coordinate as depicted by the authors or 6-coordinate with an unidentified ligand in the free coordination site. With either acetonitrile or deuterated acetonitrile being used as solvent, this may be present as a ligand on these structures.

Scheme 2.15 Development of mononuclear iron complexes containing an acylmethylpyridinol ligand; compounds **2.97** to **2.103**, synthesised by Hu *et al.*¹⁰¹



The authors also report that complexes **2.97** to **2.103** did not activate dihydrogen; however, the conditions for testing this reactivity are not outlined in the paper or supporting information.¹⁰¹ The authors suggest that the lack of dihydrogen activation accounts for the essential role of $\text{CH}\equiv\text{H}_4\text{MPT}^+$ **2.1** in this process. However, the conditions of the attempted dihydrogen activation may well be very unrepresentative of the enzymatic reaction conditions – it is impossible to provide conclusions on this without any information from the authors. The light-sensitivity and instability reported for complexes **2.97** to **2.103** suggest that the conditions used in their reactions are very important.

As can be seen from this section, there is an abundance of interest in synthesizing model complexes of the [Fe]-hydrogenase active site. However, to date only one model complex has shown hydrogenase reactivity (dehydrogenase reactivity to be precise)⁷⁹ and this is an iridium complex. With the increasing desire to convert carbon dioxide (industrially produced as well as atmospheric) into useful feedstock chemicals, understanding the way in which Nature utilizes carbon dioxide is increasingly significant. As an enzyme involved in a step of the conversion of carbon dioxide to methane, [Fe]-hydrogenase could be a vital tool in the production of industrially useful chemicals. Indeed, understanding and mimicking the chemistry carried out in [Fe]-hydrogenase could aid the development of future industrially relevant processes and it is this potential that will hopefully see the synthesis of a more refined model complex of the [Fe]-hydrogenase active site.

The next chapter (Chapter 3. Previous Work) will go on to discuss the development of amidine disalts within the Murphy Group and will discuss the use of them as models for [Fe]-hydrogenase reactivity.

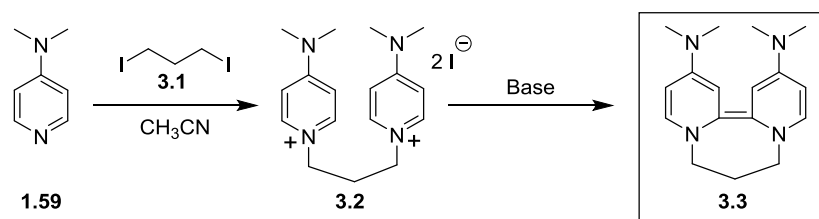
Chapter 3: Previous Work on Superelectrophiles Within the Murphy Group

Chapter 1 provided an introduction to the research that has been carried out in the area of superelectrophiles, since the concept was developed by Olah.¹ Chapter 2 reviewed the literature published on [Fe]-hydrogenase and it was shown that the Murphy group had synthesized an amidine disalt as a model for the activated amidine substrate present within the enzyme. This chapter will further elaborate on the work carried out by previous members of the Murphy Group in the area of amidine disalts as superelectrophiles.

3.1 Initial Search and Development of Superelectrophiles

The emergence of superelectrophiles as a research area within the Murphy Group was serendipitously born out of developments to novel super electron donors (SEDs). SED **3.3** (Scheme 3.1) is a very powerful 2-electron donor that was prepared in the Murphy Group and has been employed for several synthetic transformations.¹⁰²⁻¹⁰⁴

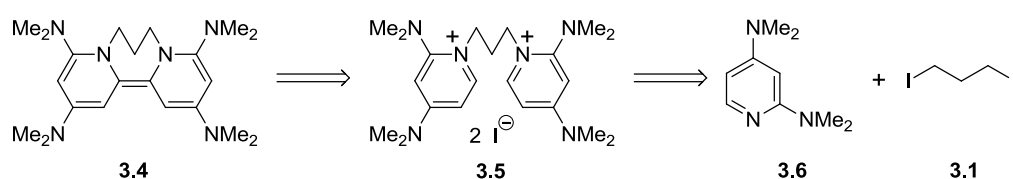
Scheme 3.1 Synthesis of SED **3.3**.



With the desire to create an even more powerful SED, the synthesis of donor **3.4** was envisioned (Scheme 3.2).^{27,105} This donor was designed to give an extra amino group

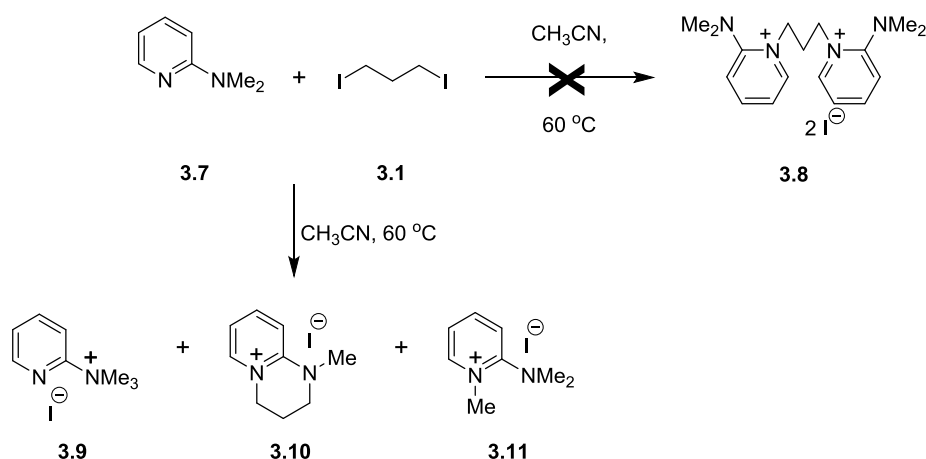
in the *ortho*-position of the pyridine rings (relative to donor **3.3**), giving extra stability to any radical cation formed during electron donation. The synthesis of this species was proposed to be possible *via* disalt **3.5** which would be formed from diiodopropane **3.1** and *bis*(dimethylamino)pyridine **3.6**. The effect of the 2-dimethylamino group on forming a bridged salt, however, was unknown.

Scheme 3.2 Retrosynthetic analysis of donor **3.4**.



This uncertainty led Zhou^{27,105} to carry out the reaction of 2-DMAP **3.7** with diiodopropane **3.1**, which did not afford disalt (donor precursor) **3.8**, but in fact a mixture of three monocationic products **3.9** to **3.11** (Scheme 3.3), identified by ¹H NMR and MS of the crude mixture.^{27,105}

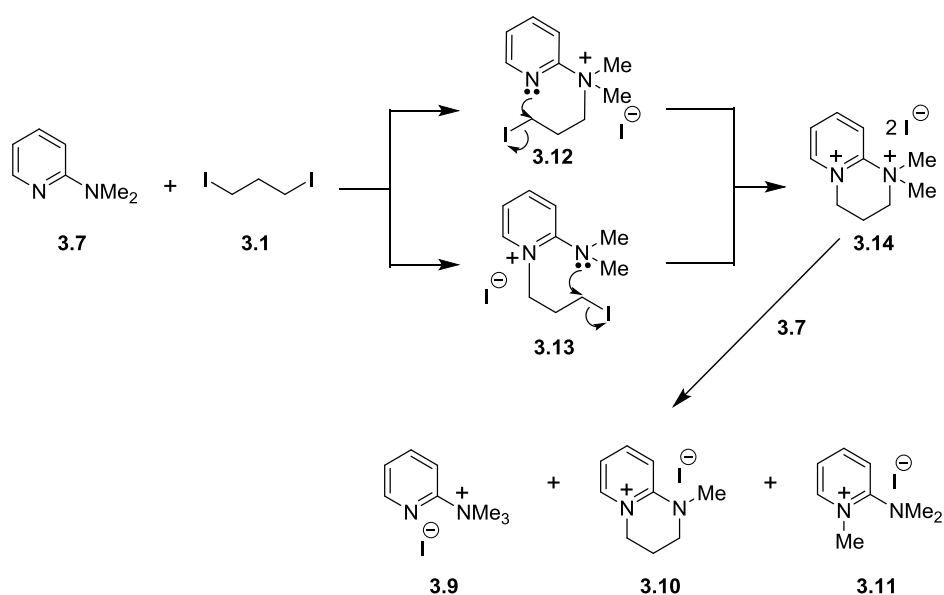
Scheme 3.3 Reaction of 2-DMAP **3.7** with diiodopropane **3.1**.



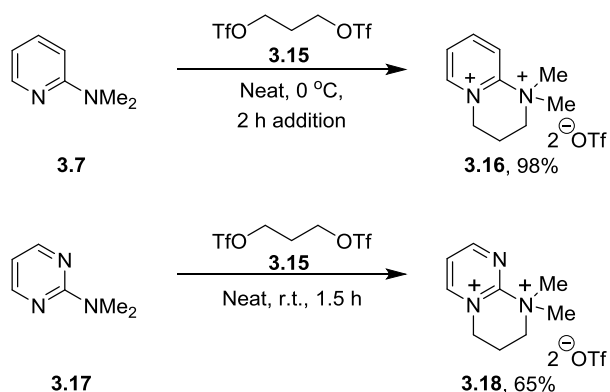
A possible mechanism (Scheme 3.4) involving an amidinium disalt **3.14** was then suggested.^{27,105} Diiodopropane **3.1** could be attacked by either of the nitrogens of 2-DMAP **3.7**, giving monocationic species **3.12** or **3.13**, both of which can undergo an intramolecular attack from the remaining nitrogen to afford disalt **3.14**. This disalt is

then sufficiently activated to transfer a methyl group to any 2-DMAP **3.7** still remaining in the reaction mixture, reacting with either the ring or the dimethylamino nitrogen to afford the observed monocations, **3.9** to **3.11**. Corr later repeated this reaction,²⁷ isolating and characterising cationic species **3.9** and **3.10**. Corr also carried out alkylation studies of 2-DMAP **3.7** that suggested intermediate **3.12** would be favoured over intermediate **3.13**, in agreement with studies on the alkylation of 2-DMAP **3.7** by other groups.¹⁰⁶⁻¹¹⁰

Scheme 3.4 Possible disalt **3.14** formation in the reaction of **3.1** and **3.7**.



Scheme 3.5 Formation of superelectrophilic dicationic species **3.16** and **3.18**.

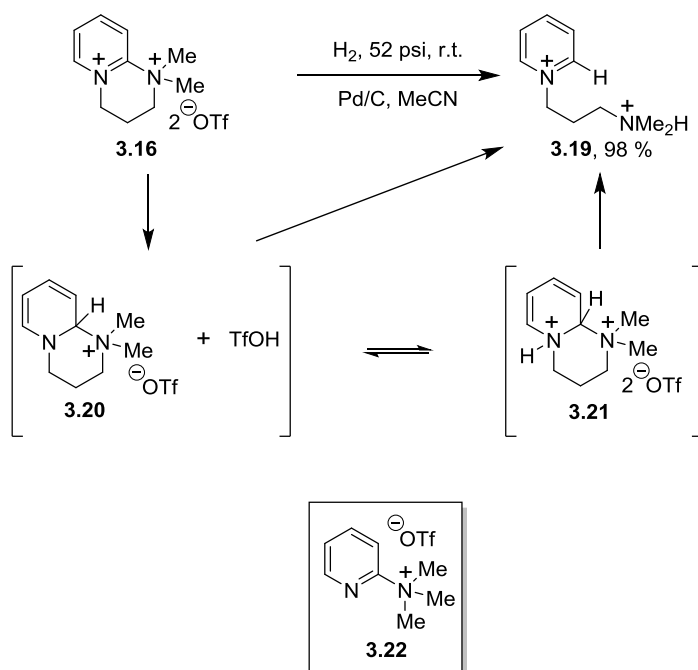


Isolation of disalt **3.14** was not possible.²⁷ However, the attempts to isolate this disalt led on to the synthesis of related disalts using alternative 1,3-disubstituted propanes.²⁷ Success was found when propane-1,3-diyl bis(trifluoromethanesulfonate) **3.15** was used, with the optimised reaction conditions affording disalt **3.16** as white

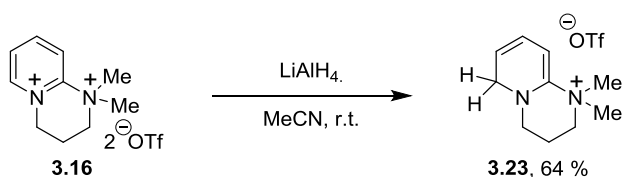
crystals in a 98 % yield (Scheme 3.5). This then led on to the synthesis of pyrimidine-derived disalt **3.18**, with a yield of 65 % (Scheme 3.5). Both species were then characterised by X-ray crystallography.

As disalt **3.16** was easier to handle (**3.18** decomposes in MeCN), it was selected for hydrogenation reactions aimed at mimicking the possible superelectrophilic activation carried out in [Fe]-hydrogenase.⁷² With 52 psi of H₂ over Pd/C catalyst, the hydrogenation of **3.16** afforded pyridinium species **3.19** in a yield of 98 % (Scheme 3.6). This disalt would be expected to be less active towards hydrogenation than disalts **2.8** and **2.9**, proposed to form from the substrate in [Fe]-hydrogenase, due to the loss of aromaticity in the proposed intermediate **3.20**. Despite this, the disalt undergoes hydrogenation in a very high yield under mild conditions. Pyridinium **3.19** was isolated without any other products and dimethylamino-alkylated 2-DMAP **3.22** was inactive to hydrogenation.²⁷

Scheme 3.6 Hydrogenation of **3.16** with Pd/C catalyst at 52 psi.



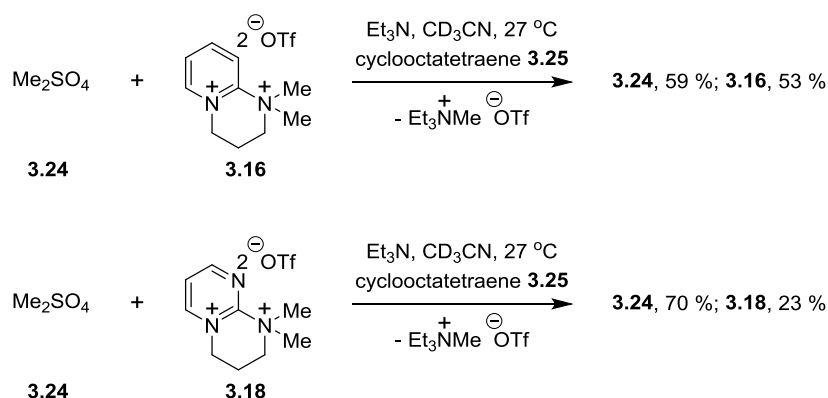
Scheme 3.7 Reduction of disalt **3.16** with LiAlH₄ to give dihydropyridine **3.23**.



The reactivity of superelectrophile **3.16** to conventional hydride donor, LiAlH_4 , was also tested, giving dihydropyridine **3.23** in a yield of 64 % (Scheme 3.7), showing rather different regioselectivity to the hydrogenation reaction.^{27,72}

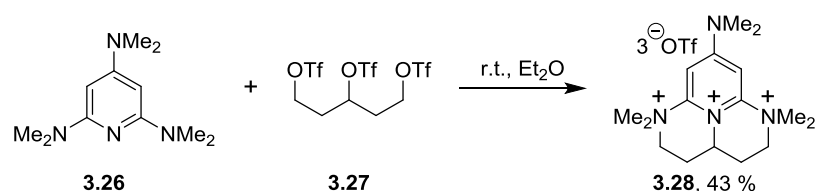
Disalts **3.16** and **3.18** were also tested as methylating reagents. In competitive ^1H NMR reactions using cyclooctatetraene **3.25** as an internal standard, both disalts were found to be more reactive than methyl sulfate **3.24** in the presence of triethylamine as nucleophile; 53 % of **3.16** remained in its reaction when 59 % of methyl sulfate **3.24** remained. Disalt **3.18** was further reactive, with only 23 % of it remaining after methylation *versus* 70 % of methyl sulfate **3.24** remaining (Scheme 3.8).^{27,73}

Scheme 3.8 Competitive methylation of triethylamine by disalts **3.16** and **3.18** against methyl sulfate **3.24**.



Trisalt **3.28** was also synthesised (Scheme 3.9).^{27,73} However, this trisalt was not found to be more reactive than dimethyl sulfate **3.24**. The trication, with its extra positive charge, was designed to be more reactive than disalts **3.16** and **3.18**. The electron-donating effect of the *p*-dimethylamino group in this species most likely balances this extra charge, resulting in the lower level of reactivity observed.

Scheme 3.9 Synthesis of trisalt **3.28**.

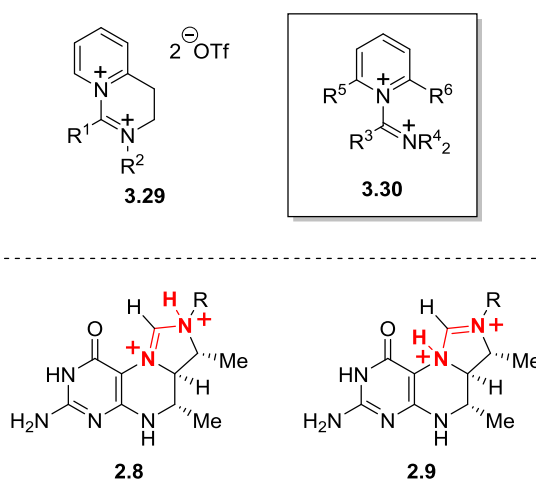


The next series of superelectrophiles that were developed within the Murphy Group are those which are a major focus in this thesis. The next section will discuss the work carried out by Corr²⁷ in developing this new series of disalts before moving on to the next Chapter which will discuss the initial work carried out for this thesis.

3.2 A New Series of Disalts

As discussed above, the reactivity of disalt **3.16** in hydrogenation reactions is affected by the loss of aromaticity on accepting a hydride (Scheme 3.6). The possible superelectrophilically activated structures of (CH≡H₄MPT⁺) **2.1** (i.e. dications **2.8** and **2.9**, Scheme 3.10) in [Fe]-hydrogenase do not incorporate the amidinium motif into an aromatic ring and so would be predicted to be more reactive. This led Corr²⁷ to design structure **3.29** as a new type of disalt (Scheme 3.10). These disalts are closely related to the superelectrophiles of structure **3.30**, proposed as reaction intermediates by Charette and Movassaghi and discussed in Chapter 1.^{13-24,31-34} These intermediates had never been isolated, so the isolation of disalts like structure **3.29** could give more credibility to the discussed mechanisms involving structures **3.30**.

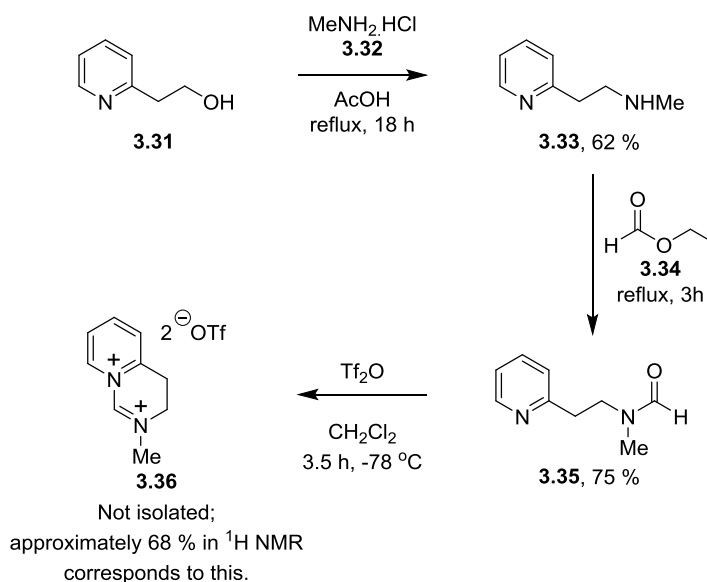
Scheme 3.10 Structure of disalt series **3.29**.



Godin¹¹¹ carried out the first attempted synthesis of disalt **3.36** (Scheme 3.11); however, pure disalt was not isolated. The product was not stable under attempted

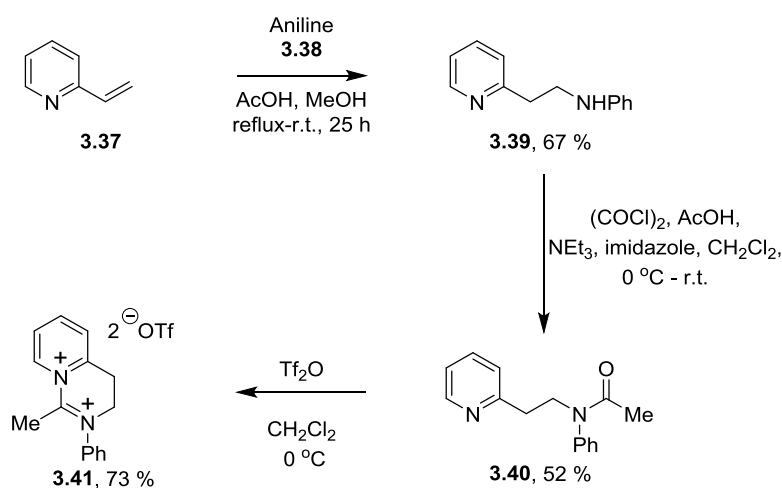
recrystallisation and the purest sample that was prepared contained approximately 68 % of material corresponding to desired disalt, observed by ^1H NMR.

Scheme 3.11 Synthetic route to disalt **3.36**.



With a desire to isolate a pure disalt, Corr²⁷ worked on developing *N*-Ph rather than *N*-Me analogues of disalt **3.36**. The first success was obtained in synthesising disalt **3.41** (Scheme 3.12) which was characterised by NMR spectroscopy. The sample was found difficult to handle with no further characterisation obtained.

Scheme 3.12 Synthesis of disalt **3.41**.

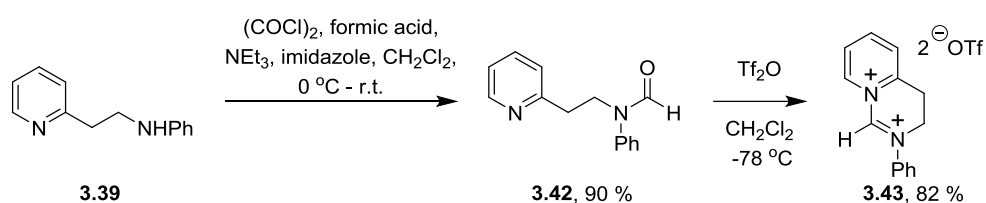


Soon after, disalt **3.43** was also synthesised (Scheme 3.13). Again, this was only characterised by NMR spectroscopy; the sample was too reactive to obtain MS and

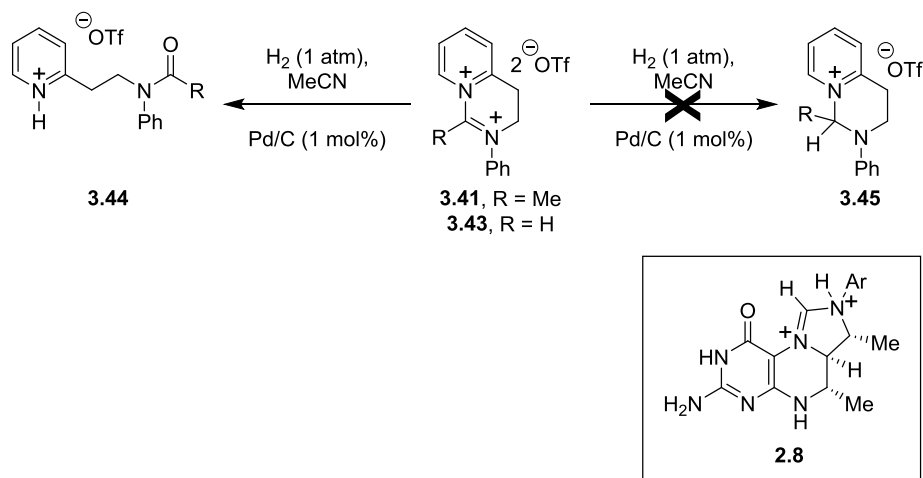
IR, was unstable under recrystallisation conditions and X-ray characterisation was not possible.²⁷

Hydrogenation reactions of both disalts **3.41** and **3.43**, aimed at modelling the [Fe]-hydrogenase reaction, were attempted using Pd/C as catalyst in dry acetonitrile. However, instead of forming any hydrogenated products such as **3.4**, amide salts **3.44** were the only products obtained (Scheme 3.14), likely arising from hydrolysis of disalts **3.41** and **3.43**.

Scheme 3.13 Synthesis of disalt **3.43**.

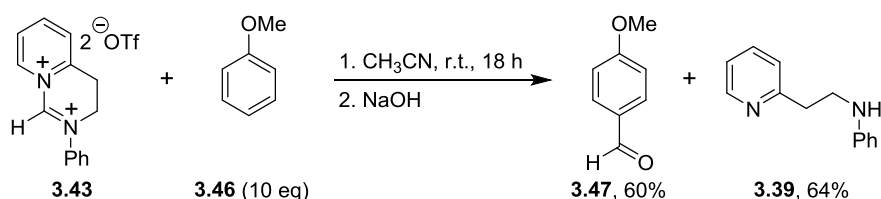


Scheme 3.14 Attempted hydrogenation of disalts **3.41** and **3.43**.



Finally, Corr²⁷ carried out the formylation of anisole **3.46** using disalt **3.43**, affording *para*-anisaldehyde **3.47** and amine **3.39** in yields of 60 % and 64 %, respectively (Scheme 3.15).

Scheme 3.15 Formylation of anisole **3.46** using disalt **3.43**.



Designing this series of disalts was seen as an important development in the Murphy Group. The fact that disalts **3.41** and **3.43** could only be analysed by NMR, and that disalt **3.36** could only be seen as part of a mixture by NMR analysis, made the isolation and full characterisation of a disalt in this series of compounds highly important.

The next chapter (Chapter 4) will go on to discuss the development of a fully characterised member of this type of disalt, the first characterised disalt to be formed from an amide. Chapter 4 will then discuss some initial attempts at [Fe]-hydrogenase-related reactivity with amidine disalts.

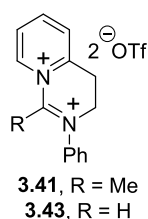
Chapter 5 will then go on to discuss the development of a modified series of disalts related to the disalts described in this chapter. These modified disalts provided improved substrates for model studies of [Fe]-hydrogenase reactivity. Chapter 6 will then discuss some alternative disalts that have been synthesised that display intriguing reactivity, not related to [Fe]-hydrogenase.

Chapter 4: Results and Discussion; Providing Evidence for the Formation of Amidine Disalts

4.1 Project Aims

As discussed in the previous chapter, Corr²⁷ synthesised disalts **3.41** and **3.43** (Figure 4.1) and proved their existence by NMR spectroscopy, although no further characterisation could be provided due to the instability of these compounds. These two disalts had a limited solubility and stability in organic solvents – the only solvent that afforded solubility and limited stability was acetonitrile. When attempting to recrystallise with dried acetonitrile/ether, these two disalts quickly decomposed to give brown oils (the starting disalts were beige solids).

Scheme 4.1 Previously synthesised disalts **3.41** and **3.43**.



The project outlined in this thesis was initiated to provide a fully characterised amidine disalt derived from an amide.

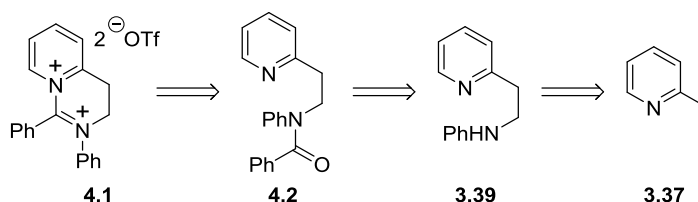
The second aim of this project was to further study the reactivity of amidine disalts in model reduction reactions of [Fe]-hydrogenase; previously Corr had only demonstrated reduction reactions of amidine disalts catalysed by palladium.²⁷

The final aim of this project was to see if additional superelectrophilic reactions could be observed with amidine disalts such as **3.41** or **3.43**.

4.2 Isolation and Full Characterisation of a New Amidine Disalt

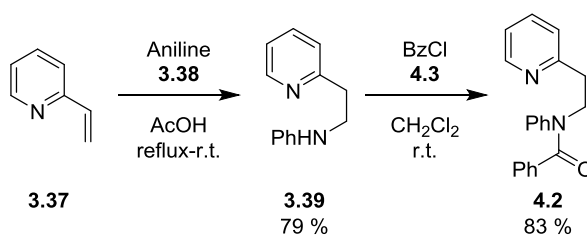
Attempting to provide a fully characterised amidine disalt related to salts **3.41** and **3.43**, a structure which could provide an alternative solubility profile was designed; it was reasoned that the alternative solubility could allow for a disalt that could be recrystallised in conventional organic solvents. Disalt **4.1** (Scheme 4.1) has a phenyl ring attached to the central carbon of the amidine group – introducing this group was hoped to give solubility in less polar and less nucleophilic solvents than acetonitrile. Additionally, it was proposed that this phenyl ring could provide additional stability and temper nucleophilic attack at the amidine centre. The synthesis of this compound was proposed to involve 3 steps from 2-vinylpyridine **3.37**, *via* intermediate compounds **3.39** and **4.2**. This route was comparable to those used for the synthesis of disalts **3.41** and **3.43**.²⁷

Scheme 4.1 Retrosynthesis of disalt **4.1**.



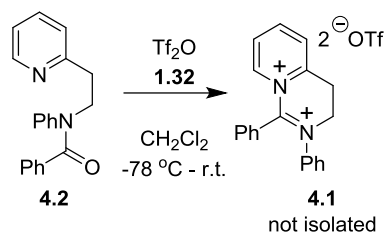
The synthesis of secondary amine **3.39** (Scheme 4.2) proceeded through a modified method from that used by Corr;²⁷ removing methanol and using high vacuum distillation achieved an improved yield of 79 % compared to the yield of 67 % previously reported. Benzamide **4.2** was then synthesised in 83 % yield by treating amine **3.39** with benzoyl chloride **4.3** in CH_2Cl_2 (Scheme 4.2).

Scheme 4.2 Synthesis of amide **4.2** *via* amine **3.39**.



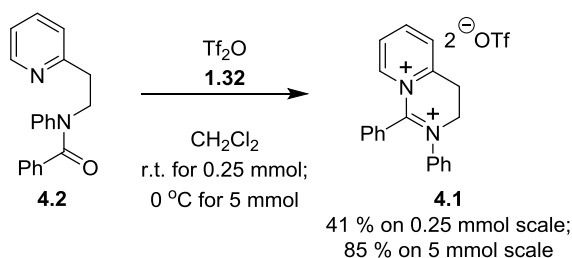
Disalt **3.43** (Figure 4.1) was prepared at $-78\text{ }^{\circ}\text{C}$,²⁷ which resulted in the initial attempt at forming disalt **4.1** (Scheme 4.3) being carried out at this temperature. Despite using a nitrogen-atmosphere dry glovebox and attempts at recrystallisation with dried diethyl ether and dichloromethane, pure **4.1** could not be isolated at this temperature.

Scheme 4.3 Attempted synthesis of amidine disalt **4.1** from amide **4.2**.



By operating at r.t. and working on a 0.25 mmol scale, disalt **4.1** was isolated in a 41 % yield, after recrystallisation from diethyl ether and dichloromethane (Scheme 4.4) – the disalt was soluble in dichloromethane and insoluble (and stable) in diethyl ether. The synthesis of disalt **4.1** was then achieved on a 5 mmol scale by operating at a temperature of $0\text{ }^{\circ}\text{C}$ (85 % yield).

Scheme 4.4 Synthesis of amidine disalt **4.1** from amide **4.2**.



The recrystallisation of disalt **4.1** afforded emerald green crystals that were suitable for X-ray crystallographic analysis. A crystal structure of 0.78 \AA resolution was obtained (Figure 4.2) in which one molecule of CH_2Cl_2 was present in relation to one amidine dication and two triflate anions. ^1H NMR analysis of disalt **4.1** showed the 2-position of the pyridinium to appear at a chemical shift of 8.69 ppm. This value is considerably different to the chemical shift obtained for the related pyridinium proton in disalt **3.43**, which comes at 9.17 ppm. This difference can be attributed to an anisotropic effect¹¹² and is understandable when considering the proximity and

direction of the proton in disalt **4.1** relative to the phenyl ring (which can be seen when analysing its X-ray crystal structure).

Figure 4.2 X-ray crystal structure of disalt **4.1**.

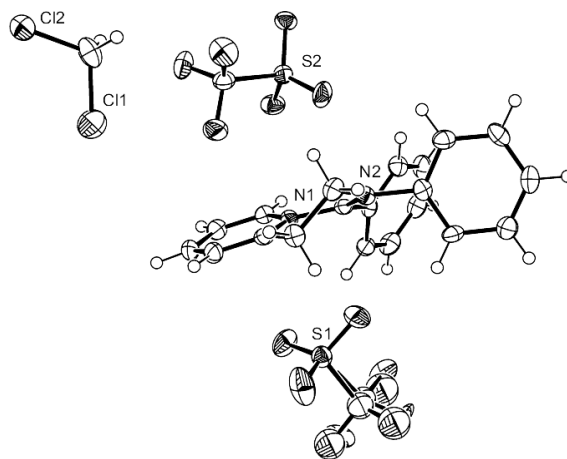
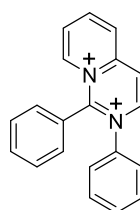


Figure 4.3 Dication **4.4** observed during mass spectrometry of disalt **4.1**.

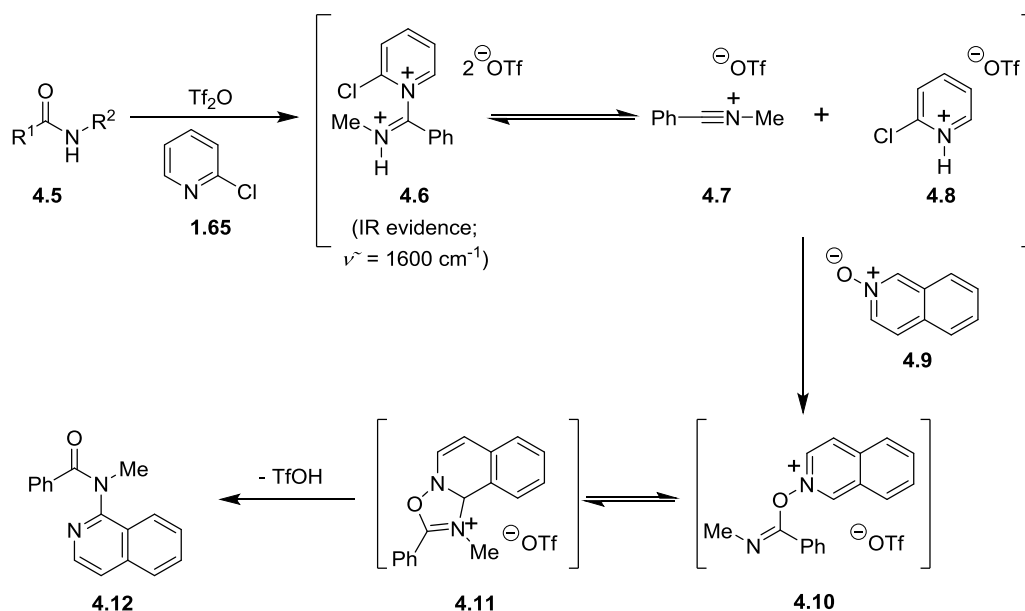


4.4, $m/z = 142$

The extra stability of disalt **4.1** compared to disalts **3.41** and **3.43** (Figure 4.1), as well as allowing NMR and X-ray crystallographic analysis, also allowed analysis by mass spectrometry. Peaks at $m/z = 143.1$ and 143.6 were seen in electrospray, with the latter peak having an intensity of approximately 24% compared to the former peak. As disalt **4.1** has a molecular weight of 286, this shows its presence as a dication in electrospray analysis. The mass at $m/z = 143.1$ corresponds to the m/z ratio of the dication, while $m/z = 143.6$ corresponds to the m/z ratio for the dication incorporating one atom of ^{13}C $[(M+1)/2]$ – the intensity of this peak would be expected to be 22%. There were also more intense peaks at $m/z = 142.1$ and 142.6 , (the latter having an intensity of 22% compared to the former) which would suggest that the disalt had lost hydrogen (H_2) on the instrument to form dication **4.4** (Figure 4.3). High resolution mass spectrometry of disalt **4.1** was attempted by the EPSRC National Mass Spectrometry Service Centre in Swansea; however, they were unable

to obtain any mass spectral data of the disalt (even at low resolution) due to the instability of the disalt in their lab conditions.

Scheme 4.5 Synthesis of amide **4.12** via proposed intermediate **4.6**.



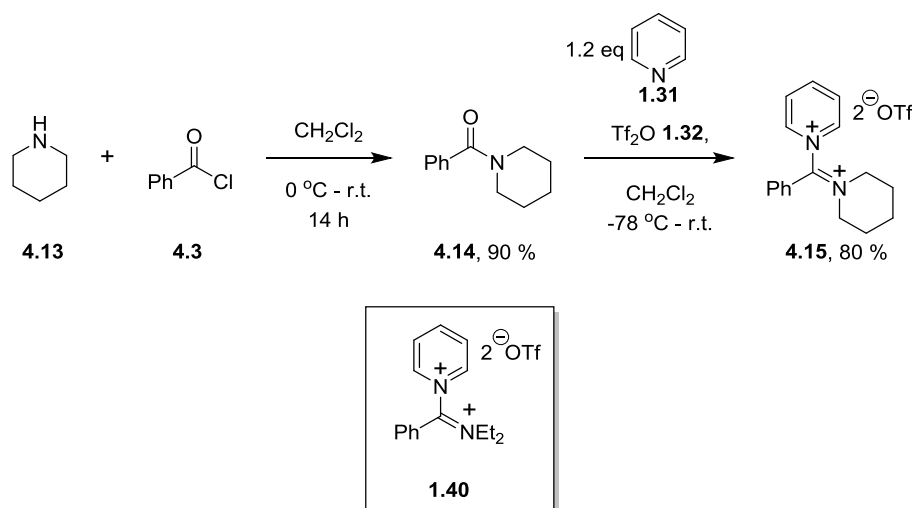
Infrared analysis of disalt **4.1** showed a peak at $\nu = 1601 \text{ cm}^{-1}$. Although this peak may be due to C=C stretching, an infrared absorption peak at 1600 cm^{-1} during the synthesis of of amide **4.12** by Medeley and Movassaghi (Scheme 4.5) was attributed to the amidine group of proposed disalt intermediate **4.6**.³⁶ As such, the characterisation of disalt **4.1** does not just provide further evidence of disalt formation (from amides, amines and triflic anhydride) within the Murphy group, but also for the formation of these species within the work of other research groups, discussed in Chapter 1 Section 4.

4.3 Synthesis of Disalts Related to Disalt 4.1

Following on from the isolation of amidine disalt **4.1**, other disalts were synthesised. The intent of extending the scope of amidine disalts in this series was twofold. Firstly, by extending the synthesis to other substrates, it could be established how broad the scope of the synthetic methodology was. Secondly, substrates more similar to those previously reported by other research groups (discussed in Chapter 1

Section 4) could be synthesised to provide further evidence for such species existing in useful synthetic transformations.

Scheme 4.6 Synthesis of disalt **4.15** related to proposed disalt **1.40**.

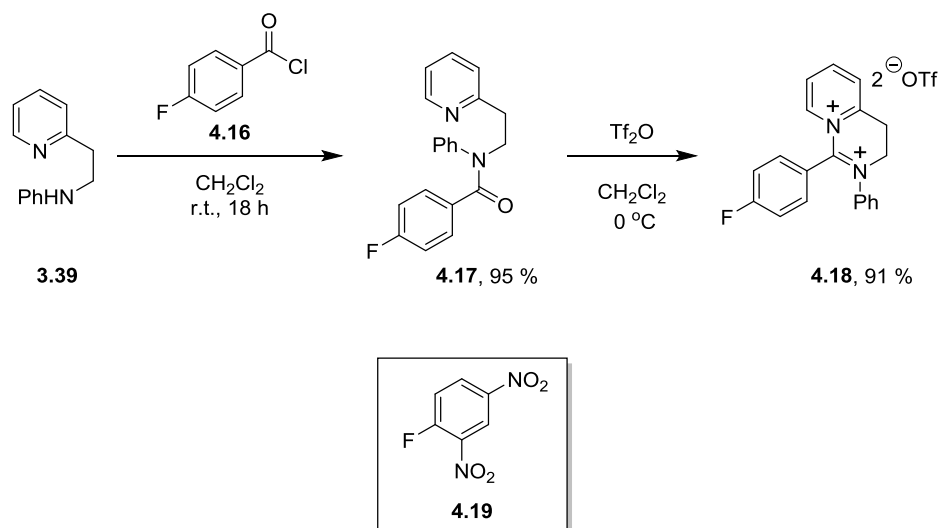


Up to this point, the isolation of a disalt derived from the bimolecular reaction of an amide and an amine (in the presence of Tf_2O **1.32**) had not been carried out; disalts **3.41**, **3.43** and **4.1** had these functional groups as part of the one molecule. Piperidine **4.13** was reacted with benzoyl chloride **4.3** to afford amide **4.14** (Scheme 4.6) in a yield of 90 %. Adding amide **4.14** to a mixture of pyridine **1.31** and triflic anhydride **1.32** (i.e. the mixture that forms triflating agent triflylpyridinium triflate, as proposed by Charette and Grenon)¹⁴ at $-78\text{ }^\circ\text{C}$ and allowing the mixture to warm to room temperature afforded disalt **4.15** which was isolated as a white precipitate. This type of disalt was similar to disalt **1.40** which was proposed as part of a reaction mixture by Charette and Grenon¹⁴ in NMR spectroscopy studies.

Returning to the same motif as disalt **4.1**, disalt **4.18** was synthesised in a related manner (Scheme 4.7); this disalt formed a brown solid in 91 % from amide **4.17**. The synthesis of this disalt provided a fluorobenzene compound, further substituted with an electron deficient dicationic amidine group. Sanger's reagent **4.19** is a well established reagent which has been used to determine the *N*-terminal amino acid

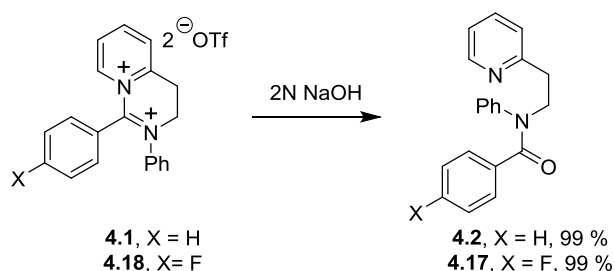
groups in polypeptide chains;¹¹³ in this compound, the C-F bond is attacked by nucleophiles at the carbon centre.

Scheme 4.7 Synthesis of disalt **4.18**.



The reaction of disalt **4.18** with sodium hydroxide, reacted at the amidine centre of the dication, just as it does with disalt **4.1** – both formed the corresponding amide (**4.17** and **4.2**, respectively) in 99 % yield. This showed that the fluoro substitution in **4.18** did not dramatically alter the reactivity of the amidine centre and did not provide a competitive centre where C-F attack related to Sanger's reagent was occurring in a competitive process.

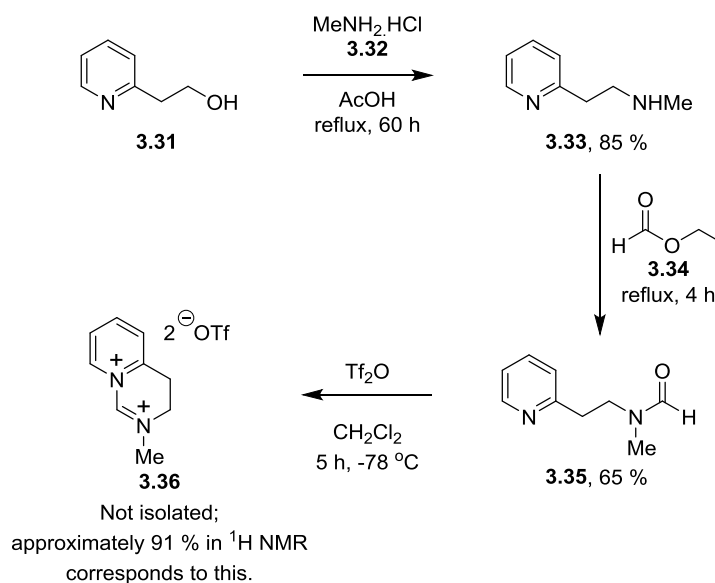
Scheme 4.8 Reaction of NaOH with disalts **4.1** and **4.18**.



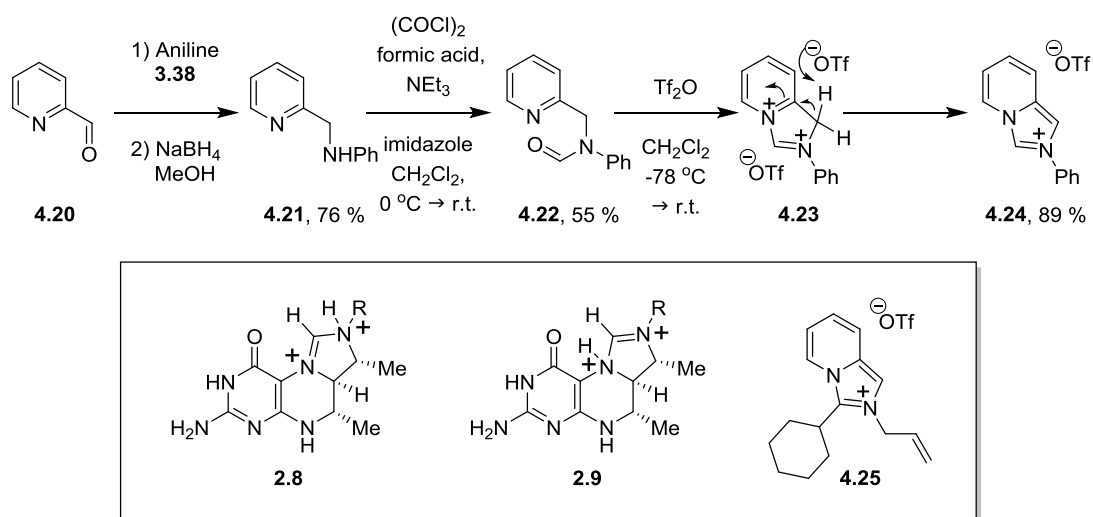
The synthesis of disalt **3.36** had previously been attempted by Godin,¹¹¹ with disalt **3.36** being proposed to be present in 68 % within an inseparable mixture of compounds. As the handling of related amidine disalts had been refined so as to allow a compound that could be crystallised for X-ray diffraction analysis (i.e. disalt

4.1), the attempt at synthesising disalt **3.36** was revisited. Disalt **3.36** was not isolated pure, but was now observed to be the main component at 91 % (by ^1H NMR) of the final mixture (this percentage was estimated from comparing the intensity of singlets in the alkyl chemical shift region, as carried out by Godin).¹¹¹

Scheme 4.9 The synthesis of disalt **3.36**, with an improved conversion over previous attempts.



Scheme 4.10 Synthesis of amidine monosalt **4.24** via intermediate **4.23**.

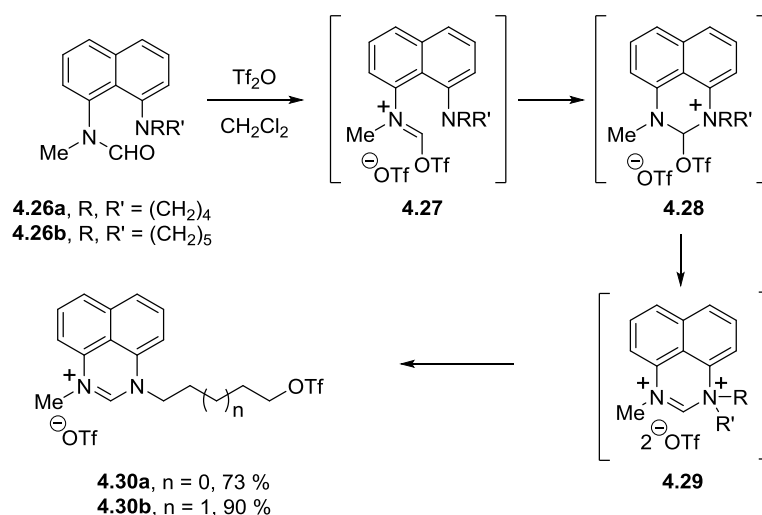


As discussed in Chapters 2 and 3, it had been proposed that [Fe]-hydrogenase may promote the formation of amidine dications **2.8** or **2.9** (Scheme 4.10). As these dications contained the amidine group as part of a five-membered ring, disalt **4.23** was proposed as a good analogue of these dications for use in model reactions.

Pyridine-2-carboxaldehyde **4.20** was reductively aminated with aniline **3.38** to form amine **4.21**. This amine was then formylated to give amide **4.22** using the conditions developed by Corr,²⁷ based on the reported formylation method of Kitagawa *et al.*¹¹⁴ Treatment with triflic anhydride then afforded monosalt **4.24** in 89 % yield. This monosalt most likely formed from disalt **4.23**, with the methylene group attached to the 2-position of the pyridine deprotonated by a triflate anion. This would then form aromatic monocation **4.24**. Since carrying out this reaction, Charette *et al.*¹¹⁵ carried out the synthesis of imidazo[1,5-*a*]azines from amides and triflic anhydride; this work included the synthesis of monocation **4.25** which most likely proceeded through a disalt related to **4.23**. As disalt **4.23** was not isolable, such a dication could not be used in model studies of [Fe]-hydrogenase reactivity.

Within the Murphy group, other members of the group have also attempted to form amidine disalts with the amidine centre being part of a heterocyclic ring. Kovacevic¹¹⁶ attempted the synthesis of naphthalene-derived amidine disalt **4.29** (Scheme 4.11); however amidine monosalts **4.30** were formed. The formation of monosalts **4.30** was modeled computationally, and suggested that disalts **4.29** were reaction intermediates on the way to these compounds. The amidine dications were so electrophilic, that dealkylation occurred with triflate anion as a nucleophile.

Scheme 4.11 Formation of amidine monosalts **4.30** *via* disalts **4.29**.

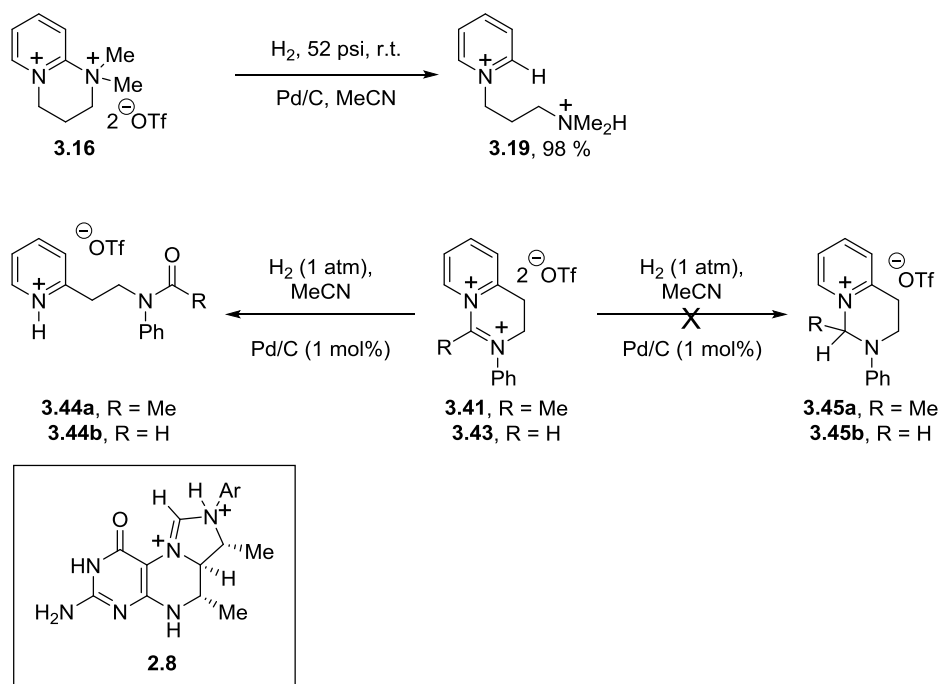


4.4 Initial [Fe]-Hydrogenase Model Reactions

As discussed in Chapter 3, Corr²⁷ carried out the successful hydrogenation reaction of amidine disalt **3.16** using palladium catalysis and 52 psi hydrogen pressure. When attempting to carry out the hydrogenation of amidine disalts **3.41** and **3.43**, no hydrogenation product was observed at atmospheric pressures, but hydrolysis to amide pyridinium salts **3.44** (Scheme 4.12) was seen.

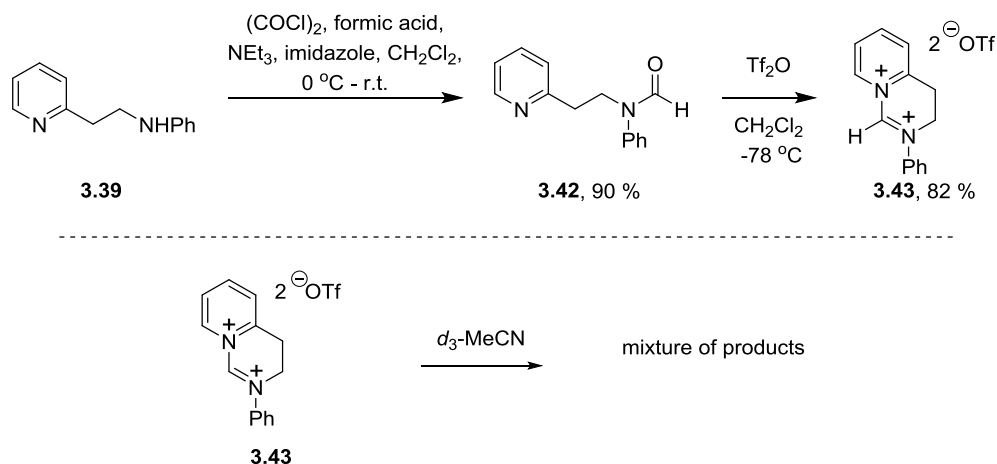
As disalts **3.41** and **3.43** were designed to be more reactive than disalt **3.16**, it was expected that hydrogenation should be achievable with this series of disalts. This area of work was revisited, with the focus being on formamide-derived disalt **3.43**.

Scheme 4.12 Hydrogenation reaction of **3.16** and attempted hydrogenation reactions of **3.41** and **3.43**.



4.4.1 Hydrogenation Under 1 Atmosphere of Hydrogen

Scheme 4.13 Synthesis of disalt **3.43** followed by decomposition in dry d_3 -MeCN.

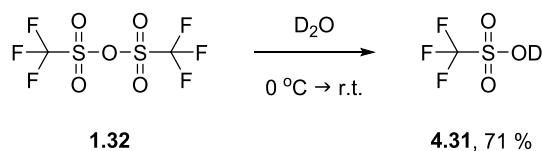


To further understand the decomposition of disalt **3.43** to amide **3.44b** (Scheme 4.12), the stability of disalt **3.43** in acetonitrile (the previously used hydrogenation solvent) was investigated. Firstly, this disalt was synthesised using the conditions employed by Corr²⁷ (Scheme 4.13). By placing disalt **3.43** in d_3 -acetonitrile, the decomposition of the salt was monitored by ^1H NMR (Scheme 4.13). The NMR solution was prepared within an inert atmosphere glovebox and a sample was removed and analysed after 2 h; approximately 77 % of the disalt was observed to remain. After 17 h, another sample was removed from the glovebox, showing approximately 35 % of the disalt to still remain. In both cases, the decomposition products were not isolated or identified, but were presumed to occur due to acetonitrile acting as a nucleophile to the disalt. Deuterated trifluoroacetic acid was also investigated as a potential solvent and, again, the disalt was found to decompose – in this case, no disalt was observed after 17 h.

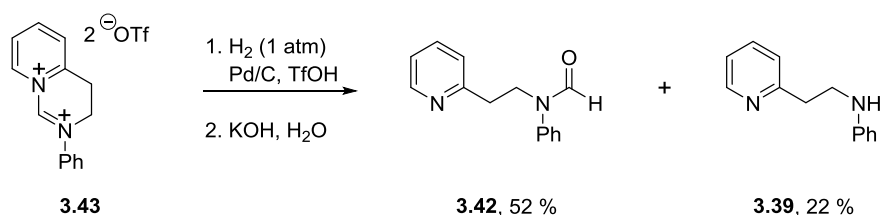
As a superacid, triflic acid is very weakly nucleophilic. As well as being available from commercial sources, d_1 -triflic acid **4.31** can be prepared easily from triflic anhydride **1.32** and deuterium oxide (Scheme 4.14).¹¹⁷ Using a slight excess of triflic anhydride **1.32**, d_1 -triflic acid **4.31** was isolated in a yield of 71 % after distillation. Disalt **3.43** was then found to be stable to d_1 -triflic acid **4.31**; a sample was kept in a sealed (nitrogen atmosphere) NMR tube for over 1 month at standard

temperature and pressure and was not observed to decompose by ^1H NMR over this time.

Scheme 4.14 Preparation of d_1 -triflic acid **4.31**.

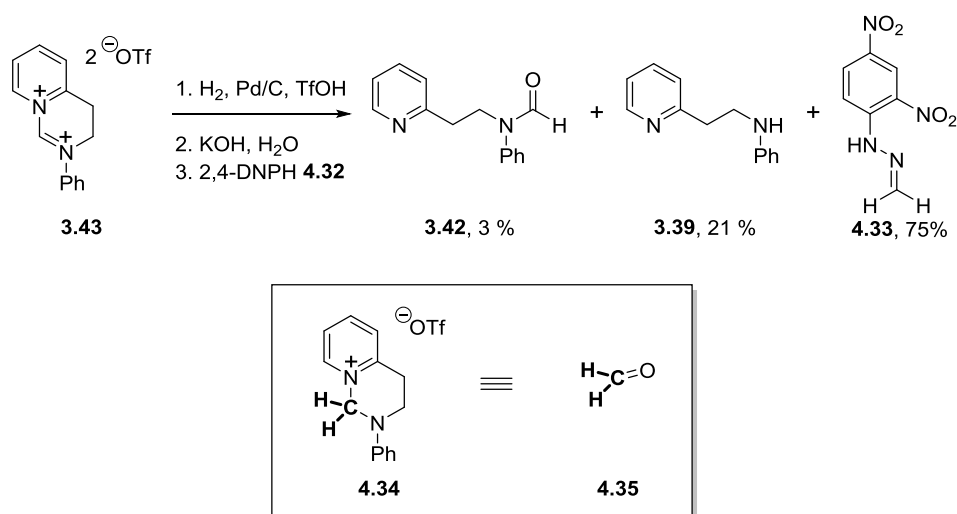


Scheme 4.15 Hydrogenation and/or hydrolysis of disalt **3.43**.



Disalt **3.43** was reacted with hydrogen (1 atm) and palladium on carbon, in triflic acid for 48 h. As this mixture was heterogeneous and triflic acid is highly corrosive, it was deemed easiest to work this reaction mixture up with a basic solution to determine what products could be observed. After reacting with potassium hydroxide, extracting with ethyl acetate and carrying out column chromatography, amide **3.42** (52 %) and amine **3.39** (22 %) were isolated (Scheme 4.15, Table 4.1 Entry 1). Both of these products could be expected to be observed from the hydrolysis of disalt **3.43** and the hydrolysis of **3.42**.

However, amine **3.39** could also result from hydrolysis of the likely product of successful hydrogenation **4.34** (Scheme 4.15). To establish whether or not hydrogenation was occurring with disalt **3.43** rather than just hydrolysis, 2,4-DNPH **4.32** was employed to derivatise the formaldehyde-equivalent **4.34** that could form from the reduction of **3.43**. After reacting disalt **3.43** under hydrogen (1 atm) in triflic acid, the reaction mixture was worked-up with potassium hydroxide. The solution was then made acidic to approximately pH = 5 (with HCl) before the addition of 2,4-DNPH **4.32** afforded amide **3.42** (3 %), amine **3.39** (21 %) and hydrazone **4.33** [(75 %) Scheme 4.15, Table 4.1 Entry 2]. Due to the detection of hydrazone **4.33**, reduction of **3.43** to **4.34** was most likely to have occurred under these conditions.

Scheme 4.15 Hydrogenation reaction of **3.43**.Table 4.1 Various reactions of disalt **3.43**.

Entry	Hydrogen	Catalyst	2,4-DNPH	Product yield (%)		
				3.42	3.39	4.33
1	1 atm	1 mol% Pd/C	None	52	22	n/a
2	1 atm	1 mol% Pd/C	1.6 eq	3	21	75
3	1 atm	none	2.0 eq	12	49	0
4	none	none	2.0 eq	13	57	0

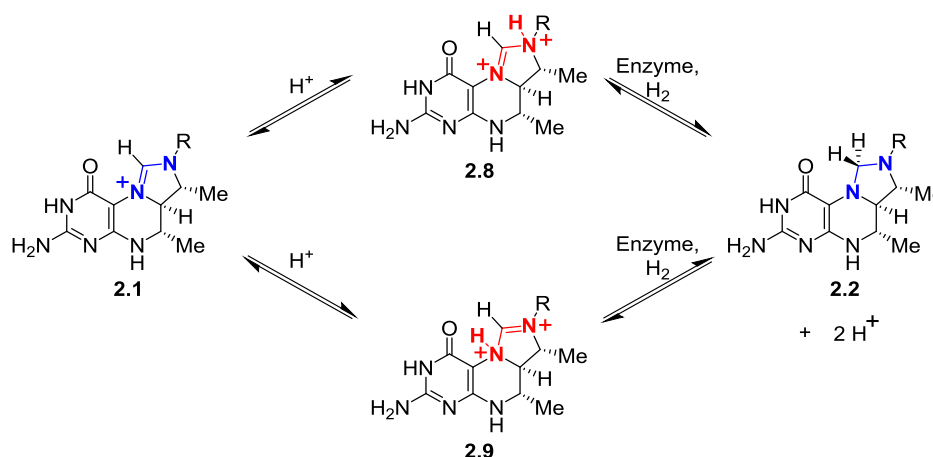
The successful hydrogenation reaction was then followed by two control reactions (Table 4.1 Entries 3 and 4). One reaction (Table 4.1 Entry 3) in which no catalyst was used, in the presence of 1 atmosphere of hydrogen afforded amide **3.42** (12 %) and amine **3.39** (49 %) without forming hydrazone **4.33**. This suggested that the palladium catalyst was essential for hydrogenation of **3.43** in the presence of 1 atm of H₂ at room temperature. The second control experiment (Table 4.1 Entry 4) involved the use of no hydrogen or catalyst. Under an atmosphere of argon, again no hydrazone **4.33** was isolated and amide **3.42** (13 %) and amine **3.39** (57 %) were isolated.

As the reactions catalysed by Pd/C involved a heterogeneous catalyst, the reduction of disalt **3.43** was also attempted with Wilkinson's catalyst in deuterated triflic acid so that any possible reduction products could be followed by NMR. Over a period of 5 days, reduction products such as **4.34** (Scheme 4.15) were not observed. This

suggested that traditional homogenous catalysts for reduction may not be suitable for reacting with amidine disalt **3.43**. The focus of investigations then moved on to attempting catalyst-free hydrogenations at higher pressures than 1 atm of hydrogen.

4.4.2 High Pressure Hydrogenation

Scheme 4.16 Proposed superelectrophilic activation in [Fe]-hydrogenase.



After the success of Pd-catalysed hydrogenation of disalt **3.43** under 1 atm of H_2 , attempts were then made at carrying out a hydrogenation without palladium catalyst. It was originally proposed by Berkessel and Thauer⁷¹ (as mentioned in Chapter 2) that if $CH\equiv H_4MPT^+$ **2.1** (Scheme 4.16) was protonated in [Fe]-hydrogenase to form a dication (**2.8** or **2.9**), that the resulting species could be reactive enough to spontaneously react with H_2 in a metal-free process. This was prior to the discovery by Thauer and co-workers⁵⁷ that [Fe]-hydrogenase was a metalloenzyme; however, it was still of interest in the Murphy group to know if it was possible for an amidine disalt to be sufficiently activated to spontaneously react with H_2 in a metal-free process.

As the control experiments of **3.43** in H_2 without Pd/C catalyst did not afford any reduction under 1 atm of H_2 , high-pressure, metal-free hydrogenation reactions were attempted with disalt **3.43**. A Baskerville Compact Mini (hydrogenation) Reactor was used with a Teflon[®] insert – this insert prevented contact of the reaction mixture placed within it with the metallic structure of the Reactor (minimising potential for metal-catalysed processes). This reactor and the insert were reserved solely for these catalyst-free reactions to prevent potential for contamination. Reactions were

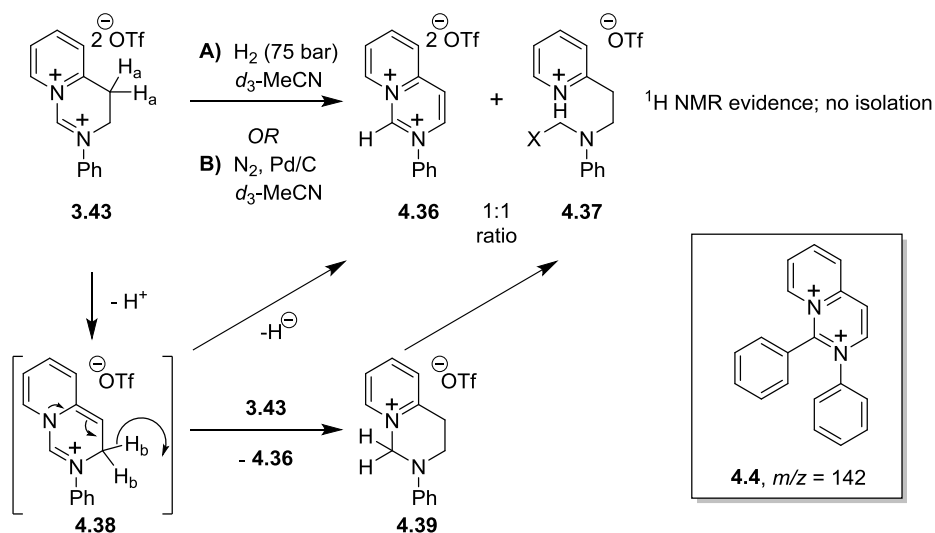
prepared in a dry, nitrogen-atmosphere glovebox before being sealed, removed and connected to a hydrogen cylinder (Conditions A, Scheme 4.17). Disalt **3.43** was reacted in deuterated acetonitrile for 7 days under 75 bar of H₂. Analysis of the resulting solution by ¹H NMR followed by DEPT and HSQC suggested two main products had been formed within a mixture. One product had a singlet at 4.22 ppm in ¹H NMR which was assigned to a methylene signal (corresponded to a ¹³C signal at 49.0 ppm). Nuclear Overhauser effect (nOe) studies of the singlet showed an effect with a signal corresponding to the *ortho* protons of a phenyl ring, while no signal was seen due to nOe with pyridine signals. As such, structure **4.37** was proposed to be part of the mixture (the X-group was unknown). The second component of the reaction mixture was proposed to be disalt **4.36**. This was proposed due to an increase in the integration of aromatic signals in ¹H NMR. No further analysis was obtained of this reaction mixture; however an attempt was carried out at using 2,4-DNPH **4.32** to isolate a formaldehyde-equivalent. This derivatisation, however, did not afford formaldehyde-equivalent **4.33** as seen in the Pd-catalysed hydrogenation reaction. Despite not isolating either **4.36** and **4.37**, the relative integration of the compound containing the methylene signals (**4.37**) compared to the additional aromatic signals, suggested a 1:1 ratio for both compounds.

The formation of the mixture of **4.36** and **4.37** was proposed to occur *via* initial deprotonation of a methylene on disalt **3.43** to afford monosalt **4.38**. One equivalent of monosalt **4.38** could then react with one equivalent of disalt **3.43** to afford dehydrogenated product **4.36** as well as a methylene product **4.39** which could then go on to form a salt such as **4.37**, where possible nucleophiles could be triflate or *d*₃-MeCN-derived.

As proposed monosalt **4.37** had been suggested based on detailed NMR studies, while disalt **4.36** was only suggested based on the increase in integration within the aromatic region in ¹H NMR, further evidence was sought to prove that **4.36** could have been forming. Previously, dehydrogenated disalt **4.4** had been observed in (electrospray) mass spectroscopy of disalt **4.1**. If disalt **3.43** could dehydrogenate to **4.36** under high pressure under an atmosphere of hydrogen, it was postulated that Pd/C could encourage the formation of such a species without the presence of hydrogen. Employing an atmosphere of nitrogen and using Pd/C in deuterated

acetonitrile (Conditions B, Scheme 4.17), the same mixture of products was observed by ^1H NMR as observed in the metal-free and high-pressure hydrogen reaction.

Scheme 4.17 Reactivity of disalt **3.43** under **A)** 75 bar of H_2 and **B)** an atmosphere of nitrogen in the presence of Pd/C.



As disalt **3.43** showed a competitive dehydrogenative reactivity to reduction with hydrogen, a new disalt was sought to enable further model studies of [Fe]-hydrogenase reactivity. The next chapter will go on to discuss a new type of disalt that could facilitate [Fe]-hydrogenation model studies, without such side-reactions, i.e. a new series of amidine disalts that do not have the potential to undergo oxidation.

4.5 Chapter 4 Summary

This work presented in this Chapter demonstrates the first definitive evidence of the formation of an amidine dication derived from an amide, with the successful characterisation of disalt **4.1** by X-ray crystallisation. As such, the initial aim that provided a basis for this project was successfully met.

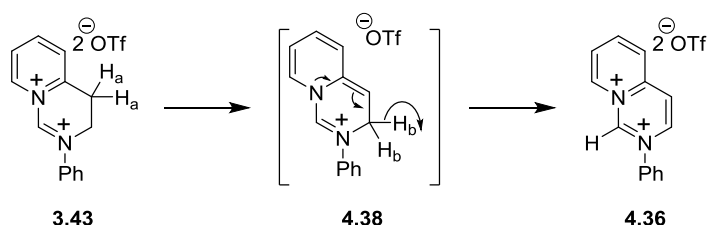
Although other disalts related to disalt **4.1** were synthesised and isolated – disalts **4.15** and **4.18** – no [Fe]-hydrogenase related reactivity was observed with these disalts. The disalt **3.43** first isolated (but not fully characterised) by Corr²⁷ was then

adopted for [Fe]-hydrogenase model reactions. Although successful Pd-catalysed hydrogenation reaction of amidine disalt **3.43** under 1 atm of hydrogen was demonstrated (an improvement compared to previous Pd-catalysed amidine disalt reductions),²⁷ Pd-free reactions showed that disalt **3.43** could be oxidised. So although the first of the project aims was met, the remaining objectives were to be further studied.

Chapter 5: Results and Discussion; Development of Amidine Disalts That Do Not Undergo Oxidation

As discussed in Chapter 4, disalt **3.43** has been proposed to dehydrogenate to form disalt **4.36**. The purpose in synthesising disalt **3.43** was to provide a compound to carry out model studies of [Fe]-hydrogenation reactivity, i.e. to undergo reduction of an amidine centre. As dehydrogenation was a competing reaction possibly occurring with disalt **3.43**, an alternative series of disalts was sought. To come up with an appropriate modification, the possible mechanism for the dehydrogenation of disalt **3.43** to disalt **4.36** can be considered (Scheme 5.1). The initial step is likely to involve deprotonation of a methylene group (one of 2 x H_a) to form monosalt **4.38**. Loss of a hydride from the neighbouring methylene (one of 2 x H_b) could then afford oxidized disalt **4.36**. To prevent the oxidation of disalt **3.43**, substitution at both of the methylene positions (H_a and H_b) could afford the basis of a new non-oxidising amidine disalt.

Scheme 5.1 Path to Dehydrogenation of Disalt **3.43**.

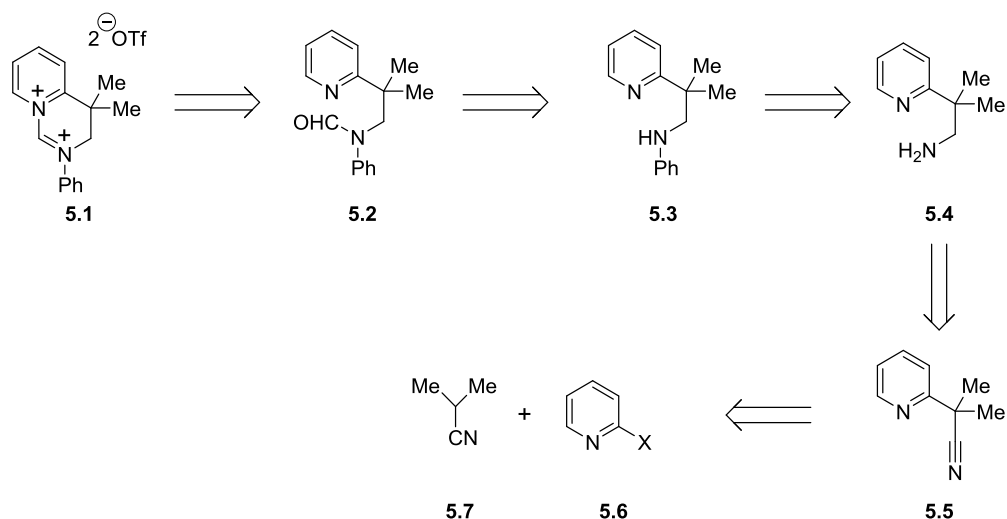


5.1 The Synthesis of a Disalt That Does Not Undergo Oxidation

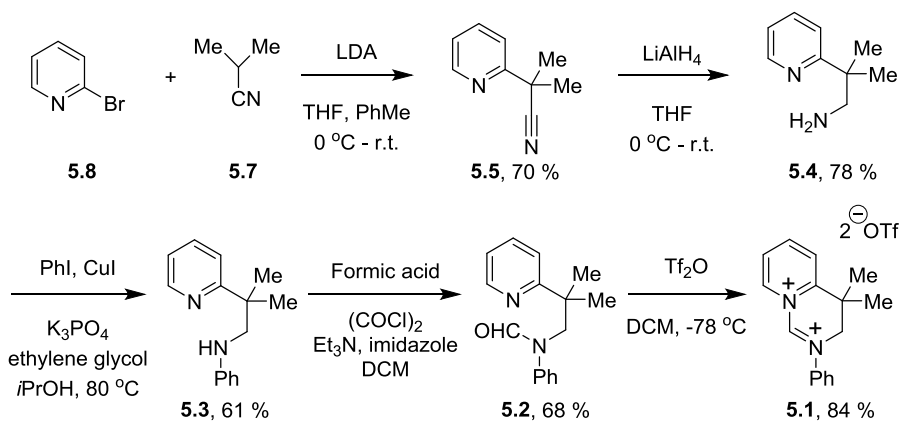
The synthesis of disalt **5.1** (Scheme 5.2) was proposed; the two *gem*-dimethyl groups of this disalt would prevent the deprotonation that enabled the dehydrogenation of disalt **3.43**. Similarly to the progenitor compound **3.43**, disalt **5.1** could be synthesised by treatment of the corresponding amide **5.2** with triflic anhydride. As before, formamide **5.2** could be synthesised from the corresponding aniline **5.3**. The aniline could be synthesised from primary amine **5.4** which, in turn, could be formed

from isobutyronitrile **5.7** and 2-halopyridine **5.6** via nitrile **5.5**. The two starting materials (**5.6** and **5.7**) are readily available, commercial materials.

Scheme 5.2 Retrosynthesis of disalt **5.1**.



Scheme 5.3 Synthesis of disalt **5.1** from commercial starting materials **5.7** and **5.8**.



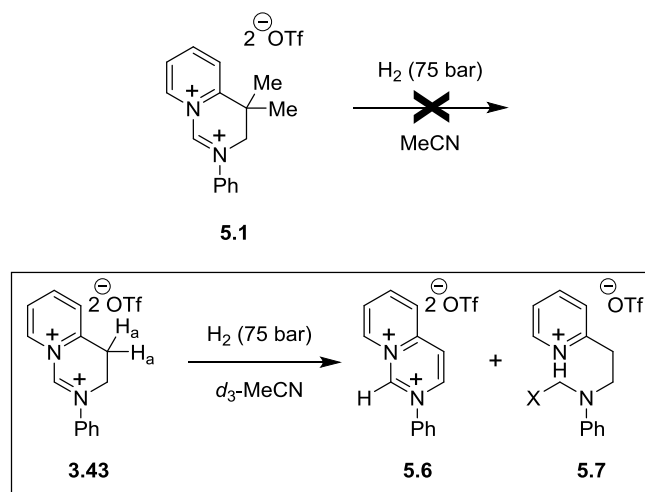
By preparing a fresh solution of LDA in THF and adding this to a toluene solution of 2-bromopyridine **5.8** and isobutyronitrile **5.7**, nitrile **5.5** was isolated in 70 % yield (Scheme 5.3). Nitrile **5.5** was then reduced with 2.2 equivalents of LiAlH_4 to afford primary amine **5.4** in a 78 % yield. By using the Ullman coupling conditions outlined by Buchwald and co-workers,¹¹⁸ aniline **5.3** was isolated in a yield of 61 %.

Using the conditions outlined to form disalt **3.43**, disalt **5.1** was synthesised in two steps *via* amide **5.2**.

Disalt **5.1**, unlike disalt **3.43**, was found to be stable in solution with d_3 -MeCN at room temperature under nitrogen (samples were left in solution for over a month and found to be stable). In the solid state, the disalt was found to be bright yellow and only partially soluble in acetonitrile (although it was sufficiently soluble in order to obtain ^1H , ^{19}F and ^{13}C NMR spectra).

Disalt **5.1**, like disalt **3.43**, was placed in acetonitrile for 7 days under 75 bar of dihydrogen. Whereas disalt **3.43** reacted to form a mixture of products under such conditions, disalt **5.1** did not react and pure starting material was recovered in 100 % yield (Scheme 5.4).

Scheme 5.4 Reactivity of disalt **5.1** in 75 bar of H_2 compared to the disproportionation reactivity of disalt **3.43**.

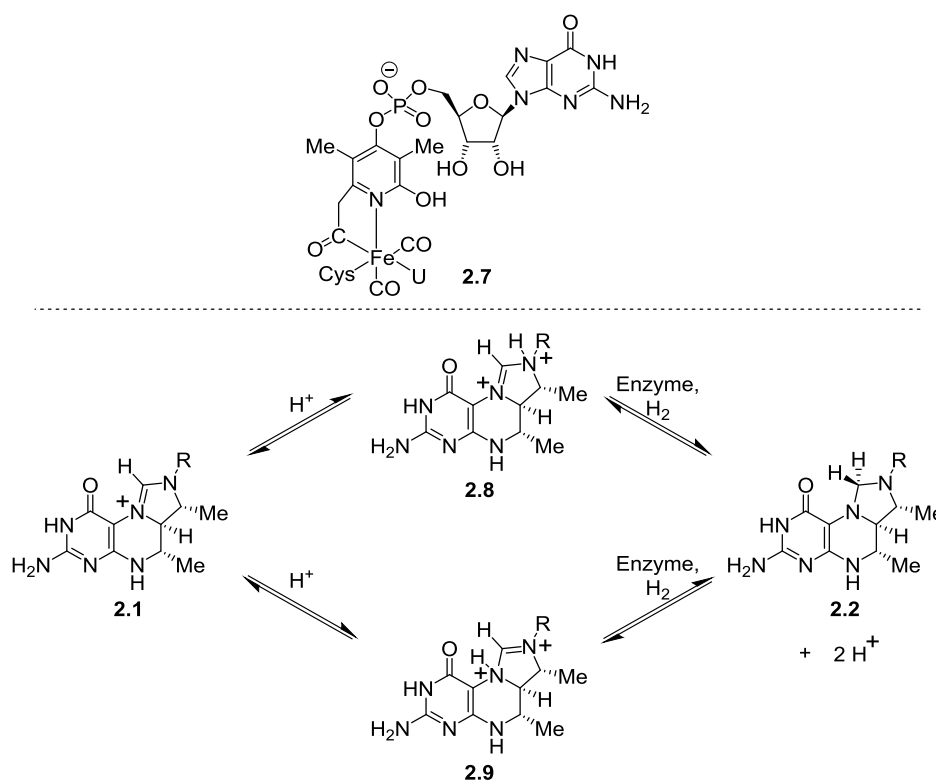


5.2 Reaction of Disalt **5.1** with Triethylsilane

After it was found that disalt **5.1** was stable to dihydrogen at high pressures, it was concluded that if a related dication (**2.8** or **2.9**) was present within the mechanism of the [Fe]-hydrogenase reaction (Scheme 5.5), then it was very unlikely to be reactive enough to abstract a hydride from dihydrogen without activation. The FeGP cofactor

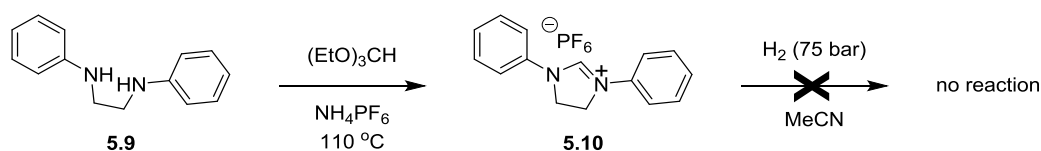
2.7 is the most likely source of dihydrogen activation in [Fe]-hydrogenase (possibly initiated from dihydrogen coordinating to the iron centre); the activated species that is formed may then be reactive enough to reduce monocation **2.1**. As a working hypothesis, it was assumed that the activation of dihydrogen proceeded with the formation of an iron hydride (similar to Hall's second proposal).⁷⁶

Scheme 5.5 FeGP cofactor **2.7** and the possible mechanism involved in the activation of [Fe]-hydrogenase substrate **2.1**.



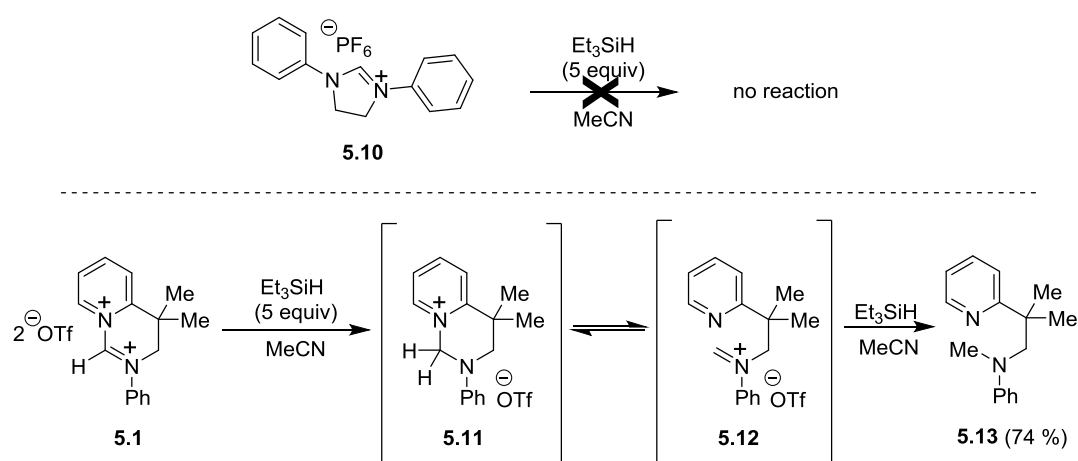
Before reacting disalt **5.1** with an iron hydride source, some other reactions were designed to give a more complete picture of the reactivity difference between amidine monosalts related to **2.1** and amidine disalts related to **2.8** and **2.9**. Firstly, monosalt **5.10** (as for disalt **5.1**) was subjected to catalyst-free hydrogenation conditions, with complete recovery of starting material (Scheme 5.6). This compound was prepared from commercially *N,N'*-diphenylethylenediamine **5.9**

Scheme 5.6 Synthesis of monosalt **5.10** and its stability towards 75 bar of dihydrogen.

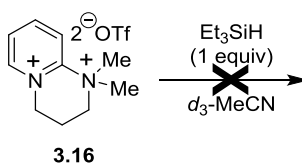


The reactivity of monosalt **5.10** and disalt **5.1** was then studied towards a well defined source of hydride that is used to react with cationic species; triethylsilane is well known as a cation scavenger.¹¹⁹ Monosalt **5.9** was found to be unreactive towards an excess of triethylsilane at room temperature in acetonitrile, while disalt **5.1** was reduced to *N*-Me aniline **5.13** (Scheme 5.7) in a yield of 74 %. The reduction of disalt **5.1** could be envisioned to go through methylene species **5.11** which, in turn, could form iminium cation **5.12**. This could then accept a second hydride to form *N*-methyl aniline **5.13**.

Scheme 5.7 Reaction of triethylsilane with monosalt **5.9** and disalt **5.1**.



Scheme 5.8 Disalt **3.16** treated with triethylsilane.

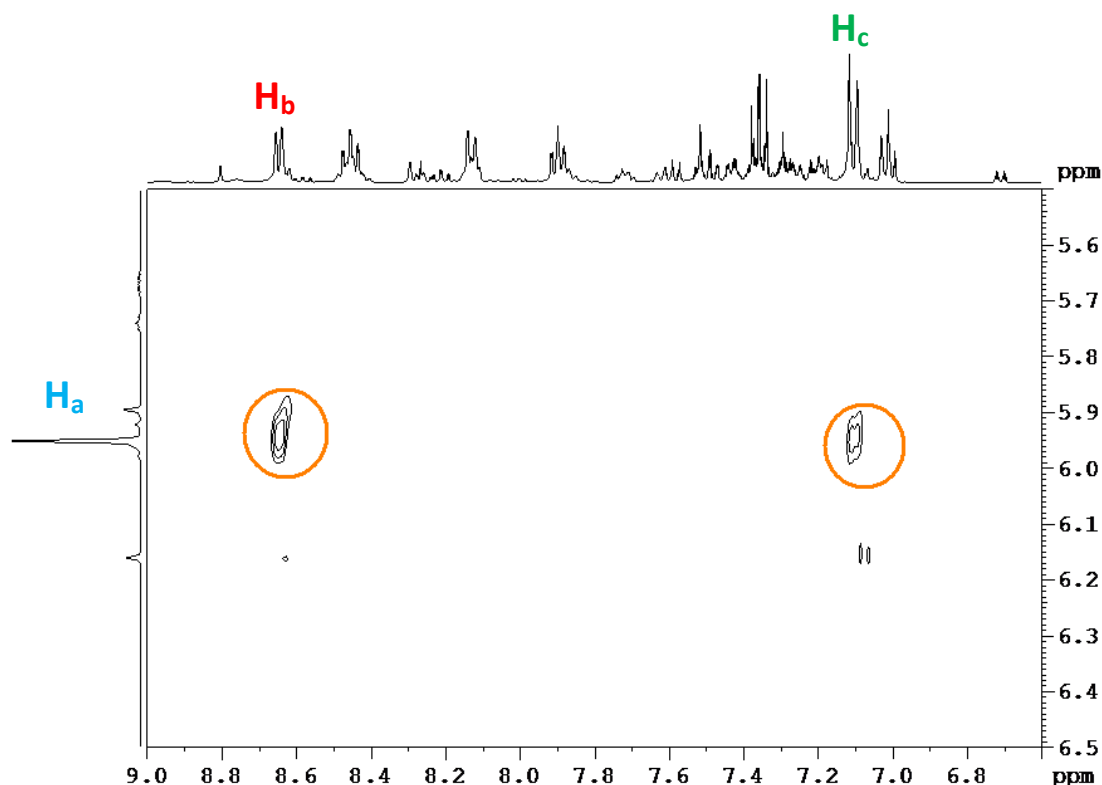


This marked difference between monosalt **5.10** and disalt **5.1** then prompted an interest in how disalt **3.16**, previously published by Corr *et al.*,^{72,73} would react towards triethylsilane. This disalt has the amidine carbon centre as part of an aromatic ring and, as such, should be less reactive than disalt **5.1**. Indeed, disalt **3.16** was found to be completely unreactive towards triethylsilane with the disalt starting material being completely recovered, after a 24 h reaction in deuterated acetonitrile. Proposed disalts **2.8** and **2.9**, that may be present in [Fe]-hydrogenase, do not contain the amidine carbon centre as part of an aromatic ring; the lack of reactivity of disalt **3.16** with triethylsilane compared with the reactivity observed with disalt **5.1**,

highlights the importance in the recent development of amidine disalts such as disalt **5.1**. Disalt **5.1** should provide a much better basis for model studies of [Fe]-hydrogenase reactivity than disalt **3.16**.

To further understand the mechanism involved in the reduction of disalt **5.1** to *N*-Me aniline **5.13** (Scheme 5.7), the reaction was repeated as an NMR experiment in deuterated acetonitrile with 1 equivalent of silane (Scheme 5.8). After approximately 14 minutes of monitoring by ^1H NMR spectroscopy, disalt **5.1** was completely consumed and a species corresponding to monosalt **5.11** was observed. HSQC analysis showed that a singlet found at 5.93 ppm in ^1H NMR correlated to a ^{13}C signal at 72 ppm. DEPT-Q135 NMR then established this signal to belong to a CH_2 signal. Two cross-correlation peaks were observed by NOESY (Figure 5.1); one corresponded to the nOe of H_a interacting with the *ortho*-phenyl protons H_b and the other corresponded to H_a interacting with the *ortho* proton H_c of the pyridinium ring.

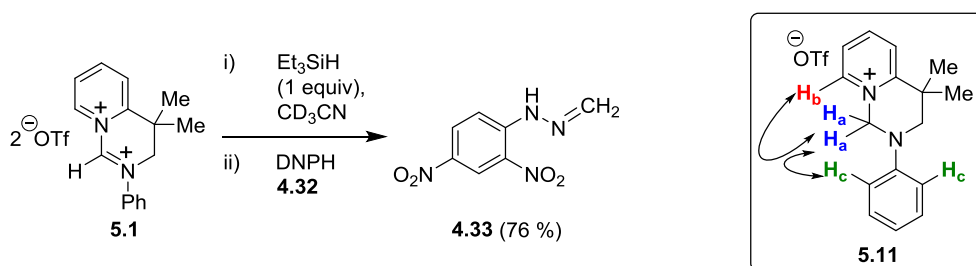
Figure 5.1 Section of NOESY spectra from reaction of disalt **5.1** with triethylsilane.



After carrying out these NMR spectroscopy studies, the reaction sample was worked up with 2,4-DNPH **4.32** to afford formaldehyde-equivalent **4.33**. This gave

additional evidence that a methylene compound was forming in the reaction mixture between disalt **5.1** and triethylsilane. As such, the steps through monocations **5.11** and **5.12** would seem likely on the way to form *N*-Me aniline **5.13** in the presence of an excess of triethylsilane.

Scheme 5.8 Reaction of disalt **5.1** with 1 equivalent of triethylsilane.



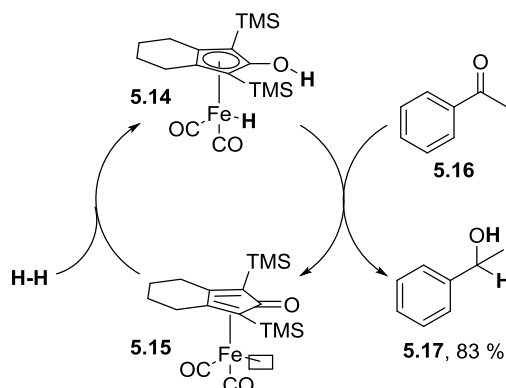
These results with triethylsilane highlight the enhanced reactivity of amidine disalts related to **5.1** compared to monosalts such as **5.10** and disalts such as **3.16**. It was then of interest to examine the reactivity of disalt **5.1** towards an iron-hydride source, which may be more representative of the reaction occurring in [Fe]-hydrogenase.

5.3 Reaction of Disalt **5.1** with an Iron Hydride

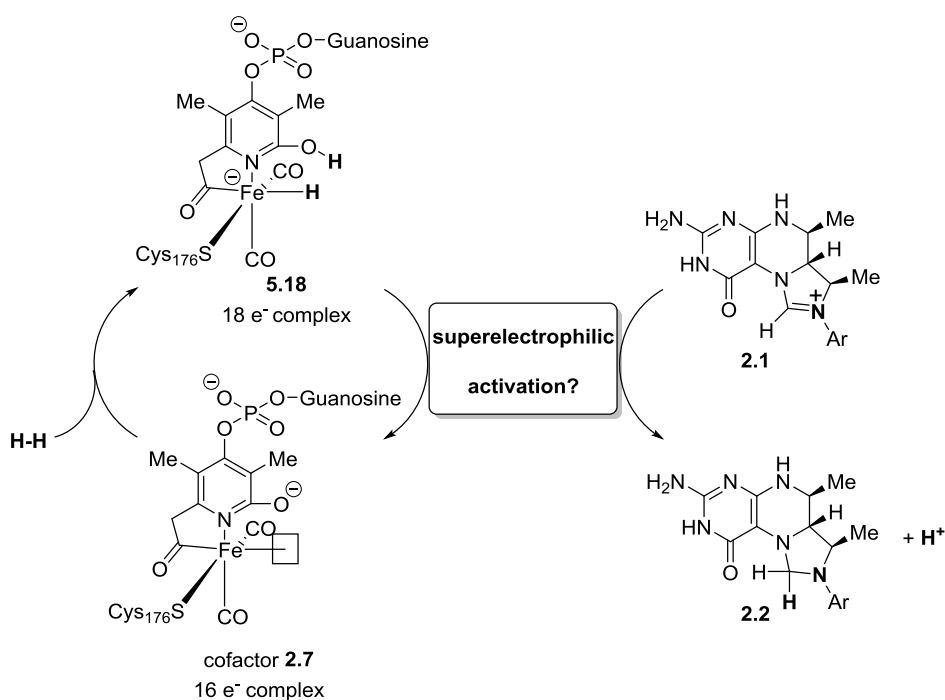
As discussed in Chapter 2 and intimated in Section 5.2, FeGP cofactor **2.7** (Scheme 5.7) is a possible source of dihydrogen activation within [Fe]-hydrogenase. This activation may occur through the formation of an iron hydride, as proposed by Yang and Hall.⁷⁶ Iron hydride complexes have been prepared and studied in various catalytic processes.¹²⁰ When considering how FeGP **2.7** may activate hydrogen and the possible iron hydride complex formed, it is worth considering how some of these processes operate; catalyst **5.14** has been used in the reduction of ketones and aldehydes to the corresponding alcohols (Scheme 5.9).^{121,122} The authors suggest that the hydroxyl hydrogen of **5.14** activates ketone **5.15** through protonation/hydrogen bonding so that the hydrogen attached to the iron can nucleophilically attack at the carbon of the ketone as a hydride. Once reacted, the free site on the iron allows complex **5.15** to bind another molecule of hydrogen,

which cleaves to reform active species **5.14**, where one of the hydrogens is formally a proton and the other is formally a hydride.

Scheme 5.9 Hydrogenation of ketone **5.15** catalysed by iron hydride **5.14**.



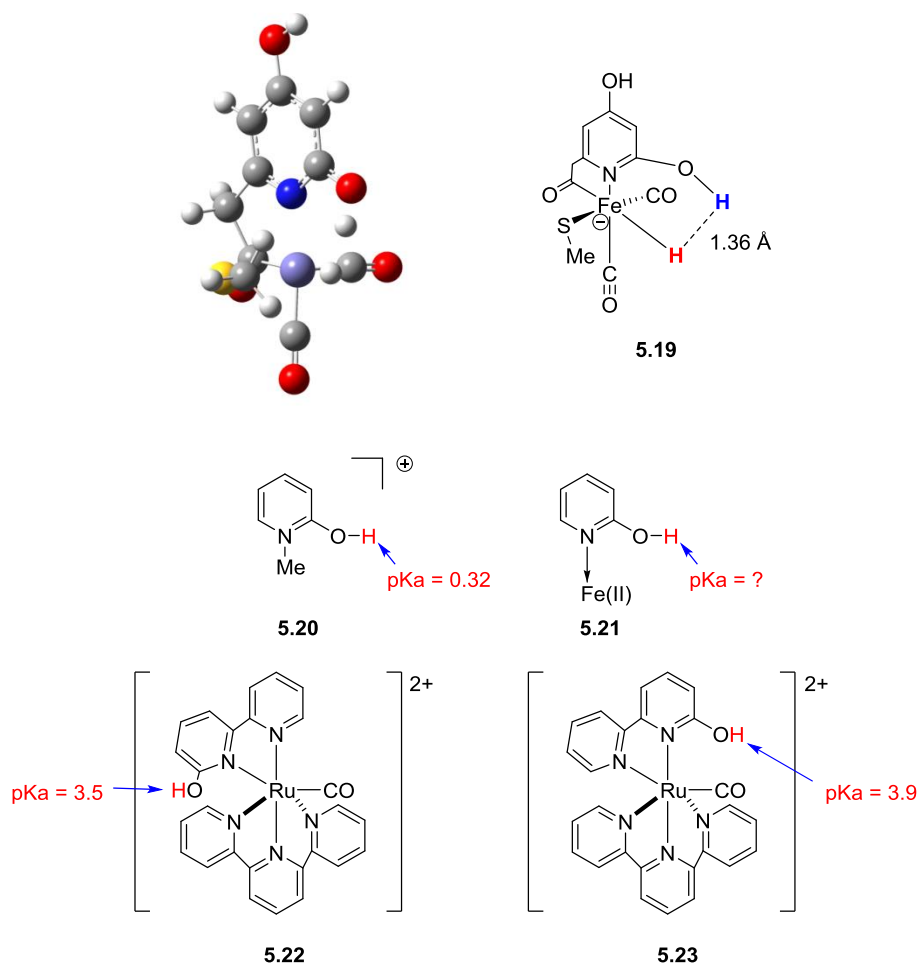
Scheme 5.10 Proposed iron hydride **5.18**, formed from the activation of hydrogen by FeGP cofactor **2.7**.



A similar mechanism can be proposed for [Fe]-hydrogenase (Scheme 5.10) and is almost the same as the mechanism proposed by Hall for this enzyme;⁷⁶ the most significant difference is removal of Cys₁₇₆-protonation. In this proposal, the hydrogen would bind to the empty site of cofactor **2.7** and then undergo cleavage so as to form iron hydride **5.18**, with the proton now existing on the hydroxyl of what

had been the pyridinium alkoxide ligand. This proton could protonate or hydrogen-bond to substrate **2.1** and form a superelectrophilic species such as **2.8** or **2.9** (Scheme 5.5).

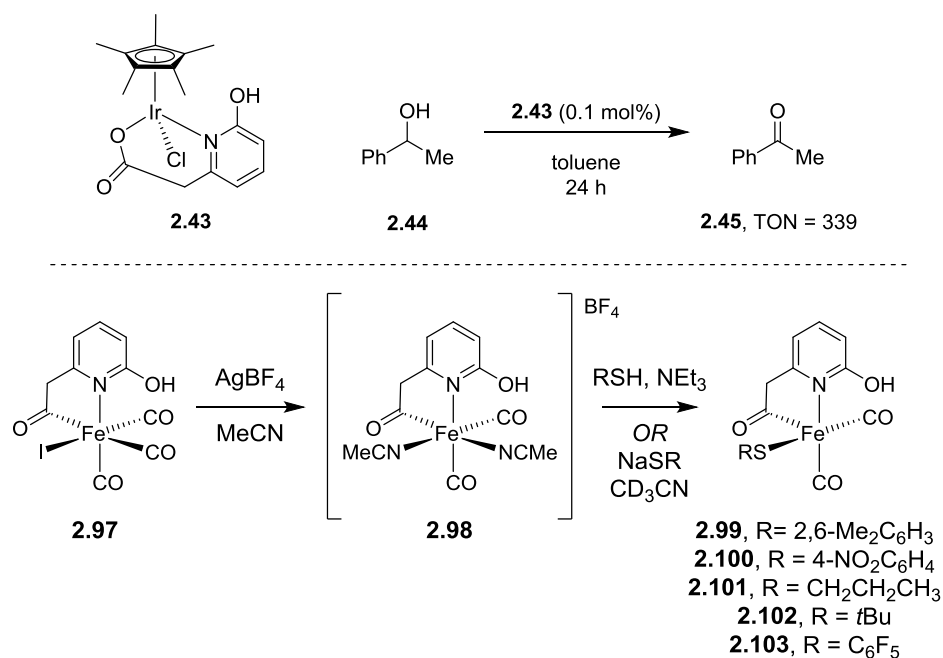
Figure 5.2 DFT (6-31 G**) calculated structure of FeGP model **5.19**.



DFT calculations were carried out based on structure **5.19** (Figure 5.2), a model of FeGP-H₂ complex **5.18**. A similar result to that obtained by Yang and Hall⁷⁶ was observed, with the hydrogen molecule being polarised. The hydrogen attached to oxygen has a Mulliken charge of 0.362 and the hydrogen attached to iron has a Mulliken charge of -0.101. An interatomic distance of 1.36 Å was calculated between both hydrogens (similar to the distance of 1.38 Å reported for Yang and Hall's model complex),⁷⁶ showing a significant dihydrogen bond. The main difference to Yang and Hall's complex is the lack of protonation on the thiolate ligand; this is due to the starting complex being deprotonated on the 2-hydroxypyridine ligand in this study. It would seem logical that a complex such as

5.21 (representing FeGP **2.7**) would be deprotonated at physiological pH; protonated *N*-methylpyridone **5.20** has a pK_a of 0.32¹²³ and ruthenium complexes **5.22** and **5.23** have pK_a values of 3.5 and 3.9, respectively.¹²⁴

Scheme 5.11 Complexes **2.42** and **2.43** and the dehydrogenation of **2.44** by iridium complex **2.43**.

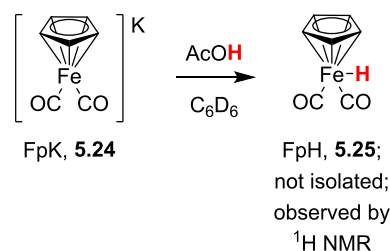


Chapter 2, Section 7 discusses the model complexes of the FeGP cofactor **2.7** that have been synthesised. Reviewing these complexes demonstrates that none of them contains an Fe-H bond. Additionally, only Royer's iridium complex **2.43** has been demonstrated to show hydrogenase-related reactivity, with the dehydrogenation of alcohol **2.44** to ketone **2.45** (Scheme 5.11).⁷⁹ Iridium complex **2.43** is also the only fully characterised complex synthesised as an FeGP cofactor model to contain a free hydroxyl group in the 2-position of the pyridine ligand; this hydroxyl could be very important for protonation/deprotonation reactivity in the catalytic cycle for hydrogenation or dehydrogenation. Complexes **2.97** to **2.103** synthesised by Hu *et al.*, although also identified as structures with 2-pyridinol ligands, have not had full structural characterisation and are challenging to handle.¹⁰¹ An additional point to note is that all of the iron-containing complexes discussed in Chapter 2 are not known to activate hydrogen and/or activate an amidine monosalt related to CH≡H₄MPT⁺ **2.1**. With the lack of a suitable FeGP model complex, a well

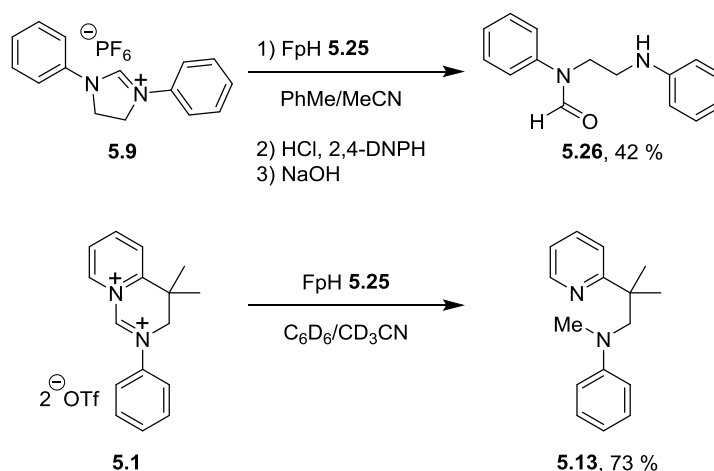
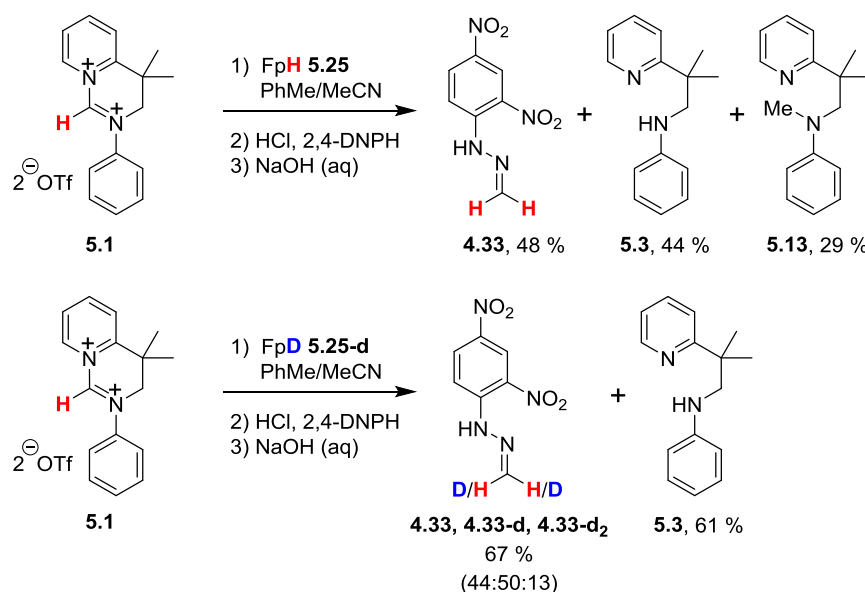
established iron hydride complex that had no previous association with [Fe]-hydrogenase studies was sought; this complex could then be used along with disalt **5.1** in an [Fe]-hydrogenase model reaction.

After reviewing the available sources of iron-hydride complex, cyclopentadienyliron dicarbonyl hydride (FpH) **5.25** was selected as the model iron-hydride complex to be used. Evaluating the structure of FpH **5.25**, this compound should essentially act in a similar manner to compound **5.14**, without having the hydroxyl. The features that can be compared to FeGP-derived structure **5.18** (Scheme 5.10) are that it contains two carbonyl ligands coordinated to an Fe(II) centre, as part of an 18-electron complex. FpH **5.25** was prepared by the method of Bullock and Samsel,¹²⁵ in which the precursor KfP **5.24** is treated with acetic acid in *d*₆-benzene and then placed under vacuum (0.01 mmbar) and collected in a cold finger (-196 °C); if the solution is concentrated or left for an extended period at room temperature, the FpH **5.25** decomposes to the Fp₂ dimer and H₂.¹²⁶ For practical reasons, the FpH **5.25** solution was prepared freshly before use (see Appendix B for a ¹H NMR check) and in the presence of an excess of the substrate that it was to be reacted with.

Scheme 5.12 Synthesis of FpH **5.25**.



Firstly, monosalt **5.9** was treated with FpH **5.25** and stirred overnight (Scheme 5.13). This afforded a brown emulsion which was transferred to a mixture of 2,4-DNPH and 4M HCl; no hydrazone derived from formaldehyde was afforded. The mixture was then worked up with sodium hydroxide to afford formamide **5.26** (42 %). Disalt **5.1** was treated with an excess of FpH **5.25** and stirred overnight to afford amine **5.13** (73 %), showing significantly greater reactivity than the monosalt **5.9**.

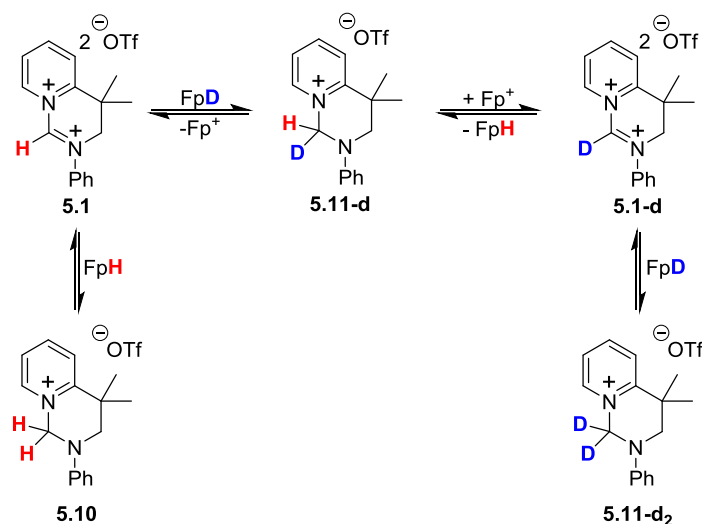
Scheme 5.13 Reactions of monosalt **5.9** and disalt **5.1** with FpH **5.25**.Scheme 5.14 Reduction of disalt **5.1** with FpH **5.25** and FpD **5.25-d**, confirming the presence of a methylene-containing intermediate.

To identify an intermediate species which has the same oxidation level as formaldehyde (on the way to forming amine **5.13**), disalt **5.1** was again treated with an excess of FpH **5.25**, and then immediately (rather than allowing to stir overnight) worked-up with 2,4-DNPH under aqueous acidic conditions (Scheme 5.14). This afforded formaldehyde-derived hydrazone **4.33** (48 %). Basic work-up and extraction then afforded a mixture of amine **5.3** (44 %) and *N*-methyl amine **5.13** (29 %); the former derived from the delivery of one hydride to **5.1** (followed by hydrolysis) and the latter derived from the delivery of two hydrides. Use of *d*₄-acetic

acid on the K_{Fp} salt affords the deuterated version of FpH **5.25** (i.e. FpD **5.25-d**), which was then reacted with disalt **5.1** to afford **4.33**, **4.33-d** and **4.33-d₂** as a mixture of isotopomers in a ratio of 44:50:13 (accounted for by high resolution mass spectrometry) and an overall yield of 67 %. It should be noted here that amine **5.3** would not be expected from the hydrolysis of formamide **5.2** – as discussed in Chapter 4, related amide **3.42** was exposed to NaOH (for longer periods than the work up of this FpH reaction) and did not hydrolyse. Only after NaOH work-up of a triflic acid solution of amide **3.42**, was hydrolysis observed.

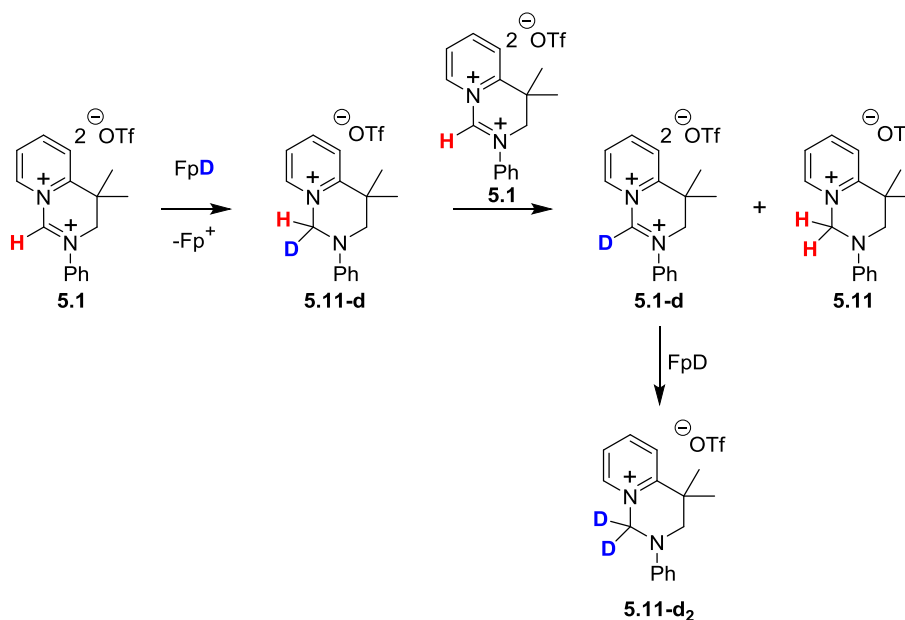
This mixture of isotopomers could imply that addition of hydride from FpH **5.25** to disalt **5.1** is a reversible process, reflecting closely the reversible conversion of **2.1** to **2.2** carried out in [Fe]-hydrogenase. A mechanism (Scheme 5.15) could be envisioned of disalt **5.1** initially reacting with FpD **5.25-d** to form (monodeutero methylene) monosalt **5.11-d**. Some monosalt **5.11-d** could then react with the Fp⁺ cation resulting from the loss of deuteride from FpD **5.25-d**. This could either reform disalt **5.1** or form monodeutero disalt **5.1-d** and FpH **5.25**. Disalt **5.1-d** could then react with another molecule of FpD **5.25-d** to form dideutero monosalt **5.11-d₂**. FpH **5.25**, which had formed from the loss of hydride from monosalt **5.11-d** could then react with a molecule of starting disalt **5.1** to form non-deuterated methylene monosalt **5.11**. All three monosalts **5.11**, **5.11-d** and **5.11-d₂** are precursors to hydrazone compounds **4.33**, **4.33-d** and **4.33-d₂**.

Scheme 5.15 Possible mechanism that forms isotopomers **5.11**, **5.11-d** and **5.11-d₂**.

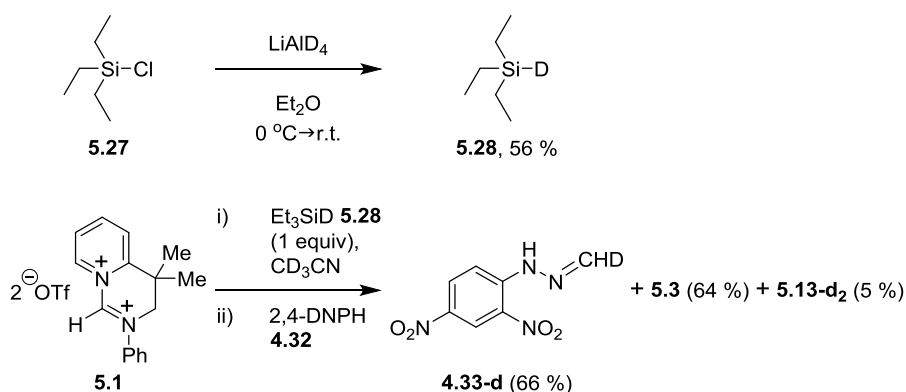


A second possible mechanism (Scheme 5.16) can also be proposed, in which the scrambling of isotopomers is not due to reaction of monosalts **5.11**, **5.11-d** or **5.11-d₂** with Fp^+ , but due to the reaction of these monosalts with disalts **5.1** and **5.1-d**. As with the previous mechanism, monosalt **5.11-d** forms from the reaction of disalt **5.1** with FpD . Monodeutero methylene monosalt **5.11-d** can then act as a hydride donor to another molecule of disalt **5.1**. This would afford monodeutero disalt **5.1-d** and non-deutero monosalt **5.11**. Deutero disalt **5.1-d**, as with the previous mechanism, could react with FpD to form dideutero monosalt **5.11-d₂**.

Scheme 5.16 Alternative mechanism for the formation of monosalts **5.11**, **5.11-d** and **5.11-d₂**.



Scheme 5.17 Reaction of disalt **5.1** with deuteriosilane **5.28**.



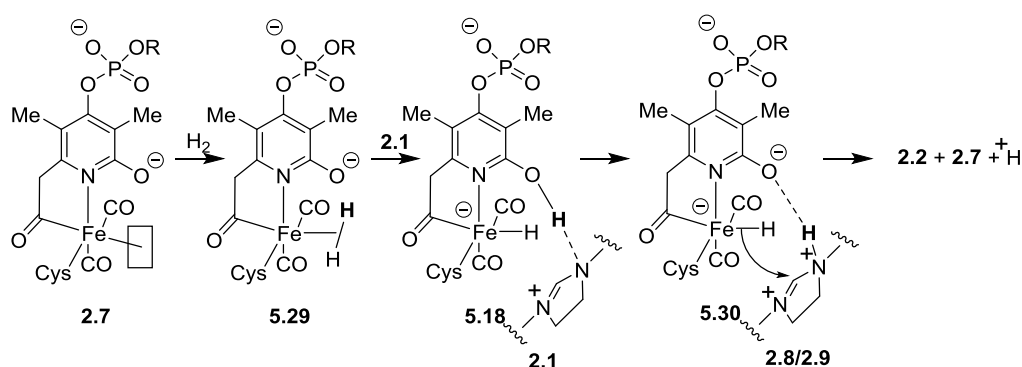
To determine the more likely mechanism in this process, the reactivity observed between disalt **5.1** and triethylsilane was revisited; if the second mechanism was possible (Scheme 5.16), then it would be possible to see this occurring in a deuterated version of the silane reaction. D_1 -triethylsilane **5.28** was prepared in 56 % yield from chlorotriethylsilane **5.27** and $LiAlD_4$ (Scheme 5.17). This was then reacted with disalt **5.1** and worked up with 2,4-DNPH **4.32** to form monodeutero hydrazone **4.33-d** as a single isotopomer. It is important to note that d_1 -triethylsilane **5.28** and disalt **5.1** were reacted in a 1:1 ratio over 16 h – after this time a small proportion of disalt **5.1** was still observed in the reaction mixture using 1H NMR (so there would still be enough disalt **5.1** present to react with monosalt **5.11-d**). These results suggests that monosalt **5.11-d** does not react as a reducing agent with disalt **5.1** as shown in Scheme 5.16; therefore, it is likely that the scrambling of isotopomers observed from the reaction of **5.1** with FpD **6.24-d** is due to the reaction of **5.11**, **5.11-d** and **5.11-d₂** with Fp^+ cation (Scheme 5.15).

In comparison with the non-reversible reaction observed with d_1 -triethylsilane **5.28**, there would appear to be reversibility to the reduction process between disalt **5.1** and FpH **5.25**. The reduction of $CH\equiv H_4MPT^+$ **2.1** to $CH_2=H_4MPT$ **2.2** in [Fe]-hydrogenase is also a reversible process;⁴⁹ as such the model reaction of disalt **5.1** with FpH **6.24** could be representative of the mechanism involved in the reduction reaction of [Fe]-hydrogenase.

Based on the results discussed in this chapter, in which disalt **5.1** was found to be considerably more reactive than monosalt **5.9** and in which the reaction of FpH **5.25** with disalt **5.1** showed a parallel reversibility to the [Fe]-hydrogenase reaction, a mechanism for the [Fe]-hydrogenation reaction can be proposed. The FeGP cofactor **2.7** may bind hydrogen in the “unknown” ligand site to form complex **5.29**. This complex could polarise the hydrogen molecule, similarly to Yang and Hall’s model,⁷⁶ to form complex **5.18**. The 2-pyridinol of complex **5.18** could hydrogen-bond to or protonate $CH\equiv H_4MPT^+$ **2.1** to form a superelectrophilic structure such as **2.8** or **2.9**. A hydride could then (or simultaneously) be delivered from structure **5.30** to form $CH_2=H_4MPT$ **2.2**, reform the original FeGP complex **2.7** and release a proton (Scheme 5.18). To further test this proposed mechanism, a model substrate with functionality closer to that of cofactor **2.7** is desirable. The proposed iron-hydrides

5.18 and **5.30** contain a negative charge formally on the iron and, as such, may be more reactive than FpH **5.25** which contains no charge. However, this work provides the first example of an amidine-containing species being reduced by an iron hydride.

Scheme 5.18 Proposed mechanism for the reduction of $\text{CH}\equiv\text{H}_4\text{MPT}^+$ **2.1** in [Fe]-hydrogenase.



After successfully isolating amidine disalts from the treatment of amides with triflic anhydride and amines and having success in carrying out [Fe]-hydrogenase model studies using disalt **5.1**, investigations into alternative reactivity were desired. The next Chapter will go on to discuss some findings of the reactivity of disalt **5.1** and related disalts which have not been discussed yet.

5.4 Chapter 5 Summary

This chapter progressed on from the work presented in Chapter 4, in which the full characterisation of an amidine disalt **4.1** derived from an amide was presented. In this chapter, the synthesis of disalt **5.1** was presented. Disalt **5.1** was recovered unreacted and quantitatively after exposure to 75 bar pressure dihydrogen under catalyst-free conditions. As disalt **5.1** presents a highly activated amidine centre, this result is the first evidence to demonstrate that dihydrogen must undergo activation within [Fe]-hydrogenase to reduce $\text{CH}\equiv\text{H}_4\text{MPT}^+$ **2.1**.

It was proposed that if the FeGP cofactor **2.7** is the source of dihydrogen activation within [Fe]-hydrogenase, that the activated reducing agent that forms may be an iron-

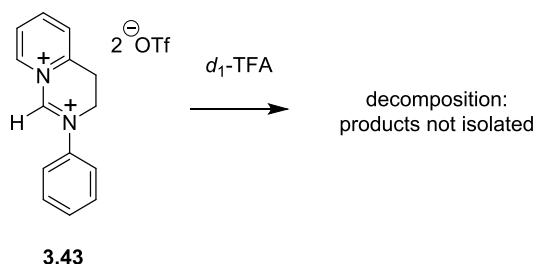
hydride. Due to the lack of suitable FeGP model complexes (see Chapter 2, Section 7), FpH **5.25** was chosen as model of the active FeGP cofactor-derived reducing agent that may be present within the enzyme.

FpH **5.25** was shown to reduce amidine disalt **5.1** in a reversible process, similarly to the reversible reaction carried out by [Fe]-hydrogenase. This chapter demonstrates the first successful [Fe]-hydrogenase model reaction in which an iron-containing reducing reagent reduces an amidine centre. As such, this chapter achieved the second of the aims outlined in Chapter 4, Section 1 (Project Aims).

Chapter 6: Results and Discussion; Extending the Reactivity of Superelectrophilic Disalts

After the success observed with amidine disalt **5.1** in [Fe]-hydrogenase model studies, the properties of this molecule were further studied in other media. As discussed in Chapter 5, disalt **3.43** was observed by ^1H NMR to decompose over 17 h in d_1 -TFA (Scheme 6.1), although decomposition products were not isolated. The decomposition was considered to be at least partially due to the acidic protons on the ethylene backbone connecting the aniline and pyridine moieties of disalt **3.43**. As disalt **5.1** did not have these acidic groups, the investigation of this reactivity was revisited with it and related disalts.

Scheme 6.1 Decomposition of disalt **3.43** in deuterated TFA.



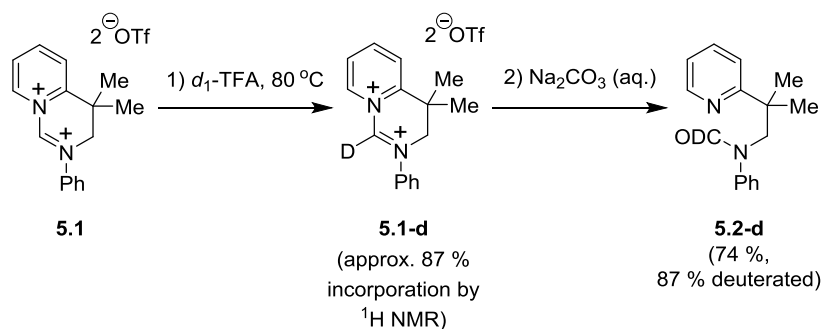
6.1 Further Investigations into the Reactivity of Disalt **5.1**

Disalt **5.1** was dissolved in d_1 -TFA in an NMR tube fitted with a J. Young's valve. The initial sample showed a peak in ^1H NMR at $\delta = 10.68$ ppm which after heating at $80\text{ }^\circ\text{C}$ for 1 h decreased by 87 %. Working up the mixture with aqueous sodium carbonate and extracting the resulting organics with diethyl ether afforded a mixture of non-deuterated amide **5.2** and deuterated amide **5.2-d** (74 % yield, 87 % deuterated, Scheme 6.2).

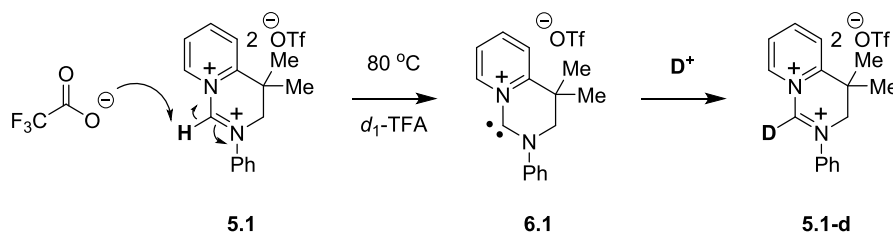
The observed deuterium exchange of disalt **5.1** in deuterated TFA provided a very intriguing result. When considering possible mechanisms, it would seem that disalt **5.1** must be deprotonated at the amidine centre. The trifluoroacetate anion would

likely deprotonate disalt **5.1** to form cationic carbene **6.1**, which could then pick up a deuteron to form disalt **5.1-d** (Scheme 6.3).

Scheme 6.2 Reactivity of disalt **5.1** in deuterated TFA.

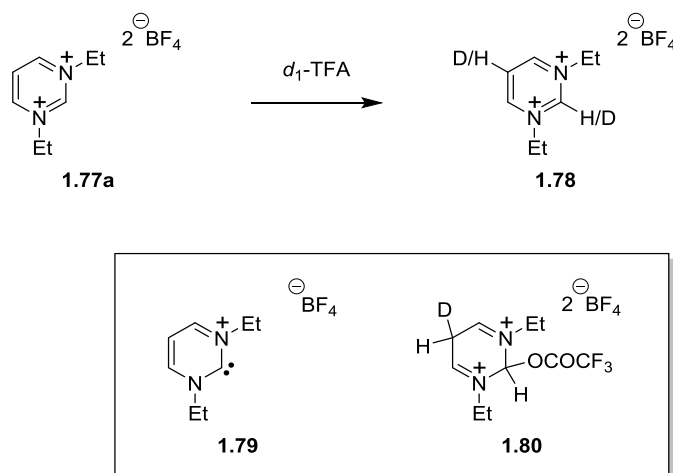


Scheme 6.3 Possible mechanism of deuterium exchange for disalt **5.1**.



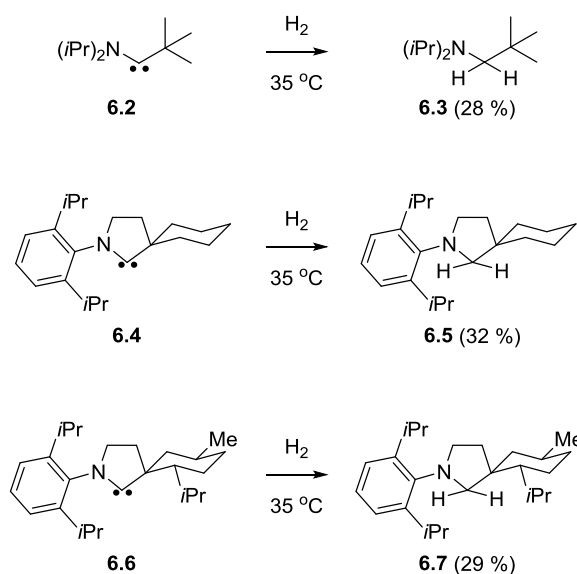
As discussed in Chapter 1, Curphey³⁷ synthesised disalt **1.77a** and carried out deuterium exchange in deuterated TFA. The author proposed the formation of cationic carbene **1.79** as an intermediate to facilitate this exchange reaction (Scheme 6.4).

Scheme 6.4 Deuterium exchange with disalt **1.77a**.



Such cationic carbenes, if they can ever be isolated, may provide some intriguing reactivity. Bertrand and co-workers¹²⁷⁻¹³⁰ have previously synthesised (alkyl)(amino)carbenes which show impressive reactivity with small molecules. Carbenes **6.2**, **6.4** and **6.6** were all reduced in catalyst-free reactions with dihydrogen at 35 °C (Scheme 6.5).¹²⁸ As the possibility of forming an amidine dication within [Fe]-hydrogenase was discussed in Chapters 4 and 5, there may also be the chance of deprotonating the amidine dication to form a carbene similar to cationic carbene **6.1**. In the FeGP cofactor binding site of [Fe]-hydrogenase, His14 (with its basic residue) is vital for enzymatic reactivity⁶² and is one of several potential bases in the active site. If a cationic carbene does form, it may behave in a related manner to an (alkyl)(amino)carbene, which also has a single donating lone pair on a nitrogen atom. In Chapter 2, the stereoselective reduction of $\text{CH}\equiv\text{H}_4\text{MPT}^+$ **2.1** was outlined, in which hydride (derived from hydrogen) was delivered to the *pro-R* position (H^b) of C_{14a} to form $\text{CH}_2=\text{H}_4\text{MPT}$ **2.2**.⁵³ This would suggest that even if a cationic carbene is formed in [Fe]-hydrogenase, this substrate is unlikely to react spontaneously with dihydrogen without the controlled orientation (most likely through complexation) of the dihydrogen molecule.

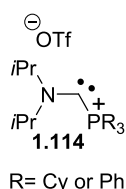
Scheme 6.5 Reduction of Bertrand and co-workers' (alkyl)(amino)carbenes **6.2**, **6.4** and **6.6** with H_2 .¹²⁸



Chapter 1 discussed phosphorus and nitrogen-based cationic carbenes **1.114** (Figure 6.1) which were also synthesised in the group of Bertrand.⁴⁷ The deuterium exchange

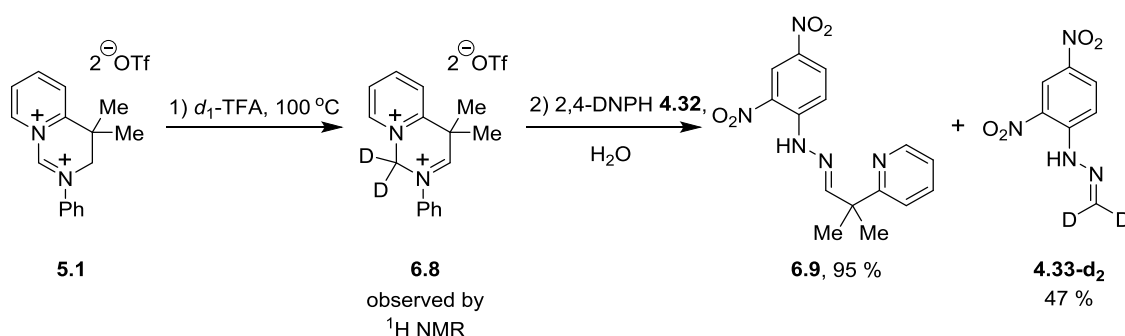
observed with disalt **5.1** in d_1 -TFA provides evidence that carbene **6.1** (a novel, all-carbon and nitrogen analogue of these cationic carbenes) may exist.

Figure 6.1 Bertrand and co-workers' cationic carbenes **1.114**.⁴⁷



A second ^1H NMR investigation into the reactivity of disalt **5.1** was carried out in deuterated TFA, this time at 100°C (Scheme 6.6). ^1H NMR analysis of the mixture showed complete consumption of starting material and the emergence of a product with a singlet (1H) at 9.81 ppm; NOESY showed that this singlet interacted with two singlets (both 3H) at 2.53 ppm and the overall integration had decreased by 2 protons. The product that had formed was proposed to be disalt **6.8**, in which two deuteriums had been incorporated into the structure and the double bond of the amidine had been shifted to the methylene carbon attached to the aniline-derived nitrogen. Work-up of the mixture with 2,4-DNPH **4.32** afforded two hydrazone products, **6.9** and **4.33-d₂**, which help confirm that disalt **6.8** must have formed. Hydrazone **4.33-d₂** showed that a dideutero methylene group had formed with disalt **5.1** and deuterated TFA, while hydrazone **6.9** confirmed that the amidine double bond had shifted to the position shown in disalt **6.8**.

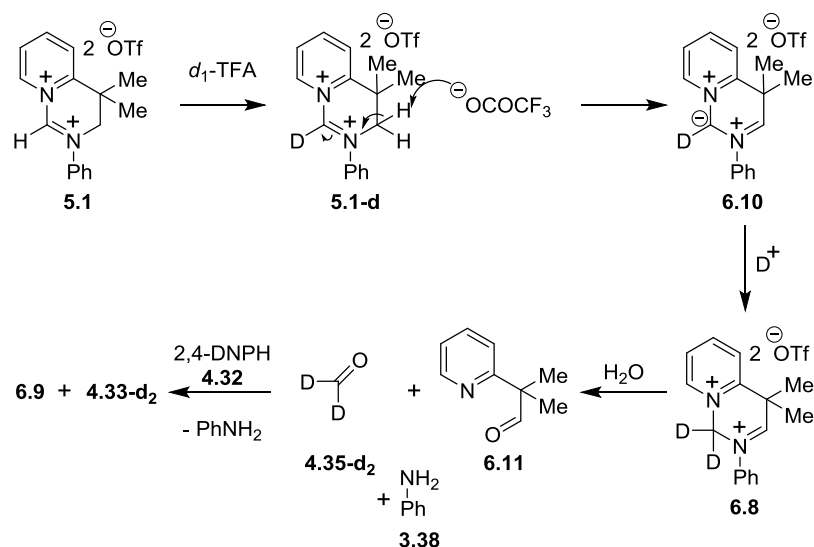
Scheme 6.6 Treatment of amidine disalt **5.1** in deuterated TFA at 100°C .



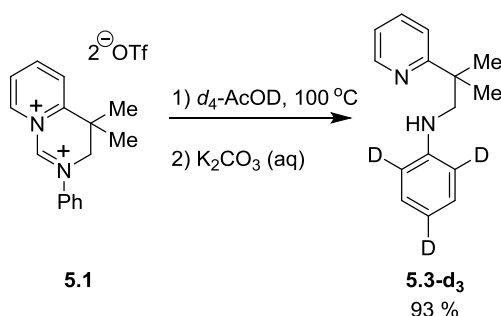
A mechanism can be proposed for this process (Scheme 6.7): as proposed in Scheme 6.5, disalt **5.1-d** may be formed from a cationic carbene; disalt **5.1-d** can be deprotonated to form cationic ylide **6.10**; cationic ylide **6.10** can pick up a deuterium

to form rearranged disalt **6.8**; when this disalt is hydrolysed, deuterated formaldehyde **4.35-d₂** and aldehyde **6.11** can be formed as precursors to hydrazones **4.33-d₂** and **6.9** with loss of aniline. Disalt **5.1** does not only appear to be a precursor to a cationic carbene **6.1**, but also appears to be a precursor to a novel type of compound, a diamino cationic ylide **6.10**.

Scheme 6.7 Reaction of disalt **5.1** in deuterated TFA at 100 °C.



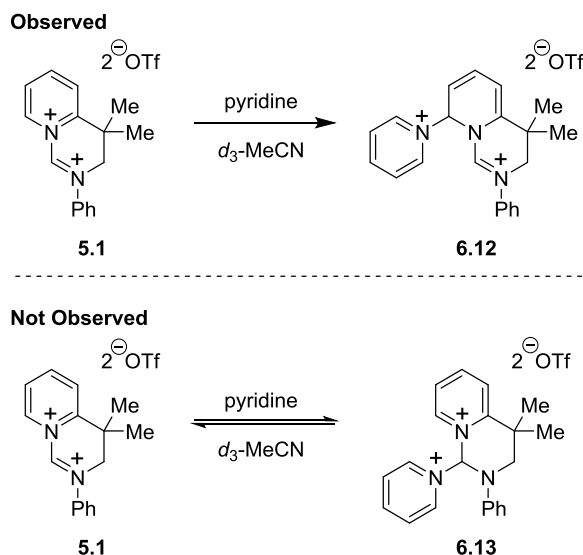
Scheme 6.8 Formation of deuterated amine **5.3-d₃** from disalt **5.1**.



After seeing the fascinating chemistry of disalt **5.1** in deuterated TFA, the reactivity of this disalt was also investigated in *d*₄-acetic acid (Scheme 6.8). After 64 h at 100 °C in this solvent, ¹H NMR revealed a compound with only 6 aromatic protons (relative to two methyl groups) as opposed to the original 9 aromatic protons of disalt **5.1**. Basic work-up and extraction with diethyl ether afforded deuterated amine **5.3-d₃** in a yield of 93 %. It is not clear whether or not the loss of the central carbon of the amidine group in disalt **5.1** was due to hydrolysis from trace amounts of water in the solvent (the deuterated acetic acid had been dried by refluxing over anhydrous

copper sulfate). Once this central carbon was lost, the observed deuterium exchange of the resulting aniline follows the documented deuterium exchange of the *ortho* and *para* positions of anilines heated in acidic media.¹³¹

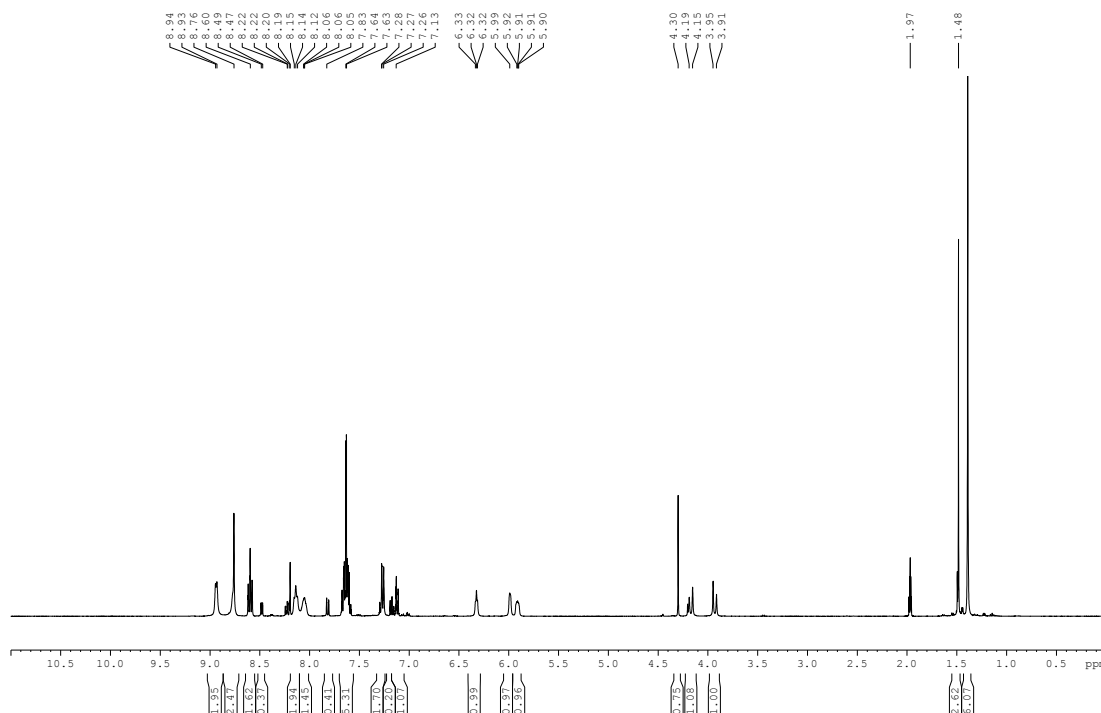
Scheme 6.9 Treatment of disalt **5.1** with pyridine.



Deprotonation/deuteration experiments had successfully been carried out on disalt **5.1** in *d*₁-TFA, and an attempt at deprotonating the disalt with pyridine was also followed by NMR studies. Pyridine was added to disalt **5.1** in deuterated acetonitrile (Scheme 6.9) and the reaction was monitored by ¹H, ¹³C, HSQC, HMBC, COSY, NOESY and DEPT-Q135 NMR spectroscopy. ¹H NMR showed a major component of the reaction mixture to have two 1H doublet signals at 3.93 and 4.17 ppm (both with *J* = 16.0 Hz), which were shown to be attached to the same carbon (57.0 ppm) by HSQC NMR and which was confirmed to be a methylene carbon by DEPT-Q135 NMR. This suggested that the pyridine had attacked disalt **5.1** to form a chiral compound with the methylene adjacent to the *gem*-dimethyl now part of a chiral system – hence the two signals at 3.93 and 4.17 ppm in ¹H NMR (Figure 6.2). The broad signals at 5.91 and 5.99 ppm in the ¹H NMR spectrum corresponded to alkene CH signals (with ¹³C signals at 109.5 and 104.9 ppm, respectively), pointing towards attack on the pyridinium ring of disalt **5.1**. The ¹H NMR spectrum displayed another broad signal at 6.32 ppm which corresponded to a ¹³C signal at 64.2 ppm in the HSQC NMR spectrum. A CH signal at 7.27 ppm in ¹H NMR was shown by HSQC to correspond to a ¹³C signal at 122.6 ppm. COSY NMR showed this CH signal to couple to the CH at 5.91 ppm only. NOESY shows the signal at 7.27 ppm in ¹H

¹H NMR to interact with the signal at 5.91 ppm as well as a broad signal at 8.76 ppm (this broad signal appears to be due to protons attached to 2 different carbon centres; it is possible that these are the amidine carbon and a pyridine carbon); this signal may be the third alkene CH. The signal at 5.99 ppm in ¹H NMR interacts with the two signals at 1.39 and 1.40 ppm in NOESY NMR, which correspond to the *gem*-dimethyl protons; this signal also interacts with the CH at 6.32 ppm. The CH at 6.32 ppm also interacts with the 2H doublet at 8.94 ppm (two *ortho* protons of the pyridine that has just added to disalt **6.12**) and the broad signal at 8.76 ppm (possibly containing the amidine proton as well as further pyridine signals); this signal is likely due to the sp³ CH attached to the pyridine nitrogen. Based on these NMR observations, disalt **6.12** (Scheme 6.9) was proposed as the structure formed on the treatment of disalt **5.1** with pyridine; this reaction occurs instead of deprotonation. It is important to note that these NMR results were observed from the major component of a reaction mixture and it would be ideal to isolate the product before proposing a structure.

Figure 6.2 ¹H NMR of the treatment of disalt **5.1** with pyridine in d₃-MeCN.



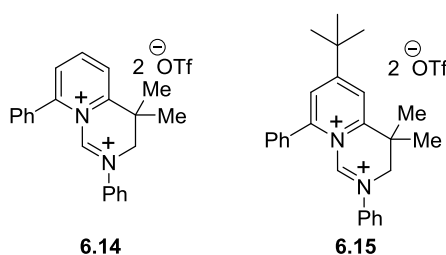
The deuterium exchange of disalt **5.1** in d₁-TFA, as previously discussed within this section, is likely to proceed *via* nucleophilic attack of a trifluoroacetate anion at the amidine centre of the disalt. It would seem likely from this observation that pyridine

would react at the amidine centre of disalt **5.1** to form disalt **6.13** (Scheme 6.9); however, the NMR studies suggest that this disalt is not formed. The reason that disalt **6.13** is not observed may be that this process is reversible. Disalts **5.1** and **6.13** both contain positive charges on nitrogens separated by a single carbon, while disalt **6.12** provides a structure with distonic² positive charges, minimising charge repulsion.

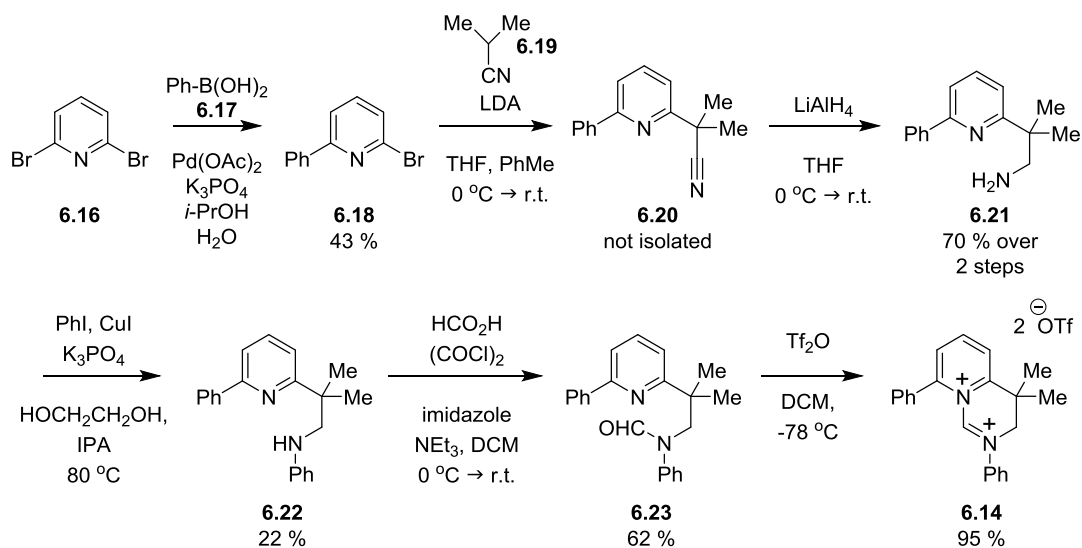
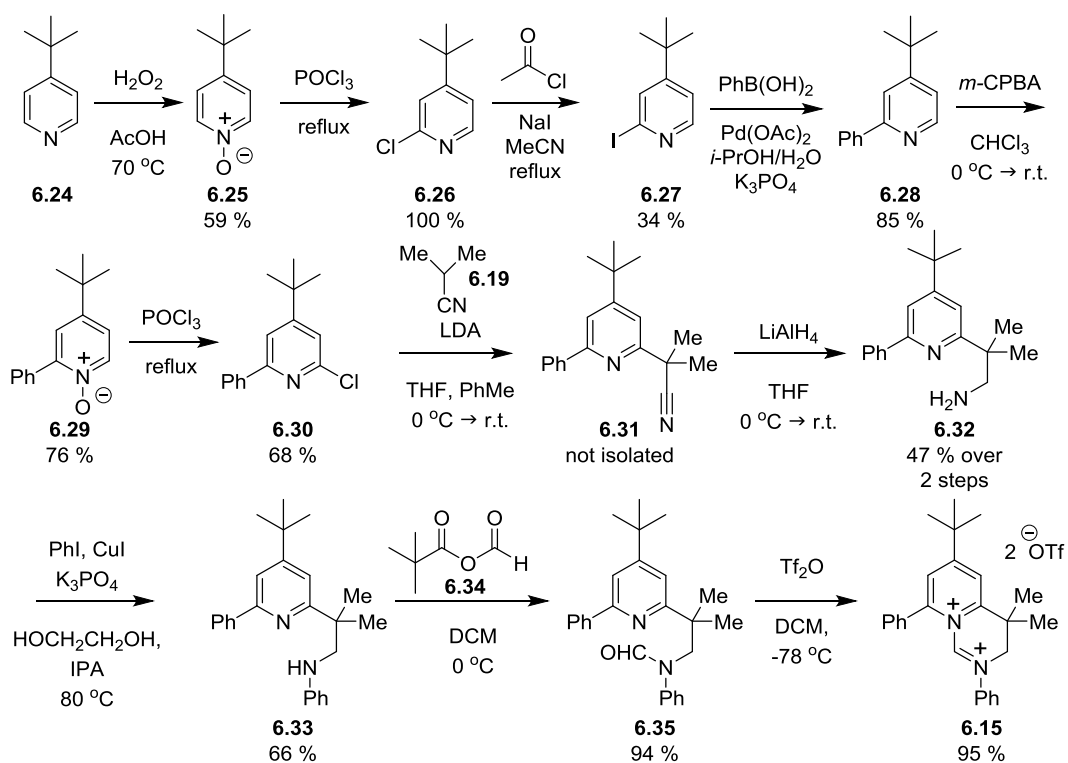
6.2 The Synthesis and Reactivity of Disalts Related to Disalt 5.1: Breaking *N*-Phenyl Bonds

During the investigations into the reactivity of disalt **5.1**, some related, but further substituted, disalts were also synthesised. Disalts **6.14** and **6.15** (Figure 6.3) were originally designed to avoid nucleophilic attack on the pyridinium ring of such systems (see structure **6.12** in Scheme 6.9); however, the synthesis of these two disalts led to the development of some unexpected and exciting reactivity. Firstly, their synthesis will be described.

Figure 6.3 Disalts **6.14** and **6.15**, additionally substituted versions of disalt **5.1**.



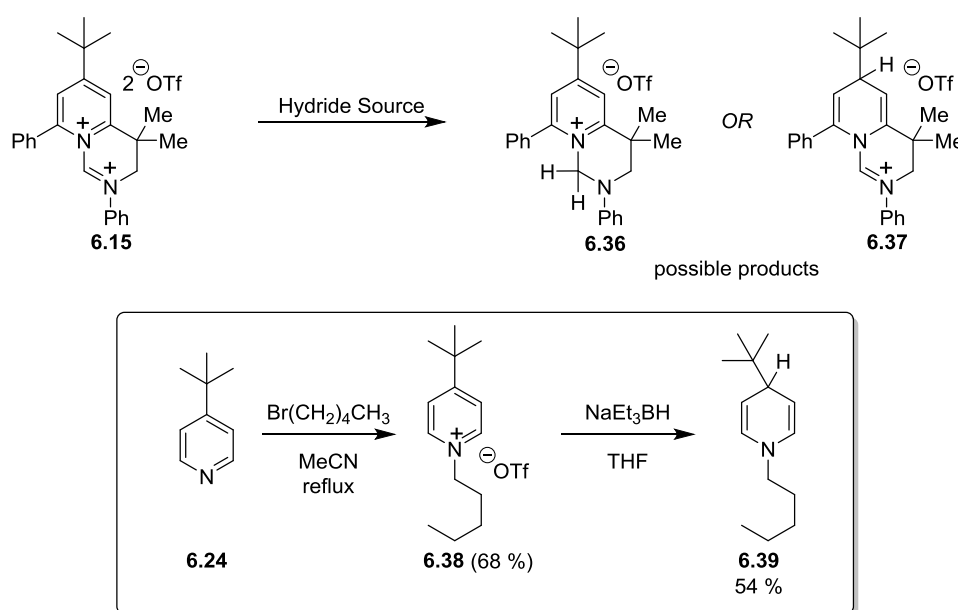
Disalt **6.14** was synthesised in 6 steps from commercially available starting materials (Scheme 6.10). Adapting the conditions of Liu and Yang for coupling 2-halopyridines and phenylboronic acid **6.17**,¹³² 2-bromo-6-phenylpyridine **6.18** was synthesised from 2,6-dibromopyridine **6.16**. The following 5 steps then followed the same synthetic route as that used to synthesise disalt **5.1**. Disalt **6.14** was isolated as a bright yellow powder.

Scheme 6.10 Synthesis of disalt **6.14**.Scheme 6.11 Synthetic route to disalt **6.15**.

Obtaining disalt **6.15** involved a more complicated synthesis than disalt **6.14**, with a total of 11 steps (Scheme 6.11). 4-*tert*-Butylpyridine **6.24** was oxidised with a mixture of hydrogen peroxide and acetic acid (a mixture that forms peracetic acid)¹⁵³ to afford pyridine-*N*-oxide **6.25**. It must be noted that to successfully carry out this reaction, careful monitoring of its temperature was required to ensure that it did not

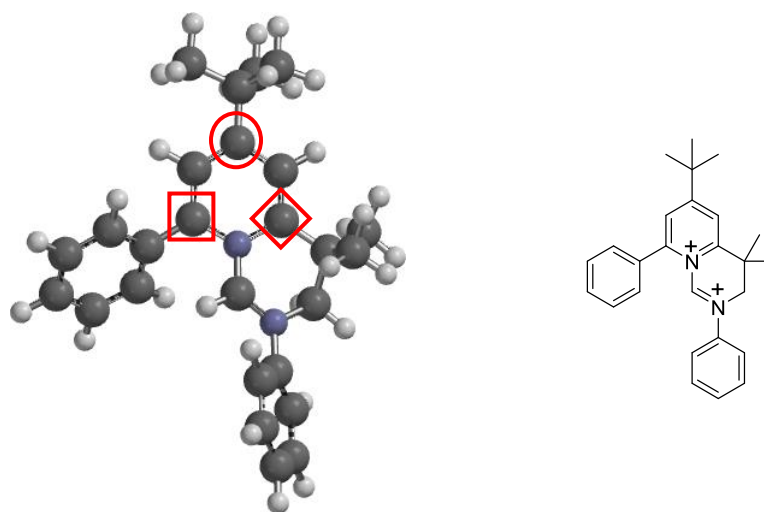
rise above 70 °C; when preliminary reactions were carried out at 80 °C, the internal reaction temperature raised quickly to temperatures as high as 180 °C. When these high temperatures were observed, no pyridine-*N*-oxide **6.25** was isolated. Pyridine-*N*-oxide **6.25** was refluxed in POCl₃ to afford 2-chloropyridine **6.26** in quantitative yield. Adapting the previously reported methods for the transhalogenation of 2-chloropyridines assisted by acetyl chloride,^{133,134} iodopyridine **6.27** was synthesised. Under the conditions outlined by Liu and Yang,¹³² 2-phenylpyridine **6.28** was synthesised in 85 % yield. Pyridine **6.28** was then oxidised with *m*-CPBA (this method was chosen after the temperature sensitivities that were observed in forming *N*-oxide **6.25**) to form pyridine-*N*-oxide **6.29**. Refluxing pyridine-*N*-oxide **6.29** in POCl₃ afforded 2-chloropyridine **6.30**, which was then used towards 3 subsequent steps (analogous steps used in the synthesis towards disalts **5.1** and **6.14**) to form secondary amine **6.33**. The formylation of amine **6.33** involved a different formylation method than those previously reported in this work; mixed anhydride **6.34** was used as formylating agent, affording formamide **6.35** in a yield of 94 %. Formamide **6.35** was then treated under the standard conditions to form disalt **6.15** as a bright yellow powder.

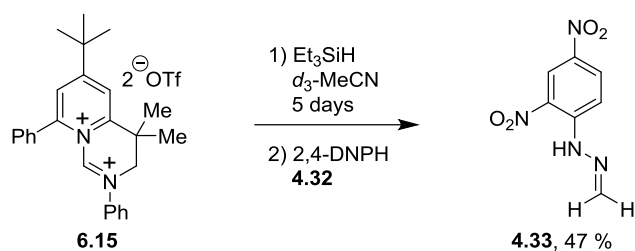
Scheme 6.12 Potential reactions of **6.15** with hydride sources and the reactivity of monosalt **6.38** with NaEt₃BH.



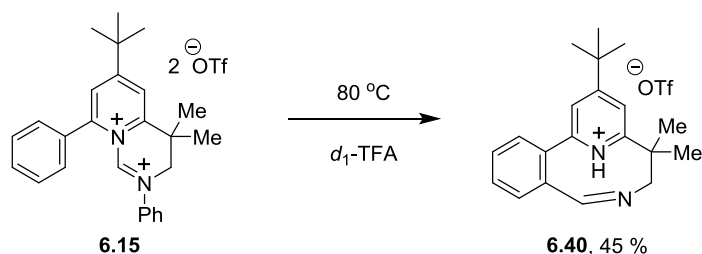
With disalt **6.15** in hand, a brief study of its reactivity with triethylsilane was carried out. ^{13}C NMR analysis showed that the pyridinium carbon which is attached to the *t*-butyl group of **6.15** has a chemical shift of 182.2 ppm which suggests that this centre is very electron-deficient. In a related system, 4-*tert*-butylpyridinium salt **6.38** (prepared from 4-*tert*-butylpyridine **6.24**) was found to react with a hydride source at the 4-position of the pyridine ring; dihydropyridine **6.39** was isolated when salt **6.38** was reacted with sodium triethylborohydride in an inert atmosphere (Scheme 6.12). This reactivity might seem surprising due to the steric bulk of the *tert*-butyl group; however, ^{13}C NMR analysis of monosalt **6.38** shows the reactive carbon attached to the *tert*-butyl to have a chemical shift of 170.4 ppm – a considerably downfield value that may indicate a substantial degree of positive charge at this centre. DFT gas-phase calculation of disalt **6.15** (minus triflates) to the 6-31G* level of theory indicates that the carbon attached to the *tert*-butyl group (circled in Figure 6.4) has a Muliken charge of +0.253, which is not the most positive value of all the carbon centres. On the pyridinium ring of disalt **6.15**, DFT showed the carbons adjacent to the nitrogen have Muliken charge values of +0.353 (square) and +0.415 (diamond), although both had more upfield ^1H NMR values.

Figure 6.4 DFT (6-31G* level of theory) structure of disalt **6.15** minus triflate anions.



Scheme 6.13 Reaction of disalt **6.15** with Et₃SiH followed by 2,4-DNPH **4.32** work-up.

Triethylsilane was added to an NMR tube of disalt **6.15** in deuterated acetonitrile and the presence of the starting material was monitored. After 5 days, starting disalt **6.15** had been consumed (this is slower than the reaction observed for disalt **5.1** with triethylsilane) and was worked-up with 2,4-DNPH **4.32** to afford hydrazone **4.33** (47 % yield, Scheme 6.13). The formation of hydrazone **4.33** suggests that methylene-containing monosalt **6.36** (Scheme 6.12) had been formed as an intermediate, demonstrating that the possible electronic effect of the *tert*-butyl group on the pyridinium ring did not remove the reactivity at the amidine centre.

Scheme 6.14 Heating disalt **6.15** in *d*₁-TFA.

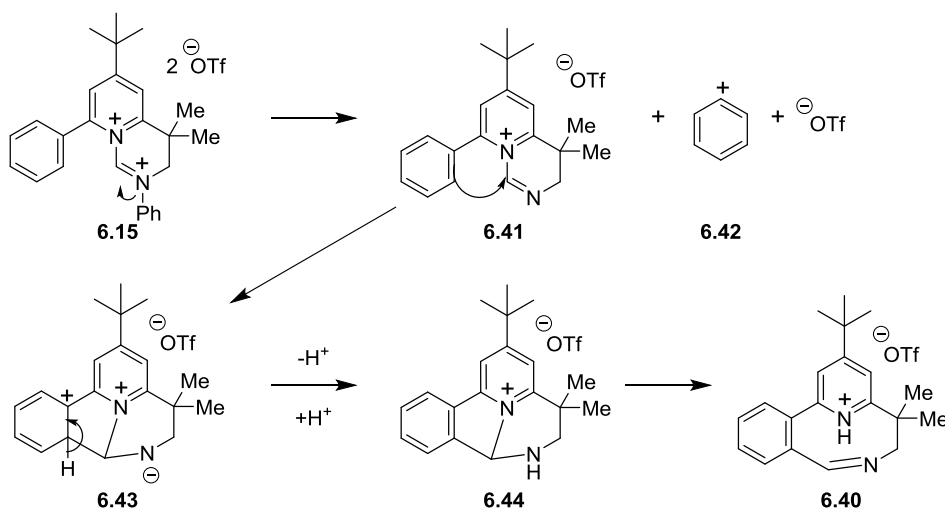
After observing that similar reactivity to disalt **5.1** at the amidine centre of disalt **6.15** was possible using triethylsilane, it was then of interest to carry out studies in deuterated TFA. When disalt **6.15** was heated at 80 °C in deuterated TFA, monosalt **6.40** (Scheme 6.14) was isolated (45 %) being characterised by ¹H, ¹³C and ¹⁹F NMR as well as IR spectroscopy – MS and X-ray evidence was not obtained. ¹H NMR in *d*₃-MeCN showed 6 well-defined peaks in the aromatic region and all integrated to single protons (disalt **6.15** has 12 ArH protons). This accounts for the loss of 6 aromatic signals. Two doublets, at 4.04 and 4.15 ppm (both integrating to one proton each and both with coupling constants of *J* = 14.4 Hz) correspond to the non-

equivalent methylene protons of monosalt **6.40**. The *gem*-dimethyl group of monosalt **6.40** corresponds to the two singlets (integrals of 3 protons each) at 1.26 and 1.61 ppm, while the *tert*-butyl group appears at 1.52 ppm. Lastly, a broad multiplet at 7.12 to 7.16 ppm could be due to the remaining NH and CH protons of structure **6.40**. Also seen in the NMR was a broad signal at 3.32 ppm that was attributed to an impurity – this signal did not integrate sensibly for any additional functional groups on the product, considering the signals already identified (see Appendix E).

In forming monosalt **6.40** from disalt **6.15**, this reaction would involve the breaking of an *N*-Ph bond as well as the formation of a 9-membered ring – new reactivity to be observed with amidine disalts.

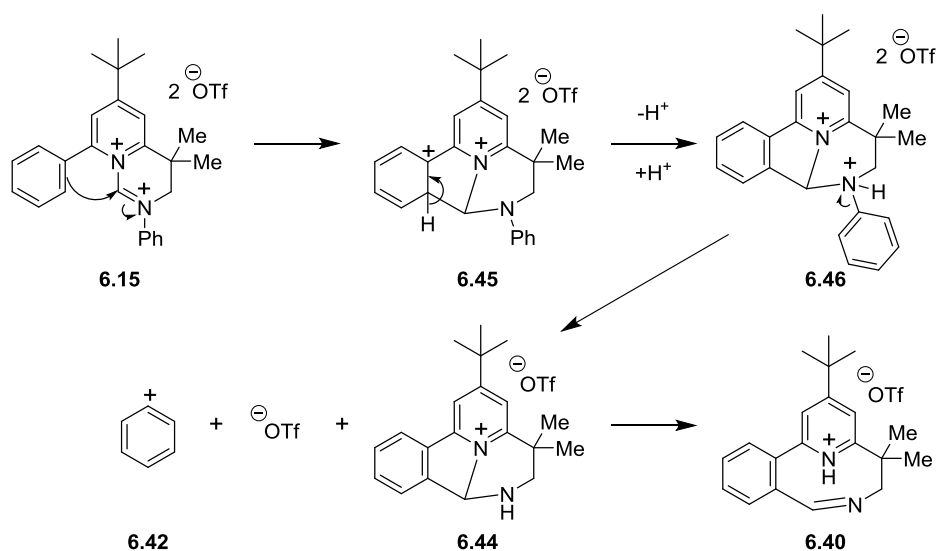
Two mechanisms were proposed for the formation of monosalt **6.40** from disalt **6.15**. The first mechanism involves the initial cleavage of the *N*-Ph bond of disalt **6.15** (Scheme 6.15) which affords monosalt **6.41**, phenyl cation **6.42** and triflate anion (the latter two can then associate to form phenyl triflate). Monosalt **6.41** could then possibly undergo a Friedel-Crafts cyclisation between the amidine centre and the phenyl ring attached to the pyridinium, forming monosalt **6.43**. Monosalt **6.43** could then rearomatise to form salt **6.44** which could then rearrange to form monosalt **6.40**.

Scheme 6.15 First possible mechanism for the formation of salt **6.40**.

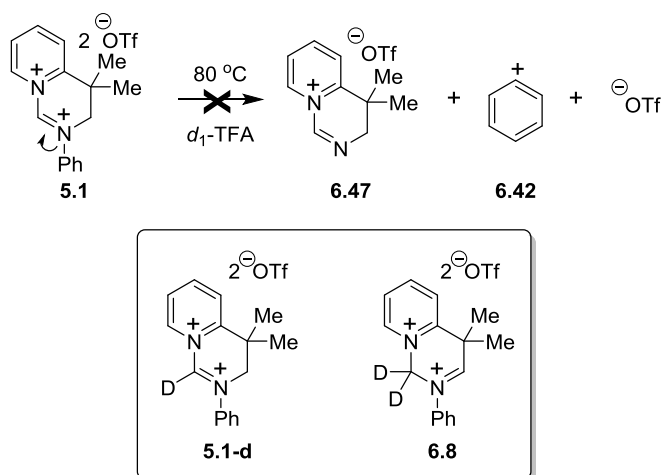


The second possible mechanism involves the initial intramolecular cyclisation of the phenyl ring on the pyridinium ring of disalt **6.15** (Scheme 6.16), attacking the amidine centre, to form disalt **6.45**. Disalt **6.45** could then rearomatise (deprotonate and protonate) to form disalt **6.46**. It is then proposed that this disalt is reactive enough to cleave the *N*-Ph bond to form monosalt **6.44**, phenyl cation **6.42** and triflate. Monosalt **6.44** can, as the previous mechanism shows, rearrange to form 9-membered-ring-containing salt **6.40**.

Scheme 6.16 The second possible mechanism for the formation of disalt **6.15**.



Scheme 6.17 C-Ph cleavage of disalt **5.1** that is not observed; protonation/deprotonation products **5.1-d** and **6.8** are observed.



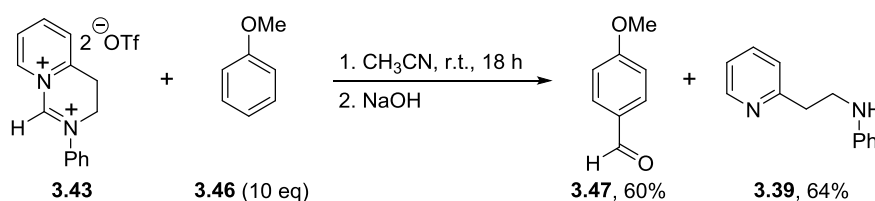
To propose which one of these two mechanisms is more likely, the reactivity of disalt **5.1** can be considered. If the mechanism illustrated in Scheme 6.15 was indeed happening, then a similar cleavage reaction should be observed with disalt **5.1** to form monosalt **6.47** (Scheme 6.17). However, as discussed in Section 6.1, the products that are observed in the reaction of disalt **5.1** in deuterated TFA purely involve deprotonation and protonation processes to form disalt **5.1-d** at 80 °C and disalt **6.8** at 100 °C. As there is no *N*-Ph cleavage reaction observed with disalt **5.1**, it would seem likely that the mechanism depicted in Scheme 6.16 is the more probable mechanism for the reactivity observed with disalt **6.15** in deuterated TFA.

One important factor remains in this uncertain reaction; both proposed mechanisms present intermediates as well as a final product with likely significant ring strain. As full characterisation was not obtained for the final product **6.40**, further investigations would have to be carried out to confirm the product in this *N*-Ph cleavage reaction. However, the mass spectral and NMR evidence is strong for the *N*-Ph cleavage reaction taking place.

6.3 Amidine Disalts As Formylating Agents

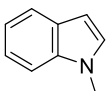
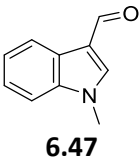
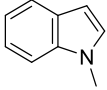
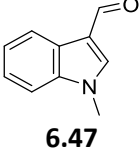
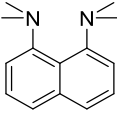
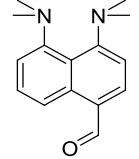
As described in Chapter 3, Corr²⁷ had successfully formylated anisole **3.46** with disalt **3.43** to afford *p*-anisidine **3.47** in a yield of 60 % (Scheme 6.18). This reaction required 10 equivalents of anisole **3.46** and no further substrates were tested in formylation studies.

Scheme 6.18 Formylation of anisole **3.46** with disalt **3.43** by Corr.²⁷



As part of the work scope in this thesis, it was of interest to return to the formylation reactions of disalt **3.43** and extend the substrate scope (Table 6.1). From the reactions studied, it was clear that disalt **3.43** requires electron-rich aromatics for successful formylation reactions. Anisole **3.46** was successful in formylation reactions (Scheme 6.18) and this work (Table 6.1) extended this success to electron-rich *N*-methylindole **6.46**, with 2 equivalents of substrate required for formylation. Formylated product **6.47** was afforded in 52 % yield after 2 days or 71 % yield after 4 days (Entries 1 and 2, Table 6.1). Entries 3 to 8, Table 6.1 highlight the lack of any formylating reactivity of disalt **3.43** with more electron-deficient substrates.

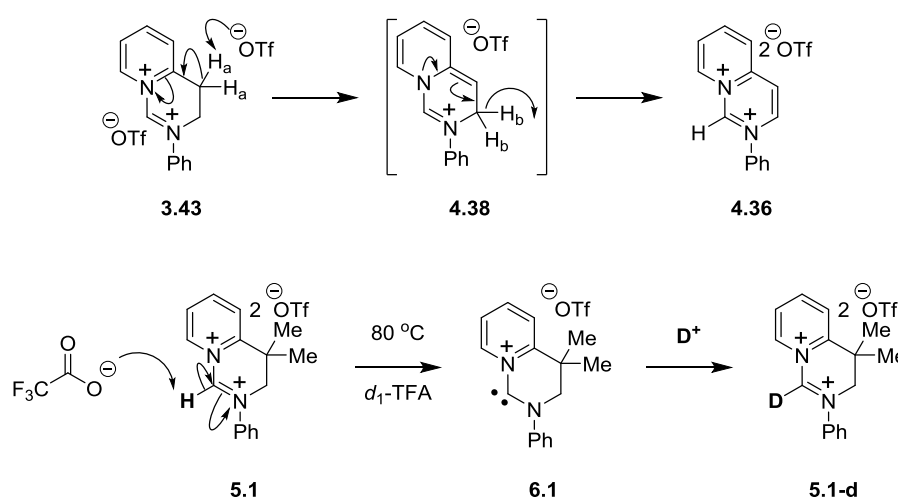
Table 6.1 Reactions of Disalt **3.43** and substrates in MeCN.

Entry	Substrate	Equiv.	Disalt 3.43 Equiv.	Reaction Time	Product	Yield (%)
1	 6.46	2	1	48 h	 6.47	52 %
2	 6.46	2	1	96 h	 6.47	71 %
3	Nitrobenzene 6.48	2	1	48 h	No formylation	n/a
4	Anthracene 6.49	2	1	48 h	No formylation	n/a
5	Chlorobenzene 6.50	2	1	48 h	No formylation	n/a
6	Acetophenone 6.51	2	1	48 h	No formylation	n/a
7	Benzene 6.52	2	1	48 h	No formylation	n/a
8	Toluene 6.53	2	1	48 h	No formylation	n/a
9	 6.54	1	1	Approx. 20 min.	 6.55	45 %

Entry 9, Table 6.1 shows the formylation of proton sponge **6.54** by disalt **3.43** in a 1:1 ratio. As deprotonation reactivity had been observed with disalts **3.43** and **5.1**

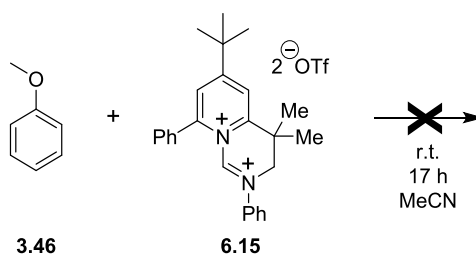
previously (Scheme 6.19), it was of surprise to observe such a significant formylation reaction with proton sponge **6.54** to form formylated product **6.55** in a yield of 45 %. The conjugate acid of proton sponge **6.54** has a pK_a of 12.34,¹³⁵ while trifluoroacetic acid has a pK_a of 0.5¹³⁶ and triflic acid has a pK_a of -12,¹³⁷ as the much weaker bases trifluoroacetate and triflate appear to be involved in deprotonation reactivity with disalts **3.43** and **5.1** (Scheme 6.19), it is a surprise that proton sponge is not dominated by deprotonation reactivity.

Scheme 6.19 Deprotonation reactivity of disalts **3.43** and **5.1**.



As disalt **6.15** is designed to prevent reactivity at centres away from the amidine centre, it was of interest to see if this disalt could be used in formylation reactions. Under conditions (1 equivalent substrate: 1 equivalent disalt) in which disalt **3.43** was found to formylate anisole **3.46** in 28 % yield, disalt **6.15** was found to be completely unreactive (with anisole re-isolated quantitatively).

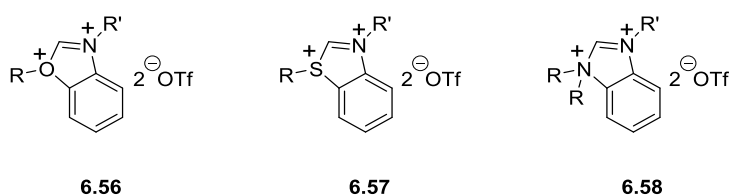
Scheme 6.20 Anisole **3.46** is unreactive to disalt **6.15**.



The cyclisation reactivity discussed regarding disalt **6.15** in the previous section (Schemes 6.15 and 6.16) illustrated some reactivity which could be viewed as intramolecular formylation. However, the result presented with anisole **3.46** (Scheme 6.20), highlights that disalt **6.15** does not provide an efficient formylating reagent for synthesis. The next section, although it also does not provide synthetically useful disalts, describes an extension from the chemistry of amidine disalts towards the potential in forming oxygen-containing equivalents.

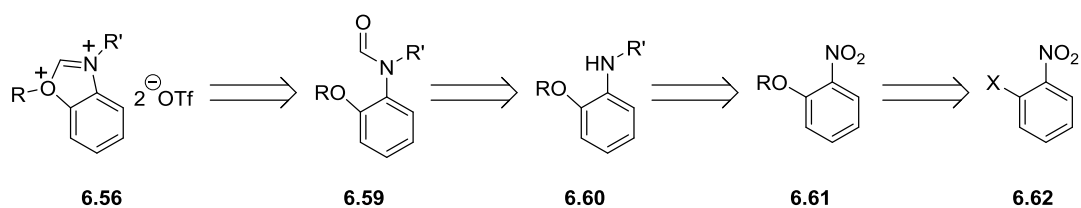
6.4 Oxygen-Containing, Amide-Derived Disalts

Figure 6.5 Disalt structures **6.56**, **6.57** and **6.58**.



After the success observed in the synthesis and reactivity of amidine disalts, there was an interest to see if some success could then be extended to disalts containing alternative heteroatoms. Disalt types **6.56** and **6.57** (Figure 6.5) were considered good candidate structures for alternative disalts to amidine disalts; Kovacevic proposed disalts of the type **6.58** as intermediates in reactions where triflate acts as a nucleophile.¹³⁸ While disalts of type **6.56** were a target for synthesis in the scope of work in this thesis, Kovacevic worked on the synthesis of disalts of type **6.57**.¹³⁸

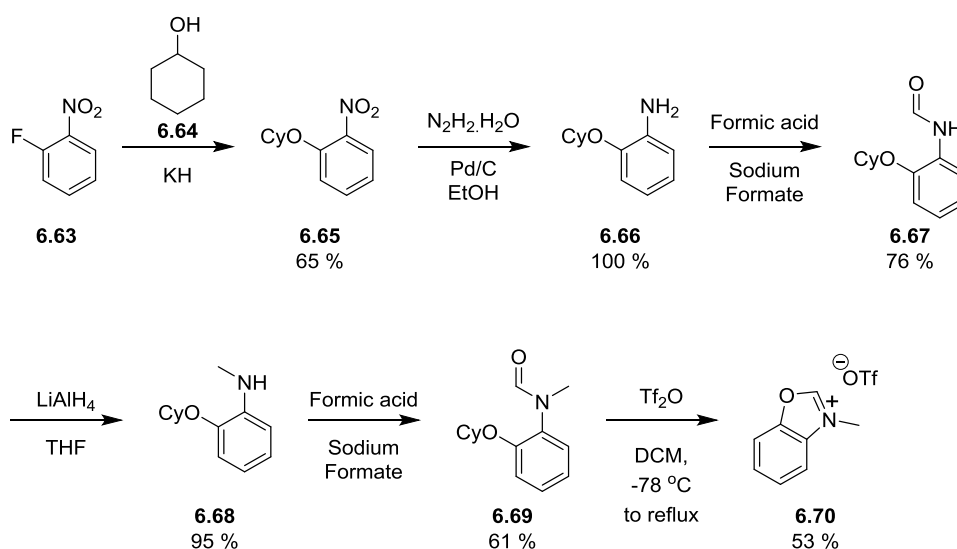
Scheme 6.21 Retrosynthesis of disalt type **6.56**.



The synthesis of disalts of type **6.56** could be relatively straightforward (Scheme 6.21). Disalt **6.56** could be formed from the intramolecular attack of an ether on an (triflic anhydride) activated amide in 1,2-disubstituted benzene **6.59**. Amide **6.59** could be synthesised from secondary amine **6.60**. In a few steps, such an amine could be synthesised from a nitro compound such as compound **6.61**. This compound could be synthesised in a nucleophilic substitution reaction from one of several commercially available 1-nitro-2-halobenzenes **6.62**.

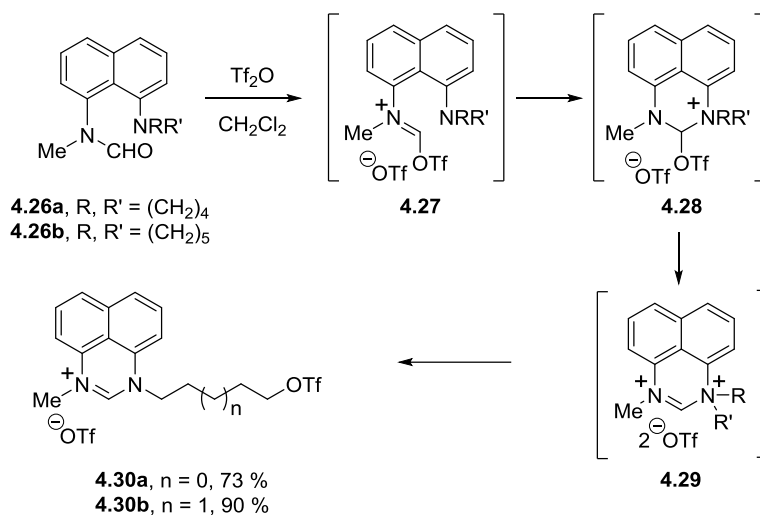
The synthesis of ether amide **6.69** was carried out in 5 steps (Scheme 6.22). Firstly, cyclohexanol **6.64** was treated with potassium hydride and the resulting salt was added to 1-nitro-2-fluorobenzene to afford nitro ether **6.65** in 65 % yield. Hydrazine monohydrate and Pd/C catalyst were used to reduce nitro compound **6.65** to primary amine **6.66** in quantitative yield. According to the method of Brahmachari and Laskar,¹³⁹ a mixture of formic acid and sodium formate was used to synthesise formamide **6.67** (76 % yield). This formamide was then reduced with LiAlH₄ to form *N*-Me amine **6.68** in 95 % yield. Using formic acid and sodium formate, formamide **6.69** was afforded in 61 % yield. This amide was then cooled to -78 °C and treated with triflic anhydride in CH₂Cl₂, before refluxing for 20 h. Instead of forming a disalt, monosalt **6.70** was afforded (53 % yield) with loss of the cyclohexyl group.

Scheme 6.22 Synthesis of amide **6.69** and subsequent formation of monosalt **6.70**.



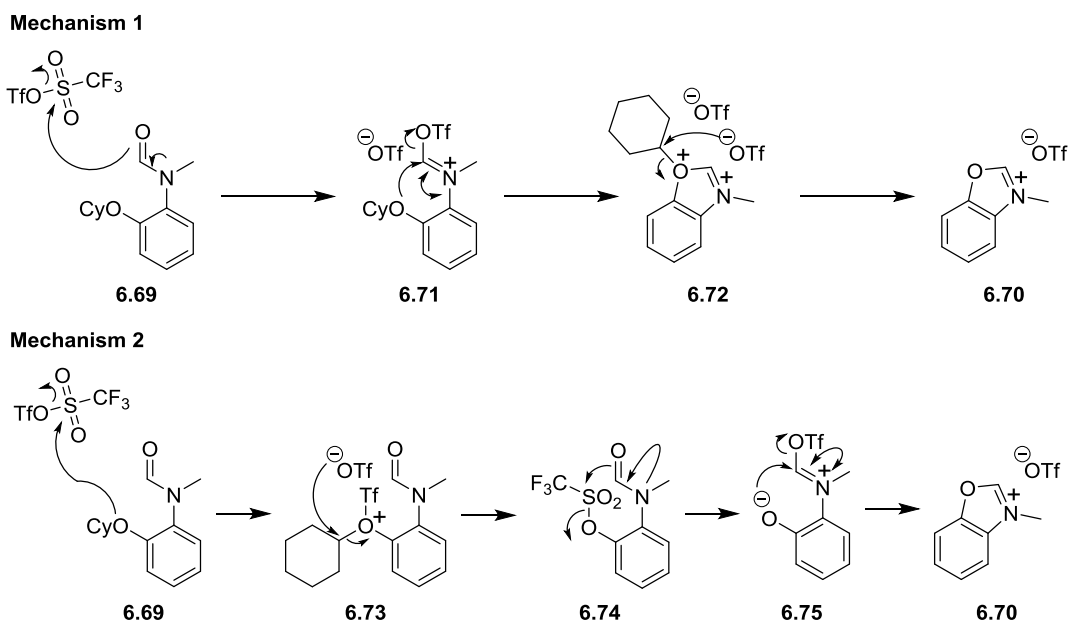
As discussed in Chapter 4, other members of the Murphy group have formed monosalts under similar circumstances.¹¹⁶ Monosalts **4.30** were suggested to form *via* disalts **4.29**, with triflate anion as a nucleophile (Scheme 6.23).

Scheme 6.23 Formation of amidine monosalts **4.30** *via* disalts **4.29**.



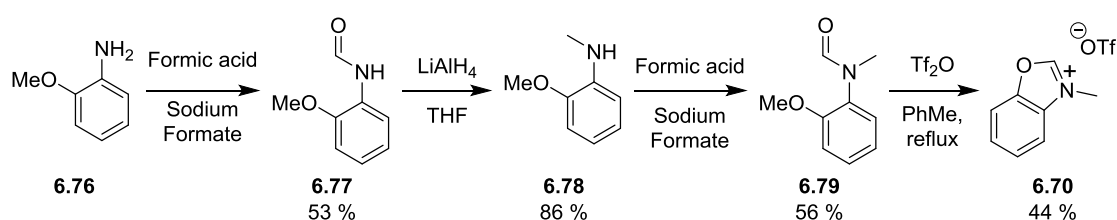
The formation of monosalt **6.70** could occur through an analogous mechanism to that of monosalts **4.30** (Mechanism 1, Scheme 6.24), with disalt **6.72** being a reaction intermediate. However, it was also considered that a mechanism involving monocations as the most positively charged species could also be occurring (Mechanism 2, Scheme 6.24).

Scheme 6.24 Possible mechanisms in the formation of monosalt **6.70** from amide **6.69**.

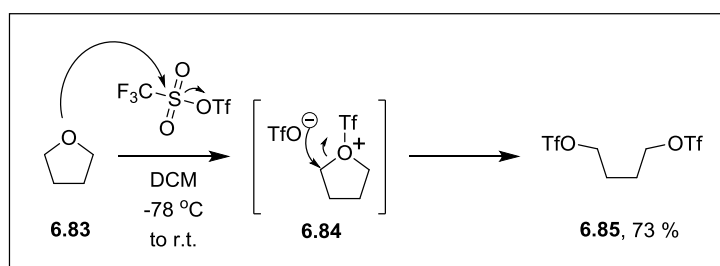
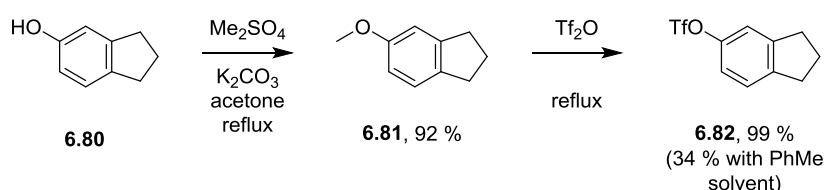


The preparation of amide **6.79** was straightforward, with starting material *o*-anisidine **6.76** being commercially available (Scheme 6.25); steps analogous to some of those used in the formation of amide **6.69** (Scheme 6.22) were found to be successful. Treatment of amide **6.79** with triflic anhydride was found to require the use of an higher boiling solvent (PhMe) than CH_2Cl_2 for the successful formation of monosalt **6.70**. The formation of monosalt **6.70** from amide **6.79** likely follows an analogous mechanism to the reaction involving amide **6.69** (either mechanism in Scheme 6.24).

Scheme 6.25 Synthesis of amide **6.79** and subsequent formation of monosalt **6.70**.



Scheme 6.26 Ether cleavage reactions with triflic anhydride.

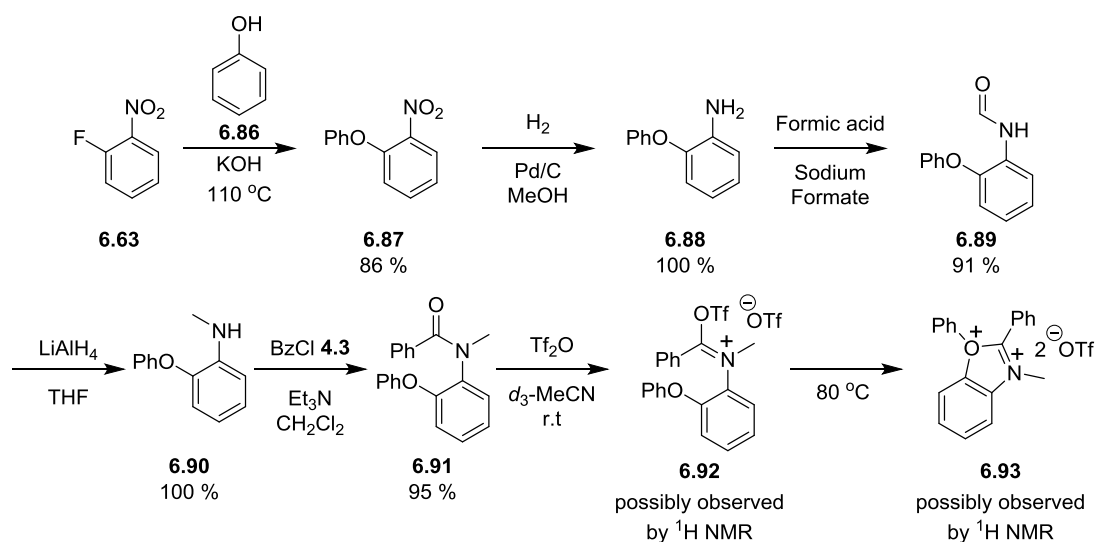


To test whether or not Mechanism 2 (Scheme 6.24) was possibly occurring in the reactions of amides **6.69** and **6.79**, ether **6.81** was synthesised from 5-indanol **6.80** and was then treated with triflic anhydride (Scheme 6.26). Reaction with neat triflic anhydride afforded aryl triflate **6.82** in 99 % yield, while reaction in toluene afforded the product in 34 % yield. This suggests that the steps from ether **6.69** to triflate **6.74** in Mechanism 2 are viable as part of a route forming monosalt **6.70** (Scheme 6.24 and Scheme 6.25). This reactivity relates to that discussed by Beard and co-workers in 1973,¹⁴⁰ in which tetrahydrofuran **6.83** was treated with triflic anhydride to form

1,4-butaneditriflate **6.85** (Scheme 6.26). In the 1970s, Subramanian *et al.* demonstrated that aryl triflates undergo nucleophilic attack at the triflate sulfur to break the S-O single bond; formation of zwitterion **6.75** from triflate **6.74** may be possible (Scheme 6.24) and this product could then form monosalt **6.70**.

Despite the dealkylation reactivity of species that do not contain disalts (Scheme 6.26), *N*-methyl-*N*-(2-phenoxyphenyl)benzamide **6.91** (Scheme 6.27) was prepared as a precursor to a potential disalt; no disalt was isolated in reactions with this amide, but some observations were made using NMR spectroscopy studies. A solution of amide **6.91** in d_3 -MeCN was prepared in an inert atmosphere glovebox and placed into an NMR tube fitted with a septum. Triflic anhydride was added to the mixture at room temperature to afford a product with two singlet signals at 4.08 and 4.13 ppm (in a ratio of 1:3, respectively) in ^1H NMR spectroscopy (Appendix F). These values were considerably more downfield than the singlet observed for the methyl group at 3.30 ppm for amide **6.91**, suggesting that positive charge had been gained in the resulting molecule; this could correspond to iminium triflate **6.92** (Scheme 6.27), which could exist as a mixture of isomers. The reaction mixture was then heated at 80 °C and cooled to r.t. to afford a mixture with two singlets at 4.55 and 4.59 ppm (a ratio of 1:2, respectively) in ^1H NMR spectroscopy. These two values indicate that even more positive charge had formed on the molecule; this could be consistent with the formation of disalt **6.93** (Scheme 6.27) although does not explain why there are two singlets.

Scheme 6.27 Preparation of amide **6.91** as a precursor to potential disalt **6.93**.

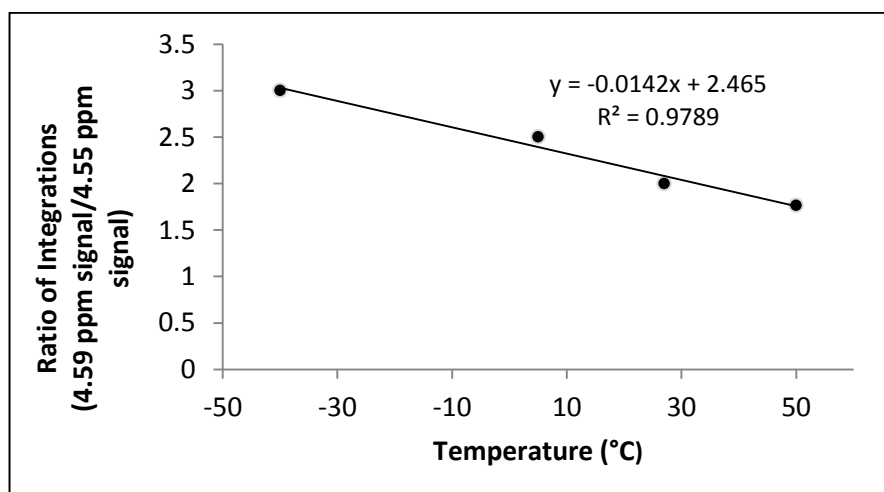


^1H NMR analysis was then carried out on this mixture at several temperatures to observe the effect on the ratio of these two singlet signals – the results are summarised in Table 6.2 (for images of spectra, see Appendix G). At $-40\text{ }^\circ\text{C}$, the ratio of the signals alters from the original values of 1:2 to the new ratio of 1:3; at $5\text{ }^\circ\text{C}$ the ratio is 1.2:3; at $50\text{ }^\circ\text{C}$ the ratio is 1.7:3. When the ^1H NMR spectrum was recorded at $27\text{ }^\circ\text{C}$ (the original measurement temperature) after having varied the temperature, the ratio returned to 1:2 for the two singlets. These values show a linear relationship between the changes in temperature of the mixture with the changes in ratio of these signals (Figure 6.6). This suggests that the formed mixture of products may contain an equilibrium between the two major species – perhaps two distinct compounds or two isomers.

Table 6.2 Influence of temperature variance on singlet signal ratios for ^1H NMR analysis of the reaction mixture of disalt **6.91** with Tf_2O **1.32**, after $80\text{ }^\circ\text{C}$ heating.

Temperature ($^\circ\text{C}$)	Relative Integration	
	Signal at 4.55 ppm	Signal at 4.59 ppm
-40	1	3
5	1.2	3
27	1.5	3
50	1.7	3

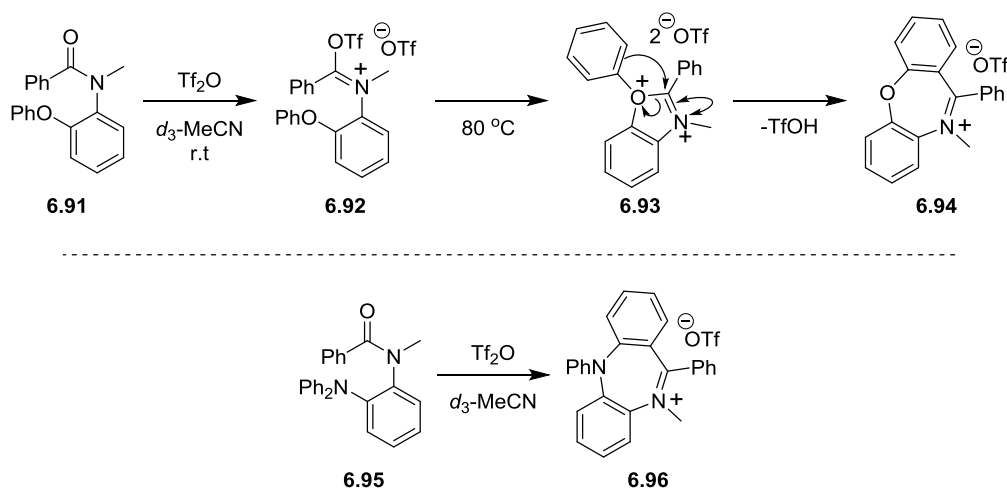
Figure 6.6 Plot of the ratio of singlet integrations from ^1H NMR against temperature.



^{19}F NMR spectroscopy (see Appendix H) showed the mixture to contain a major signal at -79.4 ppm (comparable to the triflate signal of pure disalt **5.1** which comes at -79.3 ppm); this suggests that the major product contains one type of fluorine centre and if disalt **6.93** has formed, this may correspond to two triflate anions.

In related chemistry, Kovacevic¹³⁸ reacted amino amide **6.95** with triflic anhydride to form monosalt **6.96** (Scheme 6.28), containing a seven membered ring – this could provide information on possible components of the reaction mixture with amide **6.91**. If related monosalt **6.94** was formed as the major component in the reaction mixture, this could also account for the signal at -79.4 ppm in ^{19}F NMR spectroscopy. Mass spectroscopy (electrospray) of the reaction mixture did not provide evidence of monosalt **6.94** (Scheme 6.28), but did provide a mass for the starting amide **6.91** (with $m/z = 326$ for the $[\text{M}+\text{Na}]^+$ ion). These results do not rule out or provide evidence for the formation of monosalt **6.94** or disalt **6.93**. As such, it currently remains unclear whether or not an oxygen-containing, amide-derived disalt can be obtained through similar methods to those of amidine disalts.

Scheme 6.28 Another possible reaction occurring between amide **6.91** and triflic anhydride.

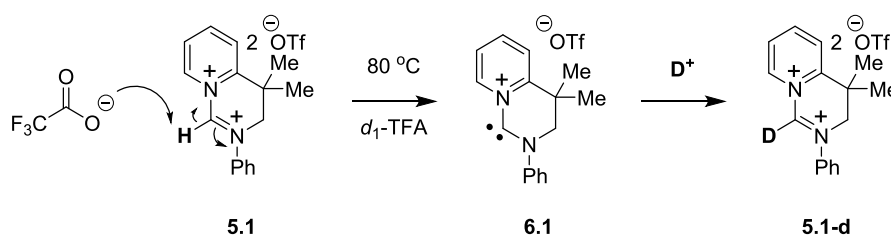


6.5 Chapter 6 Summary

This chapter successfully provided an extension to the range of reactions observed for superelectrophiles derived from amides, the third target set out in the Project Aims.

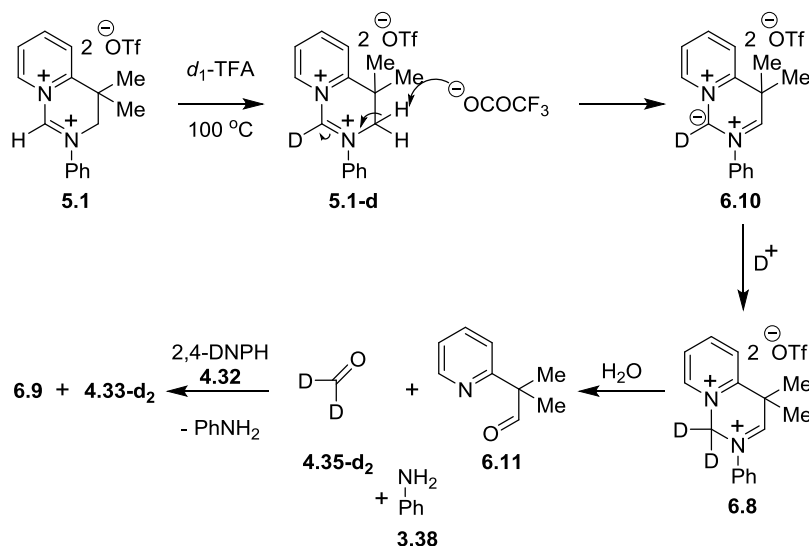
The first major success in extending the reactivity of amide-derived, amidine disalts involved deuterium exchange of disalt **5.1** at 80 °C in d_1 -TFA to form disalt **5.1-d**. The formation of disalt **5.1-d** is likely to proceed through monocationic carbene **6.1** – such a compound has never been reported to be derived from an amide.

Scheme 6.29 Formation of deuterated disalt **5.1-d** via monocationic carbene salt **6.1**.



When treated at 100 °C in d_1 -TFA, disalt **5.1** reacts to form disalt **6.8** (Scheme 6.30). This reaction is likely to proceed through the very unusual cationic ylide salt **6.10** – a very unique compound with unknown reactivity.

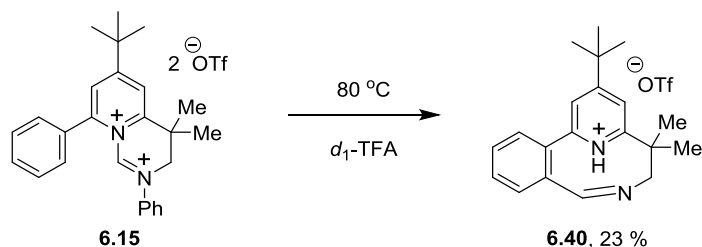
Scheme 6.30 Reaction of disalt **5.1** in deuterated TFA at 100 °C.



The reaction of disalt **6.15** in d_1 -TFA provided an *N*-Ph cleavage reaction; although the final product could not be fully characterised, mass spectroscopy and NMR evidence pointed towards the formation of monosalt **6.40** with a 9-membered ring

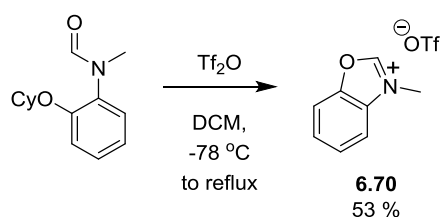
(Scheme 6.31). This is an unprecedented transformation to be carried out with an amidine disalt.

Scheme 6.31 Heating disalt **6.15** in d_1 -TFA.



In attempts to form an oxygen-containing, amide-derived disalt, amide **6.66** was treated with triflic anhydride. Instead of finding evidence of a disalt, monosalt **6.70** was isolated. Various reactions were carried out to determine the most likely mechanism to forming this monosalt; however it remains unclear whether or not the reaction intermediates were monocationic or dicationic.

Scheme 6.32 Formation of monosalt **6.70** from amide **6.66**.

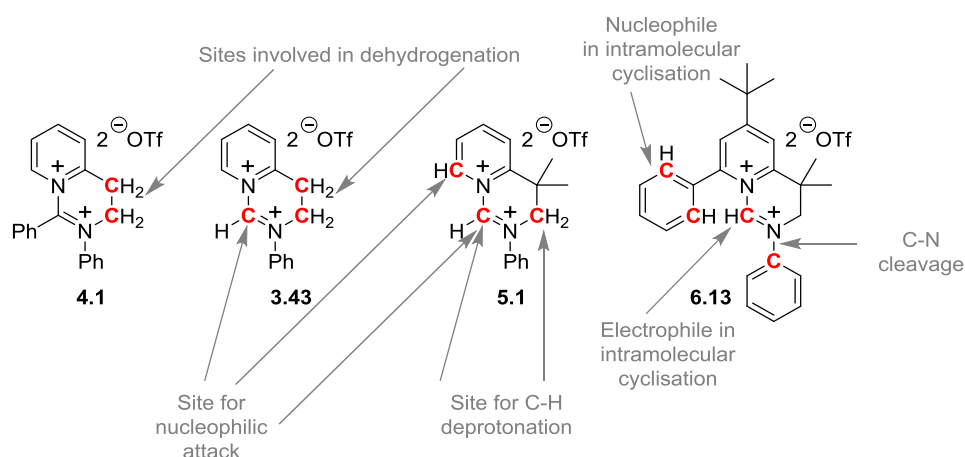


As is evident, this chapter successfully extended the scope of reactions for amide-derived superelectrophiles. Some of the more unusual reactions described merit future investigations, and this will be described in the next chapter (Chapter 7: Conclusions & Future Work).

Chapter 7: Conclusions and Future Work

The treatment of amides with triflic anhydride and amines can form amidine disalts. Amidine disalt **4.1**, was the first such disalt isolated and characterized by X-ray crystallography (Figure 7.1). After characterising disalt **4.1**, disalt **3.43** was used in palladium-catalysed hydrogenation reactions. The limitations of this disalt due to the reactivity of its ethylene backbone resulted in the need for the synthesis of disalt **5.1**. Disalt **5.1** was found to be stable to 75 bar of dihydrogen in MeCN under catalyst-free conditions, while disalt **3.43** was shown to be unstable to d_3 -MeCN in an inert atmosphere glovebox. Disalt **5.1** was then used in model studies of [Fe]-hydrogenase with an iron-hydride complex, showing reactivity when an amidine monosalt showed no reactivity with the iron-hydride. Amidine disalt **6.13** was designed to provide a compound with greater selectivity for nucleophilic attack at the amidine centre rather than the pyridinium; although this change actually reduced the reactivity at the amidine ring, the disalt did provide new, intriguing reactivity. Figure 7.1 highlights (in bold and red) the different sites where reactivity is observed with disalts **3.43**, **5.1** and **6.13**; throughout the “evolution” of these amidine disalts, new reactivity has continually been observed.

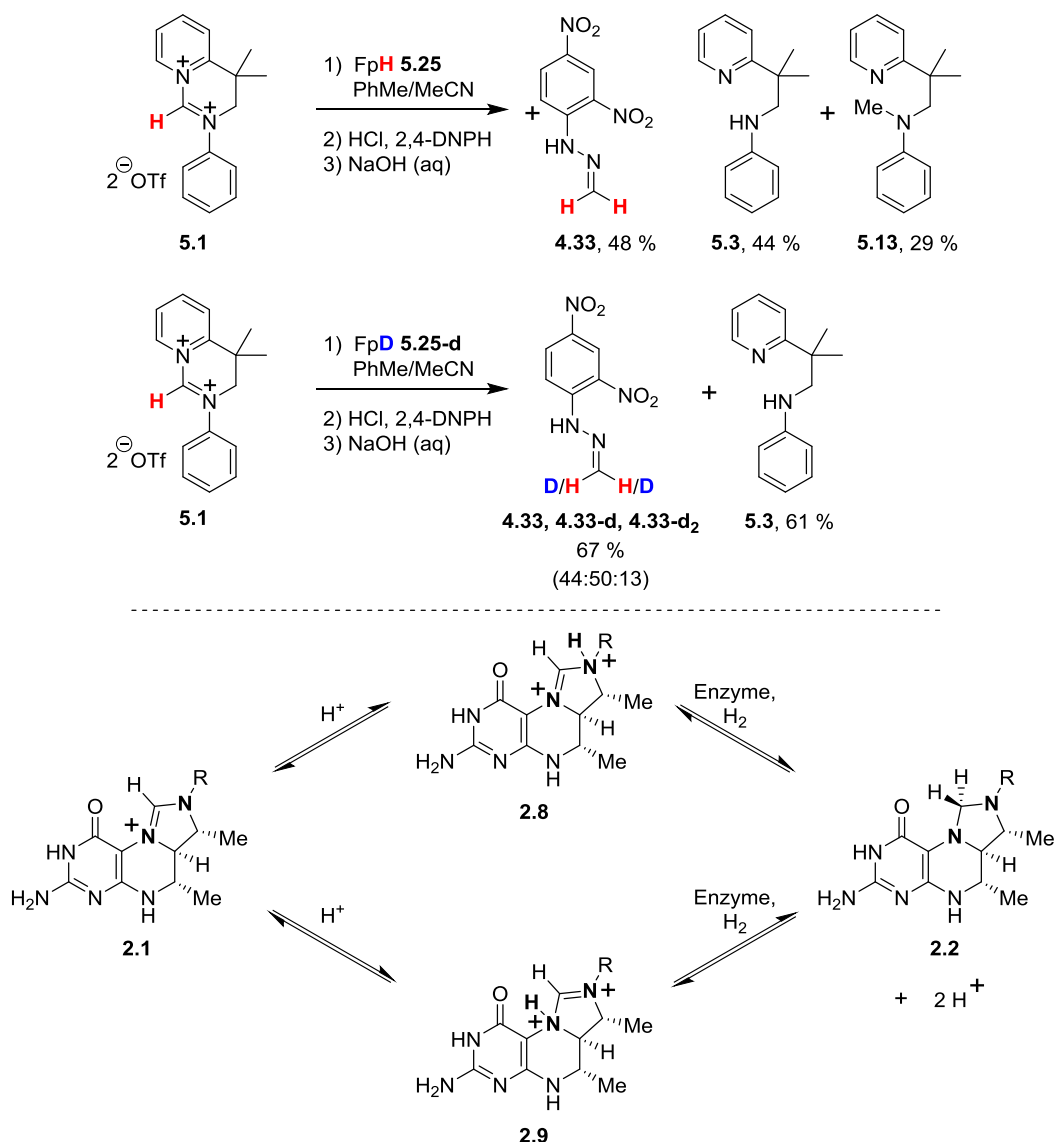
Figure 7.1 Fully characterized disalt **4.1** and related disalts **3.43**, **5.1** and **6.13**.



The [Fe]-hydrogenase model reactions carried out with amidine disalt **5.1** and FpH **5.25** and FpD **5.25-d** (Scheme 7.1) are the first model studies between iron hydride complexes and amidines. The isotopomeric scrambling in the reaction with FpD

5.25-d showed the reaction to be reversible, just as the reaction in Nature is reversible. The model studies show that if amidine dications **2.8** and/or **2.9** are formed within [Fe]-hydrogenase, these compounds are likely to react with an iron hydride, if such a complex forms in the enzyme.

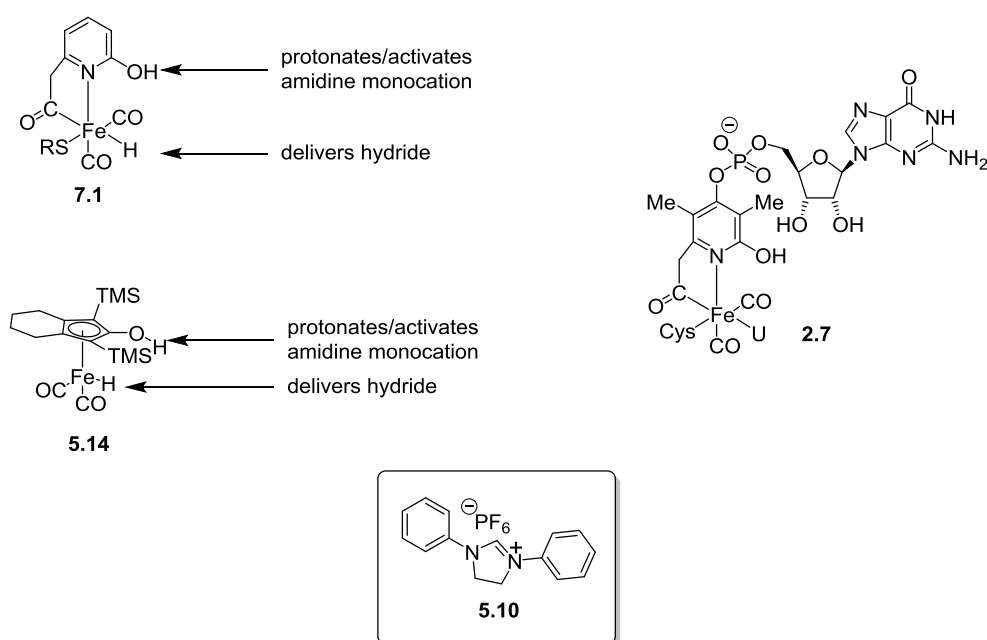
Scheme 7.1 [Fe]-hydrogenase model reactions using disalt **5.1** and FpH **5.25** or FpD **5.25-d**.



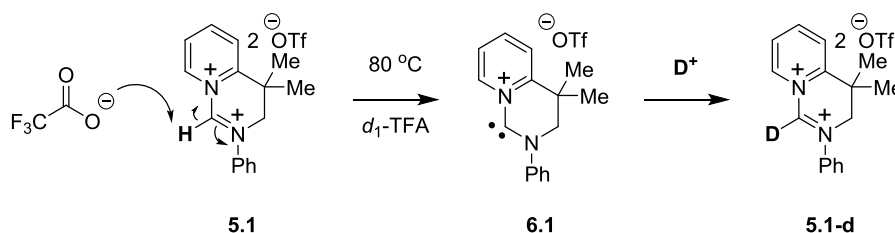
To further test the possibility of superelectrophilic activation in [Fe]-hydrogenase in model reactions, complexes of type **7.1** (Figure 7.2) would be ideal candidates to react with amidine monosalts related to N^5, N^{10} -methenyltetrahydromethanopterin ($CH\equiv H_4MPT^+$) **2.1**. The formation of similar complexes has been reported by Hu *et al.* in 2014;¹⁰¹ however, none of these structures were isolated and a lack of

definitive data was provided to definitively assign their structures. From discussions with Prof. Pickett at the University of East Anglia (one of the main researchers in forming FeGP cofactor **2.7** model complexes), the main reason that complexes such as **7.1** have not been isolated is due to coordination of the free hydroxyl to iron centres other than the one that the pyridinol is coordinated to. This results in structures with multiple iron sites. Casey and co-workers' complex **5.14**,^{121,122} may provide a surrogate for complex **7.1** and allow the study of reduction reactions with amidine monocations. Amidine monosalt **5.9** was not shown to be reduced by FpH **5.25**. If complex **5.14** was found to reduce amidine monosalts (such as monosalt **5.9**), this would demonstrate that the presence of a hydroxyl group is vital in activating the amidine; however, the fact that the 2-hydroxypyridine ligand is not present on structure **5.14** means that any results could not be directly related to the reaction in [Fe]-hydrogenase.

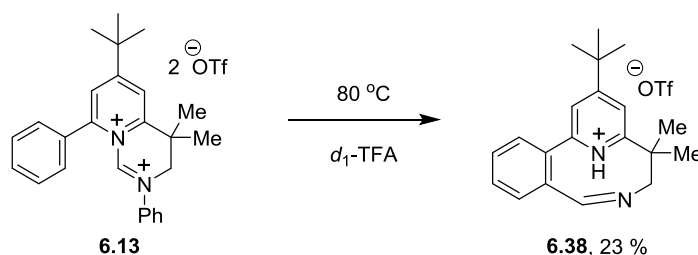
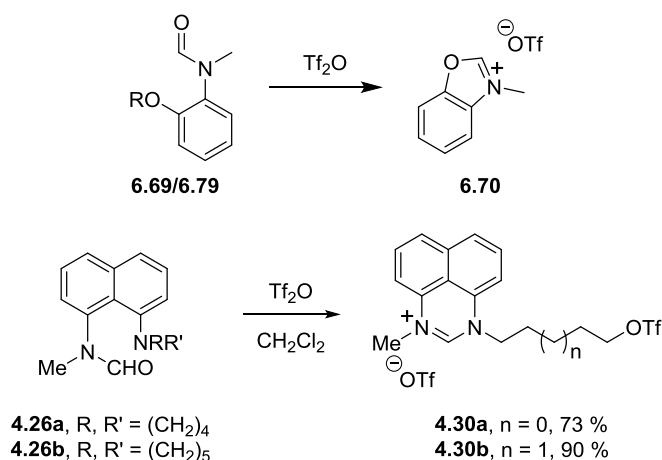
Figure 7.2 Possible FeGP model complexes **9.1**, FeGP cofactor **2.7**, Casey's complex **5.14** and amidine monosalt **5.9**.



Evidence for the formation of an amidine disalt-derived carbene **6.1** was highlighted in the deuterium exchange reaction of disalt **5.1** in deuterated TFA (Scheme 7.2). The isolation of such a carbene could provide a molecule with useful reactivity and could, therefore, form the basis of useful future investigations.

Scheme 7.2 Possible mechanism of deuterium exchange for disalt **5.1**.

The reaction of disalt **6.13** in deuterated TFA (Scheme 7.3) provided some very unusual reactivity. In particular, the loss of the phenyl group (*via* a C-N cleavage) is a reaction that merits future investigation. The exact nature of the C-N cleavage mechanism remains unknown and mechanistic investigations could provide useful. As the phenyl ring may have left disalt **6.13** as a phenyl cation (Chapter 6 Schemes 6.15 and 6.16), this reaction may provide a new way in which to generate this highly reactive species. Additionally, if further evidence for the formation monosalt **6.38** can be provided, this gives provides a new synthetic route to 9-membered rings.

Scheme 7.3 Heating disalt **6.13** in d_1 -TFA.Scheme 7.4 Reactivity of molecules **6.69** and **6.79** compared to molecules **4.26**.

Lastly, the reactions of triflic anhydride with molecules **6.69** and **6.79** (Scheme 7.4) were observed to form monosalt **6.70**. These results appear to be related to the

reaction of amides **4.26** with triflic anhydride, that are proposed to form monosalts **4.30** *via* amidine disalts.¹¹⁶ However, ethers are shown to undergo cleavage reactions under such conditions and this fact could provide an alternative mechanism to the formation of disalts on the way to forming monosalt **6.70**. Future studies involving isotopic labeling of the oxygens (one at a time) in amides **6.69** and **6.79** could shed light on the mechanism involved in this process.

The successful isolation and characterisation of amidine disalts and the extension of this success into observing novel reactions has been presented within this work. Of particular significance to the wider scientific community, a possible relation to the reactivity observed in [Fe]-hydrogenase has been demonstrated. However, there still remains a great scope in the future investigation of amidine disalts as well as scope in investigations of related disalts (containing alternative heteroatoms as part of the dicationic centre).

Chapter 8: Experimental Section

General Methods

All reagents were purchased from Alfa Aesar, Sigma Aldrich, Acros Organics or Fluorochem Ltd., with the exception of deuterated solvents (other than CDCl_3 and d_6 -DMSO), which were purchased from Goss Scientific Instruments Ltd. d_3 -Acetonitrile, acetonitrile and Tf_2O **1.32** were distilled from P_2O_5 (0.5-1.0 mol%) under argon. d_4 -Acetic acid and acetic acid were dried over CuSO_4 . Tetrahydrofuran, dichloromethane, hexane, diethyl ether and toluene were dried and deoxygenated with a Pure-Solv 400 solvent purification system by Innovative Technology Inc., U.S.A. and the moisture content of the solvents was analysed using a Karl Fischer coulometer (METTLER TOLEDO DL39). Tetrahydrofuran was additionally dried by refluxing over potassium benzophenone ketyl under nitrogen. All glassware was oven or flame-dried prior to use. Inert reactions were carried out under argon or nitrogen.

Infra-red spectra were recorded on a Perkin Elmer Spectrum One FT-IR spectrometer or an A₂ Technologies ML FTIR fitted with an ATR. Proton NMR (^1H) and carbon NMR (^{13}C) spectra were recorded on a Bruker AVIII400 spectrometer, Bruker AV400 spectrometer or Bruker DRX500 spectrometer. The chemical shifts (δ) are quoted in parts per million (ppm). Multiplicities are abbreviated as s, singlet; d, doublet; t, triplet; m, multiplet for the ^1H NMR spectra. The coupling constants (J) are reported in Hertz (Hz), with values averaged between coupling nuclei to allow clarity when reporting, and these coupling constants were only averaged if the difference between them was within 0.3 Hz of each other.

High resolution mass spectra were recorded at the EPSRC National Mass Spectrometry Service Centre, Swansea.

Melting points (mp) were carried out on a Griffin melting point apparatus and are uncorrected.

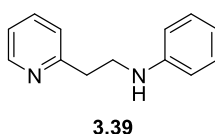
Flash chromatography was performed using silica gel 60 (200-400 mesh). Thin layer chromatography (TLC) was performed using aluminium sheets of silica gel 60 F₂₅₄ and was visualised under a Mineralight UVGL-58 lamp (254 nm). The plates were developed with vanillin, potassium permanganate, iodine or phosphomolybdic acid.

Glovebox experiments were carried out in an Innovative Technology Inc., System One glovebox under oxygen-free, moisture-free conditions. Solvents and reagents to be used in glovebox experiments were dried and degassed prior to handling in the glovebox. For reactions involving superelectrophilic disalts, solvents were further dried in the glovebox.

The IUPAC names of some compounds were obtained using ChemDraw Ultra version 12.

Single crystal X-ray diffraction measurements were made on an Oxford Diffraction Gemini S instrument at 123 K. Final refinement was to convergence on F² and used the SHELXL-97 program.

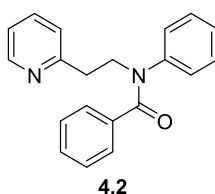
Preparation of *N*-(2-(Pyridin-2-yl)ethyl)aniline, **3.39**²⁷



Aniline **3.38** (13.68 mL, 150 mmol, 3 eq) was added to a solution of 2-vinylpyridine **3.37** (5.39 mL, 50 mmol, 1 eq) in glacial acetic acid (30 mL). The reaction mixture was refluxed for 18 h and, after cooling to room temperature, was concentrated *in vacuo*. The resultant residue was then triturated with diethyl ether to remove the aniline acetate salt side-product. The filtrate was then concentrated *in vacuo*, treated with water (60 mL) and extracted with chloroform (4 x 40 mL). The organic layers were combined, dried (Na₂SO₄) and concentrated *in vacuo* to yield a brown oil. Purification by vacuum distillation (140-152 °C at 0.01 mbar) afforded *N*-[2-(pyridin-2-yl)ethyl]aniline **3.39** (7.5 g, 79 %) as a yellow oil that later solidified on

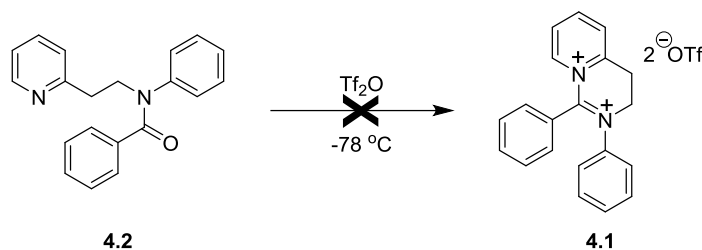
cooling;²⁷ mp 41-43 °C (lit. 40.6-41.5 °C);²⁷ ¹H NMR (400 MHz, CDCl₃) δ = 3.12 (2H, t, J = 6.7 Hz, CH₂), 3.56 (2H, t, J = 6.7 Hz, CH₂), 4.05 (1H, bs, NH), 6.66 (2H, dd, J = 1.0, 7.4 Hz, ArH), 6.71 (1H, t, J = 7.3 Hz, ArH), 7.16-7.22 (4H, m, ArH), 7.65 (1H, ddd, J = 1.9, 7.4, 7.6 Hz, ArH), 8.58 (1H, dd, J = 1.6, 4.8 Hz, ArH); ¹³C NMR (125 MHz, CDCl₃) δ = 37.5 (CH₂), 43.6 (CH₂), 113.0 (CH), 117.3 (CH), 121.5 (CH), 123.3 (CH), 129.2 (CH), 136.5 (CH), 148.2 (C), 149.4 (CH), 159.8 (C); IR (KBr disk) ν = 3655, 3022, 1591, 1498, 1474, 1435, 1326, 1266, 1177, 1150, 1093, 1071, 1050, 997, 988, 746, 694, 502 cm⁻¹; m/z (CI) 199 (100 %) [M+H]⁺; HRMS: m/z calcd for C₁₃H₁₅N₂ [M+H]⁺: 199.1230; found: 199.1229.

Preparation of *N*-Phenyl-*N*-(2-(pyridin-2-yl)ethyl)benzamide, **4.2**



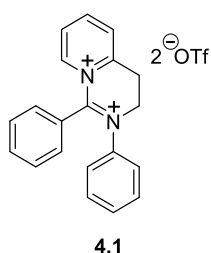
A solution of benzoyl chloride **4.3** (9.29 mL, 80 mmol, 2.0 eq) in CH₂Cl₂ (20 mL) was added dropwise to a flask containing *N*-(2-(pyridin-2-yl)ethyl)aniline **3.39** (7.93 g, 40 mmol, 1.0 eq) in CH₂Cl₂ (20 mL) under argon. The reaction mixture was stirred for 18 h, concentrated *in vacuo*, treated with saturated NaHCO₃ solution (50 mL) and extracted with ethyl acetate (4 x 50 mL). The combined organic layers were washed with NaOH (aq) (2N, 6 x 200 mL), brine (200 mL), dried (Na₂SO₄) and concentrated *in vacuo* to afford *N*-phenyl-*N*-[2-(pyridin-2-yl)ethyl]benzamide **4.2** (9.87 g, 83 %) as a white solid;¹⁴² mp 101-103 °C; ¹H NMR (500 MHz, CDCl₃) δ = 3.21 (2H, t, J = 7.6 Hz, CH₂), 4.31 (2H, t, J = 7.6 Hz, CH₂), 6.93 (2H, d, J = 7.6 Hz, ArH), 7.08-7.28 (10H, m, ArH), 7.59 (1H, dd, J = 8.5, 8.7 Hz, ArH), 8.51 (1H, d, J = 4.2 Hz, ArH); ¹³C NMR (125 MHz, CDCl₃) δ = 36.2 (CH₂), 50.8 (CH₂), 121.5 (CH), 123.7 (CH), 126.6 (CH), 127.7 (CH), 127.8 (CH), 128.7 (CH), 129.1 (CH), 129.5 (CH), 136.2 (C), 136.4 (CH), 143.6 (C), 149.2 (CH), 159.2 (C), 170.6 (C); IR (KBr disk) ν = 3717, 3060, 2937, 2809, 1638, 1584, 1493, 1393, 1308, 1141, 1020, 990, 780, 698 cm⁻¹; m/z (ESI) 303 (100 %) [M+H]⁺; HRMS: m/z calcd for C₂₀H₁₉N₂O [M+H]⁺: 303.1492; found: 303.1490.

Attempted Low Temperature Preparation of 1,2-Diphenyl-3,4-dihydropyrido[1,2-*c*]pyrimidine-2,9-dium Bis(trifluoromethanesulfonate) **4.1**



A solution of *N*-phenyl-*N*-(2-(pyridin-2-yl)ethyl)benzamide **4.2** (151 mg, 0.5 mmol, 1.0 eq) in dry CH₂Cl₂ (0.5 mL) was added to a solution of Tf₂O **1.32** (169 mg, 0.6 mmol, 1.2 eq) in dry CH₂Cl₂ (0.5 mL) at -78 °C under argon, using a syringe pump (0.254 mL h⁻¹). Addition of the amide and stirring were carried out over a time of 3 h, with the reaction mixture then warmed to room temperature and stirred for 30 min. The reaction mixture was concentrated *in vacuo* and attempted recrystallisation (diethyl ether and CH₂Cl₂) failed to yield desired product.

Small Scale Preparation of 1,2-Diphenyl-3,4-dihydropyrido[1,2-*c*]pyrimidine-2,9-dium Bis(trifluoromethanesulfonate) **4.1**



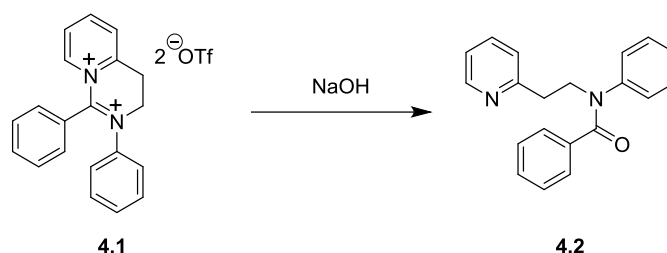
The procedure reported directly above was carried out at r.t. instead of -78 °C, using *N*-phenyl-*N*-(2-(pyridin-2-yl)ethyl)benzamide **4.2** (76 mg, 0.25 mmol, 1.0 eq) in CH₂Cl₂ (0.25 mL) and Tf₂O **1.32** (50 μL, 0.30 mmol, 1.2 eq) in CH₂Cl₂ (0.25 mL). The reaction mixture was concentrated *in vacuo* and recrystallised (diethyl ether and CH₂Cl₂) to yield 1,2-diphenyl-3,4-dihydropyrido[1,2-*c*]pyrimidine-2,9-dium bis(trifluoromethanesulfonate) **4.1** (62 mg, 41 %) as green crystals; mp 72 °C (dec.); data

were consistent with those reported in the Larger Scale Preparation of 1,2-Diphenyl-3,4-dihydropyrido[1,2-*c*]pyrimidine-2,9-dium Bis(trifluoromethanesulfonate) **4.1**.

Larger Scale Preparation of 1,2-Diphenyl-3,4-dihydropyrido[1,2-*c*]pyrimidine-2,9-dium Bis(trifluoromethanesulfonate) **4.1**

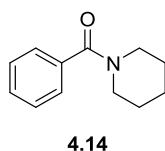
A solution *N*-phenyl-*N*-(2-(pyridin-2-yl)ethyl)benzamide **4.2** (1.51 g, 5 mmol, 1.0 eq) in dry CH₂Cl₂ (5 mL) was added to a solution of Tf₂O **1.32** (1.69 g, 6 mmol, 1.2 eq) in dry CH₂Cl₂ (5 mL) at 0 °C under argon, using a syringe pump (1.78 mL h⁻¹). Addition of the amide and stirring were carried out over a time of 4 h, then the reaction mixture was allowed to warm to r.t. and stirred for a further hour. The reaction mixture was concentrated *in vacuo* and fresh CH₂Cl₂ (5 mL) was added to the resultant residue, which was stirred. The green precipitate that had formed was filtered and residual CH₂Cl₂ removed *in vacuo*. Recrystallisation (CH₂Cl₂ and ether) afforded 1,2-diphenyl-3,4-dihydropyrido[1,2-*c*]pyrimidine-2,9-dium bis(trifluoromethanesulfonate) **4.1** (2.65 g, 85 %) as a green solid; mp 72 °C (dec.); ¹H NMR (400 MHz, CD₃CN) δ = 4.28 (2H, t, *J* = 7.5 Hz, CH₂), 4.97 (2H, t, *J* = 7.5 Hz, CH₂), 7.53-7.60 (7H, m, ArH), 7.75-7.80 (3H, m, ArH), 8.11 (1H, ddd, *J* = 1.4, 6.8, 7.8 Hz, ArH), 8.43 (1H, dd, *J* = 1.4, 7.9 Hz, ArH), 8.69 (1H, dd, *J* = 1.2, 6.8 Hz, ArH), 9.01 (1H, ddd, *J* = 1.2, 7.8, 7.9 Hz, ArH); ¹³C NMR (100 MHz, CD₃CN) δ = 25.1 (CH₂), 52.0 (CH₂), 120.6 (quartet, *J*(C,F) = 330 Hz, CF₃), 122.8 (C), 123.4 (CH), 127.0 (CH), 129.0 (CH), 129.3 (CH), 130.3 (CH), 131.4 (CH), 132.4 (CH), 135.5 (CH), 141.2 (C), 146.0 (CH), 154.1 (C), 155.8 (CH), 166.8 (C); ¹⁹F NMR (376 Hz, CD₃CN) δ = -79.4; IR (KBr disc) ν = 3258, 3026, 2932, 2862, 1601, 1535, 1497, 1435, 1328, 1283, 1175, 987, 744, 694 cm⁻¹; *m/z* (ESI) 143.1 (67 %) [M]²⁺, 143.6 (16 %) [M+1]²⁺, 142.1 (100 %) [M-H₂]²⁺, 142.6 (21 %) [M-H₂+1]²⁺.

Hydrolysis of 1,2-Diphenyl-3,4-dihydropyrido[1,2-*c*]pyrimidine-2,9-dium Bis(trifluoromethanesulfonate) **4.1** with NaOH



NaOH (aq) (2N, 2mL, 4 mmol, 8 eq) was added to 1,2-diphenyl-3,4-dihydropyrido[1,2-*c*]pyrimidine-2,9-dium bis(trifluoromethanesulfonate) **4.1**, stirred overnight and then extracted with CH₂Cl₂ (3 x 5 mL). The combined organic layers were washed with water (15 mL), brine (15 mL), dried (Na₂SO₄) and concentrated *in vacuo* to afford *N*-phenyl-*N*-(2-(pyridin-2-yl)ethyl)benzamide **4.2** (150 mg, 99 %); data were consistent with those reported for compound **4.2**.

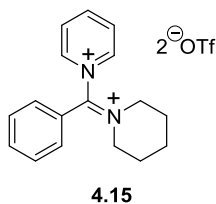
Preparation of Phenyl(piperidin-1-yl)methanone, **4.14**



A solution of benzoyl chloride **4.3** (2.32 mL, 20 mmol, 1.0 eq) in CH₂Cl₂ (5 mL) was added dropwise to a solution of piperidine **4.13** (5.93 mL, 60 mmol, 2.0 eq) in CH₂Cl₂ (5 mL) at 0 °C under argon. The mixture was then allowed to warm to room temperature, stirred for 14 h and then concentrated *in vacuo*. The resultant residue was acidified with 2N HCl (aq) and extracted with CH₂Cl₂ (3 x 30 mL). The pooled organics were washed with water (60 mL) and brine (60 mL), dried (Na₂SO₄) and concentrated *in vacuo* to yield phenyl(piperidin-1-yl)methanone **4.14** (3.41 g, 90 %) as a colourless oil; ¹H NMR (400 MHz, CDCl₃) δ = 1.54-1.74 (6H, m, CH₂), 3.36 (2H, bs, CH₂), 3.73 (2H, bs, CH₂), 7.40 (5H, bs, ArH); ¹³C NMR (100 MHz, CDCl₃) δ = 24.1 (CH₂), 25.1 (CH₂), 26.1 (CH₂), 42.6 (CH₂), 48.2 (CH₂), 126.3 (CH), 127.9 (CH), 128.8 (CH), 136.1 (C), 169.8 (C); IR (thin film) ν̄ = 2937, 2855, 1631, 1432,

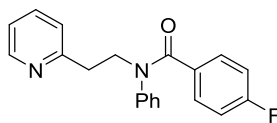
1275, 1111, 1003, 787, 707, 632, 455 cm^{-1} ; m/z (ESI) 190 (11 %) $[\text{M}+\text{H}]^+$, 212 (100 %) $[\text{M}+\text{Na}]^+$; HRMS: m/z calcd for $\text{C}_{12}\text{H}_{16}\text{NO}$ $[\text{M}+\text{H}]^+$: 190.1226; found: 190.1222.

Preparation of 1-(Phenyl(piperidin-1-ium-1-ylidene)methyl)pyridin-1-ium bis(trifluoromethanesulfonate), 4.15



A solution of pyridine **1.31** (95 mg, 1.2 mmol, 1.2 eq) in dry CH_2Cl_2 (0.7 mL) was added dropwise to a solution of Tf_2O **1.32** (282 mg, 1.0 mmol, 1.0 eq) in dry CH_2Cl_2 (0.3 mL) at $-78\text{ }^\circ\text{C}$ under argon using a syringe pump (0.508 mL h^{-1}). After full addition of pyridine **1.31**, the reaction mixture was allowed to warm to room temperature and stirred for 1.5 h before recooling to $-78\text{ }^\circ\text{C}$. A solution of phenyl(piperidin-1-yl)methanone **4.14** (227 mg, 1.2 mmol, 1.2 eq) in dry CH_2Cl_2 (1.0 mL) was then added to the reaction mixture, using a syringe pump (0.508 mL h^{-1}). After full addition of amide, the mixture was stirred for 20 min, allowed to warm to room temperature and stirred for a further 14 h. The reaction mixture was then stirred for 1 h with extra CH_2Cl_2 (2 mL) before being filtered, washed (6 x 3 mL CH_2Cl_2) and concentrated *in vacuo* to yield 1-[phenyl(piperidin-1-ium-1-ylidene)methyl]pyridin-1-ium bis(trifluoromethanesulfonate) **4.15** (438 mg, 80 %) as a white powder; mp $55\text{--}59\text{ }^\circ\text{C}$; ^1H NMR (400 MHz, CDCl_3) δ = 1.95 (2H, m, CH_2), 2.14 (2H, quintet, J = 5.8 Hz, CH_2), 2.26 (2H, quintet, J = 5.8 Hz, CH_2), 4.07 (2H, t, J = 5.8 Hz, CH_2), 4.51 (2H, t, J = 5.8 Hz, CH_2), 7.75–7.76 (4H, m, ArH), 7.98–8.02 (1H, m, ArH) 8.43–8.46 (2H, m, ArH), 9.04 (1H, ddd, J = 1.4, 8.0, 7.6 Hz, ArH), 9.08 (2H, dd, J = 1.4, 7.0 Hz, ArH); ^{13}C NMR (100 MHz, CDCl_3) δ = 21.4 (CH_2), 25.9 (CH_2), 26.0 (CH_2), 58.8 (CH_2), 60.5 (CH_2), 120.7 (quartet, $J(\text{C},\text{F})$ = 319 Hz, CF_3), 127.6 (C), 129.7 (CH), 129.9 (CH), 133.0 (CH), 138.2 (CH), 144.8 (CH), 153.7 (CH), 166.2 (C); IR (KBr disk) $\tilde{\nu}$ = 3558, 3081, 2947, 2865, 1615, 1542, 1490, 1451, 1286, 1168, 1031, 759, 640, 576, 518 cm^{-1} . The disalt was too unstable for MS analysis.

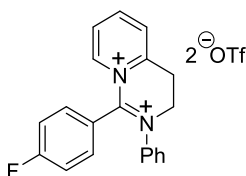
Preparation of 4-Fluoro-*N*-phenyl-*N*-(2-(pyridin-2-yl)ethyl)benzamide, **4.17**



4.17

This compound was prepared using the same procedure as for *N*-phenyl-*N*-[2-(pyridin-2-yl)ethyl]benzamide **4.2**, using 4-fluorobenzoyl chloride **4.16** (4.73 mL, 40 mmol, 2.0 eq) in CH₂Cl₂ (10 mL) and *N*-(2-(pyridin-2-yl)ethyl)aniline **3.39** (3.97 g, 20 mmol, 1.0 eq) in CH₂Cl₂ (10 mL). Column chromatography (1:1 EtOAc in petroleum ether, 40-60 °C) afforded 4-fluoro-*N*-phenyl-*N*-[2-(pyridin-2-yl)ethyl]benzamide **4.17** (6.10 g, 95 %) as an off-white solid; mp 71-73 °C; ¹H NMR (500 MHz, CDCl₃) δ = 3.22 (2H, t, *J* = 7.6 Hz, CH₂), 4.33 (2H, t, *J* = 7.6 Hz, CH₂), 6.84 (2H, dd, *J* = 8.5, 8.8 Hz, ArH), 6.96 (2H, d, *J* = 7.4 Hz, ArH), 7.11-7.32 (7H, m, ArH), 7.61 (1H, dd, *J* = 8.4, 8.6 Hz, ArH) 8.52 (1H, dd, *J* = 1.7, 4.8 Hz, ArH); ¹³C NMR (125 MHz, CDCl₃) δ = 36.1 (CH₂), 50.9 (CH₂), 114.7 (d, *J*(C,F)= 22.5 Hz, CH), 121.6 (CH), 123.7 (CH), 126.8 (CH), 127.7 (CH), 129.3 (CH), 131.1 (d, *J*(C,F)= 7.5 Hz, CH), 132.2 (C), 136.5 (CH), 143.6 (C), 149.2 (CH), 160.0 (C), 163.2 (d, *J*(C,F)= 251.5 Hz, CF), 169.4 (C); IR (KBr disk) ν = 3065, 3008, 2931, 1641, 1589, 1493, 1382, 1304, 1219, 1142, 858, 759, 699, 526 cm⁻¹; *m/z* (ESI) 343 (100 %) [M+Na]⁺; HRMS: *m/z* calcd for C₂₀H₁₈FN₂O [M+H]⁺: 321.1398; found: 321.1394.

Small Scale Preparation of 1-(4-Fluorophenyl)-2-phenyl-3,4-dihydropyrido[1,2-*c*]pyrimidine-2,9-dium Bis(trifluoromethanesulfonate), **4.18**



4.18

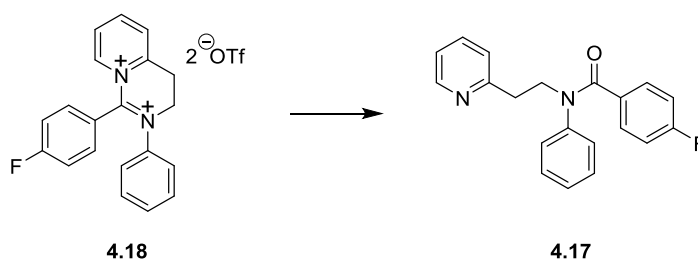
Disalt **4.18** was prepared using the same method as that used for 1,2-diphenyl-3,4-dihydropyrido[1,2-*c*]pyrimidine-2,9-dium bis(trifluoromethanesulfonate) **4.1**, using 4-fluoro-*N*-phenyl-*N*-[2-(pyridin-2-yl)ethyl]benzamide **4.17** (161 mg, 0.5 mmol, 1.0 eq) in CH₂Cl₂ (0.5 mL) and Tf₂O **1.32** (0.1 mL, 0.6 mmol, 1.2 eq) in CH₂Cl₂ (0.5

mmol). Recrystallisation (CH₂Cl₂ and ether) afforded 1-(4-fluorophenyl)-2-phenyl-3,4-dihydropyrido[1,2-*c*]pyrimidine-2,9-dium bis(trifluoromethanesulfonate) **4.17** (273 mg, 91 %) as a brown solid; mp 80 °C (dec.); ¹H NMR (400 MHz, CD₃CN) δ = 4.28 (2H, t, *J* = 7.6 Hz, CH₂), 4.97 (2H, t, *J* = 7.6 Hz, CH₂), 7.31 (2H, m, ArH), 7.56-7.57 (5H, m, ArH), 7.83-7.87 (2H, m, ArH), 8.13 (1H, ddd, *J* = 1.4, 6.4, 7.6 Hz, ArH), 8.42 (1H, m, ArH), 8.75 (1H, dd, *J* = 1.2, 6.4 Hz, ArH), 9.04 (1H, ddd, *J* = 1.2, 7.6, 8.0 Hz, ArH); ¹³C NMR (125 MHz, CD₃CN) δ = 25.5 (CH₂), 52.4 (CH₂), 117.3 (CH), 120.6 (quartet, *J*(C,F) = 324 Hz, CF₃), 123.7 (CH), 127.4 (CH), 129.5 (CH), 130.8 (CH), 131.9 (CH), 136.4 (d, *J*(C,F) = 35 Hz, CH), 141.5 (C), 146.3 (CH), 147.3 (C), 154.5 (C), 156.3 (CH), 166.3 (C), 166.7 (C, d, *J*(C,F) = 258.7 Hz, C). The disalt was too reactive for MS, HRMS or IR analysis.

Larger Scale Preparation of 1-(4-Fluorophenyl)-2-phenyl-3,4-dihydropyrido[1,2-*c*]pyrimidine-2,9-dium bis(trifluoromethanesulfonate), **4.18**

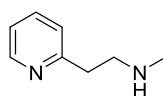
A solution 4-fluoro-*N*-phenyl-*N*-(2-(pyridin-2-yl)ethyl)benzamide **4.17** (1.51 g, 4.7 mmol, 1.0 eq) in dry CH₂Cl₂ (5 mL) was added to a solution of Tf₂O **1.32** (1.0 mL, 6.0 mmol, 1.2 eq) in dry CH₂Cl₂ (5 mL) at 0 °C under argon, using a syringe pump (1.78 mL h⁻¹). Addition of the amide was carried out with stirring over 5 h and the reaction mixture was then warmed to r.t. and stirred for 30 min. The reaction mixture was concentrated *in vacuo* to yield 1-(4-fluorophenyl)-2-phenyl-3,4-dihydropyrido[1,2-*c*]pyrimidine-2,9-dium bis(trifluoromethanesulfonate) **4.18** as a brown solid (2.74 g, 91 %); data were consistent with those reported for compound **4.18**.

Hydrolysis of 1-(4-Fluorophenyl)-2-phenyl-3,4-dihydropyrido[1,2-*c*]pyrimidine-2,9-dium Bis(trifluoromethanesulfonate) **4.18** with NaOH



NaOH (aq) (2N, 2 mL) was added to 1-(4-fluorophenyl)-2-phenyl-3,4-dihydropyrido[1,2-*c*]pyrimidine-2,9-dium bis(trifluoromethanesulfonate) **4.18** (301 mg, 0.5 mmol, 1.0 eq), stirred for 30 min and then extracted with CH₂Cl₂ (3 x 5 mL). The combined organic layers were washed with water (15 mL), brine (15 mL), dried (Na₂SO₄) and concentrated *in vacuo* to afford 4-fluoro-*N*-phenyl-*N*-(2-(pyridin-2-yl)ethyl)benzamide **4.17** (159 mg, 99 %); data were consistent with those reported above.

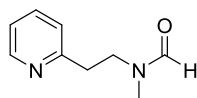
Preparation of *N*-Methyl-2-(pyridin-2-yl)ethanamine, **3.33**



3.33

Methylamine hydrochloride **3.32** (20.26 g, 300 mmol, 3 eq) was added to a solution of 2-ethanopyridine **3.31** (11.27 mL, 100 mmol, 1 eq) in glacial acetic acid (125 mL) and stirred under reflux for 60 h. After cooling, the reaction mixture was concentrated *in vacuo* and the resultant residue was then triturated with 2-propanol (80 mL) and stirred for 30 min. The white precipitate formed (unreacted methylamine hydrochloride **3.32**) was filtered off. The filtrate was then concentrated *in vacuo*, with the residue then treated with NaOH solution (2N, 70 mL) and NaOH pellets until the pH was greater than 10 (indicated by pH paper). Water (30 mL) was added and the product was extracted with chloroform (6 x 100 mL). The combined organic layers were dried (Na₂SO₄) and concentrated *in vacuo*. Column chromatography (89:10:1; chloroform: methanol: triethylamine) afforded *N*-methyl-2-(pyridin-2-yl)ethanamine **3.33** (11.51 g, 85 %) as a yellow oil;¹¹¹ ¹H NMR (400 MHz, CDCl₃) δ= 1.51 (1H, s, NH), 2.44 (3H, s, CH₃), 2.95 - 2.99 (4H, m, CH₂), 7.09 (1H, ddd, *J* = 1.0, 4.0, 6.2 Hz, ArH), 7.15 (1H, dd, *J* = 1.0, 7.8 Hz, ArH), 7.57 (1H, ddd, *J* = 1.1, 6.2, 7.8 Hz, ArH), 8.51 (1H, dd, *J* = 1.1, 4.0 Hz, ArH); ¹³C NMR (125 MHz, CDCl₃) δ= 36.3 (CH₂), 38.3 (CH₃), 51.4 (CH₂), 121.1 (CH), 123.2 (CH), 136.2 (CH), 149.3 (CH), 160.3 (C); IR (thin film) ν= 3298, 3066, 3010, 2932, 2844, 2793, 1592, 1475, 1436, 1150, 1112, 750 cm⁻¹; *m/z* (CI) 137 (100 %) [M+H]⁺; HRMS: *m/z* calcd for C₈H₁₃N₂ [M+H]⁺: 137.1073; found: 137.1072.

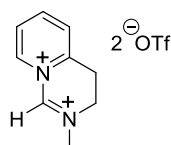
Preparation of *N*-Methyl-*N*-(2-(pyridin-2-yl)ethyl)formamide, **3.35**



3.35

N-methyl-2-(pyridin-2-yl)ethanamine **3.33** (8.30 mL, 60 mmol, 1.0 eq) was added to ethyl formate **3.34** (10.91 mL, 135.6 mmol, 2.26 eq) and stirred under argon at reflux for 4 h. After cooling, the reaction mixture was concentrated *in vacuo* to give a brown oil. Vacuum distillation (143-152 °C, 0.1 mbar) afforded *N*-methyl-*N*-(2-(pyridin-2-yl)ethyl)formamide **3.35** (6.41 g, 65 %) as a clear, yellow oil and an unseparated mixture of two rotamers (in approx. 3:2 ratio);¹¹¹ ¹H NMR (400 MHz, CDCl₃) δ = 2.52 (3H, s, CH₃, both rotamers), 2.94 - 2.99 (2H, m, CH₂, both rotamers), 3.62 - 3.69 (2H, m, CH₂, both rotamers), 7.00 - 7.10 (3H major rotamer, 2H minor rotamer, m, ArH), 7.15 (1H, d, J = 7.6 Hz, ArH, minor rotamer), 7.74 (1H, s, CHO, major rotamer), 7.86 (1H, s, CHO, minor rotamer), 8.46 - 8.49 (1H, m, ArH, both rotamers); ¹³C NMR (125 MHz, CDCl₃) δ = 29.4 (CH₂, major rotamer), 34.9 (CH₂, minor rotamer), 35.4 (CH₃, minor rotamer) 36.6 (CH₃, major rotamer), 44.2 (CH₂, minor rotamer) 49.0 (CH₂, major rotamer), 121.5 (CH, minor rotamer), 121.7 (CH, major rotamer), 123.2 (CH, minor rotamer), 123.5 (CH, major rotamer), 136.4 (CH, minor rotamer), 136.5 (CH, major rotamer), 149.2 (CH, minor rotamer), 149.5 (CH, major rotamer), 157.7 (CHO, major rotamer), 158.6 (CHO, minor rotamer), 162.4 (C, minor rotamer) 162.6 (C, minor rotamer); IR (thin film) ν = 3064, 3010, 2929, 2861, 1668, 1593, 1435, 1395, 1070, 763 cm⁻¹; m/z (ESI) 165 (100 %) [M+H]⁺; HRMS: m/z calcd for C₉H₁₃N₂O [M+H]⁺: 165.1022; found: 165.1020.

Attempted Preparation of 2-Methyl-3,4-dihydropyrido[1,2-*c*]pyrimidine-2,9-dium Bis(trifluoromethanesulfonate), **3.36**

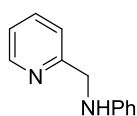


3.36

A solution of *N*-methyl-*N*-(2-(pyridin-2-yl)ethyl)formamide **3.35** (82 mg, 0.5 mmol, 1.0 eq) in dry CH₂Cl₂ (0.5 mL) was added to a solution of Tf₂O **1.32** (0.1 mL, 0.6 mmol, 1.2 eq) in dry CH₂Cl₂ (0.5 mL) at -78 °C under argon, using a syringe pump (0.254 mL h⁻¹). Addition of the amide and stirring of the reaction mixture was carried out over 5 h and the reaction mixture was allowed to warm to room temperature. A purple precipitate had developed in the reaction mixture, which was then concentrated *in vacuo* and stirred for 30 min in dry CH₂Cl₂ (5 mL), filtered, washed with CH₂Cl₂ (3 x 20 mL) and concentrated *in vacuo* to give a purple solid containing a mixture of products with 2-methyl-3,4-dihydropyrido[1,2-*c*]pyrimidine-2,9-dium bis(trifluoromethanesulfonate) **3.36** being the main component (estimated as approximately 91 %, taken from the integration of what appears to be a methyl in the impurity compared to the methyl of the disalt, by ¹H NMR).

2-Methyl-3,4-dihydropyrido[1,2-*c*]pyrimidine-2,9-dium bis(trifluoromethanesulfonate) **3.36**¹¹¹ – ¹H NMR of major peaks (400 MHz, CD₃CN) δ= 3.89 (2H, t, *J* = 8.0 Hz, CH₂), 4.02 (3H, s, CH₃), 4.34 (2H, t, *J* = 8.0 Hz, CH₂), 8.24 - 8.32 (2H, m, ArH), 8.96 (1H, ddd, *J* = 1.4, 7.6, 8.0 Hz, ArH), 8.11 (1H, dd, *J* = 1.2, 6.4 Hz, ArH), 9.87 (1H, s, CH); ¹³C NMR of major peaks (125 MHz, CD₃CN) δ= 24.2 (CH₂), 47.0 (CH₂), 47.3 (CH₃), 120.8 (C, quartet, *J*(C,F)= 318 Hz), 127.7 (CH), 129.2 (CH), 145.8 (CH), 150.9 (CH), 156.2 (CH), 156.4 (C).

Preparation of *N*-(Pyridin-2-ylmethyl)aniline, **4.21**

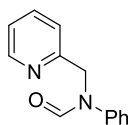


4.21

Aniline **3.39** (27.94 g, 300 mmol, 3.0 eq) was added slowly to 2-pyridylcarboxaldehyde **4.20** (17.02 g, 100 mmol, 1.0 eq) at 0 °C, then allowed to warm to r.t. and stirred for 30 min. ¹H NMR indicated imine formation. The reaction mixture was then diluted with methanol (80 mL) and treated slowly with NaBH₄ powder (5.07 g, 134 mmol, 1.34 eq) and stirred overnight. The mixture was then concentrated *in vacuo*, stirred in water (150 mL) for 1 h and extracted with CH₂Cl₂ (3 x 150 mL). The combined organic layers were dried (Na₂SO₄) and concentrated *in vacuo* to yield

a mixture of desired product **4.21** and aniline **3.38**. Column chromatography (ethyl acetate and petroleum ether, 40-60 °C) afforded *N*-(pyridin-2-ylmethyl)aniline **4.21** (14.04 g, 76 %) as a yellow solid;¹⁴⁴ mp 44 - 47 °C (lit. 48 - 50 °C);¹⁴⁵ ¹H NMR (400 MHz, CDCl₃) δ= 4.47 (2H, s, CH₂), 4.81 (1H, bs, NH), 6.68 (2H, dd, *J* = 0.9, 8.5 Hz, *ArH*), 6.74 (1H, td, *J* = 0.9, 7.3 Hz, *ArH*), 7.17 - 7.23 (3H, m, *ArH*), 7.34 (1H, d, *J* = 7.8 Hz, *ArH*), 7.64 (1H, ddd, *J* = 1.7, 7.6, 7.8 Hz, *ArH*), 8.60 (1H, dd, *J* = 1.7, 4.5 Hz); ¹³C NMR (100 MHz, CDCl₃) δ= 48.8 (CH₂), 112.6 (CH), 117.1 (CH), 121.1 (CH), 121.6 (CH), 128.8 (CH), 136.2 (CH), 147.4 (C), 148.7 (CH), 158.1 (C); IR (KBr disk) ν = 3297, 3031, 2874, 1594, 1496, 1436, 1328, 1272, 1117. 988, 871, 751, 691, 511 cm⁻¹; *m/z* (ESI) 185 (100 %) [M+H]⁺; HRMS: *m/z* calcd for C₁₂H₁₃N₂ [M+H]⁺: 185.1073; found: 185.1068.

Small Scale Preparation of *N*-Phenyl-*N*-(pyridin-2-ylmethyl)formamide, **4.22**



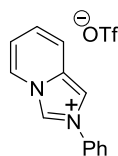
4.22

A solution of oxalyl chloride (5.70 mL, 60 mmol, 4.0 eq) in dry CH₂Cl₂ (15 mL) was added dropwise to a solution of imidazole (4.08 g, 60 mmol, 4.0 eq), triethylamine (16.87 mL, 120 mmol, 8.0 eq) and formic acid (2.26 mL, 60 mmol, 4.0 eq) in dry CH₂Cl₂ (40 mL) at 0 °C under argon. The reaction mixture was warmed to room temperature and stirred for 15 min. *N*-(pyridin-2-ylmethyl)aniline **4.21** (2.76 g, 15 mmol, 1.0 eq) in dry CH₂Cl₂ (20 mL) was added to the reaction mixture and stirred overnight. The reaction mixture was concentrated *in vacuo* and extracted between ethyl acetate (100 mL) and saturated sodium carbonate solution (100 mL). The organic layer was washed with further sodium carbonate solution (6 x 100 mL), water (100 mL), brine (100 mL), dried (Na₂SO₄) and concentrated *in vacuo* to yield *N*-phenyl-*N*-(pyridin-2-ylmethyl)formamide **4.22** with slight impurity. The product was not purified at this point, but distilled at a later point when combined with a larger scale reaction mixture (see directly below).

Larger Scale Preparation of *N*-Phenyl-*N*-(pyridin-2-ylmethyl)formamide, **4.22**

The same procedure as described in the small scale preparation of *N*-phenyl-*N*-(pyridin-2-ylmethyl)formamide **4.22** was carried out using oxalyl chloride (19.0 mL, 200 mmol, 4.0 eq) in CH₂Cl₂ (50 mL), imidazole (13.62 g, 200 mmol, 4.0 eq), triethylamine (56.2 mL, 400 mmol, 8.0 eq) and formic acid (7.6 mL, 200 mmol, 4.0 eq) in CH₂Cl₂ (120 mL) and *N*-(pyridin-2-ylmethyl)aniline **4.21** (9.21 g, 50 mmol, 1.0 eq) in CH₂Cl₂ (60 mL). After working-up, the crude material was combined with the previously made compound (see the small scale synthesis) and purified by vacuum distillation (154-162 °C, 0.005 mbar) to afford *N*-phenyl-*N*-(pyridin-2-ylmethyl)formamide **4.22** (7.54 g, 55 %) as a clear, yellow oil and a mixture of rotamers (approximately 94:6, major: minor); ¹H NMR (400 MHz, CDCl₃) δ= 4.96 (2H, s, CH₂, minor rotamer), 5.14 (2H, s CH₂, major rotamer), 7.05 - 7.37 (7H, m, ArH, major and minor rotamers), 7.60 - 7.67 (1H, m, ArH, major and minor rotamer), 8.52 - 8.60 (1H, m, ArH, major and minor rotamer), 8.66 (1H, s, CHO, major rotamer), 8.67 (1H, s, CHO, minor rotamer); ¹³C NMR of major rotamer only (100 MHz, CDCl₃) δ= 50.4 (CH₂), 121.1 (CH), 121.9 (CH), 122.7 (CH), 126.2 (CH), 129.1 (CH), 136.3 (CH), 140.8 (C), 148.9 (CH), 155.9 (C), 161.9 (CHO); IR (thin film) ν = 3434, 3055, 2928, 1676, 1591, 1497, 1432, 1355, 1196, 1096, 820, 757, 697 cm⁻¹; *m/z* (ESI) 213 (100 %) [M+H]⁺, 447 (43) [2M+Na]⁺; HRMS: *m/z* calcd for C₁₃H₁₃N₂O [M+H]⁺: 213.1022; found: 213.1018.

Preparation of 2-Phenylimidazo[1,5-a]pyridin-2-ium Trifluoromethanesulfonate, **4.24**

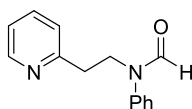


4.24

A solution of *N*-phenyl-*N*-(pyridin-2-ylmethyl)formamide **4.22** (1.061 g, 5.0 mmol, 1.0 eq) in dry CH₂Cl₂ (5 mL) was added to a solution of Tf₂O **1.32** (1.0 mL, 6.0 mmol, 1.2 eq) in dry CH₂Cl₂ (5 mL) at -78 °C under argon, using a syringe pump (1.78 mL h⁻¹). Addition of the amide and stirring of the reaction mixture was carried

out over 4 h and the reaction mixture was allowed to warm to room temperature and stirred for 30 min. The reaction mixture was concentrated *in vacuo* and stirred in diethyl ether (10 mL) for 30 min. The resulting yellow solid was filtered and washed with ether (3 x 10 mL) and concentrated *in vacuo* to afford *2-phenylimidazo[1,5-*a*]pyridin-2-ium trifluoromethanesulfonate* **4.24** (1.54 g, 89 %) as a yellow solid; m.p. 133-137 °C; ¹H NMR (500 MHz, CD₃CN) δ = 7.23 (1H, dd, *J* = 6.7, 7.1 Hz, *ArH*), 7.34 (1H, dd, *J* = 6.7, 9.3 Hz, *ArH*), 7.69 - 7.77 (5H, m, *ArH*), 7.84 (1H, d, *J* = 9.3 Hz, *ArH*), 8.22 (1H, s, *ArH*), 8.43 (1H, d, *J* = 7.1 Hz, *ArH*), 9.53 (1H, s, *ArH*); ¹³C NMR (125 MHz, CD₃CN) 112.6, (CH), 118.3 (CH), 118.6 (CH), 123.3 (CH), 123.8 (CH), 124.6 (CH), 125.6 (CH), 130.5 (CH), 131.0 (CH), 135.2 (C), 150.2 (C), no triflate carbon observed;); ¹⁹F NMR (376 Hz, CD₃CN) δ = -79.4; IR (KBr disk) ν = 3435, 3140, 1660, 1550, 1511, 1267, 1152, 1034, 804, 769, 691, 637, 517 cm⁻¹; *m/z* (ESI) 195 (100 %) [M-OTf]⁺; HRMS: *m/z* calcd for C₁₃H₁₁N₂ [M-OTF]⁺: 195.0917; found: 195.0920.

Preparation of *N*-Phenyl-*N*-(2-(pyridin-2-yl)ethyl)formamide, **3.42**

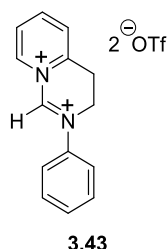


3.42

Oxalyl chloride (7.0 mL, 80 mmol, 2.0 eq) was added dropwise to a solution of imidazole (5.44 g, 80 mmol, 2.0 eq), triethylamine (22.4 mL, 160 mmol, 4.0 eq) and formic acid (3.0 mL, 80 mmol, 2.0 eq) in dry CH₂Cl₂ (100 mL) at 0 °C under argon. The reaction mixture was stirred for 30 min at 0 °C, then warmed to r.t. A solution of phenyl(2-pyridin-2-ylethyl)amine **3.39** (7.93 g, 40 mmol, 1.0 eq) in dry CH₂Cl₂ (50 mL) was added and the reaction mixture was stirred at r.t. for 18 h. The solvent was removed *in vacuo*. The resultant residue was dissolved in ethyl acetate (200 mL) and washed with saturated potassium carbonate solution (9 x 200 mL) and brine (200 mL), dried over anhydrous Na₂SO₄ and the solvent was removed *in vacuo* to give *N*-phenyl-*N*-[2-(pyridin-2-yl)ethyl]formamide **3.42** (8.15 g, 90 %) as a colourless oil;²⁷ ¹H NMR (400 MHz, CDCl₃) [2 rotamers in ratio of 1.0:0.3] δ = 2.96 (2H, t, *J* = 6.7 Hz, CH₂, minor rotamer), 3.09 (2H, t, *J* = 7.7 Hz, CH₂, major rotamer), 4.18 (2H, t, *J*

= 6.7 Hz, CH₂, minor rotamer), 4.23 (2H, t, $J = 7.7$ Hz, CH₂, major rotamer), 7.03-7.19 (4H, m, ArH, minor and major rotamer), 7.25-7.40 (3H, m, ArH, minor and major rotamer), 7.56-7.63 (1H, m, ArH, minor and major rotamer), 8.18 (1H, s, NCHO, minor rotamer), 8.38 (1H, s, NCHO, major rotamer), 8.50 (1H, dd, $J = 3.9, 0.8$ Hz, ArH, major rotamer), 8.59 (1H, m, ArH, minor rotamer); ¹³C NMR (100 MHz, CDCl₃) [2 rotamers] $\delta = 36.4$ (CH₂), 37.0 (CH₂), 45.5 (CH₂), 49.5 (CH₂), 121.8 (CH), 122.1 (CH), 123.7 (CH), 124.1 (CH), 124.5 (CH), 126.3 (CH), 127.0 (CH), 127.3 (CH), 129.5 (CH), 129.8 (CH), 136.6 (CH), 136.8 (CH), 141.1 (C), 141.2 (C), 149.6 (CH), 149.9 (CH), 157.8 (C), 158.7 (C), 162.6 (CH), 162.7 (CH); IR (thin film) $\nu = 3331, 3064, 3011, 2938, 2875, 1683, 1595, 1497, 1475, 1436, 1360, 1176, 764, 699, 674, 543, 511$ cm⁻¹; m/z (CI) 475 (90 %) [2M+Na]⁺, 249 (80 %) [M+Na]⁺, 227 (100 %) [M+H]⁺, 199 (30 %); HRMS: m/z calcd for C₁₄H₁₅N₂O [M+H]⁺: 227.1179; found: 227.1176.

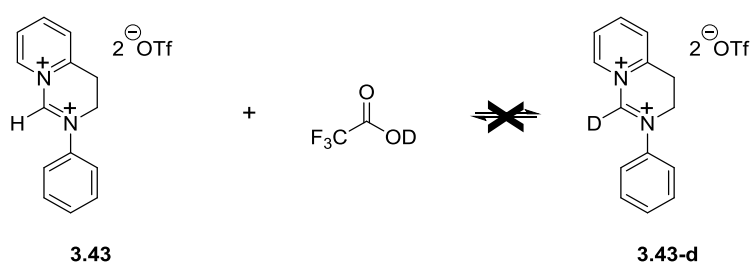
Preparation of 2-Phenyl-3,4-dihydropyrido[1,2-*c*]pyrimidine-2,9-dium Bis(trifluoromethanesulfonate), **3.43**



A solution of *N*-phenyl-*N*-[2-(pyridin-2-yl)ethyl]formamide **3.42** (1.13 g, 5.0 mmol, 1.0 eq) in dry CH₂Cl₂ (5 mL) was added using a syringe pump (1.78 mL h⁻¹) to a solution of dry trifluoromethanesulfonic anhydride **1.32** (1.0 mL, 6.0 mmol, 1.2 eq) in dry CH₂Cl₂ (5 mL) at -78 °C under argon. After the addition (~3 h), the reaction mixture was stirred for 1 h at -78 °C, then warmed to r.t. The reaction mixture was transferred to an oxygen-free, moisture-free glovebox and the resulting precipitate was collected. The precipitate was washed with dry CH₂Cl₂ (10 mL) and the solvent was removed *in vacuo* to give 2-phenyl-3,4-dihydropyrido[1,2-*c*]pyrimidine-2,9-dium bis(trifluoromethanesulfonate) **3.43** (2.08 g, 82 %) as an off-white solid;²⁷ m.p.

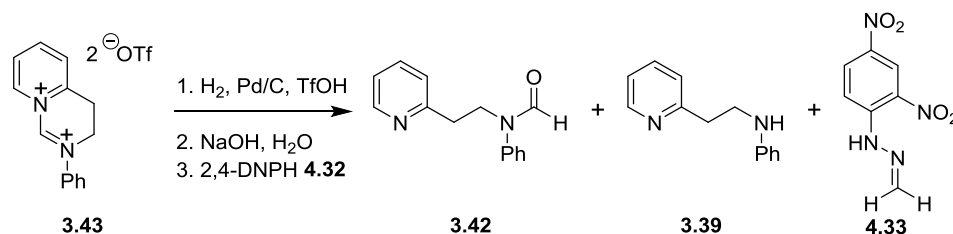
124 °C (dec.); ^1H NMR (400 MHz, CD_3CN) δ = 4.08 (2H, t, J = 7.9 Hz, CH_2), 4.84 (2H, td, J = 7.9, 1.4 Hz, CH_2), 7.76- 7.90 (5H, m, ArH), 8.31-8.34 (2H, m, ArH), 9.02 (1H, ddd, J = 8.0, 7.9, 1.5 Hz, ArH), 9.17 (1H, dd, J = 6.9, 1.4 Hz, ArH), 10.03 (1H, s, CH); ^{13}C NMR (125 MHz, CD_3CN) δ = 24.6 (CH_2), 49.0 (CH_2), 120.7 (quartet, $J(\text{C},\text{F})$ = 320 Hz, CF_3), 122.9 (CH), 128.0 (CH), 129.3 (CH), 130.9 (CH), 133.6 (CH), 139.0 (C), 146.4 (CH), 150.9 (C), 156.5 (CH), 156.8 (CH); The disalt was too unstable for MS, HRMS or IR analysis.

Attempted Deuterium Exchange Between 2-Phenyl-3,4-dihydropyrido[1,2-*c*]pyrimidine-2,9-dium Bis(trifluoromethanesulfonate) **3.43** and Deuterated TFA



Two samples of 2-phenyl-3,4-dihydropyrido[1,2-*c*]pyrimidine-2,9-dium bis(trifluoromethanesulfonate) **3.43** (76 mg) in dried, deuterated TFA (0.7 mL) were placed in two separate NMR tubes in an inert atmosphere glovebox at the same time. One sample was analysed by ^1H NMR within 10 min and showed slight decomposition of disalt (approximately 10 %). The second sample was left in the glovebox to minimise exposure to moisture and oxygen. After 17 h, both samples had gone from a light brown to a very dark brown colour. ^1H NMR of both samples showed complete consumption of starting material, affording a mixture of unidentified compounds with peaks observed more upfield compared to the spectrum of the starting disalt **3.43**.

Hydrogenation of 2-Phenyl-3,4-dihydropyrido[1,2-c]pyrimidine-2,9-dium Bis(trifluoromethanesulfonate) 3.43 in Triflic Acid with Pd/C and Work-up with 2,4-Dinitrophenylhydrazine 4.32

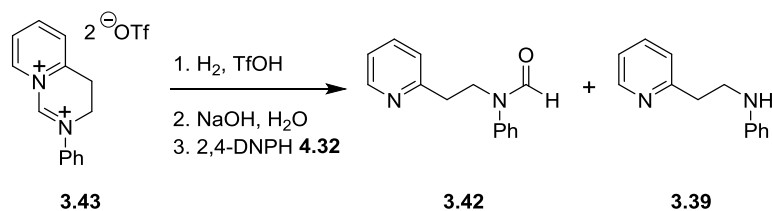


2-Phenyl-3,4-dihydropyrido[1,2-c]pyrimidine-2,9-dium bis(trifluoromethanesulfonate) **3.43** (0.160 g, 0.31 mmol, 1.0 eq) and palladium (10 wt% on activated carbon, 3.3mg, 0.003 gram-atom, 1 mol%) were weighed in an oxygen-free, moisture-free glovebox and placed in a dry round-bottomed flask. The flask was transferred from the glovebox and flushed with argon. Triflic acid (3mL) was added to the flask, which was placed under vacuum and flushed with hydrogen three times. The flask was left under hydrogen (1 atm) and stirred at r.t. for 7 days. The reaction mixture was slowly added to NaOH (aq) (2N, 30 mL), making the mixture basic. The reaction mixture was then adjusted to approximately pH 5 using concentrated HCl and 2,4-dinitrophenylhydrazine **4.32** (105 mg, 0.5 mmol, 1.6 eq) was added to the reaction mixture and stirred for 16 h. The aqueous phase was extracted with CH₂Cl₂ (3 x 30 mL) and the combined organic layers were washed through celite, dried (Na₂SO₄) and concentrated *in vacuo*. Column chromatography (gradient of 0 to 20 % diethyl ether in hexane) afforded 1-(2,4-dinitrophenyl)-2-methylenehydrazine **4.33** (49 mg, 75 %) as a yellow solid.¹⁴⁶ The aqueous phase was then made basic with NaOH (aq) (2N) and extracted with CH₂Cl₂ (3 x 30 mL). The combined organic layers were washed through celite, dried (Na₂SO₄) and concentrated *in vacuo*. Column chromatography (gradient of 0 to 20 % diethyl ether in hexane) afforded firstly *N*-[2-(pyridin-2-yl)ethyl]aniline **3.39** (13 mg, 21 %) then *N*-phenyl-*N*-[2-(pyridin-2-yl)ethyl]formamide **3.42** (2 mg, 3 %), both with data consistent with those previously reported.

1-(2,4-Dinitrophenyl)-2-methylenehydrazine **4.33**; m.p. 162-164 °C (lit. 161 °C);¹⁴⁶
¹H NMR (400 MHz, CDCl₃) δ = 6.75 (1H, d, *J* = 10.8 Hz, *CH*), 7.17 (1H, d, *J* = 10.8

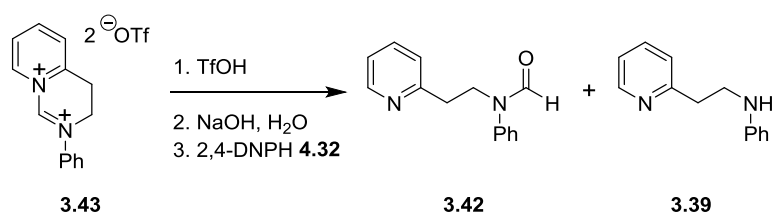
Hz, CH), 7.98 (1H, d, $J = 9.5$ Hz, ArH), 8.36 (1H, dd, $J = 2.5, 9.5$ Hz, ArH), 9.14 (1H, d, $J = 2.5$ Hz, ArH), 11.14 (1H, bs, NH); ^{13}C NMR (100 MHz, CDCl_3) $\delta = 116.3$ (CH_2), 122.8 (CH), 129.0 (C), 129.6 (CH), 136.5 (CH), 138.1 (C), 144.6 (C); IR (KBr disc) $\nu = 3301, 1622, 1584, 1517, 1430, 1335, 830$ cm^{-1} ; m/z (CI) 211 (100 %) $[\text{M}+\text{H}]^+$; HRMS: m/z calcd for $\text{C}_7\text{H}_7\text{N}_4\text{O}_4$ $[\text{M}+\text{H}]^+$: 211.0462; found 211.0457.

Attempted Hydrogenation of 2-Phenyl-3,4-dihydropyrido[1,2-*c*]pyrimidine-2,9-dium Bis(trifluoromethanesulfonate) **3.43** in Triflic Acid without Catalyst



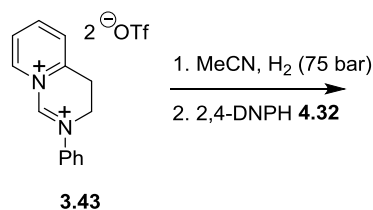
The same procedure as used in the hydrogenation of 2-phenyl-3,4-dihydropyrido[1,2-*c*]pyrimidine-2,9-dium bis(trifluoromethanesulfonate) **3.43** in triflic acid with catalyst was used. 2-Phenyl-3,4-dihydropyrido[1,2-*c*]pyrimidine-2,9-dium bis(trifluoromethanesulfonate) **3.43** (254 mg, 0.5 mmol, 1.0 eq) in triflic acid (5 mL) was reacted under hydrogen for 7 days and worked up, as previously, with 2,4-dinitrophenylhydrazine **4.32** (198 mg, 1.0 mmol, 2.0 eq). This did not afford any hydrazone product, but did afford *N*-[2-(pyridin-2-yl)ethyl]aniline **3.39** (49 mg, 49 %) and *N*-phenyl-*N*-[2-(pyridin-2-yl)ethyl]formamide **3.42** (14 mg, 12 %) both with data consistent with those previously reported in this thesis.

Blank Reaction of 2-Phenyl-3,4-dihydropyrido[1,2-*c*]pyrimidine-2,9-dium Bis(trifluoromethanesulfonate) **3.43** in Triflic Acid without Catalyst or Hydrogen



The procedure for hydrogenation reactions in triflic acid was repeated without catalyst and without the presence of hydrogen (the disalt was kept under argon), using 2-phenyl-3,4-dihydropyrido[1,2-*c*]pyrimidine-2,9-dium bis(trifluoromethanesulfonate) **3.43** (254 mg, 0.5 mmol, 1.0 eq), triflic acid (5 mL) and 2,4-dinitrophenylhydrazine **4.32** (198 mg, 1.0 mmol, 2.0 eq). This did not afford any hydrazone product, but did afford *N*-[2-(pyridin-2-yl)ethyl]aniline **3.39** (57 mg, 57 %) and *N*-phenyl-*N*-[2-(pyridin-2-yl)ethyl]formamide **3.42** (15 mg, 13 %) both with data consistent with those previously reported.

Attempted High-Pressure Catalyst-Free Hydrogenation of 2-Phenyl-3,4-dihydropyrido[1,2-*c*]pyrimidine-2,9-dium Bis(trifluoromethanesulfonate) **3.43**

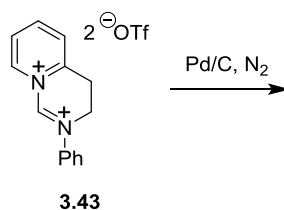


A solution of 2-phenyl-3,4-dihydropyrido[1,2-*c*]pyrimidine-2,9-dium bis(trifluoromethanesulfonate) **3.43** (2.03 g, 4.0 mmol, 1.0 eq) in MeCN (5 mL) was placed into the Teflon insert of a Baskerville Compact Mini (hydrogenation) Reactor, within an inert atmosphere glovebox. The reactor was sealed and removed from the glovebox to attach to a hydrogen cylinder. The attachments were purged with hydrogen before filling the reactor with a 75 bar pressure of hydrogen. The reaction mixture was stirred for 7 days and the pressure decreased to 10 bar before bringing the reactor back into the inert atmosphere glovebox. All pressure was then released from the reactor and the reaction mixture transferred to a round-bottomed flask. The mixture was concentrated *in vacuo* and stirred in CH₂Cl₂ (50 mL) for 2 h and filtered. The filtrate was concentrated *in vacuo* to afford a deep purple residue (1.57 g). NMR analysis was carried out on the crude material suggesting a mixture of two major compounds. In the crude mixture, one of the compounds (**4.37**) contained a singlet at 4.22 ppm by ¹H NMR; by a combination of DEPT and HSQC, this singlet was assigned to a methylene signal, showing possible reduction of the disalt. This signal

also only showed a nuclear Overhauser effect (1D spectra) on the *ortho* signal of the phenyl ring, but no effect was seen in the region of the pyridine ring. The growth in signals in the aromatic region, without growth in signals in the aliphatic region, suggested the existence of a second compound (**4.36**), which had lost hydrogen, to become fully aromatic.

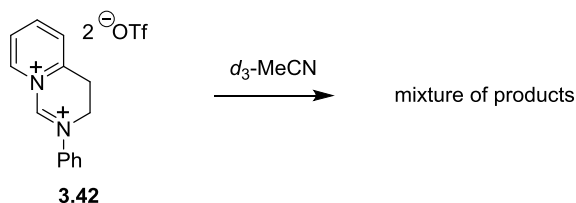
Attempted derivatisation of the mixture with 2,4-dinitrophenylhydrazine in 2N HCl, did not afford any 1-(2,4-dinitrophenyl)-2-methylenehydrazine **4.33**. *N*-[2-(pyridin-2-yl)ethyl]aniline **3.39** (223 mg, 28 %) was isolated after basic work-up, extraction with CH₂Cl₂ and column chromatography (a gradient of 0 to 20 % diethyl ether in hexane); data were consistent with those reported previously.

Treatment of 2-Phenyl-3,4-dihydropyrido[1,2-*c*]pyrimidine-2,9-dium Bis(trifluoromethanesulfonate) **3.43 with Pd/C under N₂**



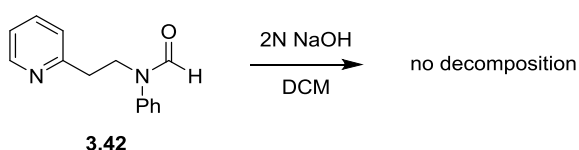
Pd/C (10 % Wt; 426 mg, 0.4 gram-atom, 0.1 eq) was added to a solution of 2-phenyl-3,4-dihydropyrido[1,2-*c*]pyrimidine-2,9-dium bis(trifluoromethanesulfonate) **3.43** (2.03 g, 4.0 mmol, 1.0 eq) in MeCN (5 mL) in an inert atmosphere glovebox and stirred for 17 h. The mixture was filtered and concentrated *in vacuo* to afford a brown residue. A sample of the residue was analysed by ¹H NMR, showing two major compounds corresponding to those in the high-pressure, catalyst-free hydrogenation experiment of 2-phenyl-3,4-dihydro-pyrido[1,2-*c*]pyrimidine-2,9-dium bis(trifluoro-methanesulfonate) **3.43**; a third minor component corresponding to starting disalt **3.43** was also observed.

Stability Test of 2-Phenyl-3,4-dihydropyrido[1,2-*c*]pyrimidine-2,9-dium Bis(trifluoromethanesulfonate) **3.43 in d_3 -MeCN.**

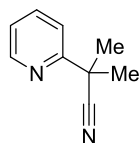


A solution of 2-phenyl-3,4-dihydropyrido[1,2-*c*]pyrimidine-2,9-dium bis(trifluoromethanesulfonate) **3.43** (180 mg, 0.35 mmol) was dissolved in d_3 -MeCN (3 mL) in an inert atmosphere glovebox. After 2 h, a sample of the solution (0.7 mL) was analysed by ^1H NMR, showing starting material (judged to be approximately still 77 % pure, by comparing methylene singlet signals for disalt **3.43** to new singlets which appeared in the aliphatic region, presumed to be due to methylene groups of new product) with several decomposition products. After 17 h, further decomposition was seen, (starting material accounted for approximately 35 % of the composition of the solution).

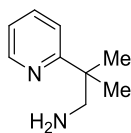
Stability Test of *N*-Phenyl-*N*-(2-(pyridin-2-yl)ethyl)formamide **3.42 with NaOH**



N-Phenyl-*N*-(2-(pyridin-2-yl)ethyl)formamide **3.42** (113 mg, 0.5 mmol, 1.0 eq) was stirred in a mixture of NaOH (2N, 2.5 mL, 5.0 mmol, 10 eq) and CH_2Cl_2 (2.5 mL) for 2 h. Two layers were then allowed to settle and separated. The aqueous layer was washed with further CH_2Cl_2 (3 x 2.5 mL) and the combined organic layers were washed with water (5 mL), brine (5 mL), dried (Na_2SO_4) and concentrated *in vacuo* to afford *N*-phenyl-*N*-(2-(pyridin-2-yl)ethyl)formamide **3.42** (112 mg, 99 %).

Preparation of 2-Methyl-2-(pyridin-2-yl)propanenitrile, **5.5****5.5**

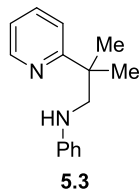
n-BuLi (2.5 M in hexane; 40 mL, 100 mmol, 1.0 eq) was added carefully to a solution of dried (over CaH₂) diisopropylamine (9 mL, 64 mmol, 0.6 eq) in THF (60 mL) at 0 °C and allowed to stir for 10 min at r.t. The resulting mixture was added slowly to a solution of isobutyronitrile **5.7** (8.98 mL, 100 mmol, 1.0 eq) and 2-bromopyridine **5.8** (9.54 mL, 100 mmol, 1.0 eq) in toluene (150 mL) at r.t. The mixture was stirred for 17 h and concentrated *in vacuo*. The resulting residue was dissolved in diethyl ether (200 mL), washed with water (3 x 200 mL), dried (Na₂SO₄) and concentrated *in vacuo* to afford a brown oil. Vacuum distillation (80–82 °C at 0.8 mbar) afforded 2-methyl-2-(pyridin-2-yl)propanenitrile **5.5** as a colourless oil (10.23 g, 70 %);¹⁴⁷ ¹H NMR (400 MHz, CDCl₃) δ = 1.79 (6H, s, CH₃), 7.26 (1H, ddd, *J* = 1.0, 4.8, 7.6 Hz, *ArH*), 7.61 (1H, dd, *J* = 1.0 Hz, 8.0 Hz, *ArH*), 7.75 (1H, ddd, *J* = 2.0 Hz, 7.6, 8.0 Hz, *ArH*), 8.62 (1H, dd, *J* = 2.0, 4.8 Hz, *ArH*); ¹³C NMR (100 MHz, CDCl₃) δ = 27.3 (CH₃), 39.0 (C), 119.31 (CH), 122.2 (CH), 123.7 (C), 136.7 (CH), 149.0 (CH), 159.0 (C); IR (thin film) ν = 2982, 2239, 1587, 1474, 1431, 785, 748 cm⁻¹; HRMS: *m/z* calcd for C₉H₉N₂ [M-H]⁺: 145.0760; found 145.0759.

Preparation of 2-Methyl-2-(pyridin-2-yl)propan-1-amine, **5.4****5.4**

A solution of 2-methyl-2-(pyridin-2-yl)propanenitrile **5.5** (10.23 g, 70 mmol, 1.0 eq) in THF (100 mL) was added slowly *via* canula to a suspension of LiAlH₄ (5.85 g, 154 mmol, 2.2 eq) in THF (400 mL) at 0 °C. The mixture was allowed to warm to

r.t. and stirred for 13 h. Sodium sulfate decahydrate (70 g) was added to the mixture followed by ethyl acetate (200 mL). The mixture was stirred for 1 h, filtered and concentrated *in vacuo*. The resulting residue was partitioned between CH₂Cl₂ (200 mL) and aq. HCl (2N, 200 mL). The aqueous layer was separated, washed with further CH₂Cl₂ (2 x 200 mL), made basic (~pH 12) with NaOH and extracted with CH₂Cl₂ (3 x 200 mL). The CH₂Cl₂ extracts from the aqueous solution were combined, dried and concentrated *in vacuo* to afford 2-methyl-2-(pyridin-2-yl)propan-1-amine **5.4** as a yellow oil (6.67 g, 78 %);¹⁴⁸ ¹H NMR (400 MHz, CDCl₃) δ = 1.36 (6H, s, CH₃), 2.96 (2H, s, CH₂), 7.12 (1H, ddd, *J* = 1.2, 4.8, 7.6 Hz, Ar*H*), 7.34 (1H, dd, *J* = 1.2, 8.0 Hz, Ar*H*), 7.65 (1H, ddd, *J* = 2.0, 7.6, 8.0 Hz, Ar*H*), 8.60 (1H, dd, *J* = 2.0, 4.8 Hz, Ar*H*); ¹³C NMR (100 MHz, CDCl₃) δ = 25.3 (CH₃), 41.8 (C), 53.2 (CH₂), 120.0 (CH), 120.4 (CH), 135.8 (CH), 148.3 (CH), 166.3 (C); IR (thin film) ν = 3368, 3291, 2959, 1661, 1587, 1473, 785, 746 cm⁻¹; HRMS: *m/z* calcd for C₉H₁₅N₂[M+H]⁺: 151.1230; found 151.1231.

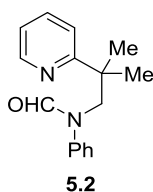
Preparation of *N*-[2-methyl-2-(pyridin-2-yl)propyl]aniline, **5.3**



CuI (190 mg, 1 mmol, 5 mol%) and K₃PO₄ (8.49 g, 40 mmol, 2.0 eq) were placed in a flask purged with argon. A solution of 2-methyl-2-(pyridin-2-yl)propan-1-amine **5.4** (4.62 g, 20 mmol, 1.2 eq) in *i*PrOH (10 mL) was added to the solids, followed by ethylene glycol (2.2 mL, 40 mmol, 2.0 eq) and iodobenzene (1.86 mL, 16.7 mmol, 1.0 eq) in *i*PrOH (10 mL). The mixture was allowed to stir for 2 h at r.t., 100 °C for 45 min and then 80 °C for 15 h. After cooling, the mixture was extracted with ether (40 mL) and water (40 mL). The aqueous layer was washed with more ether (4 x 40 mL) and the combined organics were washed with brine (40 mL), dried (Na₂SO₄) and concentrated *in vacuo*. Column chromatography (100 % toluene) afforded *N*-[2-methyl-2-(pyridin-2-yl)propyl]aniline **5.3** (3.38 g, 15 mmol, 61 %) as a yellow oil which formed a wax after 1 day; ¹H NMR (400 MHz, CDCl₃) δ = 1.49 (6H, s, CH₃), 3.41 (2H, s, CH₂), 6.61 (2H, dd, *J* = 1.0, 8.6 Hz, Ar*H*), 6.67 (1H, tt, *J* = 1.0, 7.0 Hz, Ar*H*), 7.14-7.18 (3H, m, Ar*H*), 7.38 (1H, dd, *J* = 0.9, 8.0 Hz, Ar*H*), 7.66 (1H, ddd, *J*

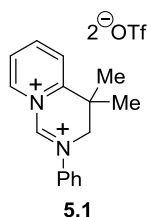
= 1.9, 7.6, 8.0 Hz, *ArH*), 8.63 (1H, dd, $J = 1.9, 4.8$ Hz, *ArH*); *NH* not observed; ^{13}C NMR (100 MHz, CDCl_3) $\delta = 26.1$ (CH_3), 40.9 (C), 54.5 (CH_2), 112.2 (CH), 116.3 (CH), 119.8 (CH), 120.7 (CH), 128.6 (CH), 136.0 (CH), 148.2 (CH), 148.5 (C), 166.0 (C); IR (thin film) $\nu = 3418, 3331, 3051, 2924, 1601, 1504, 1474, 745, 691$ cm^{-1} ; HRMS: m/z calcd for $\text{C}_{15}\text{H}_{19}\text{N}_2$ $[\text{M}+\text{H}]^+$: 227.1543; found 227.1540.

Preparation of *N*-[2-methyl-2-(pyridin-2-yl)propyl]-*N*-phenylformamide, **5.2**



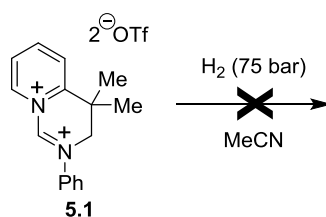
This compound was prepared following the same procedure as that used in the preparation of *N*-phenyl-*N*-[2-(pyridin-2-yl)ethyl]formamide **3.42**, using oxalyl chloride (5.3 mL, 60 mmol, 4.0 eq), imidazole (4.1 g, 60 mmol, 4.0 eq), triethylamine (16.8 mL, 120 mmol, 8.0 eq), formic acid (2.3 mL, 60 mmol, 4.0 eq) and *N*-[2-methyl-2-(pyridin-2-yl)propyl]aniline **5.3** (3.38 g, 15 mmol, 1.0 eq). Column chromatography (0-20 % ethyl acetate in petroleum ether, 40 – 60 °C) afforded *N*-[2-methyl-2-(pyridin-2-yl)propyl]-*N*-phenylformamide **5.2** as a colourless oil (2.61 g, 68 %); ^1H NMR (400 MHz, CDCl_3) [2 rotamers in ratio of 1.0:0.2] $\delta = 1.31$ (6H, s, CH_3 , minor rotamer), 1.38 (6H, s, CH_3 , major rotamer), 4.12 (2H, s, CH_2 , minor rotamer), 4.32 (2H, s, CH_2 , major rotamer), 6.86-6.91 (3H, m, *ArH*, major and minor rotamers), 7.01-7.26 (4H, m, *ArH*, major and minor rotamers), 7.37 (1H, ddd, $J = 2.0, 7.7, 7.9$ Hz, *ArH*, major rotamer), 7.53 (1H, ddd, $J = 1.8, 7.7, 7.9$ Hz, *ArH*, minor rotamer), 8.10 (1H, s, CHO , minor rotamer), 8.29 (1H, s, CHO , major rotamer), 8.32 (1H, dd, $J = 1.8, 4.7$ Hz, *ArH*, major rotamer), 8.46 (1H, dd, $J = 1.8, 4.7$ Hz, *ArH*, minor rotamer); ^{13}C NMR (100 MHz, CDCl_3) [2 rotamers] $\delta = 26.1$ (CH_3), 26.3 (CH_3), 42.6 (C), 42.8 (C), 54.1 (CH_2), 60.3 (CH_2), 120.2 (CH), 120.4 (CH), 120.9 (CH), 121.4 (CH), 124.8 (CH), 126.2 (CH), 126.3 (CH), 126.5 (CH), 128.8 (CH), 129.1 (CH), 135.9 (CH), 136.4 (CH), 139.7 (C), 141.5 (C), 148.5 (CH), 149.0 (CH), 163.3 (CHO), 163.7 (CHO), 164.6 (C), 165.5 (C); IR (thin film) $\nu = 3055, 2967, 2868, 1672, 1587, 1495, 1364, 1263, 696$ cm^{-1} ; HRMS: m/z calcd for $\text{C}_{16}\text{H}_{19}\text{N}_2\text{O}$ $[\text{M}+\text{H}]^+$: 255.1492; found 255.1489.

Preparation of 4,4-Dimethyl-2-phenyl-3,4-dihydropyrido[1,2-*c*]pyrimidine-2,9-dium Bis(trifluoromethanesulfonate), 5.1



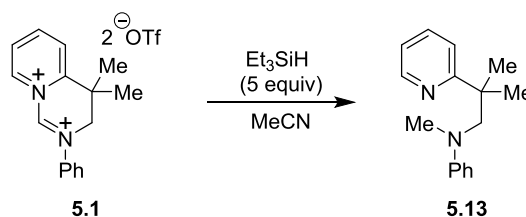
This compound was prepared following the method used for the preparation of 2-phenyl-3,4-dihydropyrido[1,2-*c*]pyrimidine-2,9-dium bis(trifluoromethanesulfonate) **3.43**, using *N*-[2-methyl-2-(pyridin-2-yl)propyl]-*N*-phenylformamide **5.2** (1.21 g, 5.0 mmol, 1.0 eq), Tf₂O **1.32** (1.0 mL, 6.0 mmol, 1.2 eq) and CH₂Cl₂ (10 mL). The crude material was washed on a sinter funnel (in a glovebox) with CH₂Cl₂ (3 x 10 mL) and placed under vacuum for 1 h to afford 4,4-dimethyl-2-phenyl-3,4-dihydropyrido[1,2-*c*]pyrimidine-2,9-dium bis(trifluoromethanesulfonate) **5.1** (2.25 g, 84 %) as a yellow solid; m.p. 130 °C (dec.); ¹H NMR (400 MHz, CD₃CN) δ = 1.74 (6H, s, CH₃), 4.79 (2H, d, *J* = 1.4 Hz, CH₂), 7.80-7.95 (5H, m, ArH), 8.40 (1H, ddd, *J* = 1.3, 6.4, 7.8 Hz, ArH), 8.49 (1H, dd, *J* = 1.3, 8.1 Hz, ArH), 9.13 (1H, ddd, *J* = 1.5, 7.8, 8.1 Hz, ArH), 9.28 (1H, dd, *J* = 1.5, 6.4 Hz, ArH), 10.21 (1H, s, CH); ¹³C NMR (100 MHz, CD₃CN) δ = 23.4 (CH₃), 34.8 (C), 58.0 (CH₂), 120.2 (quartet, *J*(C,F) = 320 Hz, CF₃), 122.4 (CH), 125.5 (CH), 127.6 (CH), 130.5 (CH), 133.3 (CH), 138.3 (C), 146.9 (CH), 156.0 (C), 156.8 (CH), 157.6 (CH); ¹⁹F NMR (376 Hz, CD₃CN) δ = -79.3; disalt was too reactive for analysis by MS or IR.

Attempted High-Pressure, Catalyst-Free Hydrogenation of 4,4-Dimethyl-2-phenyl-3,4-dihydropyrido[1,2-*c*]pyrimidine-2,9-dium Bis(trifluoromethanesulfonate) 5.1



A solution of 4,4-dimethyl-2-phenyl-3,4-dihydropyrido[1,2-*c*]pyrimidine-2,9-dium bis(trifluoromethanesulfonate) **5.1** (2.15 g, 4.0 mmol, 1.0 eq) in MeCN (5 mL) was placed into the Teflon insert of a Baskerville Compact Mini (hydrogenation) Reactor, within an inert atmosphere glovebox. The reactor was sealed and removed from the glovebox to attach to a hydrogen cylinder. The attachments were purged with hydrogen before filling the reactor with a 75 bar pressure of hydrogen. The reaction mixture was stirred for 7 days and the pressure decreased to 10 bar before bringing the reactor back into the inert atmosphere glovebox. All pressure was then released from the reactor and the reaction mixture transferred to a round bottomed flask. The mixture was concentrated *in vacuo* to afford unreacted starting material **5.1** (2.15 g, 100 %).

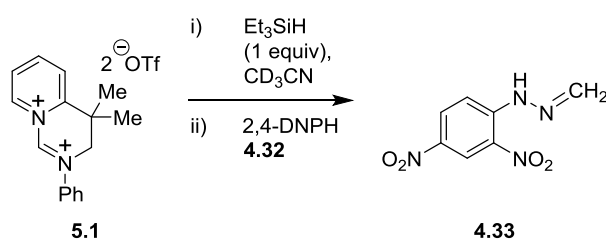
Reaction of 4,4-Dimethyl-2-phenyl-3,4-dihydropyrido[1,2-*c*]pyrimidine-2,9-dium Bis(trifluoromethanesulfonate) **5.1 with an Excess of Triethylsilane**



To a solution of 4,4-dimethyl-2-phenyl-3,4-dihydropyrido[1,2-*c*]pyrimidine-2,9-dium bis(trifluoromethanesulfonate) **5.1** (536 mg, 1.0 mmol, 1.0 eq) in dry MeCN (2 mL) was added triethylsilane (0.8 mL, 5.0 mmol, 5.0 eq) at room temperature under argon. The mixture was stirred for 3 days and concentrated *in vacuo*. The resulting residue was treated with sat. K₂CO₃ (20 mL) and extracted with CH₂Cl₂ (3 x 20 mL). The combined organics were dried (Na₂SO₄), concentrated and the resulting residue purified by column chromatography (diethyl ether in hexane) to afford *N*-methyl-*N*-[2-methyl-2-(pyridin-2-yl)propyl]aniline **5.13** (178 mg, 74 %) as a colourless oil; ¹H NMR (400 MHz, CDCl₃) δ = 1.47 (6H, s, CH₃), 2.58 (3H, s, CH₃), 3.67 (2H, s, CH₂), 6.62-6.67 (3H, m, ArH), 7.12-7.18 (3H, m, ArH), 7.32 (1H, dd, *J* = 1.1, 7.9 Hz, ArH), 7.59 (1H, ddd, *J* = 1.9, 7.6, 7.9 Hz, ArH), 8.66 (1H, dd, *J* = 1.9, 4.7 Hz, ArH); ¹³C NMR (100 MHz, CDCl₃) δ = 25.8 (CH₃), 39.7 (CH₃), 43.4 (C), 63.3 (CH₂), 111.4 (CH), 115.2 (CH), 120.1 (CH), 120.5 (CH), 128.3 (CH), 135.7 (CH),

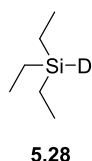
148.3 (CH), 150.0 (C), 166.6 (C); IR (thin film) $\nu = 3059, 2963, 2872, 1595, 1504, 991, 743, 691 \text{ cm}^{-1}$; m/z (ESI) 241 (100 %) $[M+H]^+$; HRMS: m/z calcd for $C_{16}H_{21}N_2$ $[M+H]^+$: 241.1699; found 241.1706.

Reaction of 4,4-Dimethyl-2-phenyl-3,4-dihydropyrido[1,2-*c*]pyrimidine-2,9-dium Bis(trifluoromethanesulfonate) 5.1 with 1 equivalent of Triethylsilane Followed by DNPH 4.32 Derivatisation



To a solution of 4,4-dimethyl-2-phenyl-3,4-dihydropyrido[1,2-*c*]pyrimidine-2,9-dium bis(trifluoromethanesulfonate) **5.1** (27 mg, 0.05 mmol, 1.0 eq) in CD_3CN (0.8 mL) in an NMR tube was added triethylsilane (8 μL , 0.05 mmol, 1.0 eq) and the mixture was inverted 3 times. The mixture was monitored by ^1H NMR with 60 experiments in 2 h. This indicated the reduction of the disalt, with a methylene signal appearing at 5.93 ppm (see ^1H NMR, HSQC and NOESY in Appendix A). The solution was then added to a suspension of 2,4-dinitrophenylhydrazine **4.32** (20 mg, 0.01 mmol, 2.0 eq) in 4N HCl (20 mL) and stirred overnight. Column chromatography (diethyl ether in hexane) afforded 1-(2,4-dinitrophenyl)-2-methylenehydrazine **4.33** (8 mg, 76 %); data are consistent with those reported previously within this thesis.

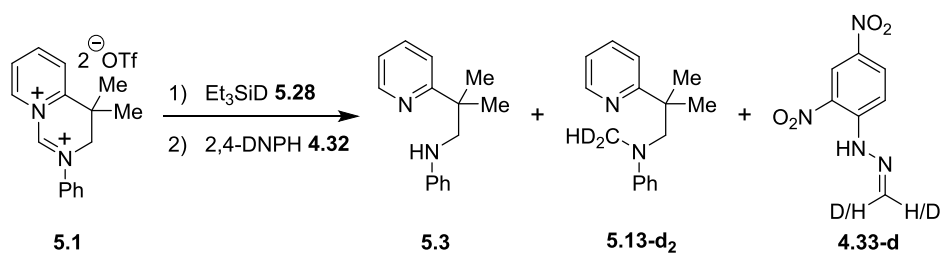
Preparation of d_1 -Triethylsilane 5.28



Chlorotriethylsilane **5.27** (3.33 mL, 19.9 mmol, 1.0 eq) was added slowly over 10 minutes to a suspension of LiAlD_4 (1.0 g, 23.8 mmol, 1.2 eq) in Et_2O (20 mL) at 0°C

under argon. After stirring for 72 h, the grey suspension had become a white suspension. Water (10 mL) was added, followed by Na₂SO₄ (9 g) and the resulting mixture was filtered. The solids were washed with further ether (3 x 10 mL). Distillation (108-110 °C, atmospheric pressure) afforded pure d₁-triethylsilane **5.28** (1.31 g, 56 %) as a colourless oil;¹⁴⁹ ¹H NMR (400 MHz, CDCl₃) δ = 0.61 (6H, quartet, *J* = 7.9 Hz, CH₂), 1.00 (9H, t, *J* = 7.9 Hz, CH₃); ²H NMR (61 MHz, CHCl₃) δ = 3.69 (s); ¹³C NMR (100 MHz, CDCl₃) δ = 1.88, 7.63; IR (ATR) ν = 2953, 2913, 2876, 1530, 1015, 733 cm⁻¹.

Reaction of 4,4-Dimethyl-2-phenyl-3,4-dihydropyrido[1,2-*c*]pyrimidine-2,9-dium Bis(trifluoromethanesulfonate) **5.1 with 1 equivalent of d₁-Triethylsilane **5.28****

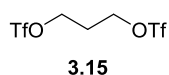


Et₃SiD **5.28** (32 μL, 0.2 mmol, 1.0 eq) was added to a solution of 4,4-dimethyl-2-phenyl-3,4-dihydropyrido[1,2-*c*]pyrimidine-2,9-dium bis(trifluoromethanesulfonate) **5.1** (107 mg, 0.2 mmol, 1.0 eq) in MeCN (2 mL) at r.t. under argon and stirred for 16 h. The mixture was added to a suspension of 2,4-dinitrophenylhydrazine **4.32** (79 mg, 0.4 mmol, 2.0 eq) in 2N HCl (10 mL) at 0 °C and stirred overnight. 10 mL of water was added and the mixture extracted with CH₂Cl₂ (3 x 20 mL), dried (Na₂SO₄) and concentrated *in vacuo*. Column chromatography (10 % EtOAc in hexane) afforded d₁-1-(2,4-dinitrophenyl)-2-methylenehydrazine **4.33-d** (28 mg, 66 %) as yellow solid. The aqueous work-up solution was later made basic with sodium hydroxide pellets to give a pink solution, which was then extracted with CH₂Cl₂ (3 x 20 mL), dried (Na₂SO₄) and concentrated *in vacuo*. Column chromatography (toluene) afforded d₂-*N*-methyl-*N*-[2-methyl-2-(pyridin-2-yl)propyl]aniline **5.13-d₂** (2.5 mg, 5 %) and *N*-[2-methyl-2-(pyridin-2-yl)propyl]aniline **5.3** (29 mg, 64 %).

*d*₁-1-(2,4-dinitrophenyl)-2-methylenehydrazine **4.33-d** ¹H NMR (400 MHz, CDCl₃) δ = 6.72 (0.5H, s, CH), 7.13 (0.5H, s, CH), 7.96 (1H, d, *J* = 9.5 Hz, ArH), 8.34 (1H, dd, *J* = 2.5, 9.5 Hz, ArH), 9.12 (1H, d, *J* = 2.5 Hz, ArH), 11.12 (1H, bs, NH); ²H (61 Hz, CHCl₃) δ = 6.76 (CD), 7.17 (CD); ¹³C NMR (100 MHz, CDCl₃) δ = 116.3 (CHD), 122.8 (CH), 129.0 (C), 129.6 (CH), 136.5 (CH), 138.1 (C), 144.6 (C); IR (ATR) ν = 3308, 3092, 1614, 1585, 1504, 1418, 1310, 827 cm⁻¹; HRMS: *m/z* calcd for C₇H₆DN₄O₄ [M+H]⁺: 212.0525; found 212.0526.

*d*₂-*N*-methyl-*N*-[2-methyl-2-(pyridin-2-yl)propyl]aniline **5.13-d₂** ¹H NMR (400 MHz, CDCl₃) δ = 1.46 (6H, s, CH₃), 2.53 (1H, bs, CD₂H), 3.65 (2H, s, CH₂), 6.60-6.64 (3H, m, ArH), 7.12-7.16 (3H, m, ArH), 7.31 (1H, dd, *J* = 1.1, 7.9 Hz, ArH), 7.59 (1H, ddd, *J* = 1.9, 7.6, 7.9 Hz, ArH), 8.65 (1H, dd, *J* = 1.9, 4.7 Hz, ArH); ²H NMR (61 MHz, CHCl₃) δ = 2.54 (d, *J*(H,D) = 1.8 Hz, CHD₂); ¹³C NMR (100 MHz, CDCl₃) δ = 25.8 (CH₃), 39.7 (CH₃), 43.4 (C), 63.3 (CH₂), 111.4 (CH), 115.2 (CH), 120.1 (CH), 120.5 (CH), 128.3 (CH), 135.7 (CH), 148.3 (CH), 150.0 (C), 166.6 (C); IR (ATR) ν = 2959, 2942, 2870, 1726, 1597, 1587, 1503, 1375, 743 cm⁻¹; HRMS: *m/z* calcd for C₁₆H₁₉D₂N₂ [M+H]⁺: 243.1825; found 243.1827.

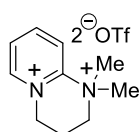
Preparation of 1,3-Bis-(trifluoromethanesulfonyloxy)propane **3.15**



A solution of 1,3-propanediol (2.9 mL, 40.0 mmol, 1.0 eq) and pyridine **1.31** (6.5 mL, 80 mmol, 2.0 eq) in CH₂Cl₂ (20 mL) was added dropwise to a solution of trifluoromethanesulfonic anhydride **1.32** (13.5 mL, 80.0 mmol, 2.0 eq) in CH₂Cl₂ (100 mL) at -78 °C under argon. The reaction mixture was warmed to r.t. and stirred for 1 h to give a pink solution with a white precipitate. The reaction mixture was washed with distilled water (3 x 20 mL), dried over anhydrous Na₂SO₄ and filtered through silica gel (40 g). The silica gel was washed with CH₂Cl₂ (50 mL) and combined with the first washing. The solvent was removed *in vacuo* to give 1,3-bis-(trifluoromethanesulfonyloxy)propane **3.15** (11.9 g, 87 %) as a red oil;²⁷ ¹H NMR (400 MHz, CDCl₃) δ = 2.41 (2H, quintet, *J* = 5.8 Hz, CH₂-CH₂-CH₂), 4.70 (4H, t, *J* =

5.8 Hz, $\text{CH}_2\text{-OTf}$); ^{13}C NMR (100 MHz, CDCl_3) δ = 29.2 (CH_2), 71.5 (CH_2), 119.1 (q, $J(\text{C},\text{F})= 322$ Hz, CF_3); IR (thin film) ν = 2991, 1417, 1248, 1207, 929, 854, 812, 735, 614, 581 cm^{-1} .

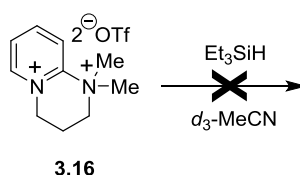
Preparation of 1,1-Dimethyl-1,2,3,4-tetrahydropyrido[1,2-a]pyrimidine-1,5-dium Bis(trifluoromethanesulfonate) 3.16



3.16

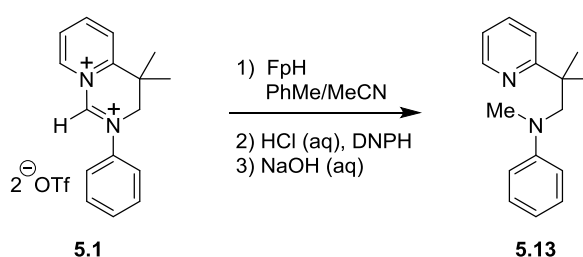
2-DMAP **3.7** (0.61 mL, 5 mmol, 1.0 eq) was added dropwise to a tube containing 1,3-*bis*-(trifluoromethanesulfonyloxy)propane **3.15** (1.021 g, 3.0 mmol, 1.2 eq) at 0 °C under argon. The reaction mixture was warmed to r.t. and stirred until solidification of the reaction mixture formed a yellow gel-like solid (approximately 5 min). The reaction mixture was washed with dry diethyl ether (10 mL) and the solvent was removed *in vacuo* to give a white powder. The powder was recrystallised from acetonitrile/diethyl ether to afford 1,1-dimethyl-1,2,3,4-tetrahydropyrido[1,2-a]pyrimidine-1,5-dium bis(trifluoromethanesulfonate) **3.16** (1.0 g, 44 %) as white crystals;²⁷ mp 113-116 °C (lit. 113-116 °C);²⁷ ^1H NMR 400 MHz, CD_3CN) δ = 2.67 (2H, tt, $J = 6.2, 5.7$ Hz, $\text{CH}_2\text{-CH}_2\text{-CH}_2$), 3.84 (6H, s, CH_3), 4.18 (2H, t, $J = 5.7$ Hz, CH_2), 4.92 (2H, t, $J = 6.2$ Hz, CH_2), 8.22 (1H, ddd $J = 7.5, 6.3, 1.1$ Hz, ArH), 8.63 (1H, dd, $J = 8.2, 1.6$ Hz, ArH), 8.79-8.83 (2H, m, ArH); ^{13}C NMR (100 MHz, CD_3CN) 17.7 (CH_2), 57.3 (CH_2), 60.8 (CH_3), 63.8 (CH_2), 122.9 (q, $J(\text{C},\text{F})= 324$ Hz, CF_3), 125.4 (CH), 131.6 (CH), 150.0 (CH), 152.3 (C), 152.5 (CH); IR (KBr disc) ν = 3136, 3102, 3080, 3050, 1638, 1591, 1519, 1488, 1452, 1256, 1228, 1155, 1033, 992, 962, 780, 636, 575, 519; MS (ESI) 313 (20 %) $[\text{M-OTf}]^+$, 82 (100 %) $[\text{M-2OTf}]^{2+}$; HRMS: m/z calcd for $\text{C}_{11}\text{H}_{16}\text{F}_3\text{N}_2\text{O}_3\text{S}$ $[\text{M-OTf}]^+$: 313.0828; found: 313.0826.

Treatment of 1,1-Dimethyl-1,2,3,4-tetrahydropyrido[1,2-a]pyrimidine-1,5-dium Bis(trifluoromethanesulfonate) **3.16 with Et₃SiH**



A solution of 1,1-dimethyl-1,2,3,4-tetrahydropyrido[1,2-a]pyrimidine-1,5-dium bis(trifluoromethanesulfonate) **3.16** (23 mg, 0.05 mmol, 1.0 eq) in CD₃CN (0.5 mL) was treated with Et₃SiH (8 μL, 0.05 mmol, 1.0 eq) in an inert atmosphere (N₂) glovebox and the sample was shaken well. The mixture was allowed to react for 24 h and monitored by ¹H NMR, showing no reaction to occur. The mixture was placed under high vacuum (0.02 mbar) for 30 min to remove the silane and afforded unreacted 1,1-dimethyl-1,2,3,4-tetrahydropyrido[1,2-a]pyrimidine-1,5-dium bis(trifluoromethanesulfonate) **3.16** (23 mg, 100%) with data consistent to those reported for this compound previously in this thesis.

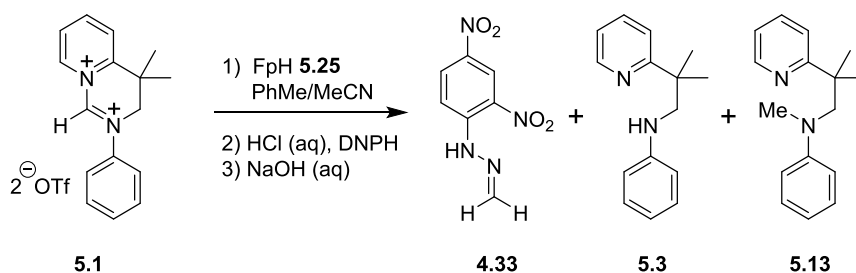
Preparation of FpH **5.25 and Subsequent Reaction with 4,4-Dimethyl-2-phenyl-3,4-dihydropyrido[1,2-c]pyrimidine-2,9-dium Bis(trifluoromethanesulfonate) **5.1****



According to the procedure reported by Bullock and Samsel,¹²⁵ AcOH (0.05 mL) was added to a suspension of KFe(CO)₂Cp (232 mg, 1.07 mmol, 10.7 eq) in C₆D₆ (10 mL) to afford FpH **5.25**, which was collected in a U-tube at -196 °C under vacuum (0.01 mbar) as a yellow solution (¹H NMR indicated the formation of the unstable FpH **5.25**; see Appendix B). This solution was placed under an atmosphere of argon and transferred *via* canula to a solution of 4,4-dimethyl-2-phenyl-3,4-dihydropyrido[1,2-c]pyrimidine-2,9-dium bis(trifluoromethanesulfonate) **5.1** (54

mg, 0.1 mmol, 1.0 eq) in CD₃CN (5 mL). The solution turned from yellow to red instantly and a sample was taken for ¹H NMR showing a possible methylene signal at 5.72 ppm (Appendix C). The NMR sample was added to the rest of the mixture and the mixture was added to a suspension of 2,4-dinitrophenylhydrazine **4.32** (40 mg, 0.2 mmol, 2.0 eq) in 4N HCl (20 mL) and allowed to stir overnight. No hydrazone formation was observed; however the aqueous solution was made basic with NaOH pellets and extracted with CH₂Cl₂ (3 x 20 mL). The combined organics were concentrated *in vacuo* and column chromatography (diethyl ether in hexane) afforded *N*-methyl-*N*-[2-methyl-2-(pyridin-2-yl)propyl]-aniline **5.13** (17.5 mg, 73 %) as a colourless oil; data were consistent with those reported above.

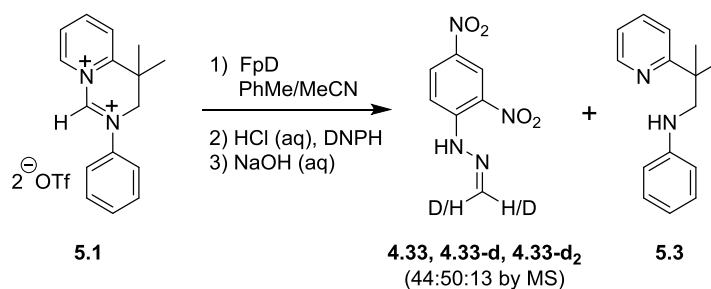
Reaction of 4,4-Dimethyl-2-phenyl-3,4-dihydropyrido[1,2-*c*]pyrimidine-2,9-dium Bis(trifluoromethanesulfonate) **5.1** with FpH **5.25** and Detection of Formaldehyde Equivalent **4.33**



The above procedure reacting FpH **5.25** with 4,4-dimethyl-2-phenyl-3,4-dihydropyrido[1,2-*c*]pyrimidine-2,9-dium bis(trifluoromethanesulfonate) **5.1** was repeated on the same scale, using PhMe instead of C₆D₆ and CH₃CN instead of CD₃CN. After addition of the FpH solution to the 4-dimethyl-2-phenyl-3,4-dihydropyrido[1,2-*c*]pyrimidine-2,9-dium bis(trifluoromethanesulfonate) **5.1** solution, the mixture was immediately treated with 4N HCl (20 mL) and 2,4-dinitrophenylhydrazine **4.32** (40 mg) was added to the mixture. The mixture was stirred overnight and then extracted with CH₂Cl₂ (3 x 30 mL). The combined organics were dried (Na₂SO₄) and concentrated *in vacuo*. The resulting residue was purified by column chromatography (diethyl ether in hexane) to afford 1-(2,4-dinitrophenyl)-2-methylenehydrazine **4.33** (10 mg, 48 %); data were consistent with those reported previously within this thesis.

The aqueous solution from the work-up was made basic with NaOH pellets and extracted with CH₂Cl₂ (3 x 30 mL). The combined organics were dried (Na₂SO₄) and concentrated *in vacuo*. Column chromatography (toluene) afforded *N*-methyl-*N*-[2-methyl-2-(pyridin-2-yl)propyl]aniline **5.13** (7 mg, 29 %) and *N*-[2-methyl-2-(pyridin-2-yl)propyl]aniline **5.3** (10 mg, 44 %); data were consistent with those reported above.

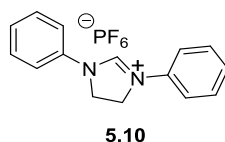
Reaction of 4,4-Dimethyl-2-phenyl-3,4-dihydropyrido[1,2-*c*]pyrimidine-2,9-dium Bis(trifluoromethanesulfonate) 5.1 with FpD 5.25-d and Isolation of Formaldehyde Equivalent (Mixture of Isotopomers) 4.33, 4.33-d and 4.33-d₂



The above procedure reacting FpH **5.25** with 4,4-dimethyl-2-phenyl-3,4-dihydropyrido[1,2-*c*]pyrimidine-2,9-dium bis(trifluoromethanesulfonate) **5.1** was repeated on the same scale, with *d*₄-acetic acid used instead of non-deuterated acetic acid. This afforded 1-(2,4-dinitrophenyl)-2-methylenehydrazine **4.33**, **4.33-d**, **4.33-d₂** as a mixture of nondeuterated, monodeuterated and dideuterated isotopomers (14.2 mg, 67 %, ratio of 44:50:13 observed by mass spectrometry) and *N*-(2-methyl-2-(pyridin-2-yl)propyl)aniline **5.3** (13.7 mg, 61 %).

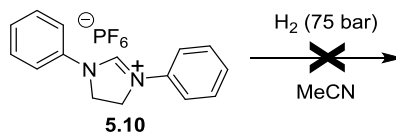
Mixture of 1-(2,4-dinitrophenyl)-2-methylenehydrazine **4.33**, **4.33-d**, **4.33-d₂** isotopomers: m.p. 140-144 °C; ²H NMR (CHCl₃, 61 MHz) δ = 6.77, 7.19; ¹H NMR (CDCl₃, 400 MHz) δ = 6.75 (0.6H, d, *J* = 10.8 Hz, *CH*), 7.17 (0.6H, d, *J* = 10.8 Hz, *CH*), 7.98 (1H, d, *J* = 9.5 Hz, *ArH*), 8.36 (1H, dd, *J* = 2.5, 9.5 Hz, *ArH*), 9.14 (1H, d, *J* = 2.5 Hz, *ArH*), 11.14 (1H, bs, NH); *m/z* (CI) 211 (88 %) [(C₇H₆N₄O₄)+H]⁺, 212 (100 %) [(C₇H₅DN₄O₄)+H]⁺; HRMS: *m/z* calcd for C₇H₇N₄O₄ [M+H]⁺: 211.0462; found 211.0460; *m/z* calcd for C₇H₆DN₄O₄ [M+H]⁺: 212.0525; found 212.0520; *m/z* calcd for C₇H₅D₂N₄O₄ [M+H]⁺: 213.0587; found 213.0581.

Preparation of 1,3-Diphenyl-4,5-dihydro-1*H*-imidazol-3-ium Hexafluorophosphate **5.10**



Triethyl orthoformate (4.2 mL, 25 mmol, 2.5 eq) was added to a mixture of *N,N'*-diphenylethylenediamine **5.9** (2.12 g, 10 mmol, 1.0 eq) and ammonium hexafluorophosphate (1.79 g, 11 mmol, 1.1 eq) and then stirred at 110 °C under a flow of argon for 2 h. The mixture was cooled to r.t. and chloroform (10 mL) was added, stirring overnight. The solid was then filtered, washed with more chloroform (6 x 10 mL) and dried under vacuum to afford *1,3-diphenyl-4,5-dihydro-1H-imidazol-3-ium hexafluorophosphate* **5.10** (3.35 g, 91 %) as a beige solid; m.p. 228 °C (dec.); ¹H NMR (400 MHz, *d*₆-DMSO) δ = 4.61 (4H, s, CH₂), 7.41 (2H, tt, *J* = 1.0, 7.5 Hz, Ar*H*), 7.59 (4H, ddd, *J* = 2.2, 7.5, 8.7 Hz, Ar*H*), 7.65 (4H, dd, *J* = 1.0, 8.7 Hz, Ar*H*), 9.96 (1H, s, CH); ¹³C NMR (100 MHz, *d*₆-DMSO) δ = 48.3 (CH₂), 118.4 (CH), 127.0 (CH), 129.7 (CH), 136.1 (C), 151.8 (CH); IR (solid) ν = 3109, 1632, 1591, 1493, 1263, 820, 756, 685 cm⁻¹; *m/z* (ESI) 223 (100 %) [M-PF₆]⁺; HRMS: *m/z* calcd for C₁₅H₁₅N₂ [M]⁺: 223.1230; found 223.1235.

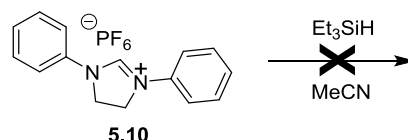
Attempted High-Pressure, Catalyst-Free Hydrogenation of 1,3-Diphenyl-4,5-dihydro-1*H*-imidazol-3-ium Hexafluorophosphate **5.10**



A solution of 1,3-diphenyl-4,5-dihydro-1*H*-imidazol-3-ium hexafluorophosphate **5.10** (368 mg, 1.0 mmol, 1.0 eq) in MeCN (5 mL) was placed into the Teflon insert of a Baskerville Compact Mini (hydrogenation) Reactor. The reactor was attached to a hydrogen cylinder with the attachments purged with hydrogen before filling the reactor with a 75 bar pressure of hydrogen. The reaction mixture was stirred for 24 h

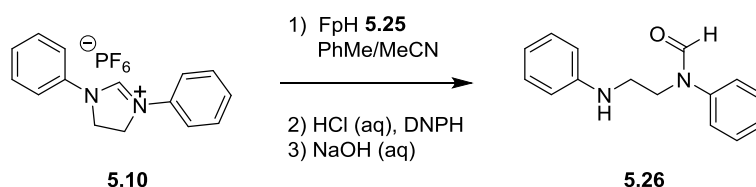
and the mixture was concentrated *in vacuo* to afford 368 mg of unreacted starting material **5.10** (100 %).

Attempted Reduction of 1,3-Diphenyl-4,5-dihydro-1*H*-imidazol-3-ium Hexafluorophosphate **5.10 with an Excess of Triethylsilane**



A solution of 1,3-diphenyl-4,5-dihydro-1*H*-imidazol-3-ium hexafluorophosphate **5.10** (368 mg, 1.0 mmol, 1.0 eq) in MeCN (5 mL) was treated with triethylsilane (0.8 mL, 5.0 mmol, 5.0 eq) and stirred for 18 h. The mixture was concentrated *in vacuo* to afford unreacted starting material **5.10** (100 %).

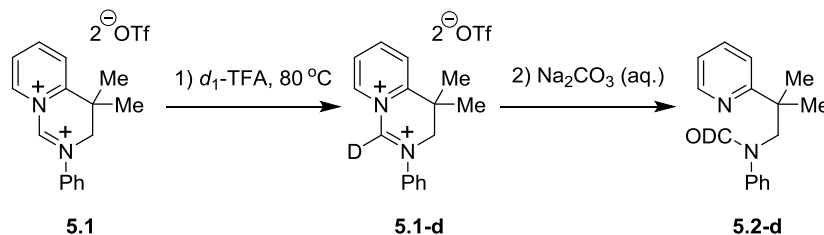
Attempted Reduction of 1,3-Diphenyl-4,5-dihydro-1*H*-imidazol-3-ium Hexafluorophosphate **5.10 with FpH **5.25****



The procedure used for the reaction of FpH **5.25** with 4,4-dimethyl-2-phenyl-3,4-dihydropyrido[1,2-*c*]pyrimidine-2,9-dium bis(trifluoro-methanesulfonate) **5.1** was repeated on the same scale, using 1,3-diphenyl-4,5-dihydro-1*H*-imidazol-3-ium hexafluorophosphate **5.10** (37 mg, 0.1 mmol, 1.0 eq) and stirring the mixture for 14 h. A precipitate formed within a red/brown solution. The mixture was transferred to a suspension of 2,4-dinitrophenylhydrazine **4.32** (40 mg, 0.2 mmol, 2.0 eq) in 4N HCl (20 mL) and stirred for 4 h. The mixture was extracted with CH₂Cl₂ (3 x 20 mL), with no hydrazone **4.33** formation observed. The aqueous layer was then made basic with NaOH pellets and extracted with CH₂Cl₂ (3 x 20 mL); throughout both acidic and basic extraction, a brown, insoluble material collected at the sides of the separating funnel – this solid had poor solubility in all solvents, so was not identified.

The combined organics were dried (Na_2SO_4) and concentrated, with the resulting residue purified by column chromatography (methanol in dichloromethane) to afford *N*-phenyl-*N*-[2-(phenylamino)ethyl]formamide **5.26** (10 mg, 42 %) as a colourless oil that formed a white solid upon standing at room temperature; m.p. 60-62 °C (lit. 65-66 °C); ^{150}H NMR (400 MHz, CDCl_3) δ = 3.37 (2H, t, J = 6.2 Hz, CH_2), 4.10 (2H, t, J = 6.2 Hz, CH_2), 4.34 (1H, bs, NH), 6.59 (2H, d, J = 7.7 Hz, ArH), 6.73 (1H, t, J = 7.3 Hz, ArH), 7.15-7.20 (4H, m, ArH), 7.34 (1H, t, J = 7.3 Hz, ArH), 7.43 (2H, dd, J = 7.3, 8.0 Hz, ArH), 8.43 (1H, s, CHO); ^{13}C NMR (100 MHz, CDCl_3) δ = 41.8 (CH_2), 44.6 (CH_2), 112.2 (CH), 117.1 (CH), 124.2 (CH), 126.8 (CH), 128.8 (CH), 129.3 (CH), 140.2 (C), 147.2 (C), 162.7 (NCHO); IR (thin film) ν = 3366, 3051, 2931, 2870, 1663, 1593, 1493, 1352, 1260, 746, 692 cm^{-1} ; m/z (ESI) 263 (100 %) $[\text{M}+\text{Na}]^+$, 241 (10 %) $[\text{M}+\text{H}]^+$.

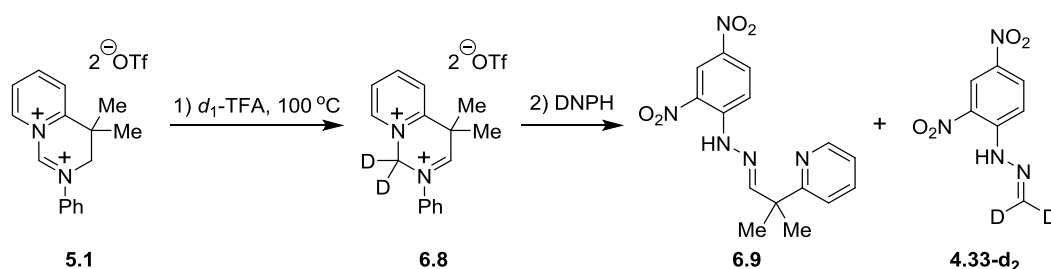
Deuterium Exchange: 4,4-Dimethyl-2-phenyl-3,4-dihydropyrido[1,2-*c*]pyrimidine-2,9-dium Bis(trifluoromethanesulfonate) 5.1 in d_1 -TFA at 80 °C



A solution of 4,4-dimethyl-2-phenyl-3,4-dihydropyrido[1,2-*c*]pyrimidine-2,9-dium bis(trifluoromethanesulfonate) **5.1** (38 mg, 0.07 mmol, 1.0 eq) in d_1 -TFA (0.7 mL) was prepared in an inert atmosphere glovebox and placed into an NMR tube fitted with a J Young valve. The tube was sealed and heated at 80 °C for 1 h. ^1H NMR analysis of the mixture showed that integration of the proton signal at δ = 10.68 ppm, corresponding to the amidine proton, had decreased by approximately 87 %. The mixture was then concentrated *in vacuo* and sat. Na_2CO_3 (5 mL) was added to the sample. Extraction with diethyl ether (3 x 5 mL), drying (Na_2CO_3) and concentration of the organics afforded a mixture of d_1 -*N*-[2-methyl-2-(pyridin-2-yl)propyl]-*N*-phenylformamide **5.2-d** and non-deuterated *N*-[2-methyl-2-(pyridin-2-yl)propyl]-*N*-phenylformamide **5.2** (87:13 deuterated to non-deuterated isotopomers determined by mass spectrometry; 13 mg, 74 %) as a yellow oil; ^1H NMR (400 MHz, CDCl_3) [2

rotamers in ratio of 1.0:0.2] $\delta = 1.31$ (6H, s, CH_3 , minor rotamer), 1.38 (6H, s, CH_3 , major rotamer), 4.12 (2H, s, CH_2 , minor rotamer), 4.32 (2H, s, CH_2 , major rotamer), 6.86-6.91 (3H, m, ArH, major and minor rotamers), 7.01-7.26 (4H, m, ArH, major and minor rotamers), 7.37 (1H, ddd, $J = 2.0, 7.7, 7.9$ Hz, ArH, major rotamer), 7.53 (1H, ddd, $J = 1.8, 7.7, 7.9$ Hz, ArH, minor rotamer), 8.10 (0.13H, s, CHO, minor rotamer), 8.29 (0.13H, s, CHO, major rotamer), 8.32 (1H, dd, $J = 1.8, 4.7$ Hz, ArH, major rotamer), 8.46 (1H, dd, $J = 1.8, 4.7$ Hz, ArH, minor rotamer); 2H NMR (61 MHz, $CDCl_3$) [2 rotamers] $\delta = 8.10$ (s, CDO), 8.29 (s, CDO); IR (ATR) $\nu = 3053, 2975, 2390, 2248, 1707, 1591, 1494, 902, 730, 695$ cm^{-1} ; HRMS m/z calcd for $C_{16}H_{18}DN_2O$ $[M+H]^+$: 256.1555; found: 256.1556.

Deuterium Exchange: 4,4-Dimethyl-2-phenyl-3,4-dihydropyrido[1,2-*c*]pyrimidine-2,9-dium Bis(trifluoromethanesulfonate) 5.1 in d_1 -TFA at 100 °C



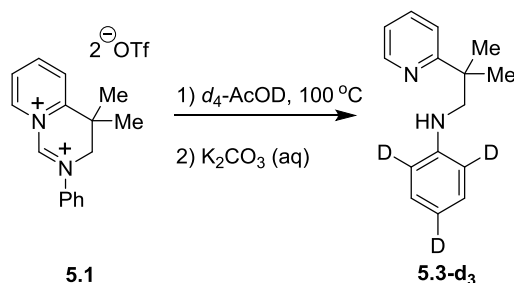
A solution of 4,4-dimethyl-2-phenyl-3,4-dihydropyrido[1,2-*c*]pyrimidine-2,9-dium bis(trifluoromethanesulfonate) **5.1** (38 mg, 0.07 mmol, 1.0 eq) in d_1 -TFA (0.7 mL) was prepared in an inert atmosphere glovebox and placed into an NMR tube fitted with a J Young valve. The tube was sealed and heated at 100 °C for 14 h. 1H NMR analysis of the mixture showed complete consumption of starting material and the emergence of a singlet (1H) at 9.81 ppm. NOESY showed that the proton associated to this singlet interacted with the two methyl groups at 2.53 ppm, with the possible disalt **6.8** being formed. The reaction mixture was treated with 2,4-dinitrophenylhydrazine **4.32** (55 mg, 0.28 mmol, 4.0 eq), 4 N HCl (4 mL) and CH_2Cl_2 (4 mL). After stirring for 5 min, the organic layer was removed and the aqueous layer extracted with more CH_2Cl_2 (2 x 4 mL). The combined organics were dried and concentrated *in vacuo*. Column chromatography (0 – 10 % ethyl acetate in hexane) afforded d₂-1-(2,4-dinitrophenyl)-2-methylenehydrazine **4.33-d₂** (7 mg, 47

%) as a yellow solid¹⁵¹ and 2-(1-(2-(2,4-dinitrophenyl)hydrazono)-2-methylpropan-2-yl)pyridine **6.9** (22 mg, 95 %) as an orange oil.

*d*₂-1-(2,4-dinitrophenyl)-2-methylenehydrazine **4.33-d₂**: m.p. 158-161 °C (lit. 167.5 – 168 °C);¹⁵¹ ¹H NMR (400 MHz, CDCl₃) δ = 7.97 (1H, d, *J* = 9.5 Hz, Ar*H*), 8.36 (1H, dd, *J* = 2.5, 9.5 Hz, Ar*H*), 9.13 (1H, d, *J* = 2.5 Hz, Ar*H*), 11.10 (1H, bs, NH); ²H NMR (77 MHz, CDCl₃) δ = 6.72 (s, CDD), 7.15 (s, CDD); IR (ATR) ν = 3314, 3094, 2922, 1617, 1588, 1502, 1312, 1092, 924, 823, 745 cm⁻¹; HRMS *m/z* calcd for C₇H₅D₂N₄O₄ [M+H]⁺: 213.0587; found: 213.0585.

(*E*)-2-(1-(2-(2,4-dinitrophenyl)hydrazono)-2-methylpropan-2-yl)pyridine **6.9**: ¹H NMR (400 MHz, CDCl₃) δ = 1.73 (6H, s, CH₃), 7.44 (1H, dd, *J* = 4.8, 7.6 Hz, Ar*H*), 7.56 (1H, d, *J* = 8.1 Hz, Ar*H*), 7.85 – 7.88 (2H, m, Ar*H* and CH), 7.96 (1H, dd, *J* = 7.6, 8.1 Hz, Ar*H*), 8.28 (1H, dd, *J* = 2.6, 9.6 Hz, Ar*H*), 8.81 (1H, d, *J* = 4.8 Hz, Ar*H*), 9.10 (1H, d, *J* = 2.6 Hz, Ar*H*), 11.08 (1H, s, NH); ¹³C NMR (100 MHz, CDCl₃) δ = 26.2 (CH₃), 45.1 (C), 116.7 (CH), 121.7 (CH), 123.2 (CH), 123.5 (CH), 129.6 (C), 130.0 (CH), 138.4 (C), 140.2 (CH), 145.3 (C), 147.4 (CH), 155.6 (CH), 163.2 (C); IR (ATR) ν = 3284, 3113, 3075, 2982, 2930, 1685, 1610, 1591, 1494, 1327, 1133, 924, 827, 715 cm⁻¹; HRMS *m/z* calcd for C₁₅H₁₆N₅O₄ [M+H]⁺ 330.1197; found: 330.1199.

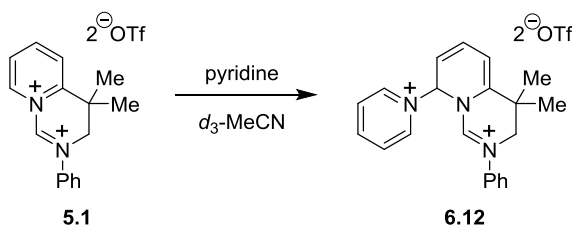
Treatment of 4,4-Dimethyl-2-phenyl-3,4-dihydropyrido[1,2-*c*]pyrimidine-2,9-dium Bis(trifluoromethanesulfonate) **5.1** in *d*₄-Acetic Acid



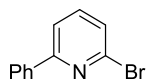
A solution of 4,4-dimethyl-2-phenyl-3,4-dihydropyrido[1,2-*c*]pyrimidine-2,9-dium bis(trifluoromethanesulfonate) **5.1** (38 mg, 0.07 mmol, 1.0 eq) in *d*₄-acetic acid (0.7 mL) was prepared in an inert atmosphere glovebox and placed into an NMR tube fitted with a J Young valve. ¹H NMR analysis indicated that all dicationic starting

material had been consumed. The mixture was then heated at 100 °C for 64 h and allowed to cool to r.t. ^1H NMR analysis showed a compound with integration for 6 aromatic protons, suggesting that some aromatic protons present in the starting material had exchanged. The mixture was added to sat. K_2CO_3 (5 mL) and extracted with diethyl ether (3 x 5 mL). The combined organics were dried (Na_2SO_4) and concentrated *in vacuo* to afford d_3 -*N*-[2-methyl-2-(pyridin-2-yl)propyl]aniline **5.3-d₃** (15, 93 %); ^1H NMR (400 MHz, CDCl_3) δ = 1.49 (6H, s, CH_3), 3.41 (2H, s, CH_2), 7.14-7.18 (3H, m, ArH), 7.38 (1H, dd, J = 0.9, 8.0 Hz, ArH), 7.66 (1H, ddd, J = 1.9, 7.6, 8.0 Hz, ArH), 8.63 (1H, dd, J = 1.9, 4.8 Hz, ArH); ^2H NMR (61 MHz, CDCl_3) δ = 6.61 (bs, ArD), 6.80 (s, ArD); IR (ATR) ν = 3374, 3053, 2963, 2867, 1655, 1584, 1476, 1431, 1259, 1095, 913, 745, 730 cm^{-1} ; HRMS: m/z calcd for $\text{C}_{15}\text{H}_{16}\text{D}_3\text{N}_2$ [M+H] 230.1731; found: 230.1730.

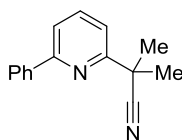
NMR Experiment: Treatment of 4,4-Dimethyl-2-phenyl-3,4-dihydropyrido[1,2-*c*]pyrimidine-2,9-dium Bis(trifluoromethanesulfonate) with Pyridine



A solution of 4,4-dimethyl-2-phenyl-3,4-dihydropyrido[1,2-*c*]pyrimidine-2,9-dium bis(trifluoromethanesulfonate) **5.1** (38 mg, 0.07 mmol, 1.0 eq) in d_3 -MeCN (0.7 mL) was prepared in an inert atmosphere glovebox and sealed in an NMR tube with a rubber cap. The tube was removed from the glovebox and a balloon of argon was attached *via* a thin-bore needle. Pyridine **1.31** (6 μL) was injected into the NMR tube, the balloon was removed and the tube inverted 3 times. ^1H , ^{13}C , COSY, NOESY, HMBC, HSQC and DEPT-Q135 NMR spectra were taken of the reaction mixture (see Appendix D and related discussion within Chapter 6, Section 1) and a major component in the reaction mixture was assigned to disalt **6.12**.

Preparation of 2-Bromo-6-phenylpyridine, **6.18****6.18**

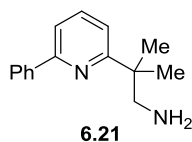
Palladium acetate trimer (67 mg, 0.1 mmol, 0.25 mol%) was added to a suspension of 2,6-dibromopyridine **6.16** (9.48 g, 40 mmol, 1.0 eq), phenylboronic acid **6.17** (4.88 g, 40 mmol, 1.0 eq) and K_3PO_4 (16.98 g, 80 mmol, 2.0 eq) in isopropanol (150 mL) and water (150 mL) at 0 °C and was stirred for 4 h before being poured into brine (200 mL). The aqueous mixture was extracted with EtOAc (3 x 200 mL) and the organic extracts were dried (Na_2SO_4) and concentrated *in vacuo*. Column chromatography (0 to 5 % EtOAc in petroleum ether, 40 – 60 °C) followed by Kugelrohr distillation (95-100 °C, 0.02 mbar) afforded 2-bromo-6-phenylpyridine **6.18** (4.03 g, 43 %) as a white solid; m.p. 54-56 °C (lit. 44 - 46 °C);¹⁵² 1H NMR (400 MHz, $CDCl_3$) δ = 7.41 (1H, dd, J = 0.7, 7.8 Hz, ArH), 7.44-7.50 (3H, m, ArH), 7.58 (1H, dd, J = 7.7, 7.8 Hz, ArH), 7.67 (1H, dd, 0.7, 7.7 Hz, ArH), 7.99 (2H, dd, 2.0, 8.1 Hz); ^{13}C NMR (100 MHz, $CDCl_3$) δ = 118.5 (CH), 125.6 (CH), 126.5 (CH), 128.3 (CH), 129.1 (CH), 137.2 (C), 138.5 (CH), 141.7 (C), 158.1 (C); IR (ATR) ν = 3040, 2324, 1572, 1547, 1427, 1391, 1125, 1051, 982, 758, 665 cm^{-1} ; m/z (CI) 234 (100 %) $[M+H]^+$, 236 (97 %) $[M+2+H]^+$ - this accounts for isotopomeric ions of ^{79}Br and ^{81}Br .

Preparation of 2-Methyl-2-(6-phenylpyridin-2-yl)propanenitrile, **6.20****6.20**

n-BuLi (2.5M in hexanes; 6.8 mL, 17 mmol, 1.0 eq) was added to a solution of freshly distilled diisopropylamine (2.6 mL, 18.7 mmol, 1.1 eq) in THF (15 mL) at 0 °C under argon and allowed to stir for 1.5 h. The mixture was then transferred *via* canula to a solution of 2-bromo-6-phenylpyridine **6.18** (4.0 g, 17 mmol, 1.0 eq) and isobutyronitrile **6.19** (1.5 mL, 17 mmol, 1.0 eq) in toluene (30 mL) at 0 °C under

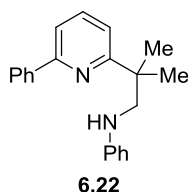
argon. After 1 h, the reaction mixture was warmed to r.t. and was then allowed to stir for a further 16 h. The mixture was concentrated *in vacuo* and the resulting residue was dissolved in diethyl ether (50 mL) before washing with water (50 mL). The aqueous layer was extracted with further ether (2 x 50 mL) and the combined organics were dried (Na₂SO₄) and concentrated *in vacuo* to afford crude 2-methyl-2-(6-phenylpyridin-2-yl)propanenitrile **6.20** (3.79 g) as a brown oil, which was used without further purification in the next step to make 2-methyl-2-(6-phenylpyridin-2-yl)propan-1-amine **6.21**.

Preparation of 2-Methyl-2-(6-phenylpyridin-2-yl)propan-1-amine, **6.21**



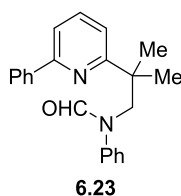
A solution of crude 2-methyl-2-(6-phenylpyridin-2-yl)propanenitrile **6.20** (3.79 g, ~ 17 mmol, 1.0 eq) in THF (20 mL) was added *via* canula to a suspension of LiAlH₄ (1.42 g, 37.5 mmol, 2.2 eq) in THF (100 mL) at 0 °C under argon. After full addition, the mixture was allowed to warm to room temperature and stirred for 16 h before being cooled to 0 °C again. Water (1.4 mL), followed by 15 % NaOH (1.4 mL) and further water (4.3 mL) was added carefully to the mixture. The mixture was dried (Na₂SO₄) and filtered through cellite and concentrated *in vacuo*. Column chromatography (20 % EtOAc in petroleum ether, 40 – 60 °C, followed by 20 % MeOH in EtOAc) afforded 2-methyl-2-(6-phenylpyridin-2-yl)propan-1-amine **6.21** (2.71 g, 70 % over two steps) as a yellow wax; ¹H NMR (400 MHz, CDCl₃) δ = 1.40 (6H, s, CH₃), 3.06 (2H, s, CH₂), 3.79 (2H, bs, NH₂), 7.25 (1H, dd, *J* = 0.7, 7.9 Hz, Ar*H*), 7.41 (1H, tt, *J* = 1.5, 7.2 Hz, Ar*H*), 7.47 (2H, dd, *J* = 7.1, 7.2 Hz, Ar*H*), 7.59 (1H, dd, *J* = 0.7, 7.8 Hz, Ar*H*), 7.71 (1H, dd, *J* = 7.8, 7.9 Hz, Ar*H*), 8.05 (2H, dd, *J* = 1.5, 7.1 Hz, Ar*H*); ¹³C NMR (100 MHz, CDCl₃) δ = 26.1 (CH₃), 41.9 (C), 52.9 (CH₂), 117.4 (CH), 118.8 (CH), 126.8 (CH), 128.7 (CH), 128.9 (CH), 137.2 (CH), 139.5 (C), 155.7 (C), 166.4 (C); IR (ATR) ν = 2963, 1570, 1443, 1402, 907, 816, 762, 727, 691 cm⁻¹; HRMS *m/z* calcd for C₁₅H₁₉N₂ [M+H]⁺: 227.1543; found: 227.1541.

Preparation of *N*-(2-Methyl-2-(6-phenylpyridin-2-yl)propyl)aniline, **6.22**



This compound was prepared using the same method as that reported for *N*-[2-methyl-2-(pyridin-2-yl)propyl]aniline **5.3**, using 2-methyl-2-(6-phenylpyridin-2-yl)propan-1-amine **6.21** (2.5 g, 11 mmol, 1.0 eq), CuI (105 mg, 0.55 mmol, 5 mol%), K₃PO₄ (4.7 g, 22 mmol, 2.0 eq), ethylene glycol (1.2 mL, 22 mmol, 2.0 eq), iodobenzene (1.8 mL, 16.5 mmol, 1.5 eq) and *i*PrOH (2 x 5 mL). This afforded *N*-(2-methyl-2-(6-phenylpyridin-2-yl)propyl)aniline **6.22** (0.73 g, 22 %) as a yellow oil; ¹H NMR (400 MHz, CDCl₃) δ = 1.52 (6H, s, CH₃), 3.44 (2H, s, CH₂), 4.65 (1H, bs, NH), 6.60 (2H, d, *J* = 8.2 Hz, ArH), 6.63 (1H, t, *J* = 7.3 Hz, ArH), 7.13 (2H, dd, *J* = 7.3, 8.2 Hz, ArH), 7.30 (1H, dd, *J* = 0.7, 7.8 Hz, ArH), 7.44 (1H, tt, *J* = 1.4, 7.3 Hz, ArH), 7.51 (2H, dd, *J* = 7.2, 7.3 Hz, ArH), 7.62 (1H, dd, *J* = 0.7, 7.8 Hz, ArH), 7.72 (1H, dd, *J* = 7.8, 7.8 Hz, ArH), 8.10 (2H, dd, *J* = 1.4, 7.2 Hz); ¹³C NMR (100 MHz, CDCl₃) δ = 26.7 (CH₃) 41.4 (C), 55.0 (CH₂), 112.8 (CH), 116.8 (CH), 117.6 (CH), 118.5 (CH), 126.8 (CH), 128.7 (CH), 128.9 (CH), 129.1 (CH), 137.3 (CH), 139.5 (C), 149.1 (C), 155.6 (C), 166.3 (C); IR (ATR) ν = 2963, 2926, 2849, 1728, 1691, 1568, 1504, 1443, 846, 760, 743, 689 cm⁻¹; HRMS: *m/z* calcd for C₂₁H₂₃N₂ [M+H]⁺: 303.1856; found 303.1857.

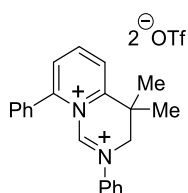
Preparation of *N*-(2-Methyl-2-(6-phenylpyridin-2-yl)propyl)-*N*-phenylformamide, **6.23**



This compound was prepared using the same procedure as used for *N*-phenyl-*N*-[2-(pyridin-2-yl)ethyl]formamide **3.42**, using *N*-(2-methyl-2-(6-phenylpyridin-2-yl)propyl)aniline **6.22** (600 mg, 1.98 mmol, 1.0 eq), oxalyl chloride (0.34 mL, 3.96

mmol, 2.0 eq), imidazole (270 mg, 3.96 mmol, 2.0 eq), triethylamine (1.1 mL, 7.92 mmol, 4.0 eq), formic acid (0.15 mL, 3.96 mmol, 2.0 eq) and CH_2Cl_2 (10 mL). This afforded *N*-(2-methyl-2-(6-phenylpyridin-2-yl)propyl)-*N*-phenylformamide **6.23** as a colourless oil (403 mg, 62 %); ^1H NMR (400 MHz, CDCl_3) [2 rotamers in ratio of 1.0:0.2] δ = 1.37 (6H, s, CH_3 , minor rotamer), 1.43 (6H, s, CH_3 , major rotamer), 4.20 (2H, s, CH_2 , minor rotamer), 4.41 (2H, s, CH_2 , major rotamer), 6.84 (2H, dd, J = 1.4, 7.1 Hz, ArH, major rotamer), 6.92 (1H, tt, J = 1.4, 7.3 Hz, ArH, major rotamer), 6.96-7.09 (3H major rotamer, 4H minor rotamer, m, ArH), 7.13 (1H, m, ArH, minor rotamer), 7.30 (1H, dd, J = 0.8, 7.9 Hz, ArH, major rotamer), 7.37-7.49 (4H major rotamer, 5 H minor rotamer, m, ArH), 7.56 (1H, dd, J = 7.8, 7.8 Hz, ArH, minor rotamer), 7.93-7.99 (2H, m, ArH, major and minor rotamers), 8.11 (1H, s, CHO, minor rotamer), 8.29 (1H, s, CHO, major rotamer); ^{13}C NMR (100 MHz, CDCl_3) [2 rotamers] δ = 25.6 (CH_3), 25.7 (CH_3), 42.3 (C), 42.4 (C), 53.6 (CH_2), 59.9 (CH_2), 116.6 (CH), 117.1 (CH), 117.8 (CH), 118.0 (CH), 124.2 (CH), 125.5 (CH), 125.6 (CH), 125.8 (CH), 126.2 (CH), 126.3 (CH), 127.9 (CH), 128.0 (CH), 128.1 (CH), 128.2 (CH), 128.3 (CH), 128.4 (CH), 136.0 (CH), 136.4 (CH), 138.8 (C), 139.0 (C), 140.8 (C), 142.6 (C), 154.8 (C), 155.4 (C), 162.7 (CH), 163.1 (CH), 163.6 (C), 164.6 (C); IR (ATR) ν = 3063, 2974, 2868, 1672, 1593, 1568, 1495, 1445, 1362, 1263, 1167, 760, 696 cm^{-1} ; HRMS: m/z calcd for $\text{C}_{22}\text{H}_{23}\text{N}_2\text{O}$ $[\text{M}+\text{H}]^+$: 331.1805; found 331.1806.

Preparation of 4,4-Dimethyl-2,8-diphenyl-3,4-dihydropyrido[1,2-*c*]pyrimidine-2,9-dium Bis(trifluoromethanesulfonate) **6.14**

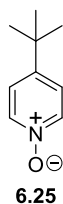


6.14

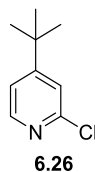
This compound was prepared using the same method as for 2-phenyl-3,4-dihydropyrido[1,2-*c*]pyrimidine-2,9-dium bis(trifluoromethanesulfonate) **3.43**, using *N*-(2-

methyl-2-(6-phenylpyridin-2-yl)propyl)-*N*-phenylformamide **6.23** (330 mg, 1.0 mmol, 1.0 eq), Tf₂O **1.32** (0.2 mL, 1.2 mmol, 1.2 eq) and CH₂Cl₂ (2 mL). This afforded 6-(*tert*-butyl)-4,4-dimethyl-2,8-diphenyl-3,4-dihydropyrido[1,2-*c*]pyridine-2,9-dium bis(trifluoromethanesulfonate) **6.14** (597 mg, 95 %) as a bright yellow solid; m.p. 60 °C (dec.); ¹H NMR (400 MHz, d₁-TFA) δ = 2.06 (6H, s, CH₃), 5.19 (2H, s, CH₂), 7.82-8.04 (8H, m, ArH), 8.10 (2H, d, *J* = 7.5 Hz, ArH), 8.59 (1H, d, *J* = 8.0 Hz, ArH), 8.63 (1H, d, *J* = 8.0 Hz, ArH), 9.21 (1H, dd, *J* = 8.0, 8.0 Hz, ArH), 9.91 (1H, s, CH); ¹³C NMR (100 MHz, d₁-TFA) δ = 23.4 (CH₃), 37.1 (C), 58.6 (CH₂), 112.7 (quartet, *J*(C,F) = 284 Hz, CF₃), 121.8 (CH), 123.4 (CH), 128.5 (CH), 129.5 (CH), 130.2 (CH), 130.5 (CH), 131.2 (CH), 133.6 (CH), 134.9 (CH), 138.6 (C), 152.1 (CH), 154.3 (C), 158.6 (C), 159.9 (C); disalt was too reactive for analysis by MS or IR.

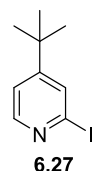
Preparation of 4-(*tert*-Butyl)pyridine-*N*-oxide, **6.25**



Hydrogen peroxide (30 % in water; 41 mL, 36 mmol, 7.2 eq) was added to acetic acid (55 mL, 96 mmol, 9.6 eq) and allowed to stir for 1 h. 4-(*tert*-Butyl)pyridine **6.24** (7.3 mL, 50 mmol, 1.0 eq) was then added and the reaction mixture was heated at 70 °C for 48 h [when this reaction was tried above 80 °C, an exothermic reaction (180 °C) was observed, with loss of product and starting material]. The mixture was added to sat. K₂CO₃ (250 mL), extracted with EtOAc (3 x 200 mL) and concentrated *in vacuo* to afford 4-(*tert*-butyl)pyridine-*N*-oxide **6.25** (4.93 g, 59 %) as a yellow oil which formed a wax on standing; ¹⁵³ ¹H NMR (400 MHz, CDCl₃) δ = 1.29 (9H, s, CH₃), 7.24 (2H, d, *J* = 7.2 Hz, ArH), 8.12 (2H, d, *J* = 7.2 Hz, ArH); ¹³C NMR (400 MHz, CDCl₃) δ = 30.0 (CH₃), 34.1 (C), 122.6 (CH), 138.1 (CH), 150.7 (C); IR (ATR) ν = 3373, 3302, 3100, 2957, 1684, 1485, 1439, 1227, 1180, 1036, 852, 823, 671 cm⁻¹; *m/z* (CI) 152 (100 %) [M+H]⁺.

Preparation of 4-(*tert*-Butyl)-2-chloropyridine, **6.26**

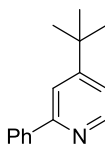
4-(*tert*-Butyl)-pyridine-*N*-oxide **6.25** (1.51 g, 10 mmol, 1.0 eq) was refluxed in phosphoryl chloride (6.1 mL, 65 mmol, 6.5 eq) under argon for 12 h. The mixture was allowed to cool and added slowly to sat K₂SO₄ (100 mL) at 0 °C. Extraction with EtOAc (3 x 100 mL), followed by drying (Na₂SO₄) and concentrating the organic layers afforded 4-(*tert*-butyl)-2-chloropyridine **6.26** (1.72 g, 100 %) as a brown oil; ¹⁵³ ¹H NMR (400 MHz, CDCl₃) δ = 1.38 (9H, s, CH₃), 7.19 (1H, dd, *J* = 1.7, 5.3 Hz, Ar*H*), 7.29 (1H, d, *J* = 1.7 Hz, Ar*H*), 8.27 (1H, d, *J* = 5.3 Hz, Ar*H*); ¹³C NMR (100 MHz, CDCl₃) δ = 29.9 (CH₃), 34.5 (C), 119.2 (CH), 120.8 (CH), 148.9 (CH), 151.3 (C), 163.1 (C); IR (ATR) ν = 3065, 2964, 2868, 1714, 1589, 1535, 1460, 1381, 1150, 1092, 991, 864, 839, 773 cm⁻¹; *m/z* (CI) 170 (100 %) [M+H]⁺, 172 (32 %) [M+2+H]⁺; HRMS: *m/z* calcd for C₉H₁₃ClN [M+H]⁺: 170.0731; found 170.0728.

Preparation of 4-(*tert*-Butyl)-2-iodopyridine, **6.27**

Acetyl chloride (4.3 mL, 60 mmol, 1.5 eq) was added to a suspension of 4-(*tert*-butyl)-2-chloropyridine **6.26** (6.78 g, 40 mmol, 1.0 eq) and sodium iodide (9.0 g, 60 mmol, 1.5 eq) in MeCN (50 mL) and the reaction mixture was refluxed for 88 h under argon. Once cooled to r.t., the mixture was added to 10 % K₂CO₃ (80 mL) and was further treated with 5 % Na₂SO₃ (80 mL) and sat. Na₂S₂O₃ (80 mL). The aqueous mixture was extracted with CH₂Cl₂ (4 x 200 mL), the combined organics were dried (Na₂SO₄) and concentrated *in vacuo*. Column chromatography (toluene) afforded 4-(*tert*-butyl)-2-iodopyridine **6.27** (3.57 g, 34 %) as a colourless oil; ¹⁵⁴ ¹H NMR (400 MHz, CDCl₃) δ = 1.28 (9H, s, CH₃), 7.23 (1H, dd, *J* = 1.6, 5.3 Hz, Ar*H*), 7.68 (1H, d, *J* = 1.6 Hz, Ar*H*), 8.24 (1H, d, *J* = 5.3 Hz, Ar*H*); IR (ATR) ν = 2963,

2866, 1578, 1524, 1454, 1375, 1261, 1136, 1074, 986, 839, 743, 681 cm^{-1} ; HRMS: m/z calcd for $\text{C}_9\text{H}_{13}\text{N}$ $[\text{M}+\text{H}]^+$: 262.0087; found 262.0087.

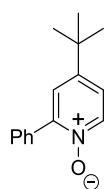
Preparation of 4-(*tert*-Butyl)-2-phenylpyridine, 6.28



6.28

A suspension of 4-(*tert*-butyl)-2-iodopyridine **6.27** (3.24 g, 12.4 mmol, 1.0 eq), palladium acetate trimer (21 mg, 0.03, 0.25 mol%), phenylboronic acid (2.27 g, 18.6 mmol, 1.5 eq) and K_3PO_4 (5.3 g, 24.8 mmol, 2.0 eq) in a mixture of isopropanol (70 mL) and water (70 mL) was heated at 80 °C for 15 h. The reaction mixture was cooled to r.t. and added to brine (150 mL). The aqueous solution was extracted with diethyl ether (3 x 200 mL) and the combined organics were dried (Na_2SO_4) and concentrated *in vacuo*. Column chromatography (toluene) afforded 4-(*tert*-butyl)-2-phenylpyridine **6.28** (2.23 g, 85 %) as a colourless oil; ^{155}H NMR (400 MHz, CDCl_3) δ = 1.38 (9H, s, CH_3), 7.24 (1H, dd, J = 1.8, 5.3 Hz, ArH), 7.41 (1H, tt, J = 1.4, 7.3 Hz, ArH), 7.48 (2H, dd, J = 7.3, 8.0 Hz, ArH), 7.71 (1H, dd, J = 0.4, 1.8 Hz, ArH), 7.97 (2H, dd, J = 1.4, 8.0 Hz, ArH), 8.60 (1H, dd, J = 0.4, 5.3 Hz); ^{13}C NMR (100 MHz, CDCl_3) δ = 30.1 (CH_3), 34.4 (C), 117.2 (CH), 118.8 (CH), 126.5 (CH), 128.1 (CH), 128.2 (CH), 139.6 (C), 149.1 (CH), 157.1 (C), 160.2 (C); IR (ATR) ν = 2961, 2864, 1595, 1545, 1477, 1445, 1393, 862, 839, 773, 743, 692, 652 cm^{-1} ; HRMS: m/z calcd for $\text{C}_{15}\text{H}_{18}\text{N}$ $[\text{M}+\text{H}]^+$: 212.1434; found 212.1433.

Preparation of 4-(*tert*-Butyl)-2-phenylpyridine-*N*-oxide, 6.29

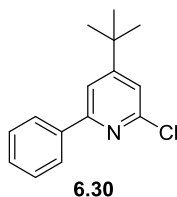


6.29

A solution of *meta*-chloroperbenzoic acid (70 %; 3.60 g, 14.6 mmol, 1.1 eq) in chloroform (20 mL) was added to a solution of 4-(*tert*-butyl)-2-phenylpyridine **6.28**

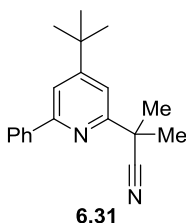
(2.81 g, 13.3 mmol, 1.0 eq) in chloroform at 0 °C and the resulting mixture was allowed to warm to r.t. and stirred for 2 h. The reaction mixture was concentrated *in vacuo* and the resulting residue was dissolved in diethyl ether (70 mL), washed with sat. Na₂CO₃ (3 x 70 mL), dried (Na₂SO₄) and concentrated *in vacuo* to afford 4-(*tert*-butyl)-2-phenylpyridine-*N*-oxide **6.29** (2.29 g, 76 %) as an orange oil; ¹H NMR (400 MHz, CDCl₃) δ = 1.34 (9H, s, CH₃), 7.21 (1H, dd, *J* = 2.9, 6.9 Hz, Ar*H*), 7.37 (1H, d, *J* = 2.9 Hz, Ar*H*), 7.43-7.50 (3H, m, Ar*H*), 7.81 (2H, dd, *J* = 1.8, 6.6 Hz, Ar*H*), 8.27 (1H, d, *J* = 6.9 Hz, Ar*H*); ¹³C NMR (100 MHz, CDCl₃) δ = 30.0 (CH₃), 34.1 (C), 121.3 (CH), 123.9 (CH), 127.8 (CH), 128.9 (CH), 129.0 (CH), 132.7 (C), 139.2 (CH), 147.8 (C), 150.0 (C); IR (ATR) ν = 2957, 2864, 1589, 1466, 1406, 1240, 827, 773, 756, 692 cm⁻¹; HRMS: *m/z* calcd for C₁₅H₁₈NO [M+H]⁺: 228.1383; found 228.1381.

Preparation of 4-(*tert*-Butyl)-2-chloro-6-phenylpyridine, **6.30**



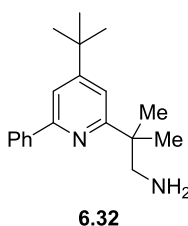
This compound was prepared using the same method as used to prepare 4-(*tert*-butyl)-2-chloropyridine **6.26**, using 4-(*tert*-butyl)-2-phenylpyridine-*N*-oxide **6.29** (2.73 g, 10 mmol, 1.0 eq) and phosphoryl chloride (6.1 mL, 65 mmol, 6.5 eq). Column chromatography (5 % EtOAc in petroleum ether, 40-60 °C) afforded 4-(*tert*-butyl)-2-chloro-6-phenylpyridine **6.30** (1.67 g, 68 %) as a light red oil; ¹H NMR (400 MHz, CDCl₃) δ = 1.36 (9H, s, CH₃), 7.25 (1H, d, *J* = 1.4 Hz, Ar*H*), 7.42-7.49 (3H, m, Ar*H*), 7.62 (1H, d, *J* = 1.4 Hz, Ar*H*), 7.97 (2H, dd, *J* = 1.6, 6.7 Hz, Ar*H*); ¹³C NMR (100 MHz, CDCl₃) δ = 30.0 (CH₃), 34.7 (C), 115.8 (CH), 119.1 (CH), 126.6 (CH), 128.2 (CH), 128.8 (CH), 137.9 (C), 151.1 (C), 157.5 (C), 163.1 (C); IR (ATR) ν = 2965, 2872, 1591, 1537, 1387, 1304, 1248, 1169, 1074, 878, 864, 819, 770, 692, 650 cm⁻¹; *m/z* (ESI) 246 (100 %) [M+H]⁺, 248 (32) [M+2+H]⁺ - the latter ion accounting for a ³⁷Cl-containing isotopomer of the former; HRMS: *m/z* calcd for C₁₅H₁₇ClN [M+H]⁺: 246.1044; found 246.1038.

Preparation of 2-(4-(*tert*-Butyl)-6-phenylpyridin-2-yl)-2-methylpropanenitrile, 6.31



This compound was prepared using the same method as 2-methyl-2-(6-phenylpyridin-2-yl)propanenitrile **6.20**, using 4-(*tert*-butyl)-2-chloro-6-phenylpyridine **6.30** (1.65 g, 6.7 mmol, 1.0 eq), *isobutyronitrile* **6.19** (0.6 mL, 6.7 mmol, 1.0 eq), *n*-BuLi (2.5 M in hexanes; 2.7 mL, 6.7 mmol, 1.0 eq) toluene (15 mL) and THF (8 mL). Column chromatography (two columns: one eluted with 0 – 10 % EtOAc in petroleum ether, 40-60 °C; the second eluted with 0-50 % CH₂Cl₂ in petroleum ether, 40-60 °C) afforded crude 2-(4-(*tert*-butyl)-6-phenylpyridin-2-yl)-2-methylpropanenitrile **6.31** (1.41 g) which was used without further purification in the preparation of 2-(4-(*tert*-butyl)-6-phenylpyridin-2-yl)-2-methylpropan-1-amine **6.32**.

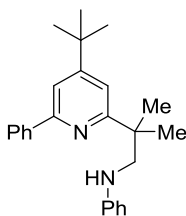
Preparation of 2-(4-(*tert*-Butyl)-6-phenylpyridin-2-yl)-2-methylpropan-1-amine, 6.32



This compound was prepared using the same method as that used for 2-methyl-2-(6-phenylpyridin-2-yl)propan-1-amine **6.21**, using crude 2-(4-(*tert*-butyl)-6-phenylpyridin-2-yl)-2-methylpropanenitrile **6.31** (1.41 g, ~5 mmol, 1.0 eq) in THF (5 mL) and LiAlH₄ (417 mg, 11 mmol, 2.2 eq) in THF (40 mL). Column chromatography (10 % EtOAc in petroleum ether, followed by 100 % EtOAc and 19:1:80 MeOH:Et₃N:petroleum ether) afforded 2-(4-(*tert*-butyl)-6-phenylpyridin-2-yl)-2-methylpropan-1-amine **6.32** (887 mg, 47 % over 2 steps) as a colourless oil; ¹H NMR (400 MHz, CDCl₃) δ = 1.37 (9H, s, CH₃), 1.40 (6H, s, CH₃), 2.81 (2H, bs,

NH_2), 3.05 (2H, s, CH_2), 7.25 (1H, d, $J = 1.5$ Hz, ArH), 7.40 (1H, tt, $J = 1.2, 6.8$ Hz, ArH), 7.47 (2H, dd, $J = 6.8, 7.1$ Hz, ArH), 7.57 (1H, d, $J = 1.5$ Hz, ArH), 8.03 (2H, dd, $J = 1.2, 7.1$ Hz, ArH); ^{13}C NMR (100 MHz, $CDCl_3$) $\delta = 25.7$ (CH_3), 30.2 (CH_3), 34.5 (C), 41.5 (C), 52.7 (CH_2), 114.3 (CH), 115.1 (CH), 126.4 (CH), 128.1 (CH), 128.1 (CH), 139.6 (C), 155.2 (C), 160.6 (C), 165.8 (C); IR (ATR) $\nu = 2963, 2867, 1595, 1551, 1406, 1362, 903, 872, 775, 756, 731$ cm^{-1} ; HRMS m/z calcd. for $C_{19}H_{27}N_2$ $[M+H]^+$: 283.2169; found: 283.2173.

Preparation of *N*-(2-(4-(*tert*-Butyl)-6-phenylpyridin-2-yl)-2-methylpropyl)aniline, **6.33**

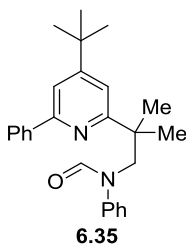


6.33

This compound was prepared using a method modified from that reported for *N*-[2-methyl-2-(pyridin-2-yl)propyl]aniline **5.3**, using 2-(4-(*tert*-butyl)-6-phenylpyridin-2-yl)-2-methylpropan-1-amine **6.32** (865 mg, 3.1 mmol, 1.0 eq), iodobenzene (0.69 mL, 6.2 mmol, 2.0 eq), CuI (30 mg, 0.16 mmol, 5 mol %), ethylene glycol (0.35 mL, 6.2 mmol, 2.0 eq), K_3PO_4 (1.97 g, 9.3 mmol, 3.0 eq) in isopropanol (5 mL). After heating at 80 °C for 38 h, further iodobenzene (0.37 mL, 3.3 mmol, 1.1 eq) was added to the reaction mixture. After heating at 80 °C for a further 96 h, the mixture was cooled and poured into water (50 mL) and extracted with diethyl ether (6 x 50 mL). The organic extracts were concentrated *in vacuo* and 2N HCl (50 mL) was added, with the mixture then extracted with CH_2Cl_2 (4 x 50 mL). The aqueous layer was then made basic with sodium hydroxide pellets and extracted with CH_2Cl_2 (4 x 50 mL). The organic layers extracted from the basic solution were then concentrated *in vacuo* to afford 2-(4-(*tert*-butyl)-6-phenylpyridin-2-yl)-2-methylpropan-1-amine **6.30** (starting material). The original reaction was repeated with this starting material, with heating at 80 °C for 24 h. All the organics extracted from the acidic solution were dried (Na_2SO_4) and concentrated *in vacuo*. Column chromatography

(0 – 20 % EtOAc in hexane) afforded *N*-(2-(4-(*tert*-butyl)-6-phenylpyridin-2-yl)-2-methylpropyl)aniline **6.33** (730 mg, 66 %) as a light brown oil; ^1H NMR (400 MHz, CDCl_3) δ = 1.37 (9H, s, CH_3), 1.54 (6H, s, CH_3), 3.43 (2H, s, CH_2), 4.83 (1H, bs, NH), 6.59 (2H, d, J = 7.8 Hz, ArH), 6.64 (1H, t, J = 7.3 Hz, ArH), 7.14 (2H, dd, J = 7.3, 7.8 Hz, ArH), 7.31 (1H, d, J = 1.4 Hz, ArH), 7.44 (1H, tt, J = 1.4, 6.8 Hz, ArH), 7.52 (2H, dd, J = 6.8, 7.3 Hz, ArH), 7.62 (1H, d, J = 1.4 Hz, ArH), 8.09 (2H, dd, J = 1.4, 7.3 Hz); ^{13}C NMR (100 MHz, CDCl_3) δ = 26.4 (CH_3), 30.2 (CH_3), 34.6 (C), 40.9 (C), 54.6 (CH_2), 112.2 (CH), 114.4 (CH), 114.9 (CH), 116.0 (CH), 126.4 (CH), 128.1 (CH), 128.2 (CH), 128.6 (CH), 139.6 (C), 148.7 (C), 155.1 (C), 160.7 (C), 165.6 (C); IR (ATR) ν = 2957, 2864, 1597, 1551, 1406, 1254, 874, 775, 746 cm^{-1} ; HRMS: m/z calcd for $\text{C}_{25}\text{H}_{31}\text{N}_2$ $[\text{M}+\text{H}]^+$: 359.2482; found 359.2485.

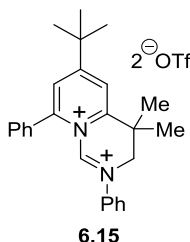
Preparation of *N*-(2-(4-(*tert*-Butyl)-6-phenylpyridin-2-yl)-2-methylpropyl)-*N*-phenylformamide, **6.35**



A solution of formic pivalic anhydride **6.34** (0.4 mL, 2.8 mmol, 1.4 eq; taken from a lab stock prepared by Luka Kovacevic)¹³⁸ in CH_2Cl_2 (10 mL) was added to a solution of *N*-(2-(4-(*tert*-butyl)-6-phenylpyridin-2-yl)-2-methylpropyl)aniline **6.33** (707 mg, 2.0 mmol, 1.0 eq) in CH_2Cl_2 (10 mL) at 0 °C under argon. The mixture was stirred at r.t. for 41 h and then washed with 2N NaOH (2 x 20 mL) and brine (20 mL), dried (Na_2SO_4) and concentrated *in vacuo*. Column chromatography (0-10 % EtOAc in hexane) afforded *N*-(2-(4-(*tert*-butyl)-6-phenylpyridin-2-yl)-2-methylpropyl)-*N*-phenylformamide **6.35** (729 mg, 94 %) as a colourless oil; ^1H NMR (400 MHz, CDCl_3) [2 rotamers in ratio of 19:3] δ = 1.22 (9H, s, CH_3 , major rotamer), 1.30 (9H, s, CH_3 , minor rotamer), 1.44 (6H, s, CH_3 , major rotamer), 1.61 (6H, s, CH_3 , minor rotamer), 4.19 (2H, s, CH_2 , minor rotamer), 4.42 (2H, s, CH_2 , major rotamer), 6.80 (2H, dd, J = 1.5, 7.0 Hz, ArH, major rotamer), 6.89 (1H, tt, J = 1.5, 7.3 Hz, ArH, major rotamer), 6.92-6.97 (3H, m, ArH, major rotamer), 6.98-7.04 (4H, m, ArH,

minor rotamer), 7.10-7.14 (2H, m, *ArH*, minor rotamer), 7.25-7.26 (1H, m, *ArH*, major rotamer), 7.37-7.42 (1H major rotamer, 2H minor rotamer, m, *ArH*), 7.44-7.49 (2H, m, *ArH*, major and minor rotamer), 7.44-7.49 (2H, m, *ArH*, major and minor rotamer), 8.11 (1H, s, *CHO*, minor rotamer), 8.29 (1H, s, *CHO*, major rotamer); ^{13}C NMR (100 MHz, CDCl_3) δ = 25.6 (CH_3), 25.8 (CH_3), 30.1 (CH_3), 30.2 (CH_3), 32.5 (C), 34.3 (C), 42.2 (C), 42.3 (C), 53.6 (CH_2), 60.1 (CH_2), 113.9 (CH), 114.4 (CH), 114.7 (CH), 115.0 (CH), 124.0 (CH), 125.4 (CH), 125.6 (CH), 125.7 (CH), 126.4 (CH), 127.9 (CH), 128.0 (CH), 128.0 (CH), 128.1 (CH), 128.1 (CH), 128.1 (CH), 128.1 (CH), 138.9 (C), 139.7 (C), 140.6 (C), 144.8 (C), 155.0 (C), 155.6 (C), 158.6 (C), 159.6 (C), 162.8 (CHO), 163.2 (CHO), 163.3 (C), 164.3 (C); IR (ATR) ν = 2967, 2868, 1680, 1597, 1497, 1364, 1263, 1166, 895, 777. 763 cm^{-1} ; HRMS: m/z calcd for $\text{C}_{26}\text{H}_{31}\text{N}_2\text{O}$ $[\text{M}+\text{H}]^+$: 387.2431; found 387.2437.

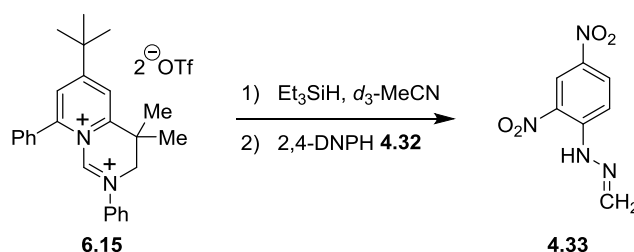
Preparation of 6-(*tert*-Butyl)-4,4-dimethyl-2,8-diphenyl-3,4-dihydropyrido[1,2-*c*]pyrimidine-2,9-dium Bis(trifluoromethanesulfonate), 6.15



This compound was prepared using the same method as for 2-phenyl-3,4-dihydropyrido[1,2-*c*]pyrimidine-2,9-dium bis(trifluoromethanesulfonate) **3.43**, with *N*-(2-(4-(*tert*-butyl)-6-phenylpyridin-2-yl)-2-methylpropyl)-*N*-phenylformamide **6.35** (650 mg, 1.7 mmol, 1.0 eq) as starting material, affording 6-(*tert*-butyl)-4,4-dimethyl-2,8-diphenyl-3,4-dihydropyrido[1,2-*c*]pyrimidine-2,9-dium bis(trifluoromethanesulfonate) **6.15** (1.07 g, 95 %) as a bright yellow solid; m.p. 70 °C (dec.); ^1H NMR (400 MHz, CD_3CN) δ = 1.57 (9H, s, CH_3), 1.79 (6H, s, CH_3), 4.85 (2H, d, J = 0.9 Hz, CH_2), 7.69-7.80 (7H, m, *ArH*), 7.86 (1H, tt, J = 1.3, 7.6 Hz, *ArH*), 7.97 (2H, dd, J = 1.3, 7.0 Hz, *ArH*), 8.30-8.32 (2H, m, *ArH*), 9.40 (1H, s, *CH*); ^{13}C NMR (100 MHz, CD_3CN) δ = 23.5 (CH_3), 28.2 (CH_3), 36.9 (C), 38.6 (C), 58.1 (CH_2), 120.4 (quartet, $J(\text{C},\text{F})$ = 317 Hz, CF_3), 121.0 (CH), 123.0 (CH), 126.7 (CH), 129.3 (C), 129.7 (CH),

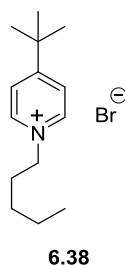
130.2 (CH), 131.7 (CH), 132.9 (CH), 133.8 (CH), 138.6 (C), 152.7 (CH), 157.3 (C), 157.4 (C), 182.8 (C); disalt was too reactive for analysis by MS or IR.

Reaction of 6-(*tert*-Butyl)-4,4-dimethyl-2,8-diphenyl-3,4-dihydropyrido[1,2-*c*]pyrimidine-2,9-dium Bis(trifluoromethanesulfonate) **6.15 with 1 equivalent of Triethylsilane Followed by 2,4-DNPH **4.32** Derivatisation**



To a solution of 6-(*tert*-butyl)-4,4-dimethyl-2,8-diphenyl-3,4-dihydropyrido[1,2-*c*]pyrimidine-2,9-dium bis(trifluoromethanesulfonate) **6.15** (33 mg, 0.05 mmol, 1.0 eq) in CD_3CN (0.8 mL) in an NMR tube was added triethylsilane (8 μL , 0.05 mmol, 1.0 eq) and the mixture was inverted 3 times. The mixture was monitored by ^1H NMR and, after 5 days, the solution was then added to a suspension of 2,4-dinitrophenylhydrazine (20 mg, 0.01 mmol, 2.0 eq) in 4N HCl (20 mL) and stirred overnight. Column chromatography (diethyl ether in hexane) afforded 1-(2,4-dinitrophenyl)-2-methylenehydrazine **4.33** (5 mg, 47 %); data were consistent with those reported previously within this thesis.

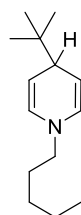
Preparation of 4-(*tert*-Butyl)-1-pentylpyridin-1-ium Bromide, **6.38**



1-Bromopentane (2.7 mL, 22 mmol, 1.1 eq) was added to a solution of 4-(*tert*-butyl)pyridine (2.9 mL, 20 mmol, 1.0 eq) in MeCN (20 mL) and refluxed for 15 h under argon. The mixture was then allowed to cool and extracted with hexane (3 x

20 mL). The MeCN solution was concentrated *in vacuo* to afford 4-(*tert*-butyl)-1-pentylpyridin-1-ium bromide **6.38** as a white crystalline solid (5.3g, ; m.p. 118 – 120 °C; ^1H NMR (500 MHz, CDCl_3) δ = 0.67 (3H, t, J = 7.0 Hz, CH_3), 1.16-1.21 (13H, m, 2 x CH_2 and 3 x CH_3), 1.88 (2H, tt, J = 7.5, 7.5 Hz, CH_2), 4.72 (2H, t, J = 7.5 Hz, CH_2), 7.87 (2H, d, J = 6.9 Hz, ArH), 9.47 (2H, d, J = 6.9 Hz, ArH); ^{13}C NMR (125 MHz, CDCl_3) δ = 13.7 (CH_3), 22.0 (CH_2), 27.9 (CH_2), 29.9 (CH_3), 31.4 (CH_2), 36.4 (C), 60.6 (CH_2), 125.2 (CH), 144.7 (CH), 170.4 (C); IR (ATR) ν = 3083, 3023, 2956, 2926, 2863, 1632, 1465, 1118, 872, 734 cm^{-1} ; HRMS m/z calcd for $\text{C}_{14}\text{H}_{24}\text{N}$ [M-Br] $^+$: 206.1903; found: 206.1903.

Reaction of 4-(*tert*-Butyl)-1-pentylpyridin-1-ium Bromide **6.38** with Sodium Triethylborohydride

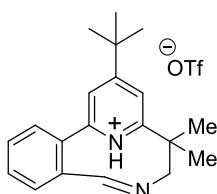


6.39

A solution of sodium triethylborohydride in THF (1M, 5.0 mL, 5.0 mmol, 1.0 eq) was added to a solution of 4-(*tert*-butyl)-1-pentylpyridin-1-ium bromide **6.38** (1.14 g, 5.5 mmol, 1.1eq) in THF (10 mL) in an inert atmosphere glovebox. A white suspension immediately developed which was stirred for 16 h and the volume was reduced under vacuum to approximately 5 mL. Hexane (10 mL) was added to the suspension and stirred for 10 min. The suspension was then filtered and the resulting orange filtrate was concentrated *in vacuo*. This afforded a mixture of an orange solid and a colourless oil (the solid likely being a mixture of salts). The oil was decanted from the solid to afford 4-(*tert*-butyl)-1-pentyl-1,4-dihydropyridine **6.39** as a colourless oil (619 mg, 54 %); ^1H NMR (400 MHz, C_6D_6) δ = 0.81 (3H, t, J = 7.2 Hz, CH_3), 0.98 (9H, s, CH_3), 1.00-1.22 (6H, m, CH_2), 2.57 (2H, t, J = 7.0 Hz, CH_2), 2.92 (1H, t, J = 4.3 Hz, CH), 4.51 (2H, dd, J = 4.3, 8.1 Hz, CH), 5.72 (2H, d, J = 8.1 Hz, CH); ^{13}C NMR (100 MHz, C_6D_6) δ = 14.2 (CH_3), 22.7 (CH_2), 26.2 (CH_3), 29.0 (CH_2), 30.2 (CH_2), 36.3 (C), 44.5 (CH), 53.4 (CH_2), 98.7 (CH), 131.5 (CH); m/z (CI)

206 (100 %) $[M-H]^+$; this dihydropyridine was too reactive for IR analysis, while MS analysis did not differentiate from starting pyridinium salt.

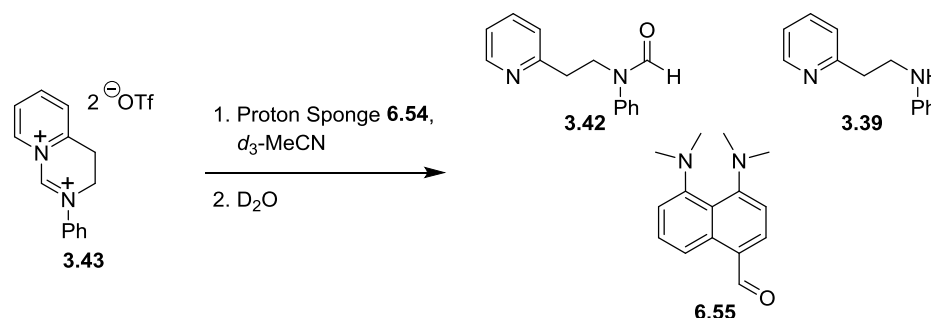
Thermal Decomposition of 6-(*tert*-Butyl)-4,4-dimethyl-2,8-diphenyl-3,4-dihydropyrido[1,2-*c*]pyrimidine-2,9-dium Bis(trifluoromethanesulfonate) **6.15 in d_1 -TFA**



6.40

6-(*tert*-Butyl)-4,4-dimethyl-2,8-diphenyl-3,4-dihydropyrido[1,2-*c*]pyrimidine-2,9-dium bis(trifluoromethanesulfonate) **6.15** (17 mg, 0.025 mmol, 1.0 eq) was heated at 80 °C in d_1 -trifluoroacetic acid for 72 h. The sample was concentrated *in vacuo* and the crude material washed with ether (3 x 2 mL). The sample was then crystallised with a mixture of chloroform and ether (in a ratio of 3:1, respectively), affording a brown solid which was then washed with further ether and concentrated *in vacuo* (3 x 2 mL) to afford 7-(*tert*-butyl)-4,4-dimethyl-3,4-dihydro-5,9-(azeno)benzo[*c*][1]azacyclo-undecine trifluoromethanesulfonic acid salt **6.40** (5 mg, 45 %) as a beige solid; m.p 60 °C (dec.); ^1H NMR (400 MHz, CD_3CN) δ = 1.26 (3H, s, CH_3), 1.52 (9H, s, CH_3), 1.61 (3H, s, CH_3), 4.04 (1H, d, J = 14.4 Hz, CHH), 4.15 (1H, d, J = 14.4 Hz, CHH), 7.12-7.16 (2H, m, NH and CH), 7.35 (1H, dd, J = 1.0, 7.7 Hz, ArH), 7.67 (1H, ddd, J = 1.0, 7.6, 7.7 Hz, ArH), 7.78 (1H, ddd, J = 1.0 Hz, 7.6, 7.8 Hz, ArH), 7.87 (1H, d, J = 1.6 Hz, ArH), 8.32 (1H, dd, J = 1.0, 7.8 Hz, ArH), 8.38 (1H, d, J = 1.6 Hz, ArH) [see Appendix E]; ^{13}C NMR (100 MHz, CD_3CN) δ = 26.1 (CH_3), 29.1 (CH_3), 30.1 (CH_3), 34.3 (C), 36.7 (C), 64.2 (CH_2), 115.6 (CH), 120.2 (CH), 123.8 (CH), 124.1 (CH), 128.7 (CH), 130.3 (C), 130.6 (CH), 132.7 (CH), 137.5 (C), 155.5 (C), 161.5 (C), 172.6 (C); ^{19}F NMR (376 Hz, CD_3CN) δ = -79.4; IR (ATR) ν = 3474, 3090, 2975, 1707, 1636, 1476, 1226, 1163, 1028, 764 cm^{-1} ; MS (ESI): reported cation could not be observed (expected m/z = 293.2012); however, undefined cations were observed at m/z = 371.2393 (100 %), 404.2371 (95 %).

Attempted Deprotonation of 2-Phenyl-3,4-dihydropyrido[1,2-*c*]pyrimidine-2,9-dium Bis(trifluoromethanesulfonate) **3.43 Using Proton Sponge **6.54****

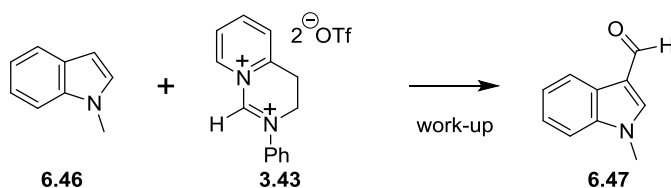


A solution of proton sponge **6.54** (54 mg, 0.25 mmol, 1.0 eq) in deuterated acetonitrile (0.7 mL) was added to 2-phenyl-3,4-dihydropyrido[1,2-*c*]pyrimidine-2,9-dium bis(trifluoromethanesulfonate) **3.43** (127 mg, 0.25 mmol, 1.0 eq), giving a solution with a red colour. 1H NMR showed that no disalt was left in the reaction mixture and the spectrum contained very broad signals in the aromatic region. The mixture was then transferred *via* canula into D_2O (3 mL) at 0 °C under argon then treated with saturated sodium bicarbonate solution (20 mL) and extracted with CH_2Cl_2 (3 x 20 mL). The combined organic layers were dried (Na_2SO_4) and concentrated *in vacuo* to yield a bright yellow oil. Column chromatography (ethyl acetate and petroleum ether, 40-60 °C) afforded 4,5-bis(dimethylamino)-1-naphthaldehyde **6.55** (27 mg, 45 %),¹⁵⁶ *N*-phenyl-*N*-(2-(pyridin-2-yl)ethyl)formamide **3.42** (18 mg, 32 %), with no decrease in the integral of the proton peak of the formamide group, and *N*-(2-(pyridin-2-yl)ethyl)aniline **3.39** (30 mg, 61 %).; data for amide **3.42** and **3.39** were consistent with those reported previously within this thesis.

4,5-Bis(dimethylamino)-1-naphthaldehyde **6.55**: 1H NMR (400 MHz, $CDCl_3$) δ = 2.79 (6H, s, CH_3), 2.98 (6H, s, CH_3), 6.85 (1H, d, J = 8.2 Hz, *ArH*), 6.97 (1H, dd, J = 1.0, 7.6 Hz, *ArH*), 7.48 (1H, dd, J = 7.6, 8.3 Hz, *ArH*), 7.72 (1H, d, J = 8.2 Hz, *ArH*), 8.90 (1H, dd, J = 1.0 Hz, 8.3 Hz, *ArH*), 10.08 (1H, s, *CHO*); ^{13}C NMR (100 MHz, $CDCl_3$) δ = 42.7 (CH_3), 42.8 (CH_3), 108.1 (CH), 112.2 (CH), 116.5 (C), 116.6 (CH), 122.1 (C), 128.4 (CH), 135.5 (C), 138.5 (CH), 150.5 (C), 156.1 (C), 190.7 (CHO); IR

(thin film) $\nu = 2940, 2838, 2790, 2709, 1662, 1558, 1516, 1218, 1195, 1123, 1095, 1044, 812, 763 \text{ cm}^{-1}$; m/z (ESI) 243 (50 %) $[M+H]^+$, 265 (27 %) $[M+Na]^+$, 507 (100 %) $[2M+Na]^+$; HRMS: m/z calcd for $C_{15}H_{19}N_2O$ $[M+H]^+$: 243.1492; found: 243.1493.

Formylation of *N*-Methylindole **6.46 Using 2-Phenyl-3,4-dihydropyrido[1,2-*c*]pyrimidine-2,9-dium Bis(trifluoromethanesulfonate) **3.43** (2 days)**



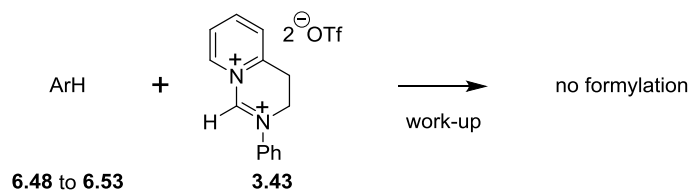
2-Phenyl-3,4-dihydropyrido[1,2-*c*]pyrimidine-2,9-dium bis(trifluoromethanesulfonate) **3.43** (254 mg, 0.5 mmol, 1.0 eq) and *N*-methylindole **6.46** (0.131 g, 1.0 mmol, 2 eq) were stirred in MeCN (2 mL) at r.t. under argon for 48 h and then concentrated *in vacuo*. The resultant residue was then dissolved in CH_2Cl_2 (5 mL) and stirred with NaOH solution (2N, 5 mL) for 3 min. The CH_2Cl_2 layer was extracted and the aqueous layer washed with more CH_2Cl_2 (5 x 10 mL). The combined organic layers were washed with water (50 mL), brine (50 mL), dried (Na_2SO_4) and concentrated *in vacuo*. Column chromatography (diethyl ether) afforded 3-formyl-*N*-methylindole **6.47** (42 mg, 52 %); ^{157}H NMR (400 MHz, $CDCl_3$) $\delta = 3.81$ (3H, s, CH_3), 7.30 - 7.37 (3H, m, ArH), 7.60 (1H, s, ArH), 8.30 (1H, m, ArH), 9.94 (1H, s, CHO); ^{13}C NMR (100 MHz, $CDCl_3$) $\delta = 33.1$ (CH_3), 109.4 (CH), 117.6 (C), 121.5 (CH), 122.4 (CH), 123.5 (CH), 124.8 (C), 137.4 (C), 138.7 (CH), 183.9 (CHO); IR (thin film) $\nu = 3099, 2923, 1655, 1535, 1473, 1193, 1074, 746 \text{ cm}^{-1}$; m/z (CI) 160 (100 %) $[M+H]^+$; HRMS: m/z calcd for $C_{10}H_{10}NO$ $[M+H]^+$: 160.0757; found: 160.0757.

Formylation of *N*-Methylindole **6.46 Using 2-Phenyl-3,4-dihydropyrido[1,2-*c*]pyrimidine-2,9-dium Bis(trifluoromethanesulfonate) **3.43** (4 days)**

The procedure directly above was followed, with a stirring time of 4 days. Column chromatography (diethyl ether) afforded 3-formyl-*N*-methylindole **6.47** (57 mg, 71

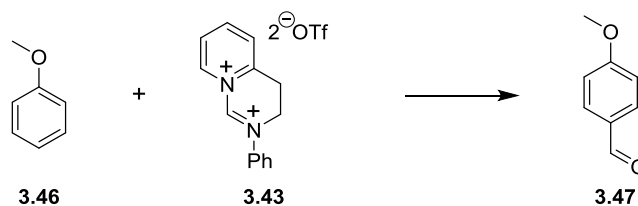
); data were consistent with those reported for 3-formyl-*N*-methylindole **6.47** reported directly above.

Attempted Formylation of Other Aromatics Using 2-Phenyl-3,4-dihydropyrido[1,2-*c*]pyrimidine-2,9-dium Bis(trifluoromethanesulfonate) **3.43**



The procedure for the formylation of *N*-methylindole using 2-phenyl-3,4-dihydropyrido[1,2-*c*]pyrimidine-2,9-dium bis(trifluoromethane-sulfonate) **3.43** was tested on several other aromatics which were found to be unreactive. The tested aromatics were nitrobenzene, anthracene, chlorobenzene, acetophenone, benzene and toluene.

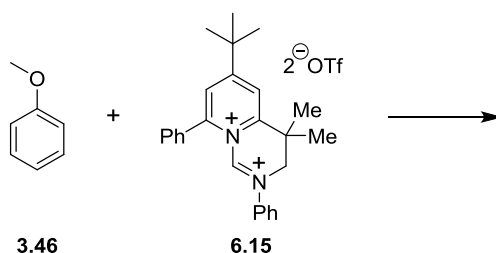
Treatment of Anisole **3.46** with 2-Phenyl-3,4-dihydropyrido[1,2-*c*]pyrimidine-2,9-dium Bis(trifluoromethanesulfonate) **3.43**



A modified procedure of that carried out by Corr was utilised.²⁷ Anisole **3.46** (22 μL , 0.2 mmol, 1.0 eq) was added to a solution of 2-phenyl-3,4-dihydropyrido[1,2-*c*]pyrimidine-2,9-dium bis(trifluoromethanesulfonate) **3.43** (102 mg, 0.2 mmol, 1.0 eq) in MeCN (1 mL). The reaction mixture was removed from the glovebox and stirred at r.t. under argon for 17 h. The reaction mixture was concentrated *in vacuo* and the resulting residue extracted between sat. Na_2CO_3 (10 mL) and diethyl ether (10 mL). The aqueous layer was extracted with further ether (3 x 10 mL) and concentrated *in vacuo*. Column chromatography (0 – 20 % ethyl acetate in petroleum ether, 40 – 60 $^\circ\text{C}$) afforded 4-anisaldehyde **3.47** (7.6 mg, 28 %) as a

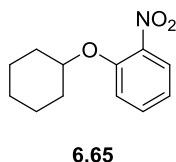
yellow oil;²⁷ ^1H NMR (400 MHz, CDCl_3) δ = 3.90 (3H, s, CH_3), 7.02 (2H, d, J = 8.8 Hz, ArH), 7.85 (2H, d, J = 8.8 Hz, ArH), 9.90 (1H, s, CH); ^{13}C NMR (100 MHz, CDCl_3) δ = 55.8 (CH_3), 144.5 (CH), 130.2 (C), 132.2 (CH), 164.8 (C), 191.0 (CH); IR (ATR) ν = 2960, 1678, 1599, 1509, 1462, 1212, 1024, 837 cm^{-1} ; m/z (EI) m/z 136 (70 %) $[\text{M}]^{+\bullet}$, 135 (100 %) $[\text{M}-\text{H}]^+$.

Treatment of Anisole 3.46 with 6-(*Tert*-butyl)-4,4-dimethyl-2,8-diphenyl-3,4-dihydropyrido[1,2-*c*]pyrimidine-2,9-dium Bis(trifluoromethanesulfonate) 6.15



The same procedure as that used for the formylation of anisole **3.46** with 2-phenyl-3,4-dihydropyrido[1,2-*c*]pyrimidine-2,9-dium bis(trifluoromethanesulfonate) **3.43** was carried out, using 6-(*tert*-butyl)-4,4-dimethyl-2,8-diphenyl-3,4-dihydropyrido[1,2-*c*]pyrimidine-2,9-dium bis(trifluoromethanesulfonate) **6.15** (133 mg, 0.2 mmol, 1.0 eq) and anisole (22 μL , 0.2 mmol, 1.0 eq) and MeCN (1 mL). No formylated anisole **3.47** was afforded from this reaction. Anisole **3.46** (22 mg, 100%) was recovered after column chromatography using 100 % petroleum ether (40 – 60 $^\circ\text{C}$) as eluent.

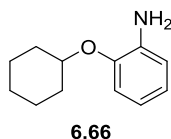
Preparation of 1-(Cyclohexyloxy)-2-nitrobenzene, 6.65



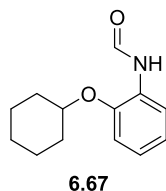
A solution of cyclohexanol **6.64** (4.7 mL, 45 mmol, 1.5 eq) in diethyl ether (10 mL) was added to a suspension of KH (30 % in mineral oil; 4.01 g, 30 mmol, 1.0 eq) in diethyl ether (40 mL) at r.t. under argon and stirred for 3 h. The resulting precipitate was filtered and washed with ether (4 x 50 mL) to give a pale yellow solid which was dissolved in THF (50 mL) and cooled to -78 $^\circ\text{C}$. 1-Fluoro-2-nitrobenzene **6.63** (3.2

mL, 30 mmol, 1.0 eq) was then added and the solution allowed to warm to r.t. and stirred overnight. CH₂Cl₂ (50 mL) was added to the mixture which was then washed with sat. NH₄Cl solution. The aqueous layer was extracted with further CH₂Cl₂ (50 mL) and the combined organics concentrated. The resulting residue was dissolved in diethyl ether (50 mL) and washed with 2N KOH solution (8 x 50 mL), dried (Na₂SO₄) and concentrated *in vacuo*. Column chromatography (gradient of 0 to 20 % of diethyl ether in cyclohexane) afforded 1-(cyclohexyloxy)-2-nitrobenzene **6.65** as a yellow oil (4.31 g, 65 %);¹⁵⁸ ¹H NMR (400 MHz, CDCl₃) δ = 1.27-1.98 (10H, m, CH₂), 4.46 (1H, tt, *J* = 3.8, 8.1 Hz, CH), 7.00 (1H, ddd, *J* = 1.1, 8.0, 7.4 Hz, ArH), 7.10 (1H, dd, *J* = 1.1, 8.3 Hz, ArH), 7.49 (1H, ddd, *J* = 1.7, 7.4, 8.3 Hz, ArH), 7.80 (1H, dd, *J* = 1.7, 8.0 Hz, ArH); ¹³C NMR (100 MHz, CDCl₃) δ = 22.6 (CH₂), 24.9 (CH₂), 30.8 (CH₂), 76.7 (CH), 115.6 (CH), 119.4 (CH), 125.0 (CH), 133.1 (CH), 140.6 (C), 150.7 (C); IR (ATR) ν = 3078, 2937, 2860, 1605, 1523, 1355 cm⁻¹; HRMS: *m/z* calcd for C₁₂H₁₆NO₃ [M+H]⁺: 222.1125; found: 222.1126.

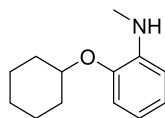
Preparation of 2-(Cyclohexyloxy)aniline, **6.66**



To a mixture of 1-(cyclohexyloxy)-2-nitrobenzene **6.65** (4.31 g, 19.5 mmol, 1.0 eq) and Pd/C (10 % Wt; 0.8 g, 0.75 mmol, 4 mol%) in ethanol (100 mL) was added hydrazine monohydrate (6.06 mL, 125 mmol, 6.25 eq) at r.t. under argon. The resulting mixture was refluxed for 1h, cooled to r.t. and stirred overnight. The mixture was filtered through celite and concentrated *in vacuo* to afford 2-(cyclohexyloxy)aniline **6.66** as a colourless oil (3.73g, 100 %);¹⁵⁸ ¹H NMR (400 MHz, CDCl₃) δ = 1.25-2.05 (10H, m, CH₂), 3.80 (2H, bs, NH₂), 4.25 (1H, tt, *J* = 3.7, 8.9 Hz, CH), 6.69-6.85 (4H, m, ArH); ¹³C NMR (100 MHz, CDCl₃) δ = 23.3 (CH₂), 25.2 (CH₂), 30.8 (CH₂), 75.5 (CH), 113.4 (CH), 114.9 (CH), 117.9 (CH), 120.6 (CH), 136.9 (C), 144.7 (C); IR (thin film) ν = 3355, 2926, 1749, 1501 cm⁻¹; HRMS: *m/z* calcd for C₁₂H₁₈NO [M+H]⁺: 192.1383; found: 192.1380.

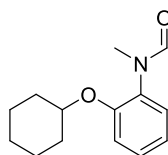
Preparation of *N*-(2-(Cyclohexyloxy)phenyl)formamide, **6.67**

Sodium formate (0.265 g, 3.9 mmol, 0.2 eq) was added to a solution of 2-(cyclohexyloxy)aniline **6.66** (4.28 g, 19.5 mmol, 1.0 eq) in formic acid (2.9 mL, 78 mmol, 4.0 eq) at r.t. under argon and stirred for 19 h. EtOAc (30 mL) was added and the mixture filtered, extracted with water (2 x 30 mL), sat. sodium bicarbonate (30 mL), dried (Na₂SO₄) and concentrated *in vacuo*. Column chromatography (ether in petroleum ether, 40-60 °C) afforded *N*-(2-(cyclohexyloxy)phenyl)formamide **6.67** (3.32 g, 76 %) as a colourless oil and a mixture of 2 rotamers (16:9, major: minor rotamers); ¹H NMR (400 MHz, CDCl₃) δ = 1.28-2.07 (10H, m, CH₂, major and minor rotamers); 4.29- 4.37 (1H, m, CH, major and minor rotamer), 6.91-7.13 (3H, m, ArH, major and minor rotamer), 7.22 (1H, dd, *J* = 1.4, 7.9 Hz, ArH, minor rotamer), 7.73, (1H, s, NH, minor rotamer), 7.84 (1H, s, NH, major rotamer), 8.40 (1H, dd, *J* = 1.6, 8.0 Hz, ArH, major rotamer) 8.49 (1H, d, *J* = 1.6 Hz, CHO, major rotamer), 8.79 (1H, d, *J* = 11.7 Hz, CHO, minor rotamer); ¹³C NMR (100 MHz, CDCl₃) δ = 23.2 (CH₂, minor rotamer), 23.3 (CH₂, major rotamer), 24.9 (CH₂, minor rotamer), 25.0 (CH₂, major rotamer), 31.3 (CH₂, minor rotamer), 31.4 (CH₂, major rotamer), 76.1 (CH, major and minor rotamer), 112.2 (CH, major rotamer), 113.4 (CH, minor rotamer), 116.1 (CH, minor rotamer), 120.1 (CH, major rotamer), 120.4 (CH, major rotamer), 123.6 (CH, major rotamer), 124.5 (CH, minor rotamer), 126.6 (C, minor rotamer), 127.2 (C, major rotamer), 145.4 (C, major rotamer), 146.2 (C, minor rotamer), 158.3 (CHO, major rotamer), 161.0 (CH, minor rotamer), 162.5 (CHO, minor rotamer); IR (thin film) ν = 3331, 3066, 2935, 2858, 1692, 1596, 1520 cm⁻¹; HRMS: *m/z* calcd for C₁₃H₁₈NO₂ [M+H]⁺: 220.1332; found: 220.1331.

Preparation of 2-(Cyclohexyloxy)-*N*-methylaniline, **6.68**

6.68

A solution of *N*-(2-(cyclohexyloxy)phenyl)formamide **6.67** (3.08 g, 14 mmol, 1.0 eq) in THF (40 mL) was added to a suspension of LiAlH₄ (1.31 g, 34.5 mmol, 2.5 eq) in THF (40 mL) and stirred for 18 h at r.t. The mixture was cooled to 0 °C and water (1.3 mL) was added dropwise followed by NaOH solution (15 %, 1.3 mL) and more water (3.9 mL). The mixture was warmed to r.t., stirred for 15 min and Na₂SO₄ was added. The salts were removed by filtration and the solution concentrated *in vacuo* to afford 2-(cyclohexyloxy)-*N*-methylaniline **6.68** as a colourless oil (2.73 g, 95 %); ¹H NMR (400 MHz, CDCl₃) δ = 1.19-2.19 (10H, m, CH₂), 2.90 (3H, s, CH₃), 4.28 (1H, m, CH), 6.64-6.69 (2H, m, ArH), 6.82 (1H, d, *J*(H,H.) = 7.9 Hz, ArH), 6.92 (1H, t, *J* = 7.6 Hz, ArH); ¹³C NMR (126 MHz, CDCl₃) δ = 23.9 (CH₂), 25.7 (CH₂), 30.5 (CH₂), 32.1 (CH₃), 75.9 (CH), 109.7 (CH), 112.4 (CH), 116.2 (CH), 121.3 (CH), 140.53 (C), 144.8 (C); HRMS: *m/z* calcd for C₁₃H₂₀NO [M+H]⁺: 206.1539; found: 206.1537.

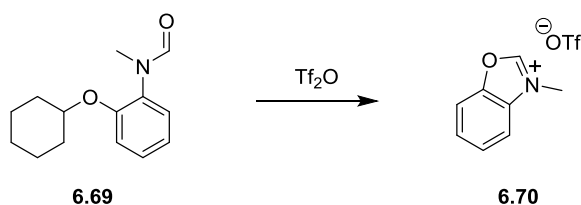
Preparation of *N*-(2-(cyclohexyloxy)phenyl)-*N*-methylformamide, **6.69**

6.69

N-(2-(Cyclohexyloxy)phenyl)-*N*-methylformamide **6.69** was prepared in an analogous manner to *N*-(2-(cyclohexyloxy)phenyl)formamide **6.67**, using 2-(cyclohexyloxy)-*N*-methylaniline **6.68** (1.39 g, 6.8 mmol, 1.0 eq), sodium formate (95 mg, 1.4 mmol, 0.2 eq) and formic acid (1.0 mL, 27.2 mmol, 4.0 eq). This afforded *N*-(2-(cyclohexyloxy)phenyl)-*N*-methylformamide **6.69** (963 mg, 61 %) as a pale yellow oil and a mixture of 2 rotamers (19:1, major:minor rotamers); ¹H NMR (400 MHz, CDCl₃) δ = 1.37-1.96 (10H, m, CH₂, major and minor rotamers), 3.24

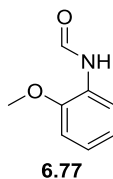
(3H, s, CH_3 , major rotamer), 3.29 (3H, s, CH_3 , minor rotamer) 4.29-4.35 (1H, m, CH , major and minor rotamers), 6.91-7.30 (4H, m, ArH , major and minor rotamers), 8.21 (1H, s, CHO , major and minor rotamers); ^{13}C NMR (126 MHz, $CDCl_3$, major rotamer only) δ = 22.9 (CH_2), 25.0 (CH_2), 31.0 (CH_2), 32.4 (CH_3), 75.4 (CH), 114.1 (CH), 120.1 (CH), 127.4 (CH), 128.3 (CH), 131.2 (C), 152.8 (C), 163.2 (CHO); IR (thin film) ν = 3067, 2932, 2857, 1672, 1595, 1497 cm^{-1} ; HRMS: m/z calcd for $C_{14}H_{20}NO_2$ $[M+H]^+$: 234.1489; found: 234.1483.

Preparation of 3-Methylbenzo[d]oxazol-3-ium Triflate 6.70 from *N*-(2-(cyclohexyloxy)phenyl)-*N*-methylformamide 6.69



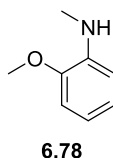
A solution of *N*-(2-(cyclohexyloxy)phenyl)-*N*-methylformamide **6.69** (117 mg, 0.5 mmol, 1.0 eq) in CH_2Cl_2 (0.5 mL) was added to a solution of Tf_2O **1.32** (0.13 mL, 0.75 mmol, 1.5 eq) in CH_2Cl_2 (0.5 mL) at -78 °C under argon, using a syringe pump (1.27 mL h^{-1}). After full addition, the mixture was stirred for 2 h at -78 °C, allowed to warm to room temperature and then stirred at 60 °C for 20 h. The mixture was allowed to cool to r.t., ether was added (5 mL) and the mixture was stirred overnight. The ether solution was then decanted from the resulting precipitate. The precipitate was then washed with further ether (2 x 5 mL) and placed under vacuum to afford 3-methylbenzo[d]oxazol-3-ium triflate **6.70** (75 mg, 53 %) as a white powder; mp 92 - 94 °C; 1H NMR (400 MHz, CD_3CN) δ = 4.22 (1H, s, CH_3), 7.84-8.07 (4H, m, ArH), 9.82 (1H, s, CH); ^{13}C NMR (126 MHz, CD_3CN) δ = 33.1 (CH_3), 113.1 (CH), 114.4 (CH), 120.5 (quartet, $J(C,F)$ = 320 Hz, CF_3) 128.3 (CH), 128.8 (C), 129.7 (CH), 148.5 (C), 156.2 (CH); IR (ATR) ν = 3092, 3041, 1585, 1462, 1254, 1159, 1028 cm^{-1} ; m/z (ESI) 134 (100 %) $[M-OTf]^+$.

Preparation of *N*-(2-Methoxyphenyl)formamide, **6.77**



N-(2-Methoxyphenyl)formamide **6.77** was prepared in an analogous manner to *N*-(2-(cyclohexyloxy)phenyl)formamide **6.67**, using *o*-anisidine **6.76** (4.5 mL, 40 mmol, 1.0 eq), sodium formate (544 mg, 8 mmol, 0.2 eq) and formic acid (6.0 mL, 160 mmol, 4.0 eq). This afforded *N*-(2-methoxyphenyl)formamide **6.77** (3.20 g, 53 %) as a brown oil and a mixture of 2 rotamers (17:8, major:minor rotamers);¹³⁹ ¹H NMR (400 MHz, CDCl₃) δ = 3.92 (3H, s, CH₃, minor rotamer), 3.95 (3H, s, CH₃, major rotamer), 6.91-7.18 (3H, m, ArH, major and minor rotamers), 7.22 (1H, d, *J* = 7.9 Hz, ArH, minor rotamer), 7.69 (1H, bs, NH, minor rotamer), 7.81 (1H, bs, NH, major rotamer), 8.38 (1H, dd, *J* = 1.6, 7.2 Hz, ArH, major rotamer), 8.48 (1H, d, *J* = 1.6 Hz, CHO, major rotamer), 8.76 (1H, d, *J* = 11.6 Hz, CHO, minor rotamer); ¹³C NMR (100 MHz, CDCl₃) δ = 55.2 (CH₃, major and minor rotamer), 109.5 (CH, major rotamer), 110.8 (CH, minor rotamer), 116.1 (CH, minor rotamer), 120.0 (CH, major rotamer), 120.5 (CH, minor rotamer), 120.6 (CH, major rotamer), 123.8 (CH, major rotamer), 124.7 (CH, minor rotamer), 126.25 (C, major rotamer), 134.9 (C, minor rotamer), 147.3 (C, major rotamer), 153.2 (C, minor rotamer), 158.2 (CHO, major rotamer), 160.9 (CHO, minor rotamer); IR (ATR) ν = 3244, 3132, 3048, 2961, 1694, 1657, 1595, 1522, 1458, 1258 cm⁻¹; HRMS: *m/z* calcd for C₈H₉NO₂ [M]⁺: 151.0628; found: 151.0624.

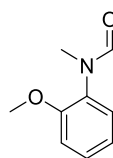
Preparation of 2-Methoxy-*N*-methylaniline, **6.78**



2-Methoxy-*N*-methylaniline **6.78** was prepared in an analogous manner to 2-(cyclohexyloxy)-*N*-methylaniline **6.68**, using *N*-(2-methoxyphenyl)formamide **6.77** (2.91 g, 40 mmol, 1.0 eq), LiAlH₄ (3.80 g, 100 mmol, 2.5 eq) and THF (2 x 150 mL).

This afforded 2-methoxy-*N*-methylaniline **6.78** as a brown oil (2.29 g, 86 %);¹⁵⁹ ¹H NMR (400 MHz, CDCl₃) δ = 2.90 (3H, s, NCH₃), 3.88 (3H, s, OCH₃), 6.64 (1H, dd, J = 1.5, 7.8 Hz, ArH), 6.71 (1H, ddd, J = 1.5, 7.6, 7.8, ArH), 6.80 (1H, dd, J = 1.3 Hz, 7.9 Hz, ArH), 6.94 (1H, ddd, J = 1.3, 7.6, 7.9 Hz, ArH); ¹³C (100 MHz, CDCl₃) δ = 29.9 (CH₃), 54.9 (CH₃), 108.8 (CH), 108.9 (CH), 115.8 (CH), 120.9 (CH), 138.9 (C), 146.4 (C); IR (thin film) ν = 3428, 3057, 2994, 2936, 2812, 1601, 1510, 1220 cm⁻¹; m/z (EI) 137 (96 %) [M]⁺, 122 (100 %) [M-CH₃]⁺; HRMS m/z calcd for C₈H₁₁NO [M]⁺: 137.0835; found: 137.0833.

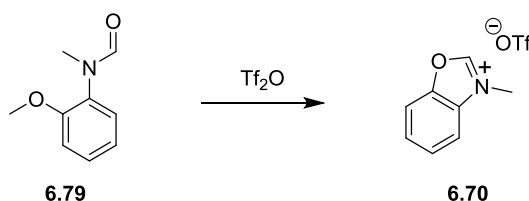
Preparation of *N*-(2-Methoxyphenyl)-*N*-methylformamide, **6.79**



6.79

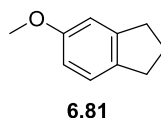
N-(2-Methoxyphenyl)-*N*-methylformamide **6.79** was prepared in an analogous manner to *N*-(2-(cyclohexyloxy)phenyl)formamide **6.67**, using 2-methoxy-*N*-methylaniline **6.78** (2.29 g, 17 mmol, 1.0 eq), sodium formate (231 mg, 3.4 mmol, 0.2 eq) and formic acid (2.6 mL, 68 mmol, 4.0 eq). This afforded *N*-(2-methoxyphenyl)-*N*-methylformamide **6.79** (1.58 g, 56 %) as a brown oil and a mixture of 2 rotamers (50:3, major to minor rotamer);¹⁶⁰ ¹H NMR (400 MHz, CDCl₃) δ = 3.23 (3H, s, NCH₃, major rotamer), 3.28 (3H, s, NCH₃, minor rotamer), 3.87 (3H, s, OCH₃, major and minor rotamers), 6.99-7.02 (2H, m, ArH, major and minor rotamers), 7.14 (1H, dd, J = 1.8, 8.0 Hz, ArH, major rotamer), 7.20 (1H, dd, 1.8 Hz, 8.1 Hz, ArH, minor rotamer), 7.31-7.36 (1H, m, ArH, major and minor rotamer), 8.19 (1H, s, CHO, major rotamer), 8.30 (1H, s, CHO, minor rotamer); ¹³C (125 MHz, CDCl₃, major rotamer only) δ = 32.8 (CH₃), 55.6 (CH₃), 112.0 (CH), 117.1 (CH), 120.9 (CH), 129.0 (CH), 130.7 (C), 155.0 (C), 163.5 (CH); IR (ATR) ν = 2918, 2839, 1670, 1595, 1501, 1342, 1271 cm⁻¹; HRMS m/z calcd for C₉H₁₂NO₂ [M+H]⁺: 166.0863; found: 166.0863.

Preparation of 3-Methylbenzo[d]oxazol-3-ium Triflate **6.70** from *N*-(2-Methoxyphenyl)-*N*-methylformamide **6.79**



A solution of *N*-(2-methoxyphenyl)-*N*-methylformamide **6.79** (83 mg, 0.5 mmol, 1.0 eq) in toluene (0.5 mL) was added to Tf_2O **1.32** (0.5 mL, 3.0 mmol, 6.0 eq) at r.t. The mixture was then refluxed for 3 h, allowed to cool to r.t. and concentrated *in vacuo* and stirred for 20 min in ether. The ether was decanted from the resulting precipitate and further ether washings were carried out (5 x 10 mL) before drying the solid *in vacuo* to afford 3-methylbenzo[d]oxazol-3-ium triflate **6.70** (62 mg, 44 %); data were consistent with those reported for 3-methylbenzo[d]oxazol-3-ium triflate **6.70** prepared from *N*-(2-(cyclo-hexyloxy)phenyl)-*N*-methylformamide **6.69**.

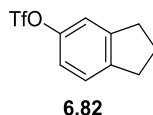
Preparation of 5-Methoxy-2,3-dihydro-1*H*-indene, **6.81**



Dimethyl sulfate (1.04 mL, 11 mmol, 1.1 eq) was added dropwise to a mixture of 5-indanol **6.80** (1.34 g, 10 mmol, 1.0 eq) and K_2CO_3 (1.52 g, 11 mmol, 1.1 eq) in acetone (20 mL) at r.t. The mixture was refluxed for 17 h, then ammonium hydroxide (0.5 mL) was added followed by an additional 15 min of stirring. The mixture was then allowed to cool to r.t., concentrated *in vacuo* and dissolved in ether (20 mL). The solution was washed with NaOH solution (2N, 2 x 20 mL) and water (20 mL), dried (Na_2SO_4) and concentrated *in vacuo* to afford 5-methoxy-2,3-dihydro-1*H*-indene **6.81** (1.363 g, 92 %) as a clear oil;¹⁶¹ ^1H NMR (400 MHz, CDCl_3) δ = 2.10 (2H, tt, J = 7.3, 7.5 Hz, CH_2), 2.89 (4H, m, 2 x CH_2), 3.82 (3H, s, CH_3), 6.72 (1H, dd, J = 2.4, 8.1 Hz, ArH), 6.82 (1H, d, J = 2.4 Hz, ArH), 7.15 (1H, d, J = 8.1 Hz, ArH); ^{13}C NMR (100 MHz, CDCl_3) δ = 25.4 (CH_2), 31.5 (CH_2), 32.7 (CH_2), 55.0 (CH_3), 109.4 (CH), 111.4 (CH), 124.2 (CH), 135.7 (C), 145.2 (C), 158.0

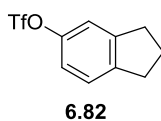
(C); IR (ATR) $\nu = 2995, 2941, 2843, 1607, 1489, 1242 \text{ cm}^{-1}$; m/z (CI) 149 (100 %) $[M+H]^+$; HRMS m/z calcd for $C_{10}H_{11}O$ $[M-H]^+$: 147.0804; found: 147.0802.

Preparation of 2,3-Dihydro-1*H*-inden-5-yl Trifluoromethanesulfonate, **6.82;
Conditions A**



A solution of 5-methoxy-2,3-dihydro-1*H*-indene **6.81** (74 mg, 0.5 mmol, 1.0 eq) in toluene (0.5 mL) was added to Tf_2O **1.32** (0.5 mL, 3.0 mmol, 6.0 eq) at r.t. under argon and the mixture was refluxed for 16 h. The mixture was cooled to r.t., concentrated *in vacuo* and stirred with sat. K_2CO_3 (10 mL). This was extracted with CH_2Cl_2 (3 x 10 mL), dried (Na_2SO_4) and concentrated *in vacuo*. Column chromatography (toluene) afforded 2,3-dihydro-1*H*-inden-5-yl trifluoromethanesulfonate **6.82** as a yellow oil (39 mg, 34 %); ^{162}H NMR (400 MHz, $CDCl_3$): $\delta = 2.45$ (2H, quintet, $J = 7.4$ Hz), 2.93 (2H, t, $J = 7.4$ Hz), 2.96 (2H, t, $J = 7.4$ Hz), 7.02 (1H, m), 7.12 (1H, d, $J = 1.8$ Hz), (1H, d, $J = 7.2$ Hz); ^{13}C NMR (100 MHz, $CDCl_3$): $\delta = 26.1$ (CH_2), 32.7 (CH_2), 33.3 (CH_2), 117.7 (CH), 119.1 (quartet, $J = 319$ Hz, CF_3), 119.2 (CH), 125.8 (CH), 145.0 (C), 147.2 (C), 148.6 (C); IR (ATR) $\nu = 2957, 2850, 1611, 1593, 1480, 1423, 1250 \text{ cm}^{-1}$; HRMS m/z calcd for $C_{10}H_9F_3O_3S$ $[M]^+$: 266.0220; found: 266.0219.

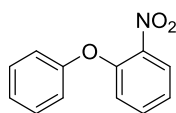
Preparation of 2,3-Dihydro-1*H*-inden-5-yl Trifluoromethanesulfonate, **6.82;
Conditions B**



Tf_2O **1.32** (0.5 mL, 3.0 mmol, 6.0 eq) was added to 5-methoxy-2,3-dihydro-1*H*-indene **6.81** (74 mg, 0.5 mmol, 1.0 eq) at r.t. under argon and the mixture refluxed

for 14 h. The mixture was cooled to r.t., concentrated *in vacuo* and stirred with sat. K_2CO_3 (5 mL). The mixture was extracted with ether (3 x 5 mL), dried (Na_2SO_4) and concentrated *in vacuo*. Column chromatography (toluene) afforded 2,3-dihydro-1*H*-inden-5-yl trifluoromethanesulfonate **6.82** as a yellow oil (132 mg, 99 %); ^1H NMR (400 MHz, CDCl_3): data were consistent with those reported for 2,3-dihydro-1*H*-inden-5-yl trifluoromethanesulfonate **6.82**, prepared under Conditions A.

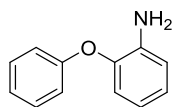
Preparation of 1-Nitro-2-phenoxybenzene, **6.87**



6.87

KOH powder (2.24 g, 40.0 mmol, 1.00 eq) and phenol (4.78 g, 50.8 mmol, 1.27 eq) were heated at 110 °C under argon for 40 min. 1-Fluoro-2-nitrobenzene **6.63** (4.60 mL, 43.6 mmol, 1.09 eq) was added dropwise to the mixture, which was then stirred for 2 h before cooling to r.t. The mixture was then dissolved in EtOAc (100 mL) and washed with 2N NaOH (100mL), brine (100 mL), 2N HCl (100 mL) and brine (100 mL). The organics were then dried (Na_2SO_4) and concentrated *in vacuo* before distillation (145-150 °C at 0.1 mbar) afforded 1-nitro-2-phenoxybenzene **6.87** as a yellow oil (7.40 g, 86 %); ^{163}H NMR (400 MHz, CDCl_3) δ = 7.03 (1H, dd, J = 1.2, 8.4 Hz, Ar*H*), 7.08 (2H, dd, J = 1.0, 8.5 Hz, Ar*H*), 7.19-7.24 (2H, m, Ar*H*), 7.39-43 (2H, m, Ar*H*), 7.52 (1H, ddd, J = 1.7, 7.4, 8.4 Hz, Ar*H*), 7.97 (1H, dd, J = 1.7, 8.1 Hz, Ar*H*); ^{13}C NMR (125 MHz, CDCl_3) δ = 119.3 (CH), 120.5 (CH), 123.1 (CH), 124.6 (CH), 125.7 (CH), 130.1 (CH), 134.1 (CH), 141.4 (C), 150.8 (C), 155.8 (C); IR (ATR) ν = 3067, 3038, 1607, 1585, 1520, 1474, 1346, 1236, 881, 841, 741, 689 cm^{-1} ; m/z (CI) 216 (100 %) $[\text{M}+\text{H}]^+$; HRMS: m/z calcd for $\text{C}_{12}\text{H}_{10}\text{NO}_3$ $[\text{M}+\text{H}]^+$: 216.0655; found: 216.0651.

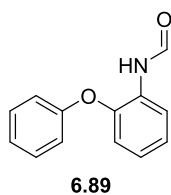
Preparation of 2-Phenoxyaniline, **6.88**



6.88

A mixture of 1-nitro-2-phenoxybenzene **6.87** (6.89 g, 32.0 mmol, 1.0 eq) and Pd/C (10 %Wt; 3.4 g, 3.2 mmol, 10 mol%) in methanol (40 mL) was placed in a round-bottomed flask fitted with a two-tapped joint. One tap was attached to a vacuum pump and the other was attached to a balloon of hydrogen. The mixture was placed under vacuum and purged with hydrogen three times and after the final purge, the mixture was allowed to stir under an atmosphere of hydrogen for 14 h at r.t. The mixture was filtered through celite, the solids were washed with ethanol (3 x 20 mL) and the resulting solution was concentrated *in vacuo* to afford 2-phenoxyaniline **6.88** as a colourless oil which later solidified to a beige solid (5.93g, 100 %); m.p. 47-49 °C (lit. 44-45 °C);¹⁶⁴ ¹H NMR (500 MHz, CDCl₃) δ = 3.80 (2H, bs, NH₂), 6.72 (1H, ddd, J = 1.4, 7.4, 7.8 Hz, ArH), 6.83 (1H, dd, J = 1.4, 7.9, ArH), 6.88 (1H, dd, J = 1.1, 8.0 Hz, ArH), 6.96-7.01 (3H, m, ArH), 7.06 (1H, t, J = 7.5 Hz, ArH), 7.31 (2H, dd, J = 6.6, 7.5 Hz, ArH); ¹³C NMR (125 MHz, CDCl₃) δ = 116.5 (CH), 117.2 (CH), 118.8 (CH), 120.3 (CH), 122.7 (CH), 125.0 (CH), 129.8 (CH), 138.8 (C), 143.1 (C), 157.6 (C); IR (ATR) ν = 3429, 3354, 3046, 1618, 1581, 1487, 1477, 1454, 1211, 1190, 1150, 876, 744, 692 cm⁻¹; HRMS: m/z calcd for C₁₂H₁₂NO [M+H]⁺: 186.0913; found: 186.0915.

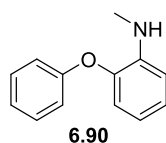
Preparation of *N*-(2-Phenoxyphenyl)formamide, **6.89**



N-(2-Phenoxyphenyl)formamide **6.89** was prepared in an analogous manner to *N*-(2-(cyclohexyloxy)phenyl)formamide **6.67**, using 2-phenoxyaniline **6.88** (5.56 g, 30 mmol, 1.0 eq), sodium formate (408 mg, 6 mmol, 0.2 eq) and formic acid (4.5 mL, 120 mmol, 4.0 eq). This afforded *N*-(2-phenoxyphenyl)formamide **6.89** (5.80 g, 91 %) as a beige solid and a mixture of 2 rotamers (in a ratio of 9:4); m.p. 93-95 °C (lit. 98-99 °C);¹⁶⁵ ¹H NMR (500 MHz, CDCl₃) δ = 6.88 (1H, dd, J = 1.2, 8.1 Hz, ArH, major rotamer), 6.93-6.95 (1H, m, ArH, minor rotamer), 6.98 – 7.18 (5H, m, ArH, major and minor rotamers), 7.31 – 7.40 (3H minor rotamer, 2H major rotamer, m, ArH), 7.69 (1H, bs, NH, minor rotamer), 7.79 (1H, bs, NH, major rotamer), 8.46-

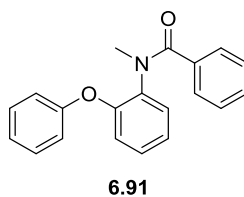
8.49 (2H, m, ArH and CHO, major rotamer), 8.81 (1H, d, $J = 11.5$ Hz, CHO, minor rotamer); ^{13}C (125 MHz, CDCl_3 , major rotamer only) $\delta = 117.9$ (CH), 118.4 (CH), 118.5 (CH), 121.4 (CH), 124.0 (CH), 124.1 (CH), 124.6 (CH), 129.0 (C), 145.5 (C), 156.4 (C), 159.0 (CH); IR (ATR) $\nu = 3130, 3022, 3001, 2922, 1678, 1584, 1487, 1231, 1206, 745, 685$ cm^{-1} ; HRMS m/z calcd for $\text{C}_{13}\text{H}_{12}\text{NO}_2$ $[\text{M}+\text{H}]^+$: 214.0863; found: 214.0867.

Preparation of *N*-Methyl-2-phenoxyaniline, **6.90**



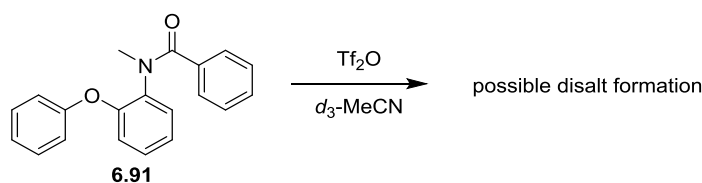
N-Methyl-2-phenoxyaniline was prepared in an analogous manner to 2-(cyclohexyloxy)-*N*-methylaniline **6.68**, using *N*-(2-phenoxyphenyl)formamide **6.89** (5.33 g, 25 mmol, 1.0 eq) and LiAlH_4 (2.37 g, 62.5 mmol, 2.5 eq) and THF (2 x 100 mL). This afforded *N*-methyl-2-phenoxyaniline **6.90** as a brown solid (4.97 g, 100 %); m.p. 51-53 °C (lit. 48 °C); ^{166}H NMR (400 MHz, CDCl_3) $\delta = 2.88$ (3H, d, $J = 4.0$ Hz, NCH_3), 4.21 (1H, bs, NH), 6.65 (1H, ddd, $J = 1.5, 7.6, 7.8$ Hz, ArH), 6.74 (1H, dd, $J = 1.5, 8.0$ Hz, ArH), 6.85 (1H, dd, $J = 1.4, 7.8$ Hz, ArH), 6.95 – 6.99 (2H, m, ArH), 7.03 – 7.12 (2H, m, ArH), 7.31 (2H, dd, $J = 7.4, 7.5$ Hz, ArH); ^{13}C (125 MHz, CDCl_3) $\delta = 30.4$ (CH_3), 111.0 (CH), 116.7 (CH), 117.3 (CH), 119.4 (CH), 122.7 (CH), 125.2 (CH), 129.8 (CH), 141.8 (C), 142.9 (C), 157.7 (C); IR (ATR) $\nu = 3433, 3419, 3048, 2913, 1607, 1579, 1512, 1487, 1427, 1256, 1217, 1163, 870, 741, 663$ cm^{-1} ; HRMS m/z calcd for $\text{C}_{13}\text{H}_{14}\text{NO}$ $[\text{M}+\text{H}]^+$: 200.1070; found: 200.1072.

Preparation of *N*-Methyl-*N*-(2-phenoxyphenyl)benzamide, **6.91**



A solution of benzoyl chloride **4.3** (2.6 mL, 22.5 mmol, 1.5 eq) in CH₂Cl₂ (10 mL) was added dropwise to a solution of *N*-methyl-2-phenoxyaniline **6.90** (2.99 g, 15 mmol, 1.0 eq) and triethylamine (4.2 mL, 30 mmol, 2.0 eq) in CH₂Cl₂ (20 mL) at r.t. under argon. After full addition, the reaction mixture was stirred for 1 h before CH₂Cl₂ was removed by distillation. The resulting residue was dissolved in EtOAc (80 mL) and washed with sat. K₂CO₃ (6 x 80 mL), brine (80 mL), 2N HCl (3 x 80 mL) and brine (80 mL). The organics were concentrated *in vacuo* and the resulting solid was purified by recrystallisation (ethanol and water) to afford *N*-methyl-*N*-(2-phenoxyphenyl)benzamide **6.91** as a white powder (4.33 g, 95 %); m.p. 92-94 °C; ¹H NMR (400 MHz, CDCl₃) δ = 3.43 (3H, bs, NCH₃), 6.68-6.82 (2H, m, ArH), 6.97-7.05 (1H, m, ArH), 7.09 – 7.41 (11H, m, ArH); ¹³C NMR (125 MHz, CDCl₃) δ = 37.6 (CH₃), 118.3 (CH), 119.1 (CH), 123.4 (CH), 124.0 (CH), 127.6 (CH), 128.3 (CH), 128.5 (CH), 129.6 (CH), 129.7 (CH), 129.8 (CH), 135.4 (C), 136.1 (C), 152.6 (C), 155.8 (C), 171.4 (C); IR (ATR) ν = 3094, 3061, 2932, 1634, 1574, 1487, 1368, 1234, 754, 689 cm⁻¹; HRMS *m/z* calcd for C₂₀H₁₇NNaO₂ [M+Na]⁺: 326.1152; found: 326.1158.

NMR Experiment: Treatment of *N*-Methyl-*N*-(2-phenoxyphenyl)benzamide **6.91 with Tf₂O **1.32** in *d*₃-MeCN**



A solution of *N*-methyl-*N*-(2-phenoxyphenyl)benzamide **6.91** (15 mg, 0.05 mmol, 1.0 eq) in *d*₃-MeCN (0.7 mL) was prepared in an inert atmosphere glovebox and was transferred to an NMR tube which was then fitted with a septum and removed from the glovebox. Tf₂O **1.32** (12 μL, 0.07 mmol, 1.4 eq) was injected into the NMR tube and the NMR tube was inverted 3 times. The solution went from being colourless to light red in colour. ¹H NMR analysis (see Appendix F) of the reaction mixture showed the emergence of 2 singlets at 4.08 and 4.13 ppm in a ratio of 1:3, respectively (in *d*₃-MeCN, the starting material has a singlet at 3.30 ppm corresponding to the methyl group). This suggested that two species were present

within the solution and that both species contained a positively charged, methyl-substituted nitrogen (possibly two isomers or two distinct compounds). ^{19}F NMR spectroscopy showed peaks at -71.7, -72.1, -72.4, -73.5, -77.0, -78.3, -79.3 and -79.8 ppm – indicating a complicated mixture of fluorine-containing compounds. The mixture was heated at 80 °C for 1.5 h under argon and then cooled to room temperature. ^1H NMR spectroscopy (at 27 °C) of the mixture then showed the two singlets to shift to 4.55 and 4.59 ppm and change ratio to 1:2, respectively (see Appendix G). By accounting for both signals being methyl signals from two different compounds, 9 aromatic proton signals (overlapping, 6.78 – 7.61 ppm) could be accounted for each compound. ^{19}F NMR (Appendix H) showed a single major peak at -79.4 ppm. The ratio of the two singlets at 4.55 and 4.59 ppm in the ^1H NMR changed to 1:3 when the measurement was recorded at -40 °C, 1.2:3 when recorded at 5 °C and 1.7:3 at 50 °C. When the ^1H NMR was recorded at 27 °C after having varied the temperature, the ratio returned to 1:2 for the two singlets. Mass spectroscopy of the reaction mixture after 80 °C heating; m/z (ESI) 326 (100 %) $[\text{M}+\text{Na}]^+$.

References

- (1) Olah, G. A.; Germain, A.; Lin, H. C.; Forsyth, D. A. *J. Am. Chem. Soc.* **1975**, *97*, 2928-2929.
- (2) Olah, G. A.; Klumpp, D. A. *Superelectrophiles and their Chemistry*; Wiley-Interscience: Hoboken NJ, **2008**.
- (3) Olah, G. A. *Angew. Chem. Int. Ed. Engl.* **1993**, *32*, 767-922.
- (4) Brouwer, D. M.; Kiffen, A. A. *Recl. Trav. Chim. Pays Bas* **1973**, *92*, 689-697.
- (5) Olah, G. A.; Lin, H. C.-H. *J. Am. Chem. Soc.* **1971**, *93*, 1259-1261.
- (6) Olah, G. A.; Klumpp, D. A. *Acc. Chem. Res.* **2004**, *37*, 211-220.
- (7) Klumpp, D. A. *Arkivoc* **2009**, 63-80.
- (8) Pictet, A.; Spengler, T. *Ber. Dtsch. Chem. Ges.* **1911**, *44*, 2030-2036.
- (9) Cox, E.; Cook, J. *Chem. Rev.* **1995**, *95*, 1797-1842.
- (10) Bischler, A.; Napieralski, B. *Ber. Dtsch. Chem. Ges.* **1893**, *26*, 1903-1908.
- (11) Yokoyama, A.; Ohwada, T.; Shudo, K. *J. Org. Chem.* **1999**, *64*, 611-617.
- (12) Nakamura, S.; Sugimoto, H.; Ohwada, T. *J. Org. Chem.* **2008**, *73*, 4219-4224.
- (13) Charette, A. B.; Chua, P. *Tetrahedron Lett.* **1997**, *38*, 8499-8502.
- (14) Charette, A. B.; Grenon, M. *Can. J. Chem.* **2001**, *79*, 1694-1703.
- (15) Charette, A. B.; Chua, P. *Synlett* **1998**, *2*, 163-165.
- (16) Charette, A. B.; Chua, P. *Tetrahedron Lett.* **1998**, *39*, 245-248.
- (17) Charette, A. B.; Chua, P. *J. Org. Chem.* **1998**, *63*, 908-909.
- (18) Charette, A. B.; Grenon, M. *Tetrahedron Lett.* **2000**, *41*, 1677-1680.
- (19) Charette, A. B.; Grenon, M. *J. Org. Chem.* **2003**, *68*, 5792-5794.
- (20) Lemire, A.; Grenon, M.; Pourashraf, M.; Charette, A. B. *Org. Lett.* **2004**, *6*, 3517-3520.
- (21) Lemire, A.; Beaudoin, D.; Grenon, M.; Charette, A. B. *J. Org. Chem.* **2005**, *70*, 2368-2371.
- (22) Charette, A. B.; Mathieu, S.; Martel, J. *Org. Lett.* **2005**, *7*, 5401-5404.
- (23) Barbe, G.; Charette, A. B. *J. Am. Chem. Soc.* **2008**, *130*, 18-19.
- (24) Pelletier, C.; Bechara, W. S.; Charette, A. B. *J. Am. Chem. Soc.* **2010**, *132*,

- 12817-12819.
- (25) Spivey, A. C.; Arseniyadis, S. *Angew. Chem. Int. Ed.* **2004**, *43*, 5436-5441.
- (26) Falmagne, J.-B.; Escudero, J.; Taleb-Sahraoui, S.; Ghosez, L. *Angew. Chem. Int. Ed. Engl.* **1981**, *20*, 878-880.
- (27) Corr, M. J. *Superelectrophiles and their Chemistry, PhD Thesis, Strathclyde University*, **2010**.
- (28) Schmit, C.; Sahraoui-Taleb, S.; Differding, E.; Dehasse-De Lombaert, C. G.; Ghosez, L. *Tetrahedron Lett.* **1984**, *25*, 5043-5046.
- (29) Thomas, E. W. *Synthesis* **1993**, 767-768.
- (30) Banwell, M. G.; Bissett, B. D.; Busato, S.; Cowden, C. J.; Hockless, D. C. R.; Holman, J. W.; Read, R. W.; Wu, A. W. *J. Chem. Soc., Chem. Commun.* **1995**, 2551-2553.
- (31) Movassaghi, M.; Hill, M. D. *J. Am. Chem. Soc.* **2006**, *128*, 4592-4593.
- (32) Movassaghi, M.; Hill, M. D. *J. Am. Chem. Soc.* **2006**, *128*, 14254-14255.
- (33) Movassaghi, M.; Hill, M. D.; Ahmad, O. K. *J. Am. Chem. Soc.* **2007**, *129*, 10096-10097.
- (34) Movassaghi, M.; Hill, M. D. *Org. Lett.* **2008**, *10*, 3485-3488.
- (35) Ahmad, O. K.; Hill, M. D.; Movassaghi, M. *J. Org. Chem.* **2009**, *74*, 8460-8463.
- (36) Medeley, J. W.; Movassaghi, M. *J. Org. Chem.* **2009**, *74*, 1341-1344.
- (37) Curphey, T. J. *J. Am. Chem. Soc.* **1965**, *87*, 2063-2064.
- (38) Curphey, T. J.; Prasad, K. S. *J. Org. Chem.* **1972**, *37*, 2259-2266.
- (39) Boon, W. R. *Chem. Ind.* **1965**, 782-788.
- (40) Black, A. L.; Summers, L. A. *J. Chem. Soc. C: Org.* **1969**, 610-611.
- (41) Campbell, E. C.; Glover, E. E.; Trenholm, G. *J. Chem. Soc. C: Org.* **1969**, 1987-1990.
- (42) Dickeson, J. E.; Eckhard, I. F.; Fielden, R.; Summers, L. A. *J. Chem. Soc., Perkin Trans. I* **1973**, 2885-2887.
- (43) Summers, L. A.; Dickeson, J. E. *Chem. Commun.* **1967**, 1183-1183.
- (44) Katritzky, A. R.; Lewis, J.; Nie, P.-L. *J. Chem. Soc., Perkin Trans. I* **1979**, 442-445.
- (45) Weiss, R.; Roth, R. *Synthesis* **1987**, 870-872.
- (46) Weiss, R.; Reichel, S.; Handke, M.; Hampel, F. *Angew. Chem. Int. Ed.* **1998**,

- 37, 344-347.
- (47) Conejero, S.; Canac, Y.; Tham, F. S.; Bertrand, G. *Angew. Chem. Int. Ed.* **2004**, *43*, 4089-4093.
- (48) Thauer, R. K.; Kaster, A.-K.; Goenrich, M.; Schick, M.; Hiromoto, T.; Shima, S. *Annu. Rev. Biochem.* **2010**, *79*, 507-536.
- (49) Zirngibl, C.; Hedderich, R.; Thauer, R. K. *FEBS Lett.* **1990**, *261*, 112-116.
- (50) Zirngibl, C.; Van Dongen, W.; Schwörer, B.; Von Büнау, R.; Richter, M.; Klein, A.; Thauer, R. K. *Eur. J. Biochem.* **1992**, *208*, 511-520.
- (51) Afting, C.; Hochheimer, A.; Thauer, R. K. *Arch. Microbiol.* **1998**, *169*, 206-210.
- (52) Schwörer, B.; Fernandez, V. M.; Zirngibl, C.; Thauer, R. K. *Eur. J. Biochem.* **1993**, *212*, 255-261.
- (53) Schleucher, J.; Griesinger, C.; Schwörer, B.; Thauer, R. K. *Biochemistry*, **1994**, *33*, 3986-3993.
- (54) Hartmann, G. C.; Santamaria, E.; Fernandez, V. M.; Thauer, R. K. *J. Biol. Inorg. Chem.* **1996**, *1*, 446-450.
- (55) Vogt, S.; Lyon, E. J.; Shima, S.; Thauer, R. K. *J. Biol. Inorg. Chem.* **2008**, *13*, 97-106.
- (56) Buurman, G.; Shima, S.; Thauer, R. K. *FEBS Lett.* **2000**, *485*, 200-204.
- (57) Lyon, E. J.; Shima, S.; Buurman, G.; Chowdhuri, S.; Batschauer, A.; Steinback, K.; Thauer, R. K. *Eur. J. Biochem.* **2004**, *271*, 195-204.
- (58) Lyon, E. J.; Shima, S.; Böcher, R.; Thauer, R. K.; Grevels, F.-W.; Bill, E.; Roseboom, W.; Albracht, S. P. J. *J. Am. Chem. Soc.* **2004**, *126*, 14239-14248.
- (59) Shima, S.; Lyon, E. J.; Sordel-Klippert, M.; Kauß, M.; Kahnt, J.; Thauer, R. K.; Steinbach, K.; Xie, X.; Verier, L.; Griesing, C. *Angew. Chem. Int. Ed.* **2004**, *43*, 2547-2551.
- (60) Shima, S.; Lyon, E. J.; Thauer, R. K.; Mienert, B.; Bill, E. *J. Am. Chem. Soc.* **2005**, *127*, 10430 -10435.
- (61) Pilak, O.; Mamat, B.; Vogt, S.; Hayemeier, C. H.; Thauer, R. K.; Shima, S.; Vonrhein, C.; Warkentin, E.; Ermler, U. *J. Mol. Biol.* **2006**, *358*, 798-809.
- (62) Shima, S.; Pilak, O.; Vogt, S.; Schick, M.; Stagni, M. S.; Meyer-Klauche, W.; Warkentin, E.; Thauer, R. K.; Ermler, U. *Science* **2008**, *321*, 572-575.
- (63) Humphrey, W.; Dalke, A.; Schulten, K. *J. Molec. Graphics* **1996**, *14*, 33-38.

- (64) Buncel, E.; Menon, B. *J. Am. Chem. Soc.* **1977**, *99*, 4457-4461.
- (65) Hiromoto, T.; Ataka, K.; Pilak, O.; Vogt, S.; Stagni, M. S.; Meyer-Klache, W.; Wakentin, E.; Thauer, R. K.; Shima, S.; Ermler, U. *FEBS Lett.* **2009**, *583*, 585-590.
- (66) Shima, S.; Schick, M.; Kahnt, J.; Ataka, K.; Steinback, K.; Linne, U.; *Dalton Trans.* **2012**, *41*, 767-771.
- (67) Schick, M.; Xie, X.; Ataka, K.; Kahnt, J.; Linne, U.; Shima, S. *J. Am. Chem. Soc.* **2012**, *134*, 3271-3280.
- (68) Hiromoto, T.; Warkentin, E.; Moll, J.; Ermler, U.; Shima, S. *Angew. Chem. Int. Ed.* **2009**, *48*, 6457-6460.
- (69) Bartoschek, S.; Buurman, G.; Thauer, R. K.; Geierstanger, B. H.; Weyrauch, J. P.; Griesinger, C.; Nilges, M.; Hutter, M. C.; Helms, V. *ChemBioChem* **2001**, *2*, 530-541.
- (70) Bartoschek, S.; Buurman, G.; Geierstanger, B. H.; Lapham, J.; Griesinger, C. *J. Am. Chem. Soc.* **2003**, *125*, 13308-13309.
- (71) Berkessel, A.; Thauer, R. K. *Angew. Chem. Int. Ed. Engl.* **1995**, *34*, 2247-2250.
- (72) Corr, M. J.; Gibson, K. F.; Kennedy, A. R.; Murphy, J. A. *J. Am. Chem. Soc.* **2009**, *131*, 9174-9175.
- (73) Corr, M. J.; Roydhouse, M. D.; Gibson, K. F.; Zhou, S.-z.; Kennedy, A. R.; Murphy, J. A. *J. Am. Chem. Soc.* **2009**, *131*, 17980-17985.
- (74) Yang, X.; Hall, M. B. *J. Am. Chem. Soc.* **2008**, *130*, 14036-14037.
- (75) Nakatani, N.; Nakao, Y.; Sato, H.; Sakaki, S. *Chem. Lett.* **2009**, *38*, 958-959.
- (76) Yang, X.; Hall, M. B. *J. Am. Chem. Soc.* **2009**, *131*, 10901-10908.
- (77) Dey, A. *J. Am. Chem. Soc.* **2010**, *132*, 13892-13901.
- (78) Shima, S.; Vogt, S.; Göbels, A.; Bill, E. *Angew. Chem. Int. Ed.* **2010**, *49*, 9917-9921.
- (79) Royer, A. M.; Rauchfuss, T. B.; Wilson, S. R. *Inorg. Chem.* **2008**, *47*, 395-397.
- (80) Sadique, A. R.; Brennessel, W. W.; Holland, P. L. *Inorg. Chem.* **2008**, *47*, 784-786.
- (81) Melarejo, D. Y.; Chiarella, G. M.; Koch, S. A. *234th ACS National Meeting, Boston, MA, August 19-23 2007*, Meeting Abstracts;

- <http://oasys2.confex.com/acs/234nm/techprogram/P1116341.HTM> (accessed 20 October 2013).
- (82) Guo, Y.; Wang, H.; Xiao, Y.; Vogt, S.; Thauer, R. K.; Shima, S.; Volkers, P. I.; Rauchfuss, T. B.; Pelmenchikov, V.; Case, D. A.; Alp, E. E.; Sturhahn, W.; Yoda, Y.; Cramer, S. *Inorg. Chem.* **2008**, *47*, 3969-3977.
- (83) Salomone-Stagni, M.; Stellato, F.; Whaley, C. M.; Vogt, S.; Morante, S.; Shima, S.; Rauchfuss, T. B.; Meyer-Klaucke, W. *Dalton Trans.* **2010**, *39*, 3057-3064.
- (84) Wang, X.; Li, Z.; Zeng, X.; Luo, Q.; Evans, D. J.; Pickett, C. J.; Liu, X. *Chem. Commun.* **2008**, *44*, 3555-3557.
- (85) Obrist, B. V.; Chen, D.; Ahrus, A.; Schünemann, V.; Scopelliti, R.; Hu, X. *Inorg. Chem.* **2009**, *48*, 3514-3516.
- (86) Li, B.; Liu, T.; Popescu, C. V.; Bilko, A.; Darensbourg, M. Y. *Inorg. Chem.* **2009**, *48*, 11283-11289.
- (87) Halder, P.; Dey, A.; Paine, T. K. *Inorg. Chem.* **2009**, *48*, 11501-11503.
- (88) Halder, P.; Paine, T. K. *Inorg. Chem.* **2011**, *50*, 708-710.
- (89) Liu, T.; Li, B.; Popescu, C. V.; Bilko, A.; Pérez, L. M.; Hall, M. B.; Darensbourg, M. Y. *Chem. Eur. J.* **2010**, *16*, 3083-3089.
- (90) Tanino, S.; Ohki, Y.; Tatsumi, K. *Chem. Asian J.* **2010**, *5*, 1962-1964.
- (91) Chen, D.; Scopelliti, R.; Hu, X. *J. Am. Chem. Soc.* **2010**, *132*, 928-929.
- (92) Turrell, P. J.; Wright, J. A.; Peck, J. N. T.; Oganessian, V. S.; Pickett, C. J. *Angew. Chem. Int. Ed.* **2010**, *49*, 7508-7511.
- (93) Chen, D.; Scopelliti, R.; Hu, X. *Angew. Chem. Int. Ed.* **2010**, *49*, 7512-7515.
- (94) Royer, A. M.; Rauchfuss, T. B.; Gray, D. L. *Organometallics* **2009**, *28*, 3618-3620.
- (95) Royer, A. M.; Salomone-Stagni, M.; Rauchfuss, T. B.; Meyer-Klaucke, W. *J. Am. Chem. Soc.* **2010**, *132*, 16997-17003.
- (96) Chen, D.; Scopelliti, R.; Hu, X. *Angew. Chem. Int. Ed.* **2011**, *50*, 5671-5673.
- (97) Chen, D.; Scopelliti, R.; Hu, X. *Angew. Chem. Int. Ed.* **2012**, *51*, 1919-1921.
- (98) Chen, D.; Ahrens-Botzong, A.; Schünemann, V.; Scopelliti, R.; Hu, X. *Inorg. Chem.* **2011**, *50*, 5249-5257.
- (99) Hu, B.; Chen, D.; Hu, X. *Chem. Eur. J.* **2013**, *19*, 6221-6224.
- (100) Song, L.-C.; Xie, Z.-J.; Wang, M.-M.; Zhao, G.-Y.; Song, H.-B. *Inorg.*

- Chem.* **2012**, *51*, 7466-7468.
- (101) Hu, B.; Chen, D.; Hu, X. *Chem. Eur. J.* **2014**, *20*, 1677-1682.
- (102) Murphy, J. A.; Garnier, J.; Park, S. R.; Schoenebeck, F.; Zhou, S.-z.; Turner, A. T. *Org. Lett.* **2008**, *10*, 1227-1230.
- (103) Cutulic, S. P. Y.; Findlay, N. J.; Zhou, S.-Z.; Chrystal, E. J. T.; Murphy, J. A. *J. Org. Chem.* **2009**, *74*, 8713-8718.
- (104) Cutulic, S. P. Y.; Murphy, J. A.; Farwaha, H.; Zhou, S.-Z.; Chrystal, E. *Synlett* **2008**, *2008*, 2132-2136.
- (105) Zhou, S.-Z. *Unpublished Work* **2006**, *University of Strathclyde*.
- (106) Tschitschibabin, A. E.; Konowalowa, R. A. *Ber. Dtsch. Chem. Ges.* **1926**, *59*, 2055-2058.
- (107) Frampton, R.; Johnson, C. D.; Katritzky, A. R. *Liebigs Ann. Chem.* **1971**, *749*, 12-15.
- (108) Barbieri, G.; Benassi, R.; Grandi, R.; Pagoni, U. M.; Ferdinando, T. *Org. Mag. Res.* **1979**, *12*, 159-162.
- (109) Dolci, L.; Dollé, F.; Jubeau, S.; Vaufrey, F. J. *Labelled Cpd. Radiopharm.* **1999**, *42*, 975-985.
- (110) Karramkam, M.; Hinnen, F.; Vaufrey, F.; Dollé, F. J. *Labelled Cpd. Radiopharm.* **2003**, *46*, 979-992.
- (111) Godin, R. P. *Thoughts on Iminium Triflate Work, Student Exchange Report, University of Strathclyde*, **2009**.
- (112) Williams, D. H.; Fleming, I. *Spectroscopic Methods in Organic Chemistry*; 6th ed.; McGraw-Hill International Ltd.: Maidenhead, **2007**.
- (113) Sanger, F. *Biochem. J.* **1945**, *39*, 507-515.
- (114) Kitagawa, T.; Ito, J.; Tsutsui, C. *Chem. Pharm. Bull.* **1994**, *42*, 1931-1934.
- (115) Pelletier, G.; Charette, A. B. *Org. Lett.* **2013**, *15*, 2290-2293.
- (116) Kovacevic, L. S.; Idziak, C.; Markevicius, A.; Scullion, C.; Corr, M. J.; Kennedy, A. R.; Tuttle, T.; Murphy, J. A. *Angew. Chem. Int Ed.* **2012**, *51*, 8516-8519.
- (117) Smith, R. J.; Pagni, R. M. *J. Org. Chem.* **1981**, *46*, 4307-4309.
- (118) Kwong, F. Y.; Klapars, A.; Buchwald, S. L. *Org. Lett.* **2002**, *4*, 581-584.
- (119) Kadereit, D.; Deck, P.; Heinemann, I.; Waldmann, H. *Chem. Eur J.* **2001**, *7*, 1184-1193.

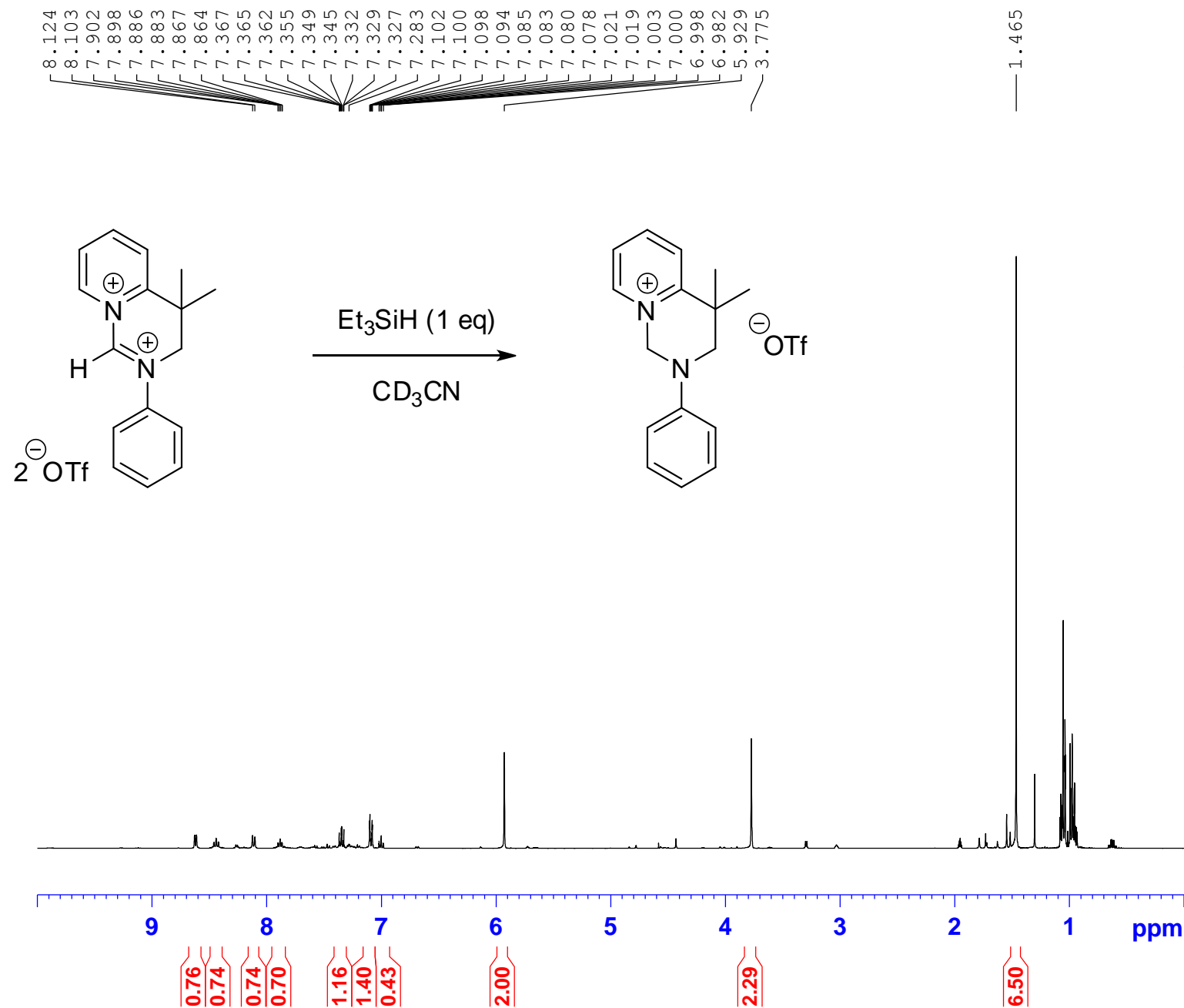
- (120) Nakazawa, H.; Itazak, M. *Top. Organomet. Chem.* **2011**, *33*, 27-81.
- (121) Casey, C. P.; Guan, H. *J. Am. Chem. Soc.* **2007**, *129*, 5816-5817
- (122) Casey, C. P.; Guan, H. *J. Am. Chem. Soc.* **2009**, *131*, 2499-2507.
- (123) Albert, A.; Phillips, J. N. *J. Chem. Soc.* **1956**, 1294-1304.
- (124) Tomon, T.; Koizumi, T.-a.; Tanaka, K. *Eur. J. Inorg. Chem.* **2005**, 285-293.
- (125) Bullock, R. M.; Samsel, E. G. *J. Am. Chem. Soc.* **1990**, *112*, 6886-6889.
- (126) Felton, G. A. N.; Vannucci, A. K.; Okumura, N.; Lockett, L. T.; Evans, D. H.; Glass, R. S.; Lichtenberger, D. L. *Organometallics* **2008**, *27*, 4671-4679.
- (127) Lavallo, V.; Canac, Y.; Donnadiou, B.; Schoeller, W. W.; Bertrand, G. *Angew. Chem. Int. Ed.* **2006**, *45*, 3488-3491.
- (128) Frey, G. D.; Lavallo, V.; Donnadiou, B.; Schoeller, W. W.; Bertrand, G. *Science* **2007**, *316*, 439-441.
- (129) Masuda, J. D.; Schoeller, W. W.; Donnadiou, B.; Bertrand, G. *J. Am. Chem. Soc.* **2007**, *129*, 14180-14181.
- (130) Masuda, J. D.; Schoeller, W. W.; Donnadiou, B.; Bertrand, G. *Angew. Chem. Int. Ed.* **2007**, *46*, 7052-7055.
- (131) Fujiwara, H.; Takagi, T.; Yamazaki, Y.; Sasaki, Y. *J. Chem. Soc., Faraday Trans. 1* **1982**, *78*, 347-356.
- (132) Liu, C.; Yang W. *Chem. Commun.* **2009**, 6267-6269.
- (133) Bissember, A. C., Banwell, M. G. *J. Org. Chem.* **2009**, *74*, 4893-4895.
- (134) Corcoran, R. C.; Bang, S. H. *Tetrahedron Lett.* **1990**, *31*, 6757-6758.
- (135) Alder, R. W.; Bowman, P. S.; Steele, W. R. S.; Winterman, D. R. *Chem. Commun.* **1968**, 723-724.
- (136) Gokel, G. W. *Dean's Handbook of Organic Chemistry*; 2nd Ed; McGraw-Hill Companies, Inc.: New York, NY, **2004**.
- (137) Raamat, E.; Kaupmees, K.; Ovsjannikov, G.; Trummal, A.; Kütt, A.; Saame, J.; Koppel, I.; Kaljurand, I.; Lipping, L.; Rodima, T.; Pihl, V.; Koppel, I. A.; Leito, I. *J. Phys. Org. Chem.* **2013**, *26*, 162-170.
- (138) Kovacevic, L. S. *PhD Thesis (Draft), Strathclyde University*, **2013**.
- (139) Brahmachari, G.; Laskar, S. *Tetrahedron Lett.*, **2010**, *51*, 2319-2322.
- (140) Beard, C. D.; Baum, K.; Grakauskas, V. *J. Org. Chem.* **1973**, *38*, 3673-3677.
- (141) Subramanian, L. R.; Hanack, M.; Chang, L. W. K.; Imhoff, M. A.; von Ragué Schleyer, P.; Effenberger, F.; Kurtz, W.; Stang, P. J.; Dueber, T. E. *J.*

- Org. Chem.* **1976**, *41*, 4099-4103.
- (142) Nagarajan, K.; Talwalker, P. K.; Kulkarni, C. L.; Shah, R. K.; Shenoy, S. J.; Prabhu, S. S. *Ind. J. Chem., Sect. B: Org. Chem. Inc Med. Chem.* **1985**, *24*, 83-97.
- (143) Das, S.; Addis, D.; Zhou, S.; Junge, K.; Beller, M. *J. Am. Chem. Soc.* **2010**, *132*, 1770-1771.
- (144) Lai, R.-Y.; Lee, C.-I.; Liu, S.-T. *Tetrahedron* **2008**, *64*, 1213-1217.
- (145) Kouznetsov, V. V.; Mendez, L. Y. V.; Sortino, M.; Vasquez, Y.; Gupta, M. P.; Freile, M.; Enriz, R. D.; Zacchino, S. A. *Bioorg. Med. Chem.* **2008**, *16*, 794-809.
- (146) Stenberg, V. I.; Singh, S. P.; Narain, N. K.; Parmar, S. S. *J. Org. Chem.* **1977**, *42*, 171-171.
- (147) Endo, T.; Saeki, S.; Hamana, M. *Chem. Pharm. Bull.* **1981**, *29*, 3105-3111.
- (148) Sanderson, P. E.; Lyle, T. A.; Dorsey, B. D.; Varsolona, R. J. (Merck & Co., Inc.), *US Pat.*, 5866573, **1999**.
- (149) Gilbert, J. C.; Giamalva, D. H. *J. Org. Chem.* **1985**, *50*, 2586-2587.
- (150) Amato, B. A.; Benkovic, S. J. *Biochemistry* **1975**, *14*, 4877-4887.
- (151) Banik, G. M.; Silverman, R. B. *J. Am. Chem. Soc.* **1990**, *112*, 4499-4507.
- (152) Vandromme, L.; Reißig, H.-R.; Gröper, S.; Rabe, J. P. *Eur. J. Org. Chem.* **2008**, *12*, 2049-2055.
- (153) Fu, R.; Bercaw, J. E.; Labinger, J. A. *Organometallics* **2011**, *30*, 6751-6765.
- (154) Taylor, S. L.; Lee, D. Y.; Martin, J. C. *J. Org. Chem.* **1983**, *48*, 4156-4158.
- (155) Seipe, I. B.; Su, S.; Rodriguez, R. A.; Giantassio, R.; Fujiwara, Y.; Sobel, A. L.; Baran, P. S. *J. Am. Chem. Soc.* **2010**, *132*, 13194-13196.
- (156) Vistorobskii, N. V.; Pozharskii, A. F. *Zh. Org. Khim.* **1989**, *25*, 2154-2161.
- (157) Liégault, B.; Petrov, I.; Gorelsky, S. I.; Fagnou, K. *J. Org. Chem.* **2010**, *75*, 1047-1060.
- (158) Haquette, P.; Dagorne, S.; Welter, R.; Jaouen, G. *J. Organomet. Chem.* **2003**, *682*, 240-247.
- (159) Jiao, J.; Zhang, X.-R.; Chang, N.-H.; Wang, J.; Wei, J.-F.; Shi, X.-Y.; Chen, Z.-G. *J. Org. Chem.* **2011**, *76*, 1180-1183.
- (160) Klapars, A.; Huang, X.; Buchwald, S. L. *J. Am. Chem. Soc.* **2002**, *124*, 7421-7428.

- (161) Aujard, I.; Roeme, D.; Arzel, E.; Johansson, M.; de Vos, D.; Sterner, O. *Bioorg. Med. Chem.* **2005**, *13*, 6145-6150.
- (162) Cacchi, S.; Lupi, A. *Tetrahedron Lett.* **1992**, *33*, 3939-3942.
- (163) Li, C.-S.; Soucy-Breau, C.; Ouimet, N. *Synthesis* **1995**, *11*, 1355-1356.
- (164) Sutter, C. M. *J. Am. Chem. Soc.* **1929**, *51*, 2581-2585.
- (165) Okubo, T, Yoshikawa, R, Chaki, S, Okuyama, S, Nakazato, A. *Bioorg. Mec. Chem.* **2004**, *12*, 423-438.
- (166) von Braun, J.; Weissbach, *Ber. Dtsch. Chem. Ges.* **1932**, *65*, 1574-1579.

Treatment of Disalt **5.1** with 1 eq Et₃SiH

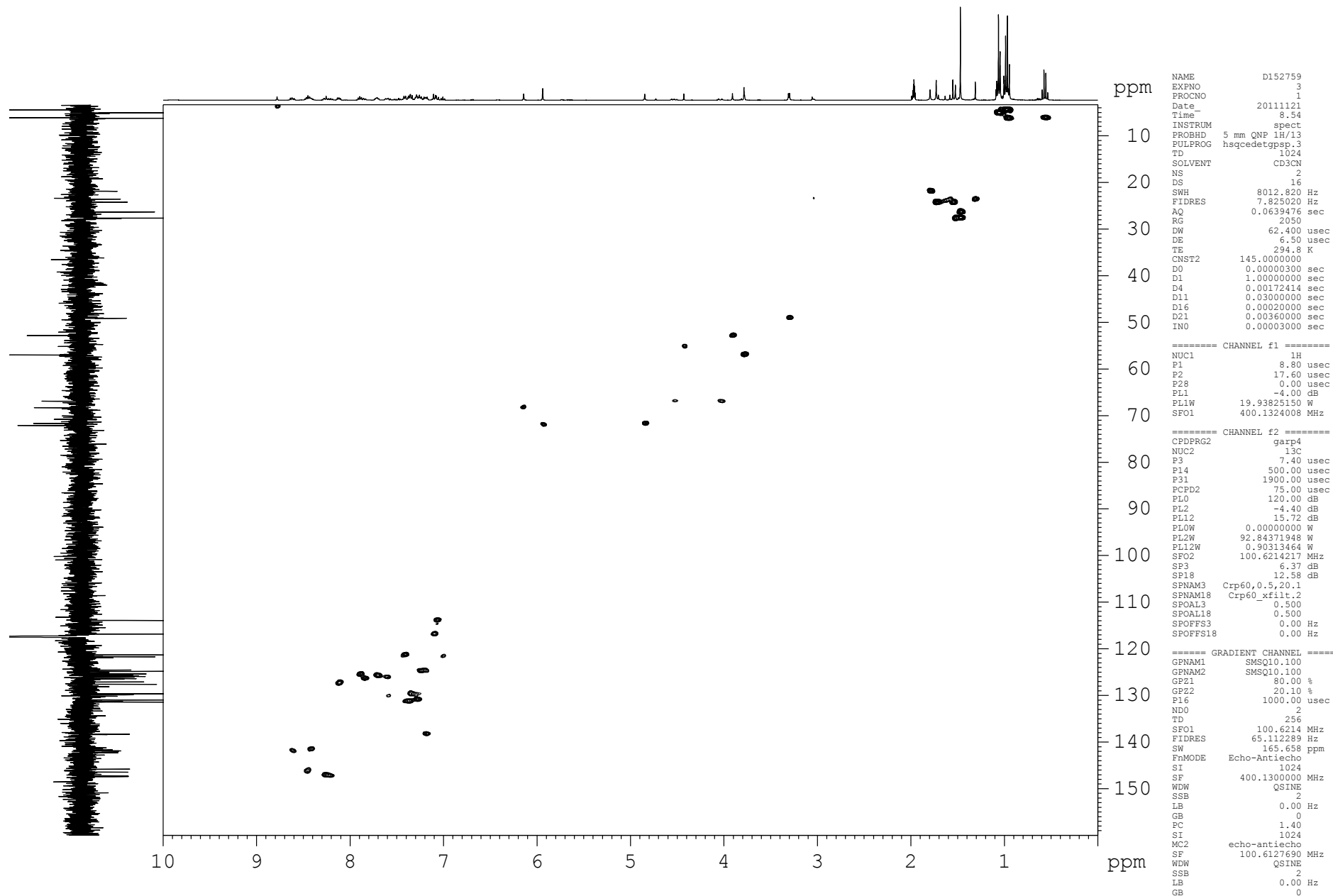
Appendix A

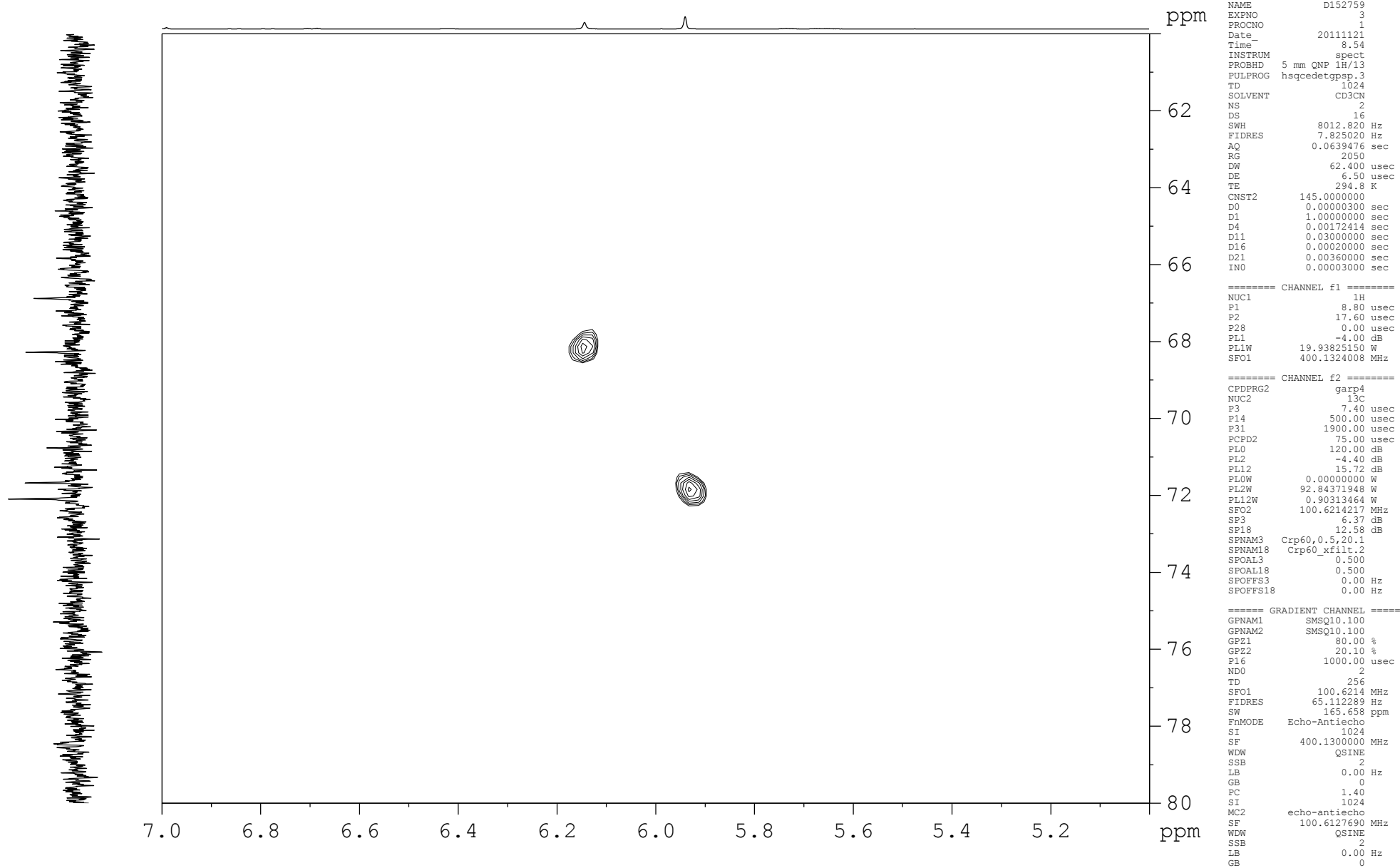


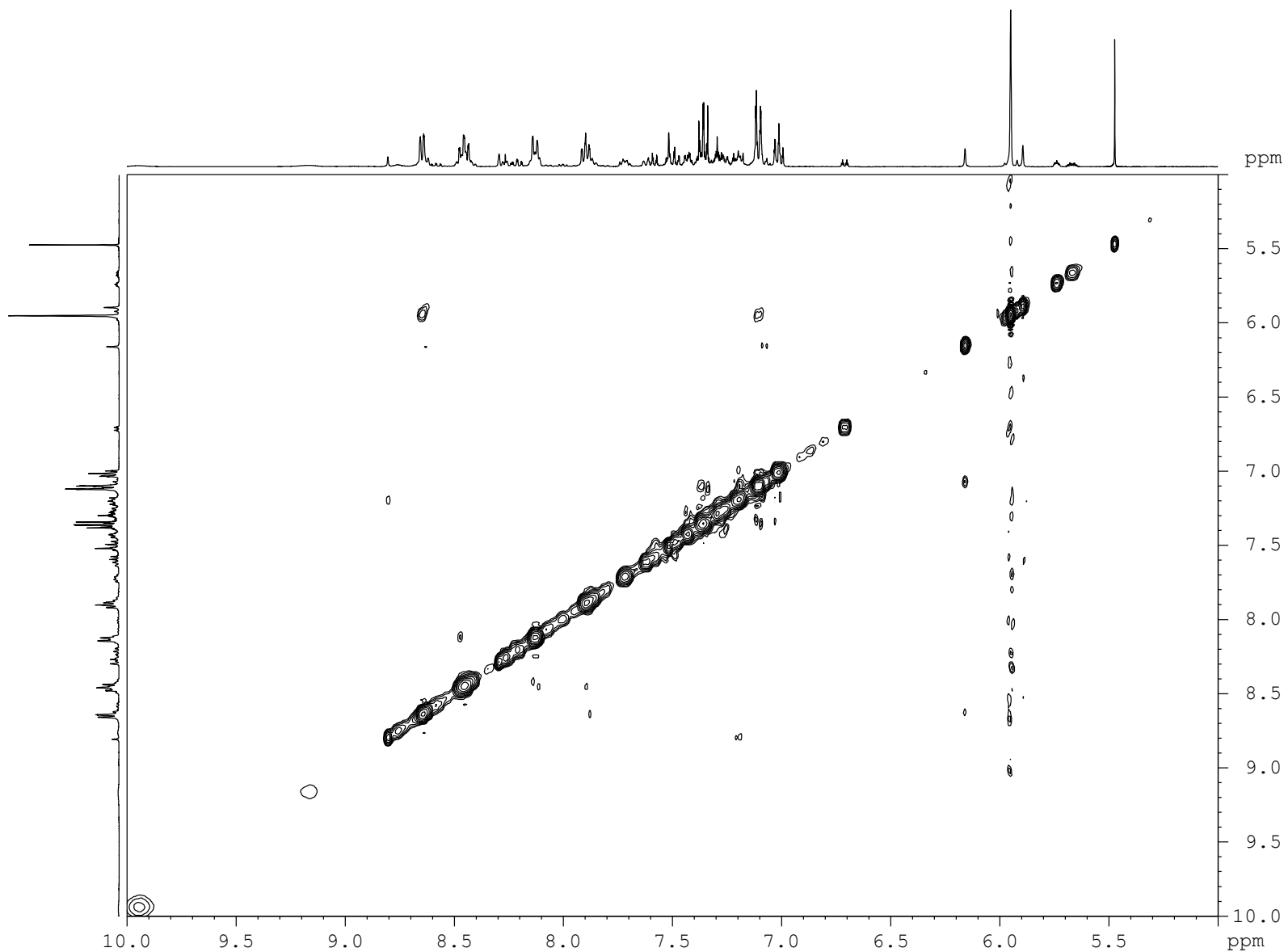
```

NAME          B20498
EXPNO         8
PROCNO        1
Date_         20120416
Time_         10.05
INSTRUM       AV400
PROBHD        5 mm PABBO BB-
PULPROG       zg k
TD            32000
SOLVENT       CD3CN
NS            4
DS            2
SWH           8012.820 Hz
FIDRES        0.250401 Hz
AQ            1.9968500 sec
RG            114
DW            62.400 usec
DE            6.00 usec
TE            300.0 K
D1            2.00000000 sec
D20           0.50000000 sec
TD0           1

===== CHANNEL f1 =====
NUC1          1H
P1            12.00 usec
PL1           -2.50 dB
PL1W         12.77515030 W
SFO1         400.0324002 MHz
SI           32768
SF           400.0300028 MHz
WDW          EM
SSB          0
LB           0.30 Hz
GB           0
PC           1.00
    
```





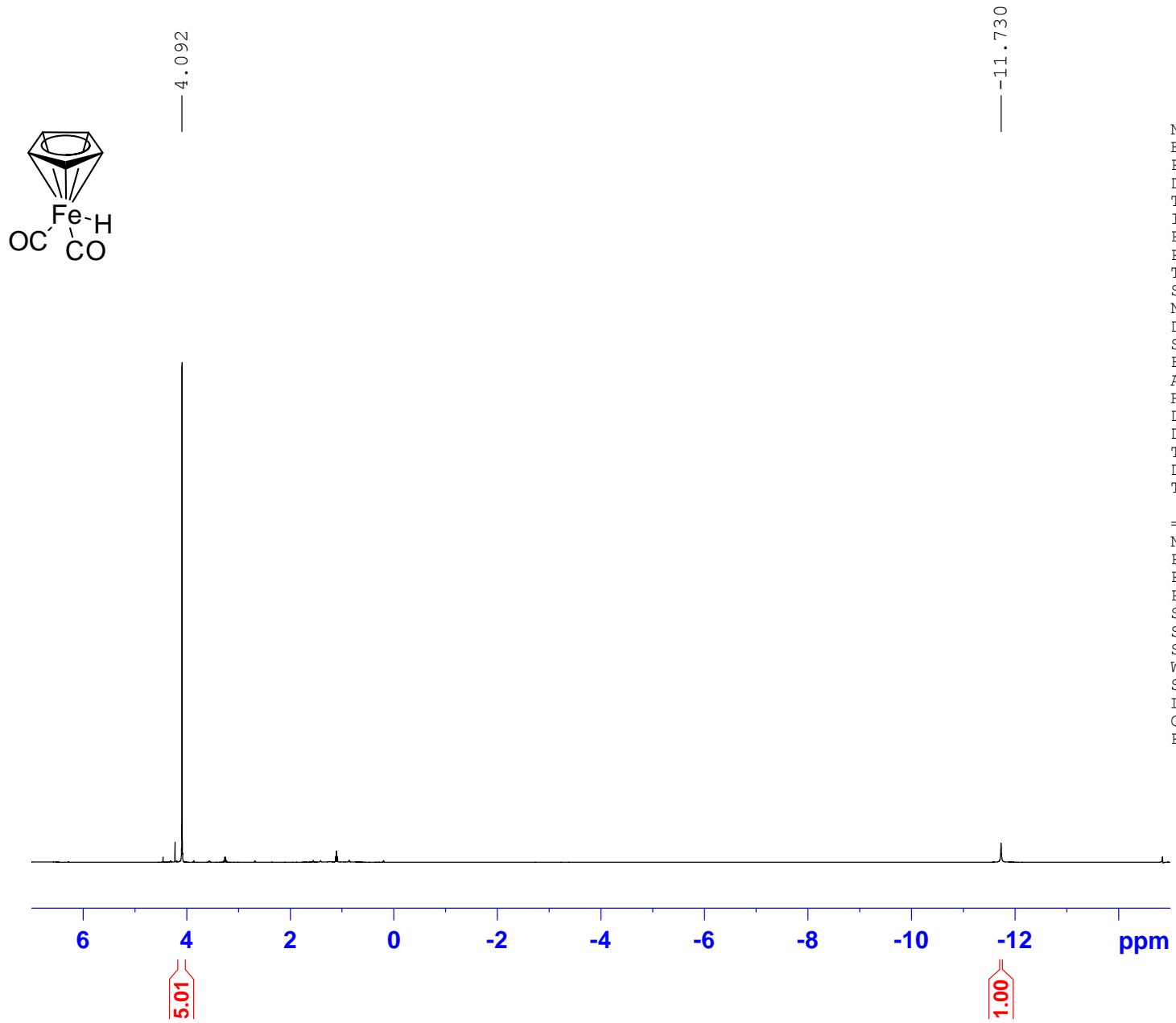


```

NAME          D155034
EXPNO         2
PROCNO        1
Date_         20120124
Time_         15.10
INSTRUM       spect
PROBHD        5 mm QNP 1H/13
PULPROG       noesygpph
TD            2048
SOLVENT       CD3CN
NS            2
DS            8
SWH           6097.561 Hz
FIDRES        2.977325 Hz
AQ            0.1679860 sec
RG            50.8
DW            82.000 usec
DE            20.62 usec
TE            300.0 K
D0            0.00007003 sec
D1            1.54560196 sec
D8            0.50000000 sec
D16           0.00020000 sec
IN0           0.00016400 sec

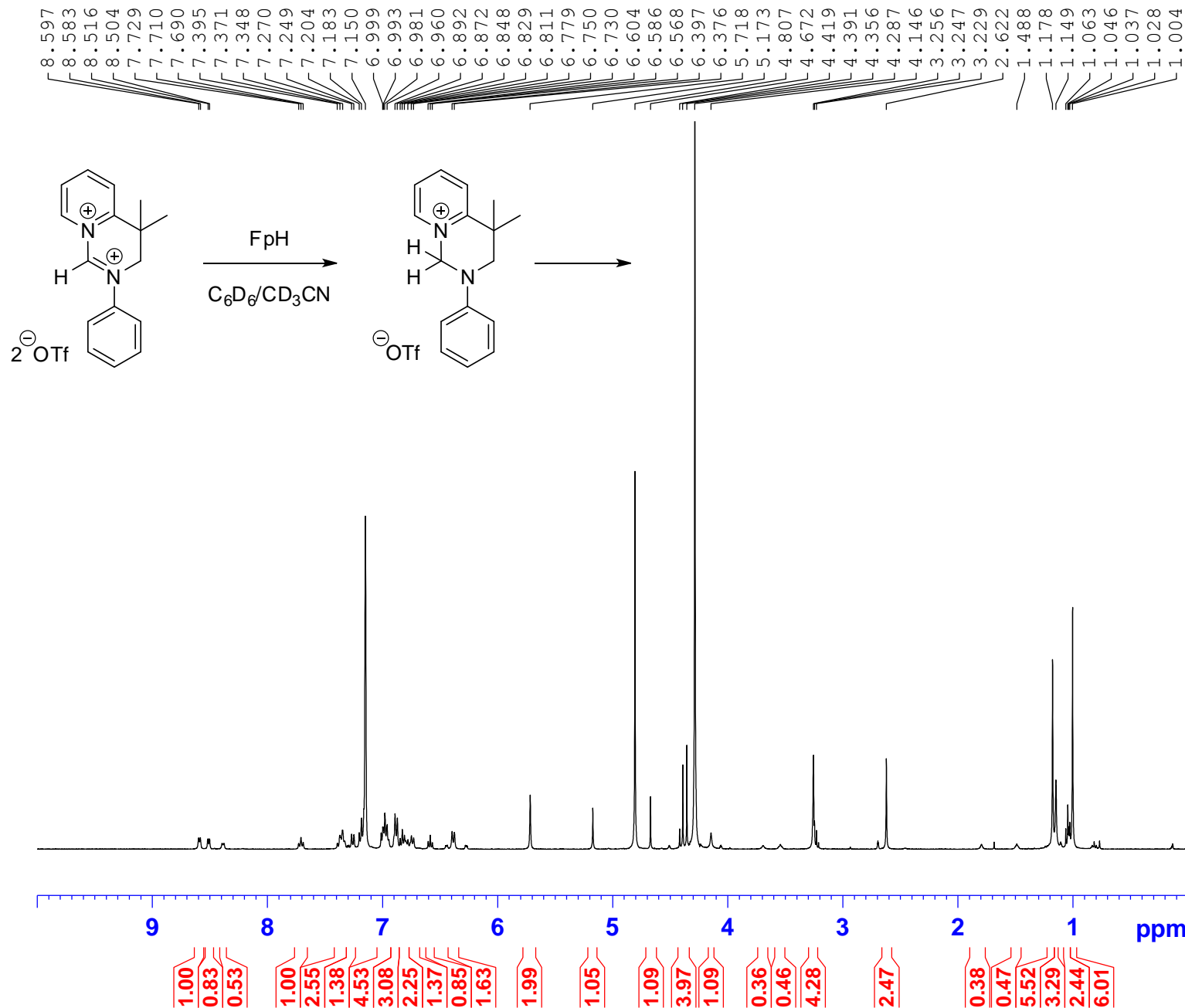
===== CHANNEL f1 =====
NUC1           1H
P1             9.40 usec
P2             18.80 usec
PL1            -4.00 dB
PL1W           19.93825150 w
SFO1           400.1329267 MHz

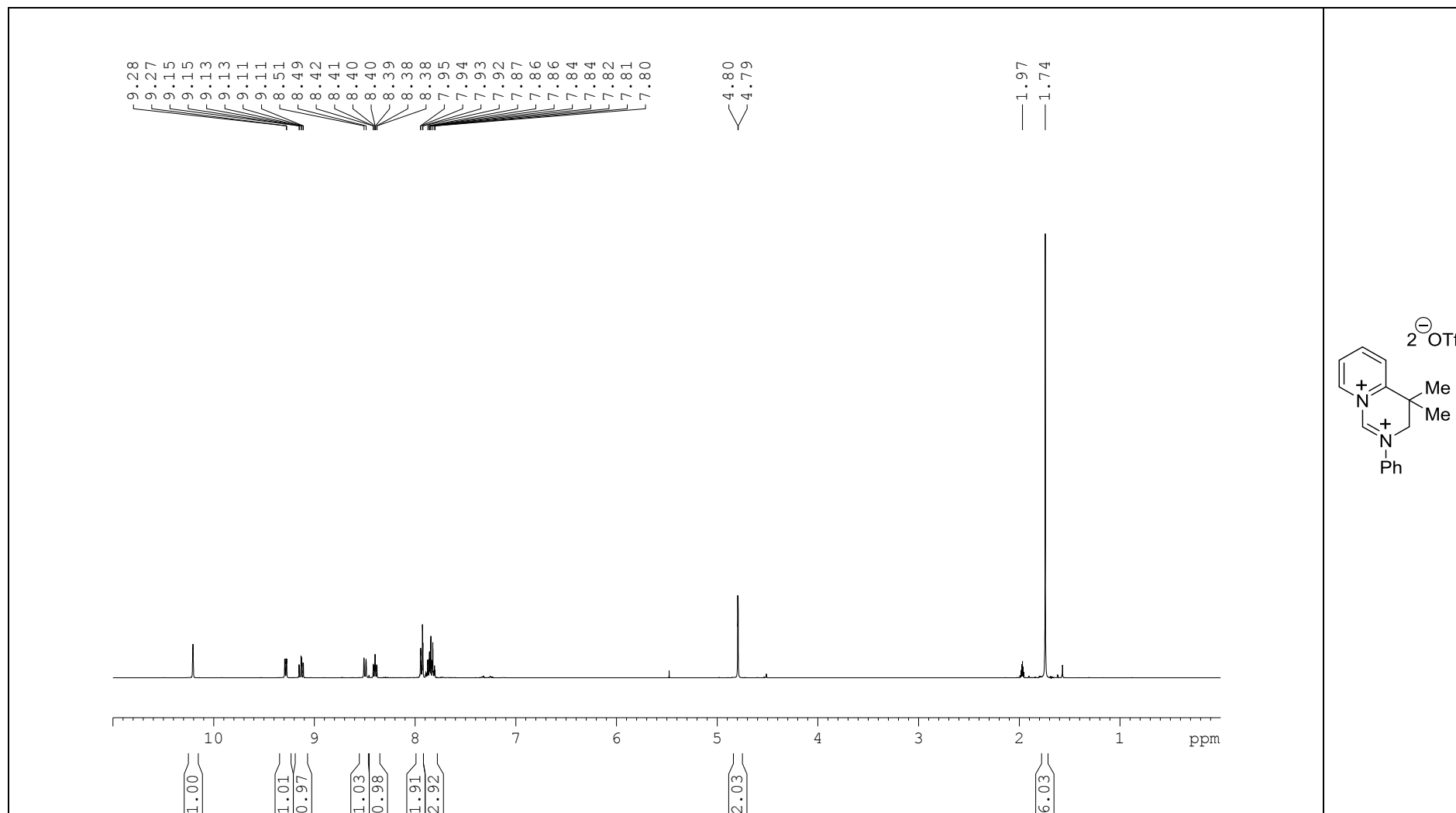
===== GRADIENT CHANNEL =====
GPNAM1        SINE.100
GPZ1           40.00 %
P16           1000.00 usec
ND0            1
TD             256
SFO1           400.1329 MHz
FIDRES         23.818598 Hz
SW             15.239 ppm
FnMODE        States-TPPI
SI             2048
SF             400.1300000 MHz
WDW            QSINE
SSB            2
LB             0.00 Hz
GB             0
PC             1.00
SI             1024
MC2           States-TPPI
SF             400.1300000 MHz
WDW            QSINE
SSB            2
LB             0.00 Hz
GB             0
    
```



```
NAME          D160658
EXPNO         1
PROCNO        1
Date_         20120503
Time_         13.16
INSTRUM       spect
PROBHD        5 mm QNP 1H/13
PULPROG       zg30
TD            32564
SOLVENT       C6D6
NS            16
DS            2
SWH           8802.817 Hz
FIDRES        0.270324 Hz
AQ            1.8496852 sec
RG            228
DW            56.800 usec
DE            6.50 usec
TE            300.0 K
D1            2.00000000 sec
TD0           1

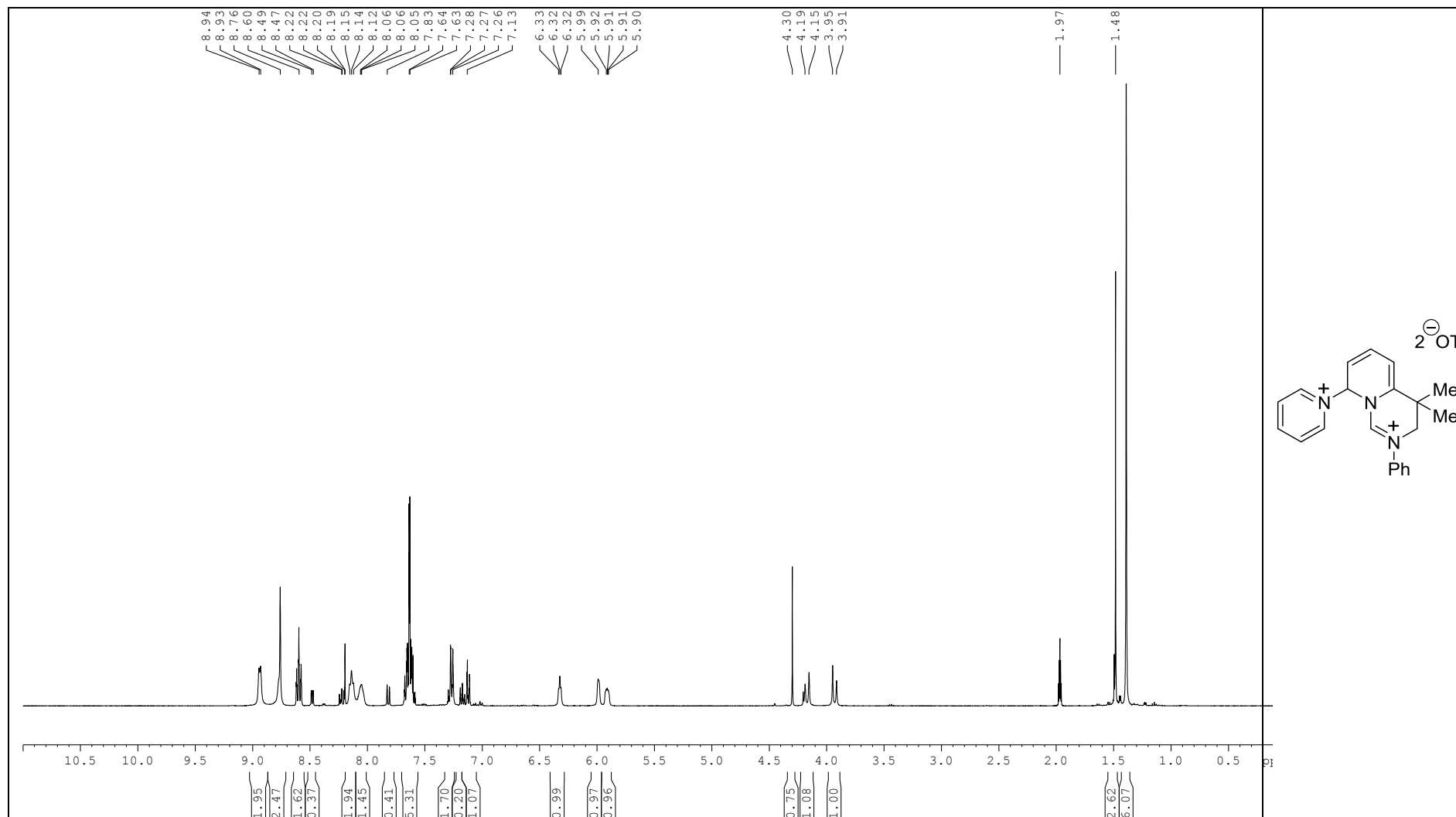
===== CHANNEL f1 =====
NUC1          1H
P1            9.40 usec
PL1           -4.00 dB
PL1W          19.93825150 W
SF01          400.1283995 MHz
SI            32768
SF            400.1300000 MHz
WDW           EM
SSB           0
LB            0.30 Hz
GB            0
PC            1.00
```

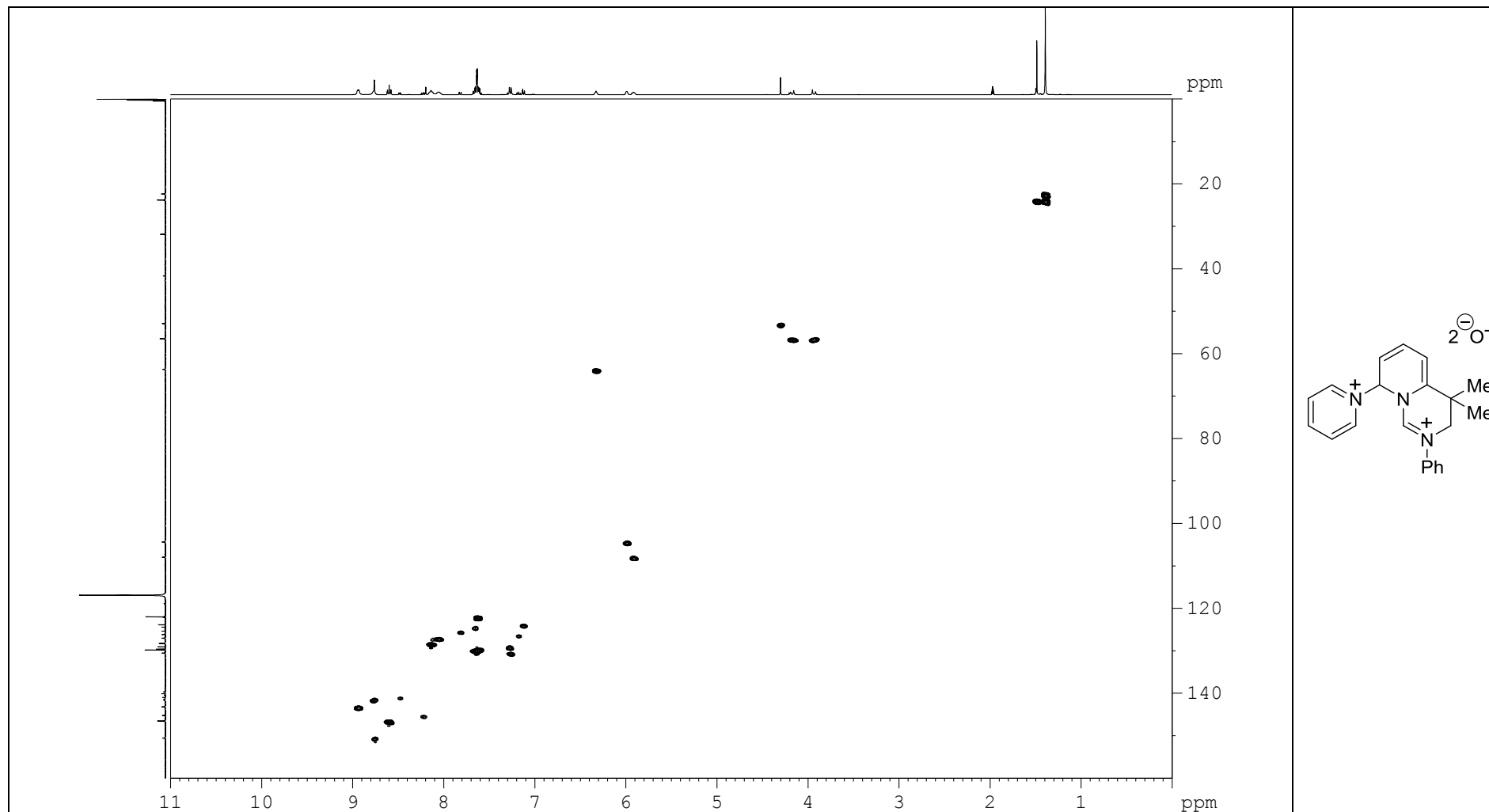


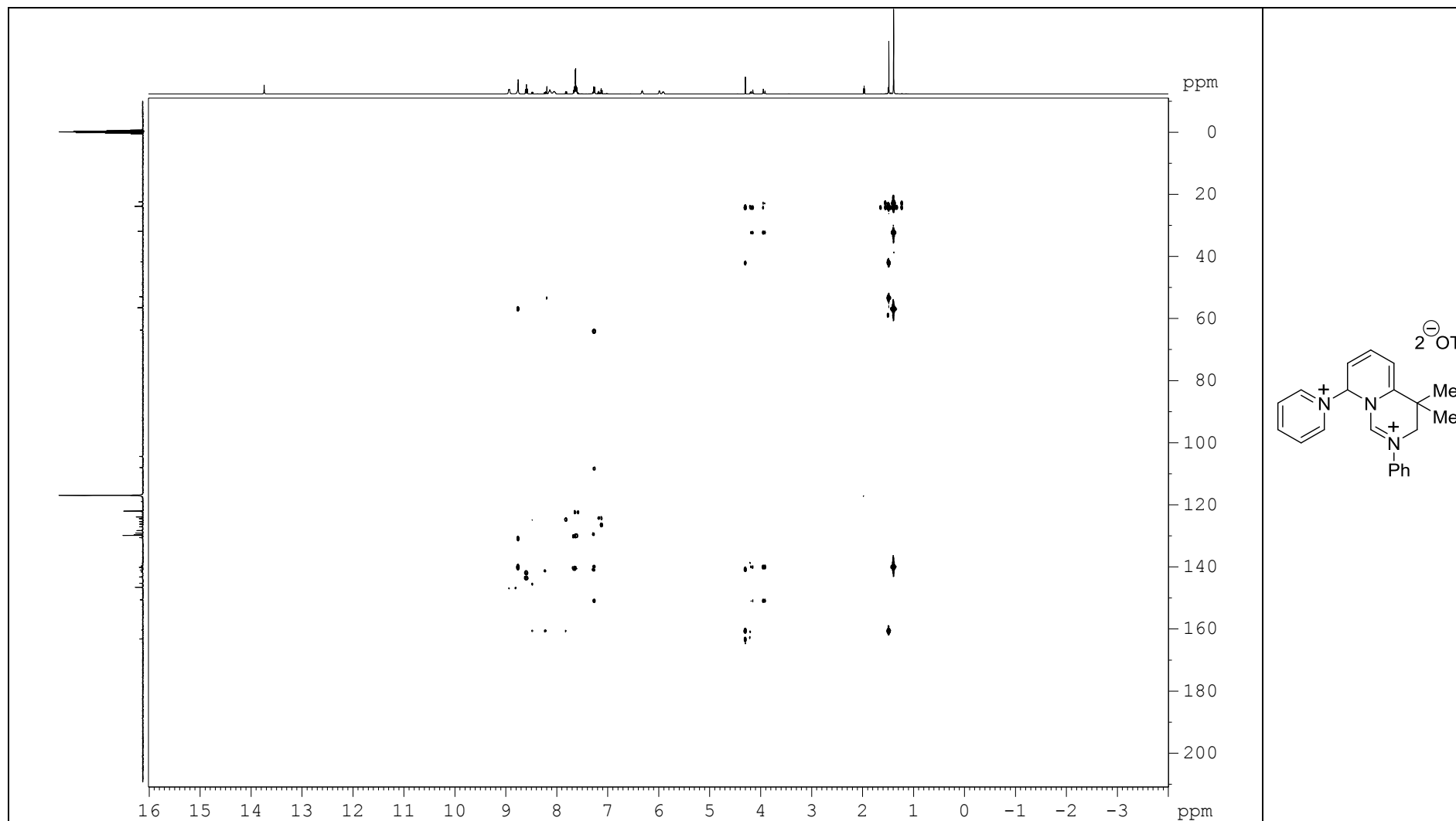


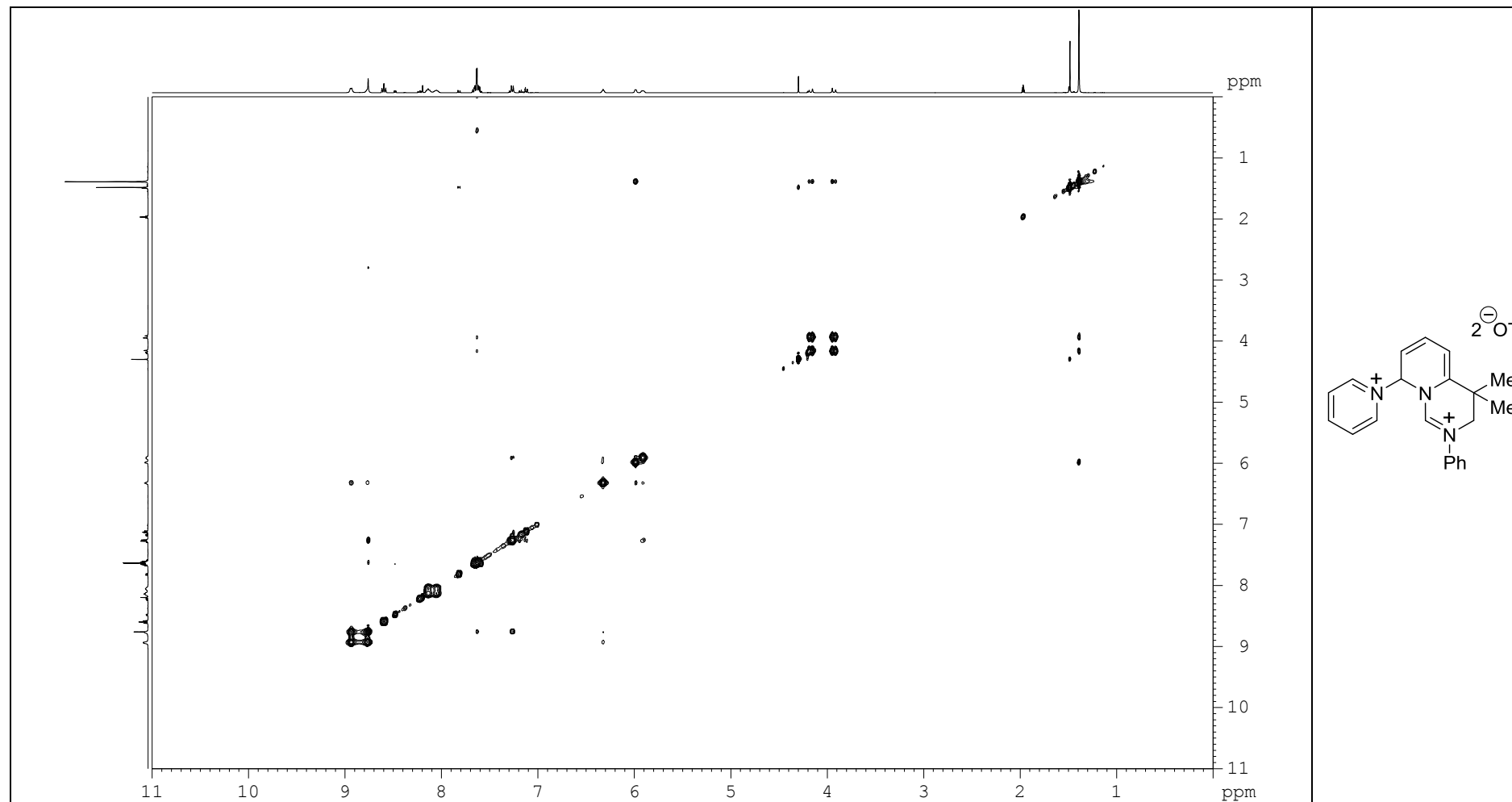
¹H NMR of Disalt **5.1** treated with pyridine **1.31**.

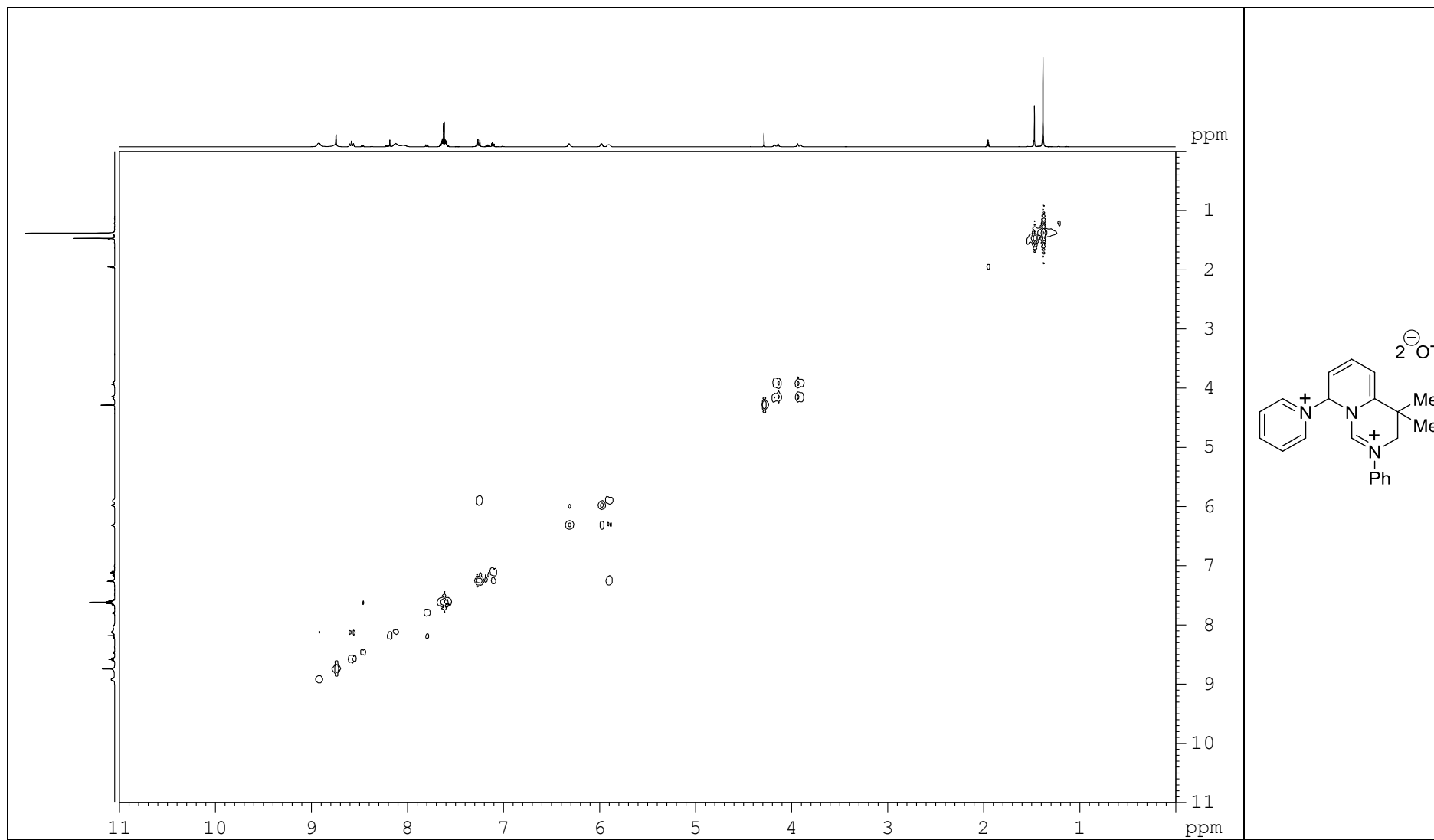
Appendix D

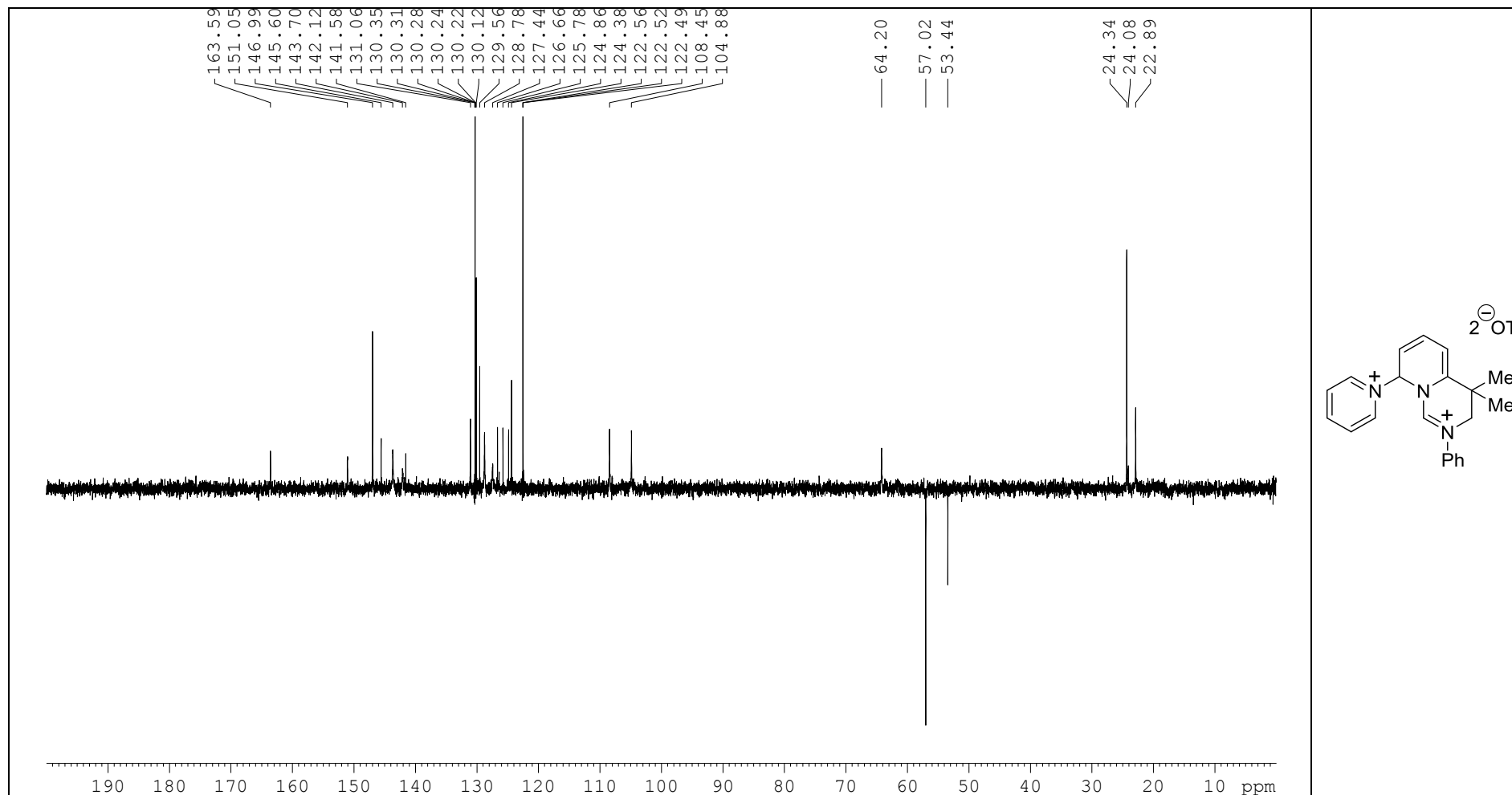






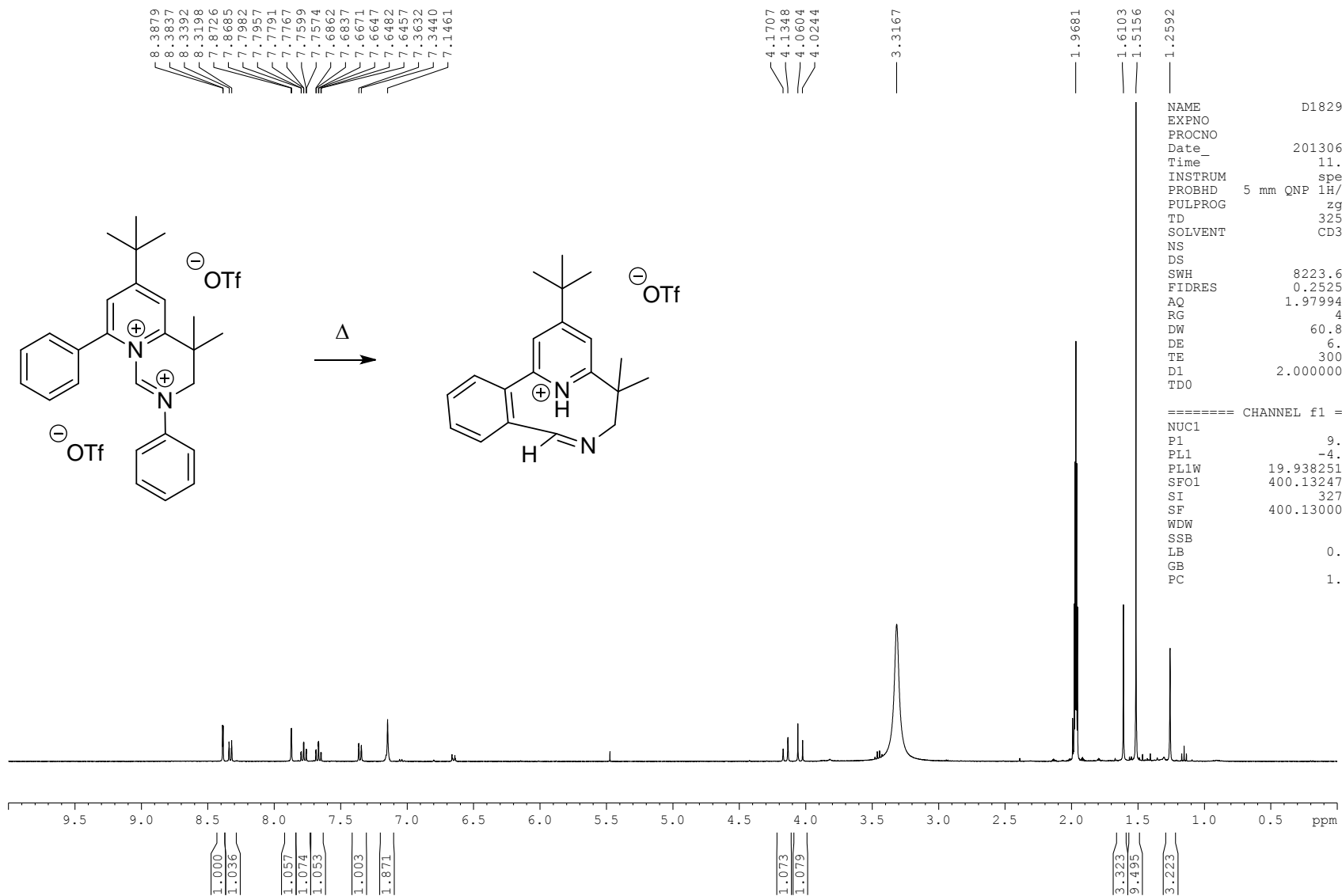




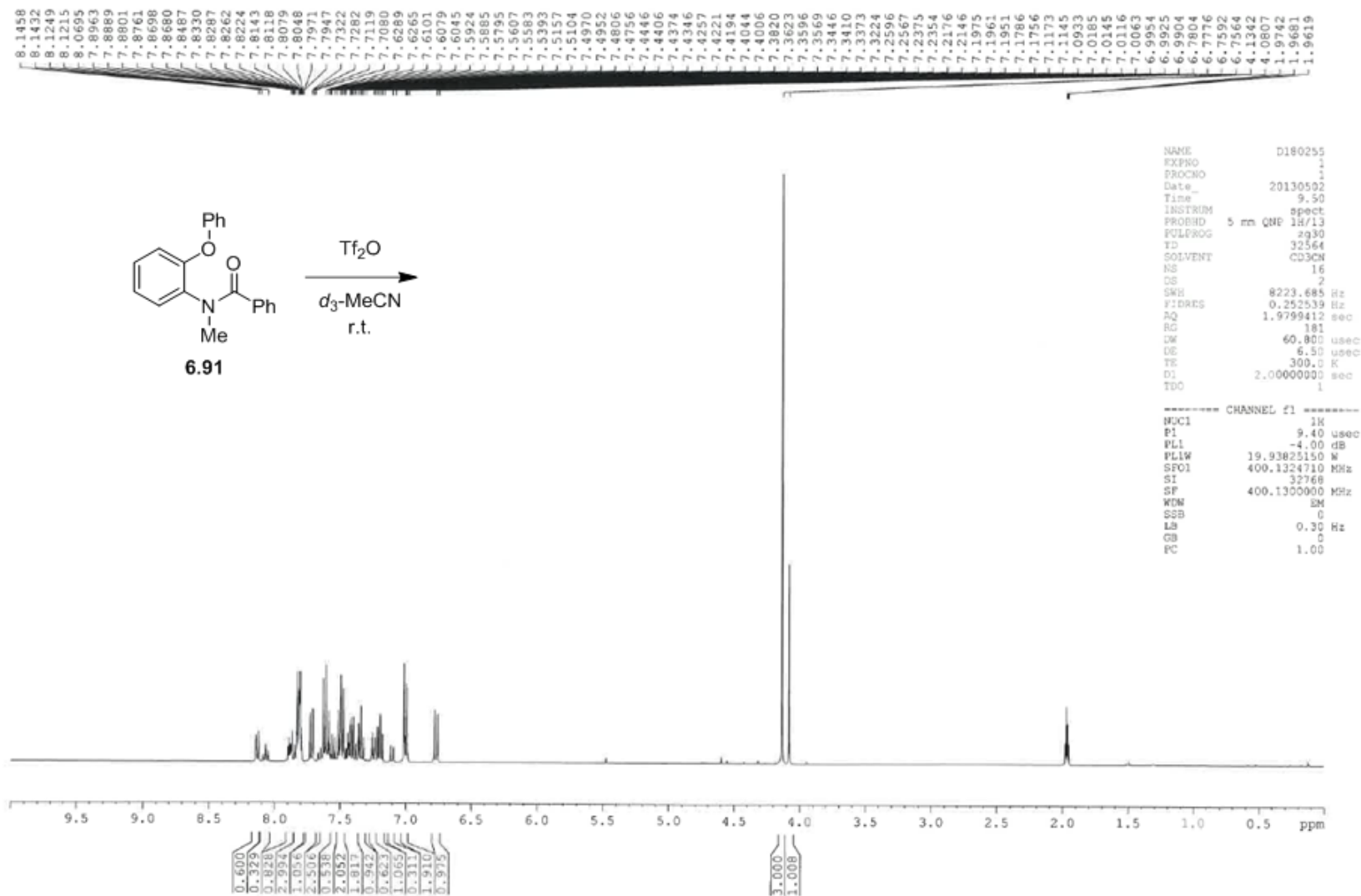


¹H NMR of Possible N-Ph Cleavage Reaction

Appendix E

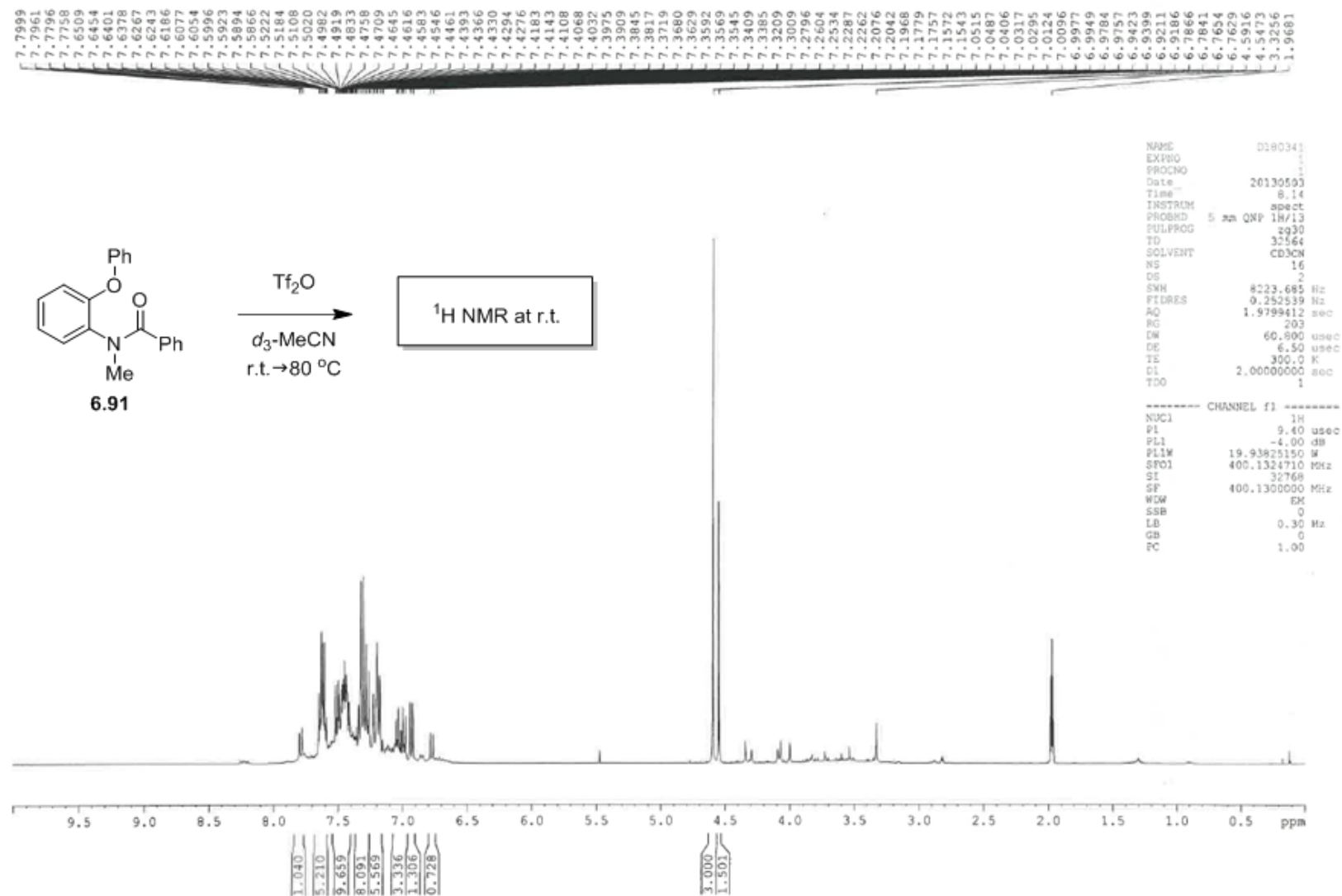


¹H NMR Experiment: Treatment of Amide **6.91** with Tf₂O at r.t.



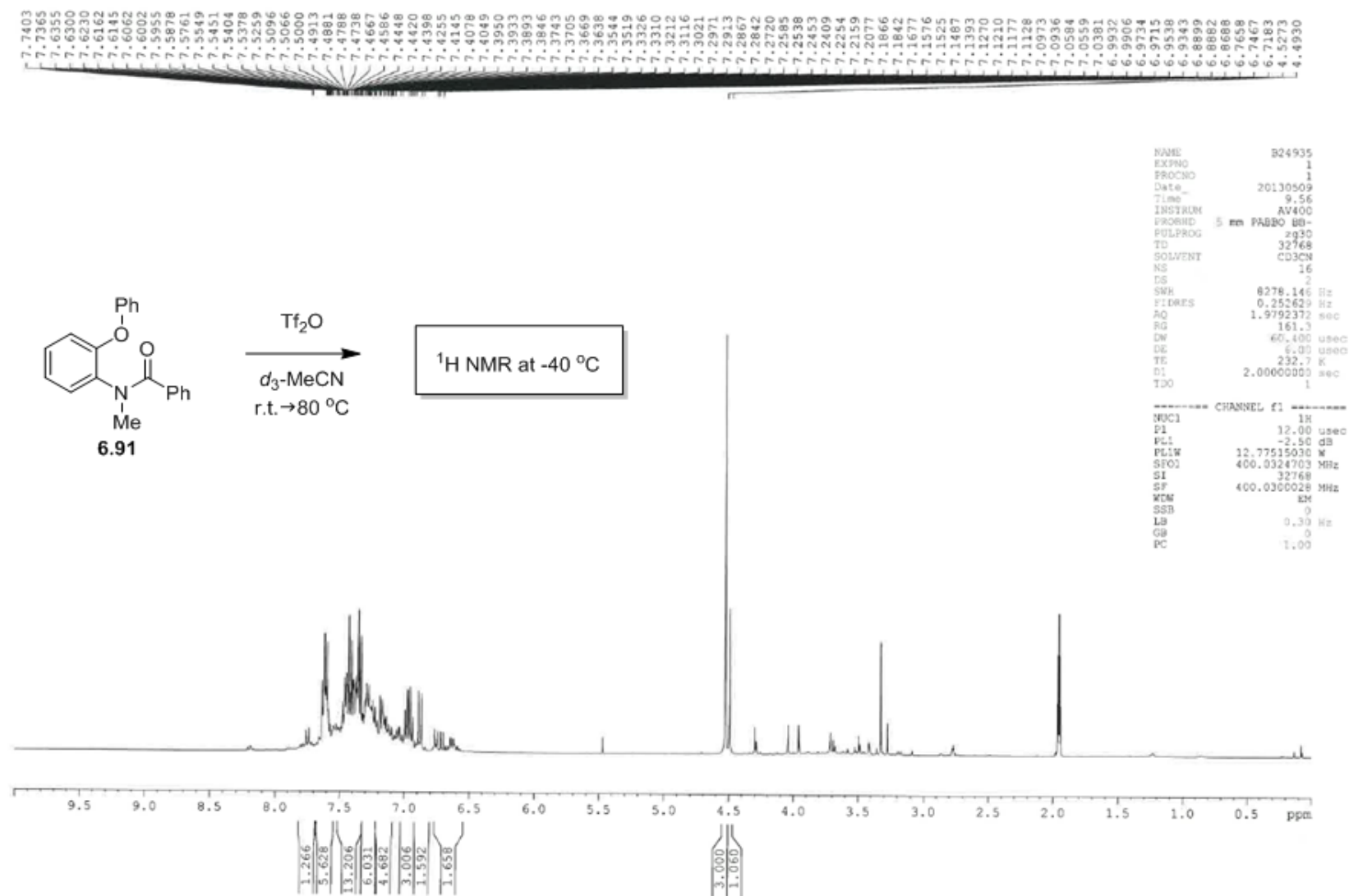
¹H NMR Experiment: Treatment of Amide **6.91** with Tf₂O at r.t. Followed by Heating at 80 °C Then Cooling to r.t.

Appendix G



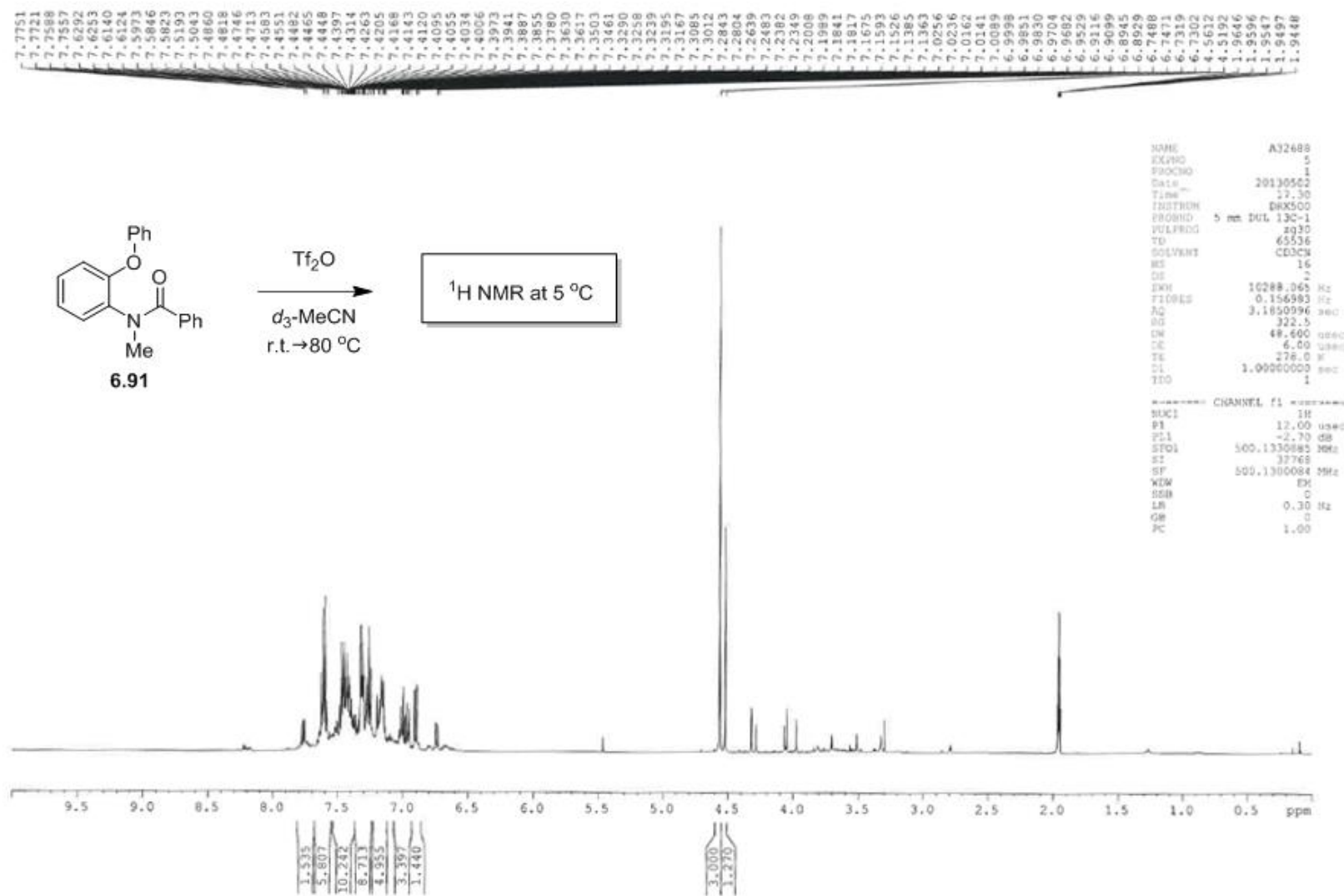
¹H NMR Experiment: Treatment of Amide **6.91** with Tf₂O at r.t. Followed by Heating at 80 °C Then Cooling to r.t.

Appendix G



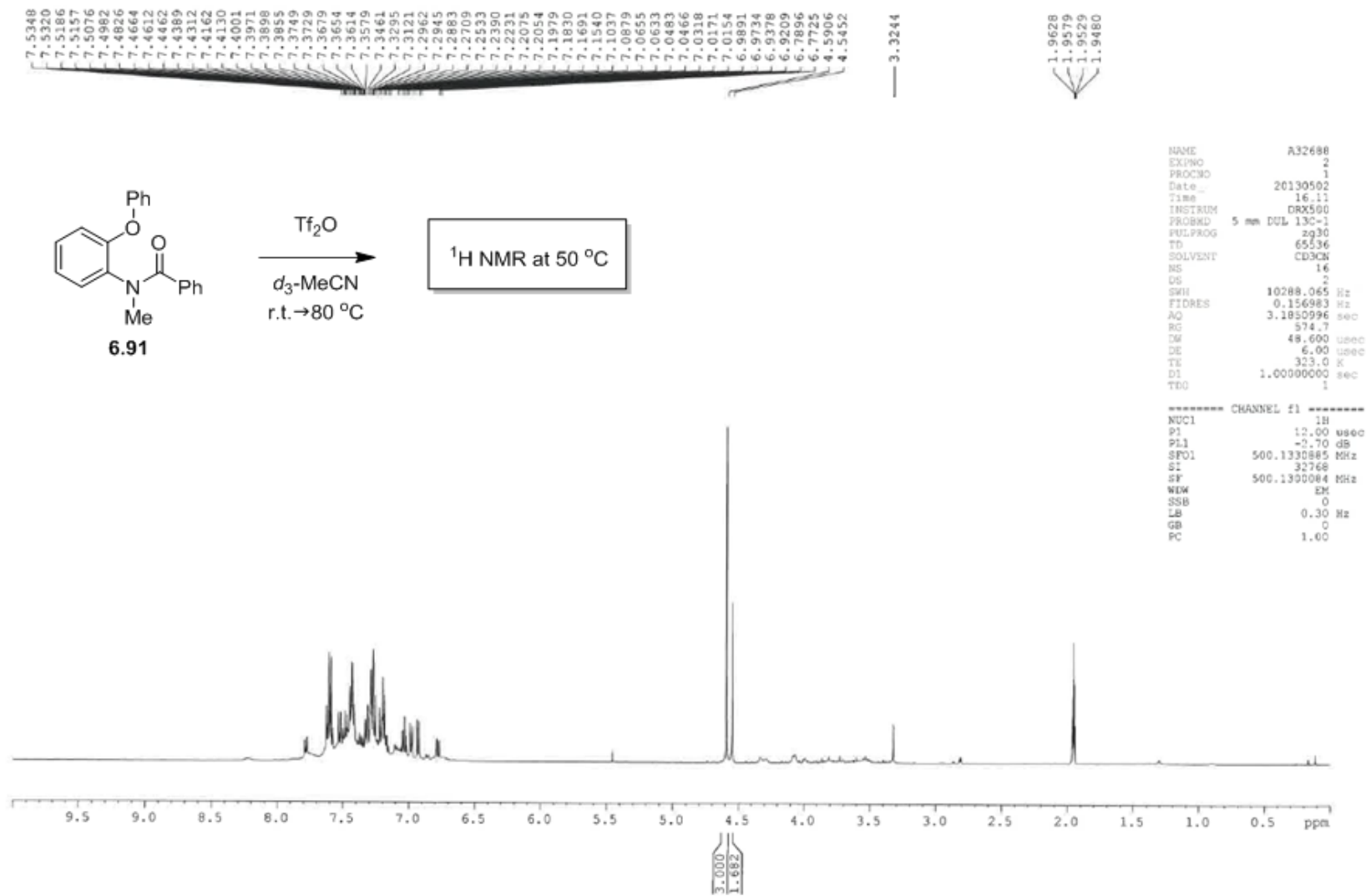
¹H NMR Experiment: Treatment of Amide **6.91** with Tf₂O at r.t. Followed by Heating at 80 °C Then Cooling to r.t.

Appendix G



¹H NMR Experiment: Treatment of Amide **6.91** with Tf₂O at r.t. Followed by Heating at 80 °C Then Cooling to r.t.

Appendix G



¹⁹F NMR experiment: Treatment of Amide **6.91** with Tf₂O at r.t. Followed by Heating at 80 °C Then Cooling to r.t.

Appendix H

